Exploration of CF_3^+ as a new reagent ion for Chemical-Ionization-Reaction Mass-Spectrometry

Thesis submitted for the degree of

Doctor of philosophy

At the University of Leicester

Saleh Alhadi Ouheda

Department of Chemistry

University of Leicester

2018

Statement of Originality

This thesis is based on work conducted by the author in the Department of Chemistry at the University of Leicester (October 2014-Sebtemper 2018). All the work in this thesis is original unless otherwise acknowledged in the text or by references.

Saleh Alhadi Ouheda

Abstract

The detection of small alkanes in a chemical ionization reaction mass spectrometer (CIR-MS) using conventional reagents presents an analytical challenge. The proton affinity of reagents such as H_3O^+ is too high, whereas the alternatives, such as O_2^+, give rise to excessive fragmentation. In this research, the use of CF_3^+, generated from CF_4, in CIR-MS is shown to be suitable to detect light n-alkanes in the range C_2-C_6 with almost no fragmentation. CF_3^+ ionization proceeds via hydride abstract ion and this is the critical difference in comparison with the proton transfer mechanism facilitated by H_3O^+.

Different reaction mechanisms are observed to be at work in the reaction of CF_3^+ with a functionally varied range of volatile organic compounds (VOCs). For example, with the larger alkanes, fluoride extraction occurs and, with aromatic and nitrile VOCs, CF_3^+ acts as a Lewis acid and a strong electrophile. Cases of charge transfer were observed as well as a metathesis reaction with aldehydes and ketones, where the oxygen in the C=O bond is replaced with C-F^+. The weakness of the bonds in longer chain VOCs were found to exhibit the same tendency to fragment as experienced with reactions with every other type of reagent, including H_3O^+.

Application of CF_3^+ as a reagent, in exhaled breath and urine headspace analysis of smokers and non-smokers was examined. The results showed that CF_3^+ was more sensitive than H_3O^+ in the detection of acetonitrile and toluene in exhaled breath. In both cases of acetonitrile and toluene, an adduct is formed with CF_3^+, which makes these molecules easily identifiable from interfering isobaric compounds. CF_3^+ reactions were not affected by the large amounts of urea and ammonia found in urine samples. When using H_3O^+ as a reagent, VOCs with lower proton affinities such as small n-alkanes cannot be detected. Hence CF_3^+ has the potential to be a useful as a complementary reagent to H_3O^+ to detect a wider range of VOCs in real-life samples.

The data of breath and urine headspace were subject to multivariate analysis, mainly Principle Component Analysis (PCA) and Partial Least Squares Discriminant Analysis (PLS-DA) which provided excellent means for distinguishing between smokers and non-smokers in breath and urine analysis.

Acknowledgment

I would first like to thank my supervisors, Professor Paul Monks and Professor Andrew Ellis, for giving me the opportunity to start a PhD with the atmospheric group. The advice and guidance given to me by Prof Monks has been excellent, and to him I must say thank you.

Special thanks to Dr Robert Blake for all of his assistance, especially in the early days while I was finding my feet in the world of research, teaching me how to run the CIR-MS, setting the experiments, analysing the data and for carefully reading this work. I must also say thank you to Dr Rebecca Cordell for all the help, proof reading and expertise I have received from her throughout my PhD, which was always greatly appreciated. Also, thanks to Luke Bryant, Jonathon Brooks and Thalassa Valkenburg for helping me with the statistical analysis and analysing GC data. Also, I would like to thank my friend Embarek Alwedi for explanations of some the mechanisms of the reactions involved.

I would also like to thank the other members of atmospheric group for many helpful discussions and support, including Dr Zoe Fleming, Dr Roberto Sommariva, Rikesh Panchal, Lloyd Hollis, Sarkawt Hama, Mario Panagi, Jasmine Wareham, Sofia Mirmigkou and Emmanuel Bermand.

I wish to thank the staff within the chemistry department's workshops, especially Carl Schieferstein and Gareth Bustin for their valuable technical support.

Finally, I am grateful to my family for their constant love and support throughout my PhD journey.

Table of contents

List of Tables

List of Figures

Chapter One: Introduction

Chemical ionization reaction mass spectrometry (CIR-MS) is an important tool for the real-time measurement of volatile organic compounds (VOCs) in a variety of environmental fields such as monitoring urban pollution as well as medical applications such as breath and urine analysis. The most popular reagent used in CIR-MS is H_3O^+ but other reagent ions such as O_2^+, NO^+ and NH_4^+ have been found to be useful for detecting VOCs in special circumstances. These reagents often cause fragmentation or do not react with a certain analytes thus making it hard or impossible to detect some VOCs. One of the most intractable situations arise with small chain alkanes.

This thesis explores the utility of CF_3^+ as novel reagent in CIR-MS and its application to detect small chain of alkanes and other VOCs. In addition, it explores the potential for its use in the detection of VOCs in breath and urine samples from smokers and non-smokers. This chapter provides context of this study through the application of the main reagent ions in CIR-MS and the chemistry of these reagents with different families of VOCs.

1.1 Applications of Proton Transfer Reaction-Mass Spectrometry

1.1.1 Environmental Measurements

The importance of PTR-MS is apparent from its high sensitivity, selectivity and its ability to measure many VOCs online as emitted from biogenic and anthropogenic sources in application areas such as environmental science, biogenic/anthropogenic VOCs emissions, oceans and seas, food and medical applications [1].

Natural and anthropogenic sources emit a wide range of VOCs into the atmosphere. VOCs may affect the chemical properties of the atmosphere such as through the formation of secondary organic aerosols during the photochemical formation of ozone. As a result, the identification and the quantification of these VOCs helps the understanding of the chemical changes occurring in the atmosphere [2]. Owing to the relative selectivity of H_3O^+ in reacting with the majority of VOCs, but not with the major constituents of air, PTR-MS can be applied to detect VOCs in the atmosphere with high sensitivity with a fast response time [2]. The first studies on the atmosphere by PTR-MS were carried out in 1990s to measure the variation of VOC concentrations in the atmosphere near Innsbruck in Austria [3, 4]. Other studies have been carried out to characterise the VOCs and their oxidation products from the forests of Surinam using PTR-M [5-7]. In another

example, PTR-MS was used to measure the aromatic and oxygenated VOCs which evaporated from an oil spill over the Gulf of Mexico [8]. Many studies have been carried out to calibrate and validate PTR-MS atmospheric measurements [1, 9-23].

Biogenic VOCs are released from biological processes within the environment and have an impact on the change of chemistry of the biosphere such as climate, formation of the tropospheric ozone, and production of aerosols [1, 2]. The major naturally occurring non-methane VOCs are isoprene, monoterpenes, other reactive and relatively nonreactive VOCs. The tropical forests, particularly those with broadleaf trees, are considered to be the main source of isoprene emissions owing to a greater exposure to higher levels of photoactive radiation and higher temperatures [1]. Emissions of isoprene and its oxidation products from tropical forests have been measured through the use of PTR-MS. PTR-MS has been used to measure the concentration of several VOCs in European forests. The findings suggest a strong diurnal variation for a number of compounds. The results were classified into three groups depending on the behaviour of their concentrations. The first class contains reactive compounds such as methanol, methyl vinyl ketone, acetone, butanol, methacrolein and hexanal, which generally had their highest concentration during the afternoon and the lowest concentration during the night. This class is affected by air temperature and light levels. The second class of compounds, monoterpenes, were correlated with mixed timescales having their highest concentration at night and minimal concentrations during the day. The third class contained long-lived compounds such as benzene [1, 24].

Anthropogenic VOCs result from human activities such as factory emissions, vehicle exhaust, oil refining storage, burning fossil fuels and agricultural activities. These emissions may affect air quality and can damage ecosystems and, as result, affect the quality of life on Earth [2]. The PTR-MS instrument has been adapted for the measurement of VOCs in many cities such as Tokyo, Mexico City, Houston, Caracas and Barcelona [1, 12, 21, 25-28]. The PTR-MS measurement showed that the concentrations of VOCs in Tokyo were very high in summer compared with autumn, while aromatic compounds showed less seasonal variation [1, 12]. The results of measurements in Caracas showed relatively low levels of pollutions [1, 27]. Langford *et al.* [29], applied PTR-MS to measure VOC fluxes in the urban areas of Manchester and London. Six VOCs were chosen for analysis in the Manchester measurements which were toluene, benzene, isoprene, acetone, acetaldehyde and methanol. In the London study, the VOCs were

toluene, isoprene, acetone, acetaldehyde, acetonitrile, methanol, and benzene and its derivatives such as ethylbenzene. The results showed the fluxes of methanol, acetone, toluene, and benzene were greater in London than Manchester. In addition, the larger organic aerosol emission fluxes were also larger in London than Manchester [2, 29, 30]. Biomass burning has two major sources: the burning of vegetation (anthropogenic) such as burning for land management in agriculture or cooking or brick making. The other source of biomass burning is natural such as wildfires resulting from lightning strikes and volcanic activity [1, 2]. Biomass burning is considered to be a major source of VOCs in the atmosphere and has a significant effect on its chemistry [2, 31, 32]. PTR-MS is a powerful tool in the detection of acetonitrile as a marker of biomass burning plumes [1, 20, 33-39], with the combination of measuring the concentration of CO, it is able to define biomass burning related to fossil fuel emissions [1, 35, 37, 38].

1.1.2 PTR-MS in the medical sciences

Conventional medical methods used to diagnose and monitor disease may cause significant discomfort or pain to a patient. These methods require collection of biological samples that are subsequently analysed in clinical laboratories, a process which is often expensive and time-consuming. Blood is considered one of the most useful biological specimens used for medical investigation. However, blood analysis is usually complicated and needs particular care.

Development of simple non-invasive and reliable methods enabling rapid and accurate monitoring of disorders or diseases is always desirable in medicine. PTR-MS has potential for use as a non-invasive tool for investigation in health science to improve the quality of life. The analysis of breath is one such application for PTR-MS in medical diagnostics. Exhaled breath contains a variety of VOCs that supply a non-invasive method to measure metabolic processes in the body and indeed their disruption in certain diseases. Lagg *et al*. [40], detected methanol, ethanol and acetone in exhaled human breath using H_3O^+ as the reagent in conventional selected ion flow drift tube (SIFDT). The measurements demonstrated that the concentration of ethanol and acetone were not affected by consumption of fruit. However, concentrations of methanol were significantly altered.

Jordan *et al*. [41], used PTR-MS to investigate the concentration of acetonitrile and benzene in the exhaled breath of smokers and non-smokers. The concentration of both

benzene and acetonitrile were found to be greater in the breath of smokers than in non-smokers. In addition, the result showed that concentrations of benzene in smokers' breath rapidly declines with time since the last time they smoked. In contrast, acetonitrile concentrations in smokers lasted around a week before declining once smoking had been stopped.

Warneke *et al*. [42], conducted experiments to measure propanol in exhaled human breath using H_3O^+ as the reagent in PTR-MS. The average concentration of propanol in healthy volunteers was about 150 ppb.

Various mycobacterial species can cause infections in humans, and the treatment depends on the type of infecting species. Fast detection could improve targeted treatment of the infecting species. Crespo *at al* [43] used PTR-MS to detect short-chain VOCs emitted from two non-tuberculosis slow-growing mycobacterial species, *Mycobacterium avium* and *Mycobacterium kansasii*, and a non-pathogenic fast-growing species, *Mycobacterium smegmatis*, in culture. The result showed that there were differences in VOCs emitted from these different species of mycobacteria. Propanethiol, dimethyl sulphide and dimethyl disulphide in particular were found to be derived from *M. avium* [43].

In another study, Wang *et al*. [44], investigated the reaction of hydronium ion with compounds released by *Pseudomonas* and related bacteria. In this study, primary and secondary aliphatic alcohols produced by the bacteria reacted with H_3O^+ to produce protonated molecular ions. However, the 2-heptanol reaction produced a protonated parent with another small fragment, characteristic of the fragility of longer alkyl chain VOCs:

1.2 Precursors in Chemical Ionization

By far the most widely used precursor in chemical ionization (CI) work is H_3O^+ which ionizes via the process of proton transfer reactions (PTR). Its main advantages are that it produces less fragmentation than most other potential candidates, and its less disruptive action results in fewer reaction pathways. The technique does have certain shortcomings, apart from its insensitivity to some VOCs, such as its inability to distinguish items with the identical m/z values as found in isomers such as methyl vinyl ketone (MVK) and methacrolein.

In situations such as these it is useful to use other reagents, which have other reaction mechanisms such as charge transfer, hydride transfer or adduct formation. This has led to

limited use of precursors like NO^+, O_2^+. Unfortunately these precursors undergo more complex reactions making the interpretation of the results more complicated. The introduction of ions produced by CF_3^+ reaction has opened up several new avenues such as hydrogen fluoride (HF) elimination (found with ethane and propane, and several CF_2^+ end products) and the behaviour as an electron acceptor or Lewis acid in reactions with aromatics and nitriles.

In this chapter we summarise the roles played by the historic CI reagents and present the case for the use of CF_3^+ as a useful addition.

1.2.1 H_3O^+ as reagent in CIR-MS

The reaction of H_3O^+ with various VOCs proceeds via exothermic proton transfer [1] . Spanel *et al.* [45], studied the reaction of H_3O^+ with several aldehydes and ketones using selected ion flow tube mass spectrometry (SIFT-MS). Formaldehyde, acetaldehyde and propanal reactions produce only a protonated molecular ion, e.g.:

$$H_3O^+ + CH_3CHO \longrightarrow CH_3CHOH^+ + H_2O \qquad (1.1)$$

Similarly, the reaction of propenal and benzaldehyde with the hydronium ion result in a protonated molecular ion. However, the reactions of longer chain saturated aldehydes such as hexanal produced two protonated fragments ions:

$$H_3O^+ + RCHO \longrightarrow RCHOH^+ + H_2O \qquad (1.2a)$$

$$H_3O^+ + RCHO \longrightarrow R^+ + 2H_2O \qquad (1.2b)$$

Ketones tend to react to produce the protonated parent ion [45].

The reaction of the hydronium ion with several alcohols and phenols have been studied using SIFT-MS. The methanol and ethanol, $C_5H_{11}(OH)$ isomers and phenols such as 2-hydroxyphenol, 2-, 3-, 4-methylphenol, 4-ethylphenol proceeded via direct, non-dissociative proton transfer forming only the protonated molecular ion, while, the reaction of 1-propanol, 2-propanol and $C_4H_9(OH)$ isomers produced the parent ion as minor product [46, 47]:

$$H_3O^+ + R(OH)CH_3 \longrightarrow R^+CH_3 + 2H_2O \qquad (1.3a)$$

$$H_3O^+ + R(OH)CH_3 \longrightarrow R(OH_2^+)CH_3 + H_2O \qquad (1.3b)$$

The reaction of 1-octanol and 2-octanol produced three fragments [46]:

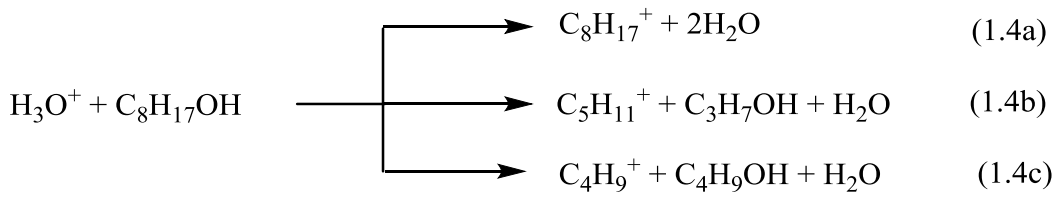

1-phenylmethanol, 1- and 2-phenylethanol produce the hydrocarbon ion by elimination of an H_2O molecule [47].

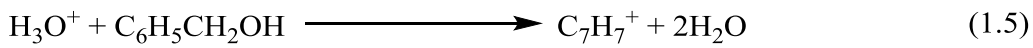

The reaction of H_3O^+ with cyclic carbonyl such as 1,4-benzoquinone and cyclohexanone proceeds via non-dissociative proton transfer, resulting in only the protonated molecular ion, e.g., as in methyl phenol [47]:

The reaction of H_3O^+ with a number of carboxylic acids and esters have been studied via SIFT-MS by Spanel *et al*. [48], who noted that the formic acid, acetic acid, methyl acetate and ethyl acetate reactions produced only the protonated parent ion after elimination of H_2O:

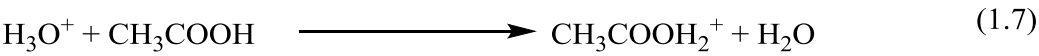

Propionic, butyric, trimethylacetic, acrylic acids and longer esters all produced two fragments but the protonated ion still had the greatest abundance:

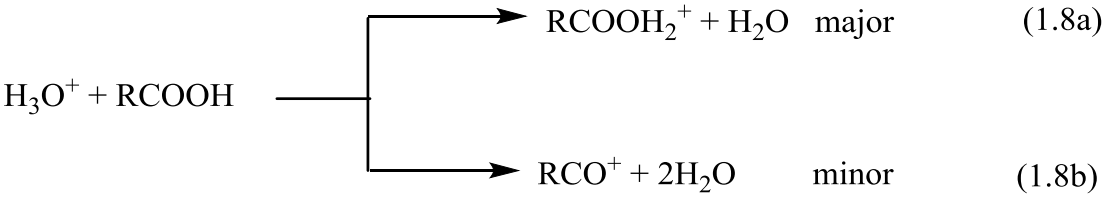

The lactic acid reaction produced a protonated ion as a minor product. It seems that the second product is more exothermic:

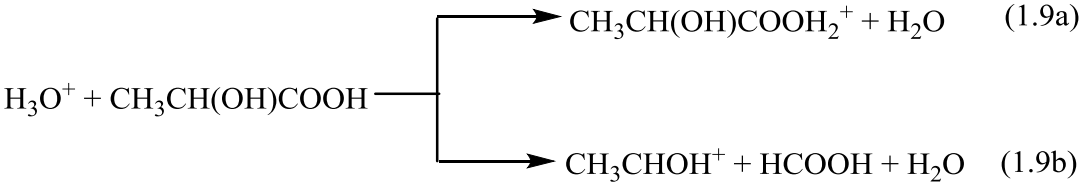

The reaction of hydronium ion with peroxyacetic acid has been studied using SIFT-MS. Acetic acid reacts with H_3O^+ through non-dissociative proton transfer resulting in only a parent ion at m/z = 61. However, another signal can be seen at 77 amu which was related to protonated peroxyacetic acid, produced via the following reactions [49]:

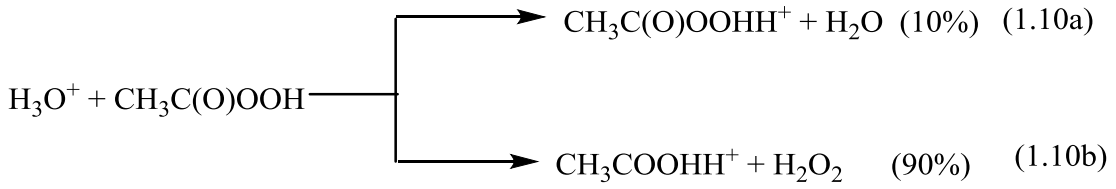

The reactions of some organosulphur compounds with H_3O^+ have been studied using SIFT-MS by Spanel *et al*. [50], where most of these reactions produced a protonated parent ion as exemplified by the dimethyl sulphide reaction:

$$H_3O^+ + (CH_3)_2S \longrightarrow (CH_3)_2S.H^+ + H_2O \qquad (1.11)$$

Thiolacetic acid reaction formed the molecular ion and another fragment [50]:

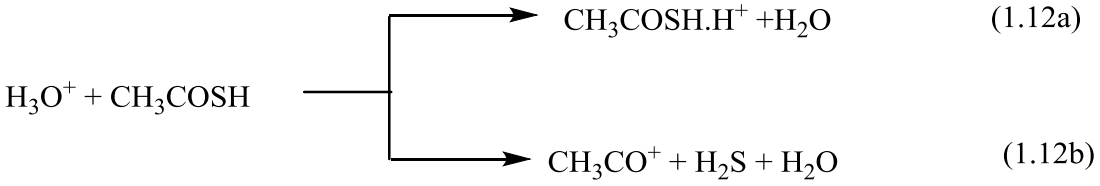

SIFT-MS was used to study the reaction of H_3O^+ with several aromatic and aliphatic hydrocarbons. Ionization of aromatic hydrocarbons proceeds via exothermic proton transfer producing a single protonated parent ion exemplified by the toluene reaction [51]:

$$H_3O^+ + C_6H_5CH_3 \longrightarrow C_6H_5CH_3.H^+ + H_2O \qquad (1.13)$$

Small chain *n*-alkanes up to C_5 do not react with H_3O^+ [52]. However, higher alkanes such as octane produce their parent ion [51].

Spanel *et al*. [53], studied the reaction of H_3O^+ with several ethers using SIFT-MS. Tetrahydrofuran, diethyl ether and anisole reactions result in the protonated parent ion:

$$H_3O^+ + C_2H_5OC_2H_5 \longrightarrow C_2H_5OC_2H_5.H^+ + H_2O \qquad (1.14)$$

Allyl ethyl ether, butyl methyl ether and the ethylene glycol dimethyl ether reactions produce protonated parent ions with some other fragment, but not always with the molecular ion as the major product [53]: An example of this is the behaviour of dimethyl ether (DME):

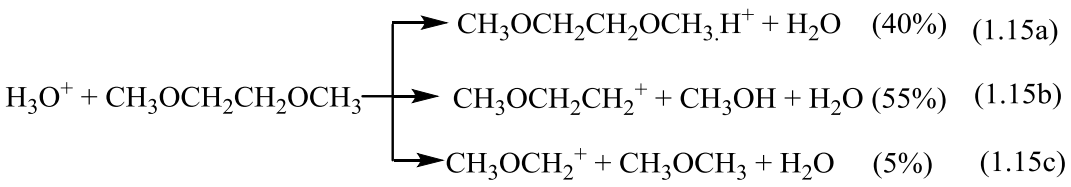

Wang *et al*. [54], described the application of SIFT-MS on the reactions of H_3O^+ with several $C_{10}H_{16}$ monoterpenes. These reactions proceeded via exothermic proton transfer

with the major product being the parent ion, $C_{10}H_{17}^+$ with $C_6H_9^+$ ions as a major additional fragment ion [54].

Spanel *et al*. [55], measured the reaction of H_3O^+ with several amines and a number of other nitrogen-containing compounds. These reactions are exothermic and proceed via transfer of a proton from the H_3O^+ ion to the analyte. The ammonia reaction produced only NH_4^+. However, the primary amine *n*-propyl amine and isopropyl amine produced a partial dissociation reaction, where parent ion with NH_4^+ are the major product fragments:

$$H_3O^+ + (CH_3)_2CHNH_2 \longrightarrow (CH_3)_2CHNH_2.H^+ + H_2O \quad (1.16a)$$

$$H_3O^+ + (CH_3)_2CHNH_2 \longrightarrow NH_4^+ + C_3H_6 + H_2O \quad (1.16b)$$

Secondary and tertiary amines produced protonated parent ions with second fragment. This additional channel is produced by elimination of H_2, as can be seen in the following equations:

$$H_3O^+ + (C_2H_5)_2NH \longrightarrow (C_2H_5)_2NH.H^+ + H_2O \quad (1.17a)$$

$$H_3O^+ + (C_2H_5)_2NH \longrightarrow C_4H_{10}N^+ + H_2 + H_2O \quad (1.17b)$$

The reaction of the hydronium ion with several N-containing heterocyclic compounds have also been studied using SIFT-MS. The pyrrole, pyridine, acetonitrile and benzonitrile reactions with H_3O^+ produces only the protonated molecular ion [55, 56].

$$H_3O^+ + CH_3CN \longrightarrow CH_3CN.H^+ + H_2O \quad (1.18)$$

However, for pyrrolidine, 1-methyl pyrrolidine and piperidine, a second minor product was also detected, as can be seen in the following equations:

$$H_3O^+ + C_5H_{11}N \longrightarrow C_5H_{11}NH^+ + H_2O \quad (1.19a)$$

$$H_3O^+ + C_5H_{11}N \longrightarrow C_5H_{10}N^+ + H_2 + H_2O \quad (1.19b)$$

The hydronium ion reacts with the O-containing heterocyclic compounds in SIFT-MS resulting in the protonated molecular ions, e.g., as with furan:

$$H_3O^+ + C_4H_4O \longrightarrow C_4H_4OH^+ + H_2O \quad (1.20)$$

1.2.2 NH_4^+ as the reagent in CIR-MS

PTR-MS faces some limitation in applications in atmospheric measurements such as the difficulty to discriminate between isobaric species. To overcome this limitation, PTR-MS could be operated using other reagent ions [57]. NH_4^+ has a higher proton affinity (8.85 eV) than the majority of organic compounds, so is not able to react with most classes of organic compounds. There are some exceptions, however, such as amines and certain other types of nitrogen-containing compounds that could react with NH_4^+ as a reagent in PTR-MS. When an air sample contains 2-ethyl-3,5-dimethylpyrazine ($C_8H_{12}N_2$) and pinene ($C_{10}H_{16}$), both compounds can react with H_3O^+ and both produce nominal molecular ions at m/z = 137. If NH_4^+ is then provided as a reagent in PTR-MS, the signal at 137 amu can only arise from the pyrazine compound, owing to the fact that pyrazine has a proton affinity exceeding that of ammonia [2, 3]. Blake *et al*. [58], studied the reaction of multiple reagents with trace gas composition in CIR-MS. The reaction of acetone, acetonitrile, ethyl acetate, methacrolein, methyl benzoate and methyl vinyl ketone mainly produced an association complex, $M.(NH_3)^+$, with small fragments of association products from the cluster ions, $NH_4^+(NH_3)$, while the hexanal reaction produced only an association complex. Reactions of acetaldehyde, benzene, 1-butene, ethanol and toluene were not observed.

1.2.3 NO^+ as the reagent in CIR-MS

NO^+ reacts with organic molecules and usually produces only one or two product ions. There are several mechanisms for reactions of NO^+ with organic compounds (M) which include charge transfer resulting in M^+ ions, hydride ion transfer (H^-) forming MH^+ ions, hydroxide ion transfer (OH^-) producing MOH^+ ions, alkoxide ion transfer (OR^-) creating MOR^+ ions and ion-molecule combination (association) forming NO^+M ions. In general, the reactions of organic species with NO^+ follow only one of these mechanisms, but in some cases can proceed via two processes [59].

Charge transfer processes occur if the ionization energy of the analyte is lower than the ionization energy of NO, which is 9.26 eV, such as aromatic hydrocarbons and organosulphur compounds, an example of which is shown in the following equation [50, 51, 59].

$$NO^+ + C_6H_5CH_3 \longrightarrow C_6H_5CH_3^+ + NO \qquad (1.21)$$

Hydride ion transfer generally occurs during the reaction of NO^+ with aldehydes and ethers, forming one product ion (MH^+); for instance [53, 59]:

$$NO^+ + CH_3CHO \longrightarrow CH_2CHO^+ + HNO \qquad (1.22)$$

In equation 1.22, a hydride ion (H^-) was extracted from the CH_3 carbon group to form HNO, which is exothermic compared with separated H and NO. Hydride transfer also occurs in the reaction of NO^+ with primary and secondary alcohols [58].

Hydroxide ion transfer occurs in some cases such as with the reaction of NO^+ with a tertiary alcohol. In this process, a nitrous acid molecule was formed as shown in the example below [46, 59]:

$$NO^+ + (CH_3)_3COH \longrightarrow (CH_3)_3C^+ + HNO_2 \qquad (1.23)$$

Ion molecule association commonly occurs in the reaction of NO^+ with certain polar organic compounds such as carboxylic acids as seen in this example [48].

$$NO^+ + CH_3COOH \longrightarrow NO^+ CH_3COOH \qquad (1.24)$$

Mochalski *et al*. [60], conducted a study to measure product ion distributions for the reaction of aldehydes with NO^+ using selective reagent ionization time-of-flight mass spectrometry (SRI-TOF-MS). The aldehydes examined consisted of several *n*-alkanals, branched chain alkanals and alkenals. They found that most of the reactions produced multiple ion products, but a common product followed hydride ion transfer. Ionization energy determines the ionic and neutral products of these reactions. Acetaldehyde produces only the CH_3CO^+ parent ion. The percentage of parent ion to the total product ions in the reaction of NO^+ with propanal is lower than 100% in a dry sample, as shown in the following equation:

$$NO^+ + C_2H_5CHO \longrightarrow \begin{cases} C_2H_5CO^+ + HNO & (1.25a) \\ C_2H_5^+ + CO + HNO & (1.25b) \\ C_2H_3^+ + (CH_2O + HNO) & (1.25c) \end{cases}$$

CO elimination was observed in the C_3-C_7 alkanals' reactions as a fragment of the parent ion. The hydride ion transfer mechanism of C_6-C_{11} *n*-alkanes could be followed by elimination of H_2O or formation of dihydroxyamine, H_3NO_2, as a neutral fragment. The percentage of hydride ion transfer products showed interesting behaviour depending on the number of carbon atoms present. The percentage of the parent ion varies from 100% and 13% for acetaldehyde and *n*-hexanal reactions, respectively, as shown in Figure1.1 [60].

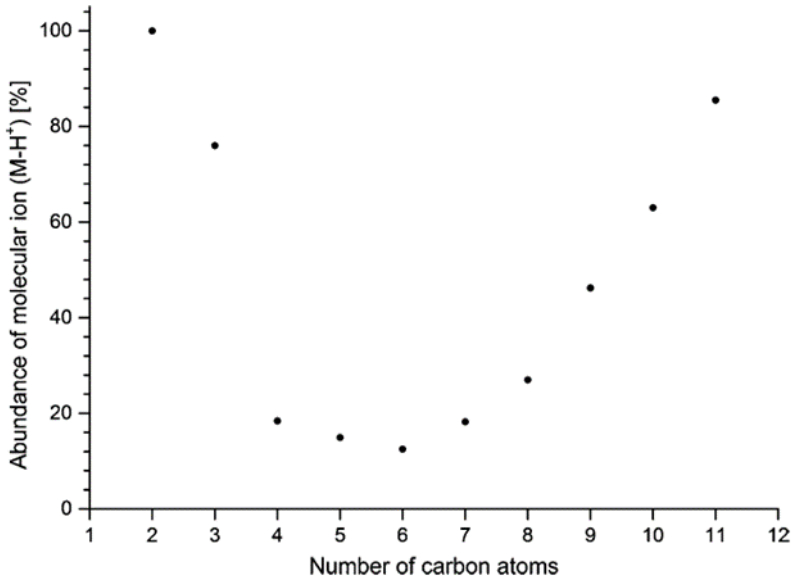

Figure 1. 1: Percentage of molecular ions in the reactions of NO^+ with n-alkanals in SRI-TOF-MS at an *E/N* of 130 Td and dry air. Adapted from Mochalski *et al* [60].

Wyche *et al.*[61], ran the first attempt to differentiate isobaric compounds using NO^+ as the reagent in CIR-MS. The results showed the product of NO^+ with aldehydes and ketones supply a possible means of differentiating between isobaric compounds compared with the results of H_3O^+. Figure 1.2 shows an example of these reactions.

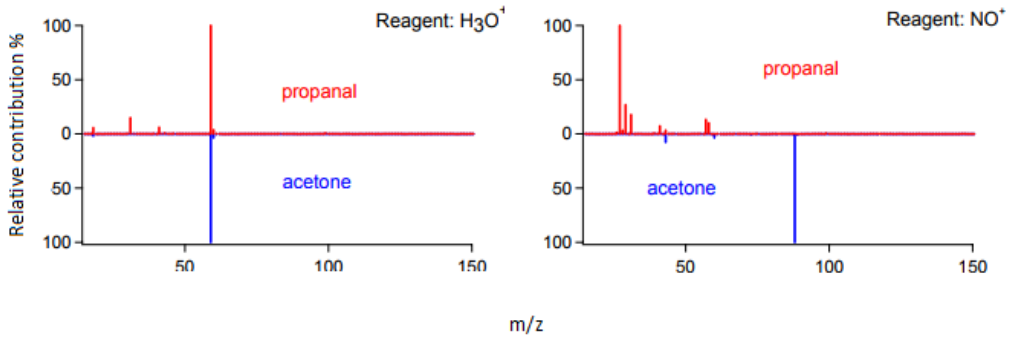

Figure 1. 2: Mass spectra of the isobaric aldehyde/ketone (propanal/ acetone), produced by a molecular ion with H_3O^+ or NO^+, adapted from Wyche *et al* [61].

Smith *et al.*'s [62], study with SIFT was carried out to measure the reaction between NO^+ and other reagents with seven isomers of hexanol with the general formula $C_6H_{14}O$ and molecular weights of 102 amu. These compounds are commonly included in food science research. The reaction of NO^+ follows a hydride ion transfer path to produce mainly $C_6H_{13}O^+$ ions (m/z = 101) for the primary and secondary hexanols. Energetics processes indicate that a hydrogen atom was removed from the alpha carbon in each instance to

form protonated aldehydes and protonated ketones for the reaction of primary and secondary alcohols, respectively, as seen in equation 1.26.

$$NO^+ + C_6H_{14}O \longrightarrow C_6H_{13}O^+ + HNO \quad (1.26)$$

A minor product of the primary alcohols formed another fragment at m/z = 83 by removal of H_2O from the major product, as shown in the following equation.

$$NO^+ + C_6H_{14}O \longrightarrow C_6H_{11}{}^+ + HNO + H_2O \quad (1.27)$$

Also, the secondary alcohols produce a minor hydrocarbon product at 85 amu and release the HONO molecule, as indicated in equation 1.28 [62].

$$NO^+ + C_6H_{14}O \longrightarrow C_6H_{13}{}^+ + HONO \quad (1.28)$$

Wang *et al*. [47], used SIFT to study the reaction of NO^+ with some phenols, phenyl alcohols and cyclic carbonyl compounds. The results showed the reaction of NO^+ with phenols follows a non-dissociative charge transfer mechanism to form the molecular ions.

$$NO^+ + HOC_6H_4CH_3 \longrightarrow C_7H_8O^+ + NO \quad (1.29)$$

NO^+ mainly follows the three processes as shown in this example.

$$NO^+ + C_6H_5CH_2OH \longrightarrow C_7H_8O^+ + NO \quad (1.30a)$$

$$NO^+ + C_6H_5CH_2OH \longrightarrow C_7H_7O^+ + HNO \quad (1.30b)$$

$$NO^+ + C_6H_5CH_2OH \longrightarrow C_7H_7{}^+ + HNO_2 \quad (1.30c)$$

Alkanes react with NO^+ and the major channel in such reactions is hydride ion transfer. In some cases, other channels were recorded. The sensitivity of multiple alkanes can be measured by PTR + SRI-MS using NO^+ as the precursor [63].

$$NO^+ + RH \longrightarrow R^+ + HNO \quad (1.31a)$$

$$NO^+ + RH \longrightarrow RHNO^+ \quad (1.31b)$$

Spanel *et al*. [51], used SIFT to detect the products of reactions of several aromatic and aliphatic hydrocarbons with NO^+. The authors found that NO^+ reacted with alkanes by hydride ion transfer and that greater fragmentation was noticed with larger alkanes [51]. Knighton *et al*. [64], detected 1,3-butadiene in the ambient atmosphere using NO^+ as the reagent in CIR-MS The result showed that the concentration of 1,3-butadiene was 35 pptv [64].

Wang *et al*. [56], measured the reaction of several N- and O-containing heterocyclic compounds with NO^+. The reactions of these compounds with NO^+ are relatively simple

and mostly yield a single product ion species. The mechanism of these reactions generally follows charge transfer owing to the ionization energies of these compounds being less than, or close to, the ionization energy of NO (9.26 eV). However, when charge transfer is only just exothermic, other mechanistic paths can proceed, and ion-molecule association and hydride ion transfer create NO^+M and MH^+, respectively. For example, the 2-piperidinone reaction follows all three processes, as seen in the following equations: [56].

$$NO^+ + C_5H_9NO \rightarrow NO^+C_5H_9NO \quad \text{dominant} \qquad (1.32a)$$

$$NO^+ + C_5H_9NO \rightarrow C_5H_8NO^+ + HNO \qquad (1.32b)$$

$$NO^+ + C_5H_9NO \rightarrow C_5H_9NO^+ + NO \quad \text{minor} \qquad (1.32c)$$

Michalcikova and Spanel [65] studied the reactions of NO^+ with various carboxylic acids. The reaction of NO^+ with carboxylic acids proceed via an association reaction or hydroxide ion transfer. The reaction rates of formic acid and acetic acid are significantly lower owing to the lack of exothermic bimolecular reaction channels and form only MNO^+. The higher carboxylic acids proceed via both mechanisms, an association reaction and hydroxide ion transfer, where the first path represents the major product.

$$HCOOH + NO^+ \longrightarrow NO^+COOH \qquad (1.33)$$

$$C_2H_5COOH + NO^+ \longrightarrow C_2H_5CO^+ + NO^+C_2H_5COOH \quad (88\%) \qquad (1.34)$$

$$C_3H_7COOH + NO^+ \longrightarrow C_3H_7CO^+ + NO^+C_3H_7COOH \quad (77\%) \qquad (1.35)$$

The reaction of NO^+ with 3-methyl-1-butyl acetate proceeds via adduct formation with small contributions from other channels.

$$NO^+ + CH_3C(=O)O(CH_2)_2CH(CH_3)CH_3 \rightarrow NO^+C_7H_{14}O_2 \qquad (1.36a)$$

$$NO^+ + CH_3C(=O)O(CH_2)_2CH(CH_3)CH_3 \rightarrow CH_3CO^+ + C_5H_{11}NO_2 \qquad (1.36b)$$

$$NO^+ + CH_3C(=O)O(CH_2)_2CH(CH_3)CH_3 \rightarrow C_7H_{13}O_2^+ + HNO \qquad (1.36c)$$

4-methyl-1,3-pentadiene reacts with NO^+ to produce the parent cation via a charge transfer process.

$$NO^+ + CH_2{=}CHCH{=}C(CH_3)_2 \longrightarrow C_6H_{10}^+ + NO \qquad (1.37)$$

Charge transfer in this instance occurs owing to the molecule's ionization energy (8.26 eV) being lower than that of NO.

The reaction of NO^+ with dimethyl trisulphide and dimethyl tetra sulphide via non-dissociative charge transfer produces only parent cations [44].

$$CH_3S_4CH_3 + NO^+ \longrightarrow CH_3S_4CH_3^+ + NO \qquad (1.38)$$

1.2.4 O_2^+ as the reagent in CIR-MS

The ionization energy of O_2 (12.06 eV) is higher than most VOCs. O_2^+ reacts with organic compounds via two processes: simple non-dissociative charge transfer to produce the molecular ion or via dissociative charge transfer reactions producing two or more fragment ions [40].

Spanel *et al*. [45], measured the rate coefficients of several aldehydes and ketones using O_2^+ as the reagent ion in SIFT. In contrast with other reagents, H_3O^+ and NO^+, the reaction of O_2^+ with aldehydes proceeds via charge transfer, which produces molecular ions and at least one other fragment. However, in some cases there is the possibility that hydride ion transfer can take place to produce $(M\text{-}H)^+$ and HO_2. As the number of carbons in the reactant increases, more complex product ions can be produced. The reaction of O_2^+ with smaller aldehydes is shown in this example:

$$O_2^+ + HCHO \longrightarrow CH_2O^+ + O_2 \qquad (1.39a)$$

$$O_2^+ + HCHO \longrightarrow HCO^+ + H + O_2 \qquad (1.39b)$$

O_2^+ reacts with propenal to produce three product ions, as shown in the following equations:

$$O_2^+ + CH_2{=}CHCHO \longrightarrow C_3H_4O^+ + O_2 \qquad (1.40a)$$

$$O_2^+ + CH_2{=}CHCHO \longrightarrow C_3H_3O^+ + H + O_2 \qquad (1.40b)$$

$$O_2^+ + CH_2{=}CHCHO \longrightarrow C_2H_4^+ + CO + O_2 \qquad (1.40c)$$

Aldehydes with greater atomicity react with O_2^+ to produce polyatomic fragment ions, carbon, hydrocarbon ions, and neutral molecules, as shown in this example:

$$O_2^+ + C_2H_5CH{=}CHCH_2CHO \longrightarrow C_2H_3O^+ + C_4H_7 + O_2 \qquad (1.41a)$$

$$O_2^+ + C_2H_5CH{=}CHCH_2CHO \longrightarrow C_5H_9^+ + HCO + O_2 \qquad (1.41b)$$

$$O_2^+ + C_2H_5CH{=}CHCH_2CHO \longrightarrow C_4H_6O^+ + C_2H_4 + O_2 \qquad (1.41c)$$

$$O_2^+ + C_2H_5CH{=}CHCH_2CHO \longrightarrow C_6H_{10}O^+ + O_2 \qquad (1.41d)$$

Ketones react with O_2^+ via charge transfer with dissociation. R_1COR_2 is representative of most of these ketones, where R_1 and R_2 represent alky groups such as CH_3 and C_2H_5. For example, in the 2-butanone reaction, parent ion production and elimination of alky radicals can be seen:

$$O_2^+ + CH_3COC_2H_5 \rightarrow C_4H_8O^+ + O_2 \quad (1.42a)$$

$$O_2^+ + CH_3COC_2H_5 \rightarrow C_2H_5CO^+ + CH_3 + O_2 \quad (1.42b)$$

$$O_2^+ + CH_3COC_2H_5 \rightarrow CH_3CO^+ + C_2H_5 + O_2 \quad (1.42c)$$

As the number of carbons increase in the reactant, more complex and additional processes such as C_2H_4 elimination can occur. The 3-pentanone reaction is an example of these processes:

$$O_2^+ + C_2H_5COC_2H_5 \rightarrow C_3H_6O^+ + C_2H_4 + O_2 \quad (1.43a)$$

$$O_2^+ + C_2H_5COC_2H_5 \rightarrow C_3H_4O^+ + C_2H_6 + O_2 \quad (1.43b)$$

$$O_2^+ + C_2H_5COC_2H_5 \rightarrow C_5H_{10}O^+ + O_2 \quad (1.43c)$$

O_2^+ reacts with 2,3-butanedione to produce dissociation of the molecular ion at the central carbon-carbon bond as the major product channel, the parent ion is still seen, albeit as a minor product [45]:

$$O_2^+ + CH_3COCOCH_3 \rightarrow CH_3CO^+ + CH_3CO + O_2 \quad (1.44a)$$

$$O_2^+ + CH_3COCOCH_3 \rightarrow C_4H_6O_2^+ + O_2 \quad (1.44b)$$

Spanel *et al*. [46], studied the reactions of several alcohols with O_2^+ as reagent in SIFT. In most cases, O_2^+ reacted with alcohols via charge transfer reactions, although in a few cases other mechanism could occur such as hydride ion transfer. Methanol and ethanol with O_2^+ produce the parent ion, as seen in the following equation:

$$O_2^+ + CH_3OH \rightarrow CH_3OH^+ + O_2 \quad (1.45a)$$

$$O_2^+ + CH_3OH \rightarrow CH_3O^+ + (H + O_2) \quad (1.45b)$$

O_2^+ reacts with 1-propanol and 2-propanol to produce different products, which in itself offers a means by which to distinguish between the two isomers. 1-Propanol produces CH_3O^+ as the main product and $C_3H_6^+$ as a minor product, 2-propanol reactions proceed via release of a terminal CH_3:

$$O_2^+ + CH_3CH_2CH_2OH \longrightarrow CH_3O^+ + C_2H_5 + O_2 \quad (1.46a)$$

$$O_2^+ + CH_3CH_2CH_2OH \longrightarrow C_3H_6^+ + H_2O + O_2 \quad (1.46b)$$

$$O_2^+ + CH_3CH(OH)CH_3 \longrightarrow CH_3CHOH^+ + (CH_3 + O_2) \quad (1.47)$$

The reaction of longer chain of alcohols such as $C_4H_9(OH)$ and $C_5H_{11}(OH)$ follow a charge transfer mechanism to produce the parent ion with a number of other fragment ions. In general, the reaction of the non-branched alcohols and most primary alcohols produces hydrocarbon ions, as shown in this example:

$$O_2^+ + C_5H_{11}OH \longrightarrow C_5H_{10}^+ + H_2O + O_2 \quad (1.48a)$$

$$O_2^+ + C_5H_{11}OH \longrightarrow C_3H_6^+ + C_2H_5OH + O_2 \quad (1.48b)$$

$$O_2^+ + C_5H_{11}OH \longrightarrow C_5H_{11}^+ + OH + O_2 \quad (1.48c)$$

$$O_2^+ + C_5H_{11}OH \longrightarrow C_4H_7^+ + (CH_3 + H_2O) + O_2 \quad (1.48d)$$

On the other hand, secondary alcohols such as 3-pentanol produce predominantly carboxyl ions rather than the parent ion, as shown in this example:

$$O_2^+ + CH_3CH_2CH(OH)CH_2CH_3 \longrightarrow C_3H_7O^+ + (C_2H_5 + O_2) \quad (1.49a)$$

$$O_2^+ + CH_3CH_2CH(OH)CH_2CH_3 \longrightarrow C_3H_6O^+ + (C_2H_6 + O_2) \quad (1.49b)$$

$$O_2^+ + CH_3CH_2CH(OH)CH_2CH_3 \longrightarrow C_4H_9O^+ + (CH_3 + O_2) \quad (1.49c)$$

The reactions of tertiary alcohols such as 2-methyl-2-propanol usually produce a single product ion, as shown in the following equation:

$$O_2^+ + (CH_3)_3COH \longrightarrow (CH_3)_2COH^+ + (CH_3 + O_2) \quad (1.50)$$

It is worth noting that 1-octanol produces hydrocarbon ions, whereas 2-octanol produces $C_2H_5O^+$ as their major products. Therefore, these reactions could be utilized so as to differentiate between these isomers.

Menthol and phenol reactions both proceed via charge transfer reactions, but whereas phenol produce its parent ion ($C_6H_5OH^+$), menthol produces several fragment ions, as shown in the following equation [46]:

$$O_2^+ + C_{10}H_{19}OH \longrightarrow C_6H_9^+, C_7H_{11}^+, C_7H_{12}^+, C_{10}H_{18}^+, C_4H_7O^+ \quad (1.51)$$

The reactions of O_2^+ with some phenols, phenyl alcohols and cyclic carbonyl compounds in SIFT were studied by Wang *et al* [47]. The reaction of O_2^+ with 2-hydroxyphenol, 2-, 3-, 4-methylphenol and 4-ethylphenol proceed via charge transfer which is non-

dissociative, resulting in molecular ions except for 4-ethylphenol which produces two fragments, as seen in the following equations:

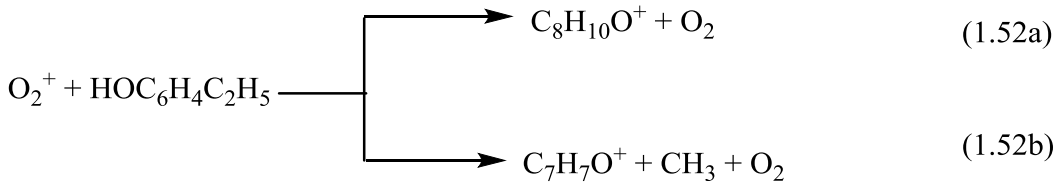

(1.52a)

(1.52b)

The relative simplicity of these reactions allows for the use of O_2^+ as a reagent in SIFT to detect these compounds.

O_2^+ reacts with 1-phenylmethanol, 1- and 2-phenylethanol to produce several fragments. The relative complexities of these products leave O_2^+ an unsuitable reagent for the detection of these compounds.

Again, O_2^+ reacts with 1,4-benzoquinone and cyclohexanone to result in multiple product ions, making O_2^+ an unfavourable precursor ion for the measurement of these compounds [47].

In another study, Spanel *et al*. [48], measured the reactions of several volatile carboxylic acids and esters using O_2^+ as reagent in SIFT. The reactions of carboxylic acids with O_2^+ are fast, but their mechanisms do not apparently follow the same trend as above. The formic acid reaction produced the parent ion via dissociative charge transfer, while the trimethylacetic acid reaction occurs by elimination of a COOH fragment from the molecular ion, these equations being represented by the mechanisms below:

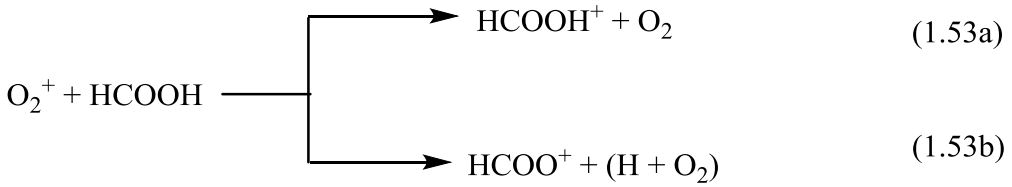

(1.53a)

(1.53b)

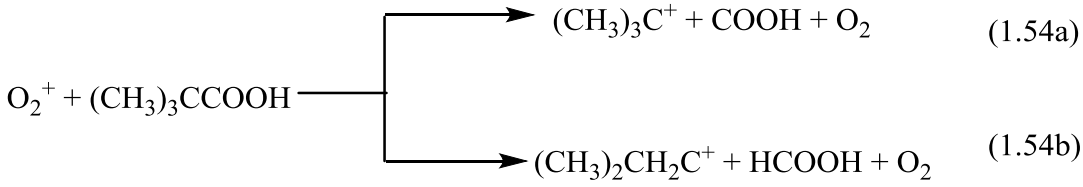

(1.54a)

(1.54b)

Spanel *et al*. [49], studied the reaction of peroxyacetic acid wit O_2^+ as reagent in SIFT. It is most probable that the reaction between O_2^+ and peroxyacetic acid proceeds via dissociative charge transfer as shown in the following equations [49].

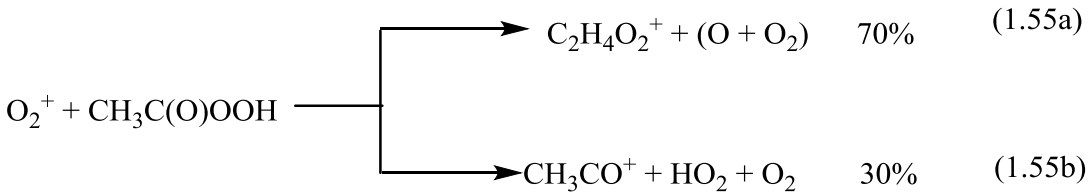

O_2^+ reacts with esters via charge transfer to produce a range of fragments. Most reactions occur by breaking the $R_1CO\text{-}OR_2$ bond in the compound, resulting in the carboxyl ion (R_1CO^+) as, for instance, in the methyl acetate reaction [48]:

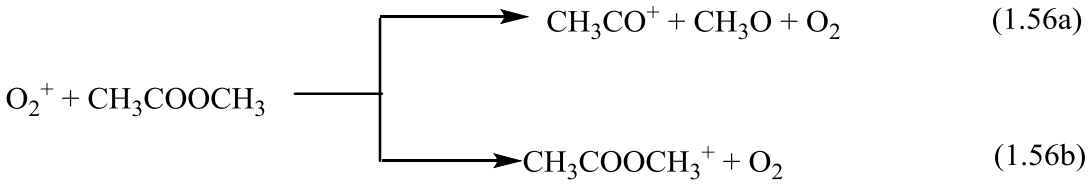

Norman *et al*. [66] used O_2^+ as a reagent in CIR-MS to detect gas phase ammonia. The reaction of O_2^+ with ammonia proceeded via charge transfer due to the ionization energy of ammonia (10.07 eV) being lower than the recombination energy of O_2^+, as can be seen in the following equation:

$$O_2^+ + NH_3 \longrightarrow NH_3^+ + O_2 \qquad (1.57)$$

The reaction of O_2^+ with several amines have been measured using O_2^+ as precursor in SIFT by Spanel *et al*. These reactions follow non-dissociative (parent ion production) or dissociative charge transfer mechanisms. Generally, primary amine reactions produce $CH_2NH_2^+$ as a result of cleaving the carbon bond at $R\text{-}CH_2NH_2^+$. In this reaction a C_2H_5 fragment was removed, as seen in the equation below:

$$O_2^+ + CH_3CH_2CH_2NH_2 \longrightarrow CH_2NH_2^+ + C_2H_5 + O_2 \qquad (1.58)$$

In the secondary and tertiary amine reaction, most likely the CH_3 radical was removed as seen in this equation [55]:

$$O_2^+ + (C_2H_5)_3N \longrightarrow (C_2H_5)_2CH_2N^+ + CH_3 + O_2 \qquad (1.59)$$

In another study, Wang *et al*. [56], studied the reaction of O_2^+ with several N- and O-containing heterocyclic compounds using SIFT. Generally, reaction of N-containing heterocyclic compounds with O_2^+ produce two or more product ions, with the exception of the pyrrole and indole reactions, which form the parent cations. A specific case was the reaction of nicotine with O_2^+ to produce the parent ion at a minor abundance and other fragments with greater abundances as seen in the following equations:

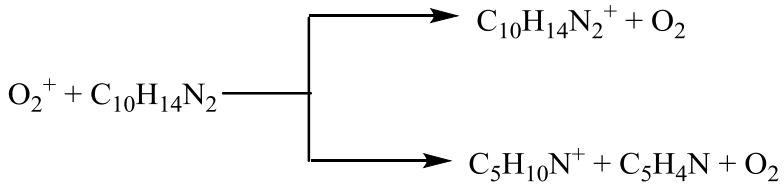

(1.60a)

(1.60b)

It seems that O_2^+ as a reagent in SIFT is not suitable for the detection of these heterocyclic compounds.

The reaction of O_2^+ with O-containing heterocyclic compounds generally produce two or more fragments, except the furan and 5-methyl-2-furancarboxaldehyde reactions which produced just the molecular ion [56].

Spanel *et al*. [50], studied the reaction of O_2^+ with some organosulphur compounds in SIFT. In most cases, the O_2^+ reaction with organosulphur compounds can be considered to be one of dissociative charge transfer:

$$O_2^+ + CH_3COSH \longrightarrow CH_3CO^+ + SH + O_2 \qquad (1.61)$$

Sulphide and diallyl disulfide produced multiple products and 1,3-dithiane reaction forming $C_3H_6S^+ + CH_2S$.

A few cases such as the CS_2 reaction follow non-dissociative charge transfer processes, producing only the parent ion [50]:

$$O_2^+ + CS_2 \longrightarrow CS_2^+ + O_2 \qquad (1.62)$$

Small hydrocarbons' reactions with O_2^+ have been investigated by Wilson *et al.* using SIFT. Methane was found to react with O_2^+ to produce two channels, as shown in the following equations:

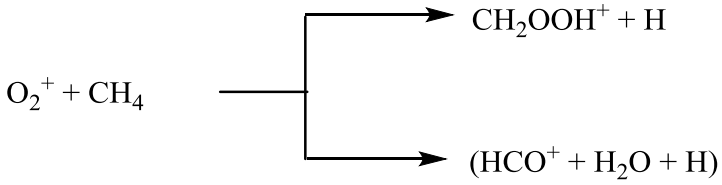

(1.63a)

(1.63b)

Large alkanes' reactions are rapid and proceed via charge transfer and dissociative charge transfer mechanism as their main routes. Ethane produces parent ions, whilst other large alkanes produce a greater number of fragments; for example:

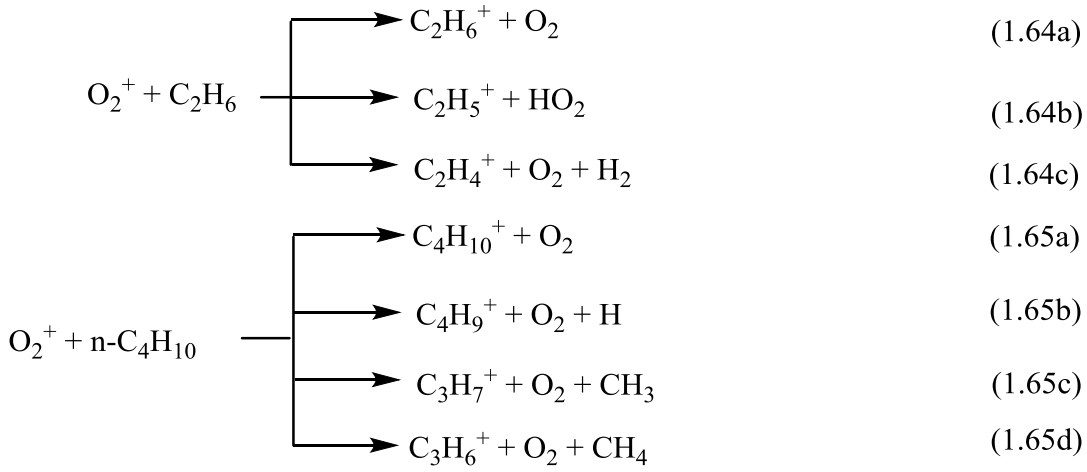

The reactions of alkenes with O_2^+ are fast, with ethene and propene exhibiting non-dissociative charge transfer reactions. However, higher alkenes, such as 2-butene, react via dissociative charge transfer reactions; for example:

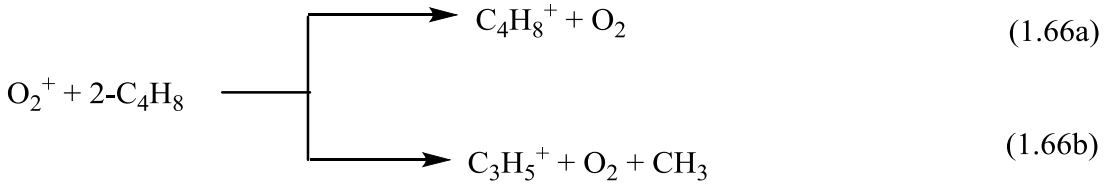

The reactions of alkynes with O_2^+ are proceeding via non-dissociative charge transfer reactions [52].

The aromatic hydrocarbons follow a charge transfer mechanism. Benzene and toluene reactions produce only the parent ion, while xylene isomers and trimethylbenzene isomers produce the molecular ion with other products produced by ejecting a CH_3 fragment, as shown in the following equation [51]:

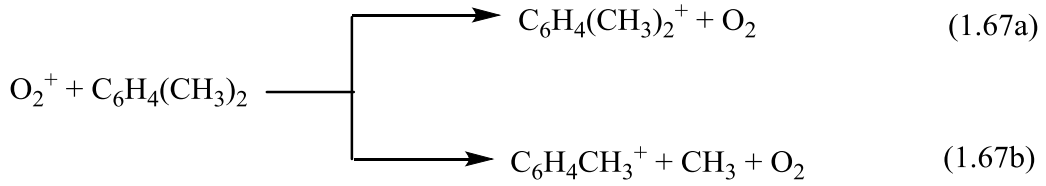

Ethyl benzene and propylbenzene produce dissociative products, for instance:

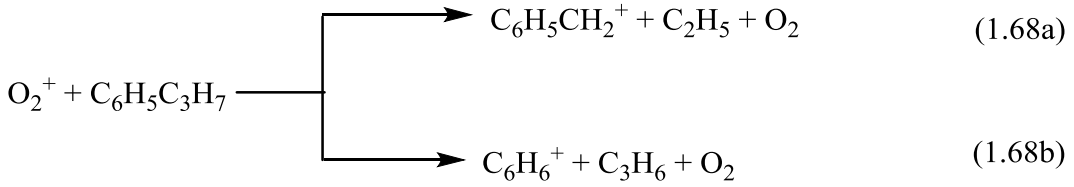

The reaction of ethers with O_2^+ have been studied using SIFT by Spanel *et al*. Most of these reactions follow a charge transfer process and produce the parent ion as seen in the following equation:

$$O_2^+ + C_6H_5OCH_3 \longrightarrow C_7H_8O^+ + O_2 \quad (1.69)$$

Other types of reaction proceed via dissociative charge transfer processes producing further fragmentation. In these cases, it is not simple to identify these products, for example [53]:

$$O_2^+ + C_4H_9OCH_3 \longrightarrow (C_2H_5O^+ + C_3H_7) \text{ or } (C_3H_9^+ + C_2H_3O) + O_2 \quad (1.70a)$$

$$O_2^+ + C_4H_9OCH_3 \longrightarrow (C_4H_8^+ + CH_3OH) \text{ or } (C_3H_4O^+ + C_2H_8) + O_2 \quad (1.70b)$$

Wang *et al*. [54], studied the reaction of O_2^+ with several monoterpenes (C_6H_{10}) using SIFT. Owing to the relatively large recombination energy of O_2^+, the major products for these reactions are multiple product ions rather than the parent ion cations, $C_{10}H_{16}^+$. As a consequence, O_2^+ is not a suitable reagent to investigate monoterpenes reactions in SIFT.

1.2.5 CF_3^+/CF_2H^+ as a reagent in CIR-MS

CF_3^+ can be generated from pure CF_4 in Fourier-transform ion cyclotron resonance mass spectrometry (FT-ICR). CF_3^+ is electrophilic and a Lewis acid, reacting with nucleophilic precursors to allow the formation of most carbenium ions in the gas phase. CF_3^+ has the ability to react with the n-centre of several carbonyl compounds, causing cleavage of their C-O bond due to migration of fluorine atom. CF_3^+ does not react with the CF_4 molecule and H_2O when run at 2 x 10^{-7} Torr in the FT-ICR, even though the reaction is exothermic (CF_3^+ addition/ HF elimination reaction). Methanol can react in these conditions, resulting in the fragments seen in Figure 1.3 [67].

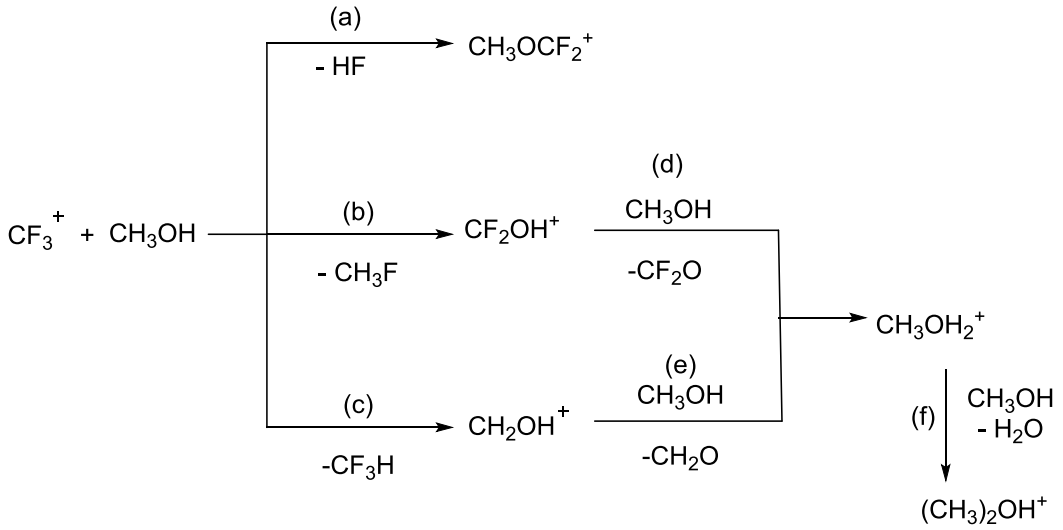

Figure 1. 3: Reaction of CF_3^+ with CH_3OH; adapted from Grandinetti *et al* [67].

The reactions of benzene, ethylbenzene, ethynylbenzene, toluene and styrene with CF_3^+ have been studied using an ion-beam apparatus [68]. The reaction of benzene proceeds via electrophilic addition followed by HF elimination and hydride transfer:

$$CF_3^+ + C_6H_6 \rightarrow C_6H_5CF_2^+ + HF \quad (93.4\%) \qquad (1.71a)$$

$$CF_3^+ + C_6H_6 \rightarrow C_6H_5^+ + CF_3H \quad (6.6\%) \qquad (1.71b)$$

Toluene's reactions were similar to those of benzene with an extra fragment produced by charge transfer:

$$CF_3^+ + C_6H_5CH_3 \rightarrow C_6H_5CH_2CF_2^+ + HF \quad (84.3\%) \qquad (1.72a)$$

$$CF_3^+ + C_6H_5CH_3 \rightarrow C_6H_5CH_3^+ + CF_3 \quad (7.9\%) \qquad (1.72b)$$

$$CF_3^+ + C_6H_5CH_3 \rightarrow C_6H_5CH_2^+ + CF_3H \quad (7.8\%) \qquad (1.72c)$$

Ethylbenzene reacts to form three fragments. All channels proceed via electrophilic addition followed by molecular elimination:

$$CF_3^+ + C_6H_5C_2H_5 \rightarrow C_6H_6CF_3^+ + C_2H_4 \quad (29.4\%) \qquad (1.73a)$$

$$CF_3^+ + C_6H_5C_2H_5 \rightarrow C_6H_5CF_2^+ + C_2H_4 + HF \quad (49.4\%) \qquad (1.73b)$$

$$CF_3^+ + C_6H_5C_2H_5 \rightarrow C_2H_5^+ + C_6H_5CF_3 \quad (21.1\%) \qquad (1.73c)$$

Styrene with CF_3^+ produced four products and electrophilic addition can occur at the unsaturated substituent bond and in the aromatic ring:

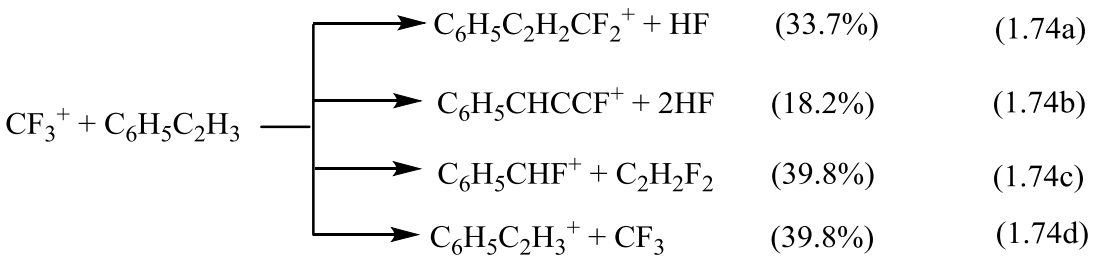

Ethynylbenzene with CF_3^+ produced three products. The most notable product is the detection of a small amount of the $C_9H_6F_3^+$ ion [68].

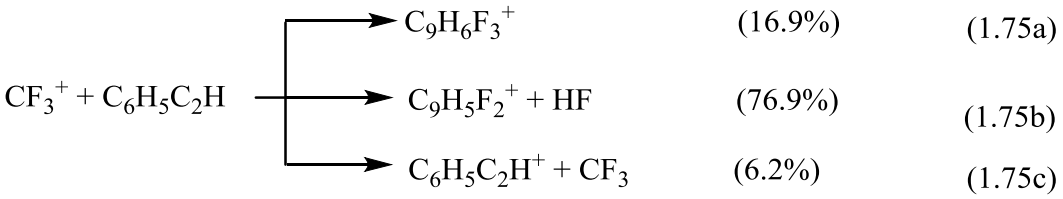

Dehon *et al.* [69], studied the reaction of CF_3^+ with small alkanes using a compact FT-ICR mass spectrometer. CF_3^+ reacted with water vapour at a pressure of 10^{-4} Torr with a slow rate, resulting in a very minor fragment at 67 amu belong to CF_2OH^+ followed by a proton transfer reaction:

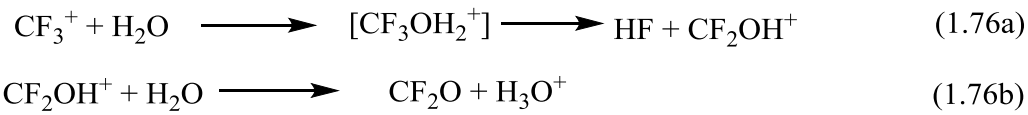

With the exception of methane, CF_3^+ reacts with all the alkanes. For C_2-C_4 alkanes and cyclohexane, the reaction can proceed via this formula:

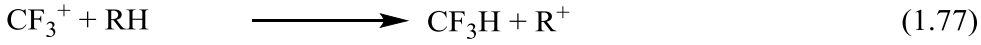

Pentane experiences complete fragmentation to produce the $C_3H_7^+$ ion whilst losing an ethene molecule:

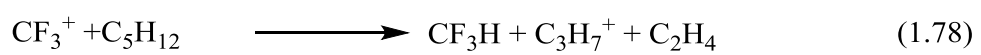

Higher alkanes also produced fragments that ranged from C_2-C_6 ions. Usually, fragmentation resulted in ions with fewer than four carbon atoms or ethene elimination. In some cases, the molecular ions of some alkanes were detected by hydride elimination [69].

Lias *et al*. [70], studied the reaction of CF_4 with alkanes and cycloalkanes using low energy electrons in a pulsed ion cyclotron resonance spectrometer at a pressure of 10^{-7}-10^{-5} Torr. The predominant products were produced by a hydride transfer reaction [70]:

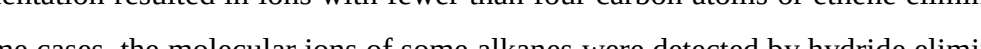

CF_3^+ reacts with acetylene using ion-beam apparatus to produce electrophilic addition to a C≡C bond [68]:

$$CF_3^+ + C_2H_2 \longrightarrow C_2H_2CF_3^+ \quad (100\%) \qquad (1.80)$$

The reaction of C_2H_4 with CF_3^+ produces four products:

$$CF_3^+ + C_2H_4 \longrightarrow \begin{cases} C_3H_3F_2^+ + HF & (62\%) \quad (1.81a) \\ C_2H_3^+ + CF_3H & (29\%) \quad (1.81b) \\ CHF_2^+ + C_2H_3F & (7\%) \quad (1.81c) \\ CH_2F^+ + C_2H_2F_2 & (2\%) \quad (1.81d) \end{cases}$$

Channel (1.81a), (1.81c), and (1.81d) proceed via electrophilic addition followed by molecular elimination, whilst channel (1.81b) occurs by hydride transfer.

Eyler *et al.* [71], studied the reaction of CF_3^+ with the carbonyl bond in ketones and aldehydes using a pulsed ICR mass spectrometer. CF_3^+ reacts with acetone and acetaldehyde to produce $C_3H_6F^+$ and $C_2H_4F^+$, respectively, as the major product ions:

$$CF_3^+ + CH_3COCH_3 \longrightarrow CH_3CF^+CH_3 + CF_2O \qquad (1.82)$$

$$CF_3^+ + CH_3CHO \longrightarrow CH_3CHF^+ + CF_2O \qquad (1.83)$$

CF_3^+ reacts with larger ketones, though the product seen in reaction (1.82) is not detected. Instead, the main product ions are usually produced by elimination of HF from the monofluorinated ions.

$$CF_3^+ + C_2H_5COCH_3 \longrightarrow CF_2O + (C_4H_8F^+)^* \longrightarrow CF_2O + HF + C_4H_7^+ \qquad (1.84)$$

$$CF_3^+ + (CH_3)_2CHCOCH_3 \longrightarrow CF_2O + (C_5H_{10}F^+)^* \longrightarrow CF_2O + HF + C_5H_9^+ \qquad (1.85)$$

Some ketones and aldehydes reacted with CF_3^+ to produce fragments ions rather than molecular ions owing to carbonyl compounds containing a weak bond [71]:

$$CF_3^+ + n\text{-}C_4H_9COCH_3 \longrightarrow CF_2O + HF + C_2H_4 + C_4H_7^+ \qquad (1.86)$$

$$CF_3^+ + (CH_3)_2CHCHO \longrightarrow C_3H_7^+ + (CF_3CHO) \qquad (1.87)$$

The mechanism of reaction of CF_3^+ with carbonyl groups such as acetone may proceed via the fluoronium metathesis reaction, as can be seen in Figure 1.4:

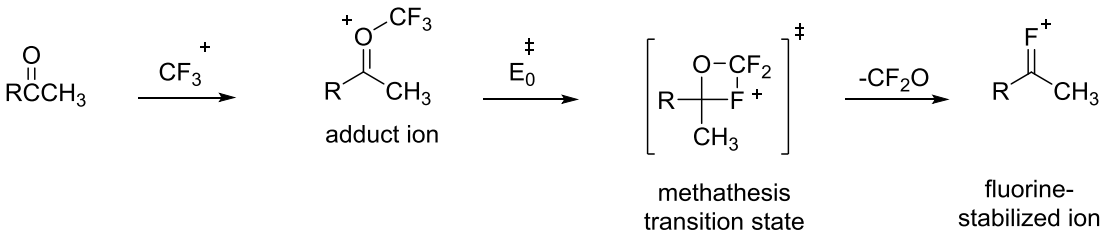

Figure 1. 4**:** Reaction of CF_3^+ with carbonyl groups; adapted from Oomens *et al* [72].

The reaction of CF_3^+ with esters, carboxylic acids and acetic anhydride proceeds via displacement involving a split of the acyl-oxygen bond to produce the acylium ion [73]:

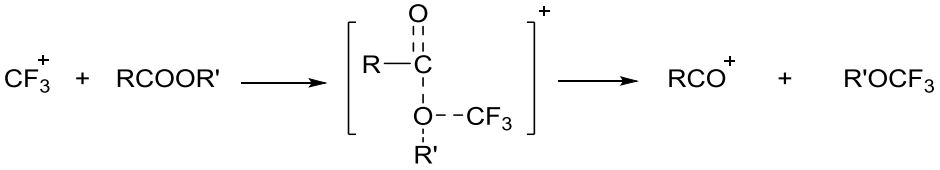

Figure 1. 5**:** Reaction of CF_3^+ with esters and carboxylic acids; adapted from de Gouw *et al* [73].

The reaction of formic acid with CF_3^+ produce different fragments compared with the previous reaction. The intermediate state (four-centre reaction) in this reaction is more exothermic, as a result cleave occur at different position as can be seen in Figure 1.6, [73].

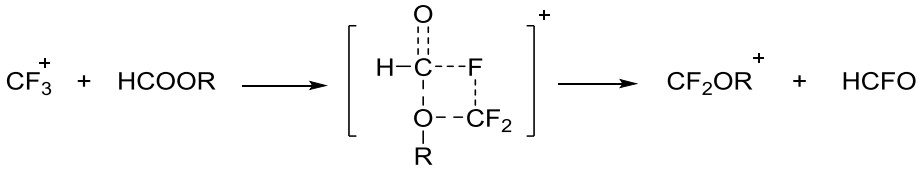

Figure 1. 6: Reaction of CF_3^+ with formic acid; adapted from de Gouw *et al* [73]**.**

From this review, it appears that CF_3^+ is the soft chemical ionization reagent of choice in pulsed ion cyclotron resonance spectrometry for the detection of compounds such as small chain of alkanes. These are difficult to detect with other reagents so CF_3^+ will be used in CIR-TOF-MS for the detection VOCs.

1.3 Study objectives

The objective of this thesis was to explore the utility of the novel reagent CF_3^+ in the real-time mass spectrometric technique CIR-TOF-MS to detect small chain alkanes (C_2-C_6) and other types of VOCs in breath and urine samples of smokers and non-smokers. To achieve this, standards of alkanes (C_2-C_6) were measured using CF_3^+ as the reagent in CIR-MS. In addition, VOCs which represented the main groups in organic compounds,

were chosen in accordance with the possibility of their existence in exhaled breath and human urine samples and were measured using the reagent ion CF_3^+.
Furthermore, samples of breath and urine were collected from smokers and non-smokers and measured using CF_3^+ as a reagent in CIR-MS. The results of alkanes and other types of VOCs were used to help interpret the data from breath and urine samples of smokers and non-smokers and draw conclusions on the efficacy as reagent in breath analysis.

1.4 Summary

This chapter has discussed at length the behaviour of several precursors in CIR-MS. Most of them have been used extensively in the past so that the literature is well supplied with their behaviour. The chapter has discussed some of the principles of the reactions of H_3O^+, NH_4^+, NO^+ and O_2^+ with a variety of VOCs and gave examples. Some of the applications of these precursors were also reviewed in this chapter.

The aim of this thesis is to explore CF_3^+/CF_2H^+ as a novel precursor in chemical ionization mass spectrometry able to detect VOCs which have so far proved difficult or impossible to detect.

1.5 References

[1] R.S. Blake, P.S. Monks, A.M. Ellis, Proton-transfer reaction mass spectrometry, Chemical reviews, 109 (2009) 861-896.

[2] A.M. Ellis, C.A. Mayhew, Proton transfer reaction mass spectrometry: principles and applications, John Wiley & Sons, 2013.

[3] W. Lindinger, A. Hansel, A. Jordan, On-line monitoring of volatile organic compounds at pptv levels by means of proton-transfer-reaction mass spectrometry (PTR-MS) medical applications, food control and environmental research, International journal of mass spectrometry and ion processes, 173 (1998) 191-241.

[4] A. Hansel, A. Jordan, C. Warneke, R. Holzinger, W. Lindinger, Improved detection limit of the proton-transfer reaction mass spectrometer: On-line monitoring of volatile organic compounds at mixing ratios of a few pptv, Rapid communications in mass spectrometry, 12 (1998) 871-875.

[5] P. Crutzen, J. Williams, U. Pöschl, P. Hoor, H. Fischer, C. Warneke, R. Holzinger, A. Hansel, W. Lindinger, B. Scheeren, High spatial and temporal resolution measurements of primary organics and their oxidation products over the tropical forests of Surinam, Atmospheric Environment, 34 (2000) 1161-1165.

[6] J. Williams, U. Pöschl, P. Crutzen, A. Hansel, R. Holzinger, C. Warneke, W. Lindinger, J. Lelieveld, An atmospheric chemistry interpretation of mass scans obtained from a proton transfer mass spectrometer flown over the tropical rainforest of Surinam, Journal of Atmospheric Chemistry, 38 (2001) 133-166.

[7] C. Warneke, R. Holzinger, A. Hansel, A. Jordan, W. Lindinger, U. Pöschl, J. Williams, P. Hoor, H. Fischer, P. Crutzen, Isoprene and its oxidation products methyl vinyl ketone, methacrolein, and isoprene related peroxides measured online over the tropical rain forest of Surinam in March 1998, Journal of Atmospheric Chemistry, 38 (2001) 167-185.

[8] J. De Gouw, A. Middlebrook, C. Warneke, R. Ahmadov, E. Atlas, R. Bahreini, D. Blake, C. Brock, J. Brioude, D. Fahey, Organic aerosol formation downwind from the Deepwater Horizon oil spill, Science, 331 (2011) 1295-1299.

[9] J. De Gouw, P. Goldan, C. Warneke, W. Kuster, J. Roberts, M. Marchewka, S. Bertman, A. Pszenny, W. Keene, Validation of proton transfer reaction-mass spectrometry (PTR-MS) measurements of gas-phase organic compounds in the atmosphere during the New

England Air Quality Study (NEAQS) in 2002, Journal of Geophysical Research: Atmospheres, 108 (2003).

[10] P. Prazeller, P.T. Palmer, E. Boscaini, T. Jobson, M. Alexander, Proton transfer reaction ion trap mass spectrometer, Rapid communications in mass spectrometry, 17 (2003) 1593-1599.

[11] C. Warneke, C. Van der Veen, S. Luxembourg, J. de Gouw, A. Kok, Measurements of benzene and toluene in ambient air using proton-transfer-reaction mass spectrometry: calibration, humidity dependence, and field intercomparison, International Journal of Mass Spectrometry, 207 (2001) 167-182.

[12] S. Kato, Y. Miyakawa, T. Kaneko, Y. Kajii, Urban air measurements using PTR-MS in Tokyo area and comparison with GC-FID measurements, International Journal of Mass Spectrometry, 235 (2004) 103-110.

[13] M. Steinbacher, J. Dommen, C. Ammann, C. Spirig, A. Neftel, A. Prevot, Performance characteristics of a proton-transfer-reaction mass spectrometer (PTR-MS) derived from laboratory and field measurements, International Journal of Mass Spectrometry, 239 (2004) 117-128.

[14] J. de Gouw, C. Warneke, R. Holzinger, T. Klüpfel, J. Williams, Inter-comparison between airborne measurements of methanol, acetonitrile and acetone using two differently configured PTR-MS instruments, International Journal of Mass Spectrometry, 239 (2004) 129-137.

[15] C. Ammann, C. Spirig, A. Neftel, M. Steinbacher, M. Komenda, A. Schaub, Application of PTR-MS for measurements of biogenic VOC in a deciduous forest, International Journal of Mass Spectrometry, 239 (2004) 87-101.

[16] W. Kuster, B. Jobson, T. Karl, D. Riemer, E. Apel, P. Goldan, F.C. Fehsenfeld, Intercomparison of volatile organic carbon measurement techniques and data at la porte during the TexAQS2000 Air Quality Study, Environmental science & technology, 38 (2004) 221-228.

[17] A. Lee, G. Schade, R. Holzinger, A. Goldstein, A comparison of new measurements of total monoterpene flux with improved measurements of speciated monoterpene flux, Atmospheric Chemistry and Physics, 5 (2005) 505-513.

[18] S. Inomata, H. Tanimoto, S. Kameyama, U. Tsunogai, H. Irie, Y. Kanaya, Z. Wang, Technical Note: Determination of formaldehyde mixing ratios in polluted air with PTR-

MS: laboratory experiments and field measurements, Atmospheric Chemistry and Physics Discussions, 7 (2007) 12845-12876.

[19] C. Warneke, S. Kato, J.A. de Gouw, P.D. Goldan, W.C. Kuster, M. Shao, E.R. Lovejoy, R. Fall, F.C. Fehsenfeld, Online Volatile Organic Compound Measurements Using a Newly Developed Proton-Transfer Ion-Trap Mass Spectrometry Instrument during New England Air Quality Study Intercontinental Transport and Chemical Transformation 2004: Performance, Intercomparison, and Compound Identification, Environmental science & technology, 39 (2005) 5390-5397.

[20] J.A. de Gouw, C. Warneke, A. Stohl, A. Wollny, C. Brock, O. Cooper, J. Holloway, M. Trainer, F. Fehsenfeld, E. Atlas, Volatile organic compounds composition of merged and aged forest fire plumes from Alaska and western Canada, Journal of Geophysical Research: Atmospheres, 111 (2006).

[21] T. Karl, T. Jobson, W.C. Kuster, E. Williams, J. Stutz, R. Shetter, S.R. Hall, P. Goldan, F. Fehsenfeld, W. Lindinger, Use of proton-transfer-reaction mass spectrometry to characterize volatile organic compound sources at the La Porte super site during the Texas Air Quality Study 2000, Journal of Geophysical Research: Atmospheres, 108 (2003).

[22] D. Sprung, C. Jost, T. Reiner, A. Hansel, A. Wisthaler, Acetone and acetonitrile in the tropical Indian Ocean boundary layer and free troposphere: Aircraft-based intercomparison of AP-CIMS and PTR-MS measurements, Journal of Geophysical Research: Atmospheres, 106 (2001) 28511-28527.

[23] C. Warneke, J.A. de Gouw, W.C. Kuster, P.D. Goldan, R. Fall, Validation of atmospheric VOC measurements by proton-transfer-reaction mass spectrometry using a gas-chromatographic preseparation method, Environmental science & technology, 37 (2003) 2494-2501.

[24] J. Rinne, T.M. Ruuskanen, A. Reissell, R. Taipale, H. Hakola, M. Kulmala, On-line PTR-MS measurements of atmospheric concentrations of volatile organic compounds in a European boreal forest ecosystem, Boreal environment research, 10 (2005) 425-436.

[25] L. Molina, C. Kolb, B.d. Foy, B. Lamb, W. Brune, J. Jimenez, R. Ramos-Villegas, J. Sarmiento, V. Paramo-Figueroa, B. Cardenas, Air quality in North America's most populous city–overview of the MCMA-2003 campaign, Atmospheric Chemistry and Physics, 7 (2007) 2447-2473.

[26] T. Rogers, E. Grimsrud, S. Herndon, J. Jayne, C.E. Kolb, E. Allwine, H. Westberg, B. Lamb, M. Zavala, L. Molina, On-road measurements of volatile organic compounds in the Mexico City metropolitan area using proton transfer reaction mass spectrometry, International Journal of Mass Spectrometry, 252 (2006) 26-37.

[27] R. Holzinger, B. Kleiss, L. Donoso, E. Sanhueza, Aromatic hydrocarbons at urban, sub-urban, rural (8° 52′ N; 67° 19′ W) and remote sites in Venezuela, Atmospheric Environment, 35 (2001) 4917-4927.

[28] I. Filella, J. Penuelas, Daily, weekly, and seasonal time courses of VOC concentrations in a semi-urban area near Barcelona, Atmospheric Environment, 40 (2006) 7752-7769.

[29] B. Langford, E. Nemitz, E. House, G. Phillips, D. Famulari, B. Davison, J. Hopkins, A. Lewis, C.N. Hewitt, Fluxes and concentrations of volatile organic compounds above central London, UK, Atmospheric Chemistry and Physics, 10 (2010) 627-645.

[30] B. Langford, B. Davison, E. Nemitz, C. Hewitt, Mixing ratios and eddy covariance flux measurements of volatile organic compounds from an urban canopy (Manchester, UK), Atmospheric Chemistry and Physics, 9 (2009) 1971-1987.

[31] J.M. Lobert, D.H. Scharffe, W.M. Hao, P.J. Crutzen, Importance of biomass burning in the atmospheric budgets of nitrogen-containing gases, Nature, 346 (1990) 552-554.

[32] S. Akagi, R.J. Yokelson, C. Wiedinmyer, M. Alvarado, J. Reid, T. Karl, J. Crounse, P. Wennberg, Emission factors for open and domestic biomass burning for use in atmospheric models, Atmospheric Chemistry and Physics, 11 (2011) 4039-4072.

[33] R. Holzinger, J. Williams, G. Salisbury, T. Klüpfel, M.d. Reus, M. Traub, P. Crutzen, J. Lelieveld, Oxygenated compounds in aged biomass burning plumes over the Eastern Mediterranean: evidence for strong secondary production of methanol and acetone, Atmospheric Chemistry and Physics, 5 (2005) 39-46.

[34] G. Salisbury, J. Williams, R. Holzinger, V. Gros, N. Mihalopoulos, M. Vrekoussis, R. Sarda-Esteve, H. Berresheim, R.v. Kuhlmann, M. Lawrence, Ground-based PTR-MS measurements of reactive organic compounds during the MINOS campaign in Crete, July–August 2001, Atmospheric Chemistry and Physics, 3 (2003) 925-940.

[35] J. De Gouw, C. Warneke, D. Parrish, J. Holloway, M. Trainer, F. Fehsenfeld, Emission sources and ocean uptake of acetonitrile (CH3CN) in the atmosphere, Journal of Geophysical Research: Atmospheres, 108 (2003).

[36] T. Karl, A. Hansel, T. Märk, W. Lindinger, D. Hoffmann, Trace gas monitoring at the Mauna Loa Baseline observatory using proton-transfer reaction mass spectrometry, International Journal of Mass Spectrometry, 223 (2003) 527-538.

[37] A. Wisthaler, A. Hansel, R.R. Dickerson, P.J. Crutzen, Organic trace gas measurements by PTR-MS during INDOEX 1999, Journal of Geophysical Research: Atmospheres, 107 (2002).

[38] J. De Gouw, O. Cooper, C. Warneke, P. Hudson, F. Fehsenfeld, J. Holloway, G. Hübler, D. Nicks Jr, J. Nowak, D. Parrish, Chemical composition of air masses transported from Asia to the US West Coast during ITCT 2K2: Fossil fuel combustion versus biomass-burning signatures, Journal of Geophysical Research: Atmospheres, 109 (2004).

[39] T.J. Duck, B.J. Firanski, D.B. Millet, A.H. Goldstein, J. Allan, R. Holzinger, D.R. Worsnop, A.B. White, A. Stohl, C.S. Dickinson, Transport of forest fire emissions from Alaska and the Yukon Territory to Nova Scotia during summer 2004, Journal of Geophysical Research: Atmospheres, 112 (2007).

[40] A. Lagg, J. Taucher, A. Hansel, W. Lindinger, Applications of proton transfer reactions to gas analysis, International journal of mass spectrometry and ion processes, 134 (1994) 55-66.

[41] A. Jordan, A. Hansel, R. Holzinger, W. Lindinger, Acetonitrile and benzene in the breath of smokers and non-smokers investigated by proton transfer reaction mass spectrometry (PTR-MS), International journal of mass spectrometry and ion processes, 148 (1995) L1-L3.

[42] C. Warneke, J. Kuczynski, A. Hansel, A. Jordan, W. Vogel, W. Lindinger, Proton transfer reaction mass spectrometry (PTR-MS): propanol in human breath, International journal of mass spectrometry and ion processes, 154 (1996) 61-70.

[43] E. Crespo, H. de Ronde, S. Kuijper, A. Pol, A.H. Kolk, S.M. Cristescu, R.M. Anthony, F.J. Harren, Potential biomarkers for identification of mycobacterial cultures by proton transfer reaction mass spectrometry analysis, Rapid communications in mass spectrometry : RCM, 26 (2012) 679-685.

[44] T. Wang, D. Smith, P. Španěl, Selected ion flow tube, SIFT, studies of the reactions of H_3O^+, NO^+ and O_2^+ with compounds released by Pseudomonas and related bacteria, International Journal of Mass Spectrometry, 233 (2004) 245-251.

[45] P. Španěl, Y. Ji, D. Smith, SIFT studies of the reactions of H_3O^+, NO^+ and O_2^+ with a series of aldehydes and ketones, International journal of mass spectrometry and ion processes, 165 (1997) 25-37.

[46] P. Spanel, D. Smith, SIFT studies of the reactions of H_3O^+, NO^+ and O_2^+ with a series of alcohols, International journal of mass spectrometry and ion processes, 167 (1997) 375-388.

[47] T. Wang, P. Španěl, D. Smith, A selected ion flow tube study of the reactions of H_3O^+, NO^+ and O_2^+ with some phenols, phenyl alcohols and cyclic carbonyl compounds in support of SIFT-MS and PTR-MS, International Journal of Mass Spectrometry, 239 (2004) 139-146.

[48] P. Ŝpaněl, D. Smith, SIFT studies of the reactions of H_3O^+, NO^+ and O_2^+ with a series of volatile carboxylic acids and esters, International journal of mass spectrometry and ion processes, 172 (1998) 137-147.

[49] P. Španěl, A.M. Diskin, T. Wang, D. Smith, A SIFT study of the reactions of H_3O^+, NO^+ and O_2^+ with hydrogen peroxide and peroxyacetic acid, International Journal of Mass Spectrometry, 228 (2003) 269-283.

[50] P. Španěl, D. Smith, Selected ion flow tube studies of the reactions of H_3O^+, NO^+, and O_2^+ with some organosulphur molecules, International Journal of Mass Spectrometry, 176 (1998) 167-176.

[51] P. Španěl, D. Smith, Selected ion flow tube studies of the reactions of H_3O^+, NO^+, and O_2^+ with several aromatic and aliphatic hydrocarbons, International Journal of Mass Spectrometry, 181 (1998) 1-10.

[52] P.F. Wilson, C.G. Freeman, M.J. McEwan, Reactions of small hydrocarbons with H_3O^+, O_2^+ and NO^+ ions, International Journal of Mass Spectrometry, 229 (2003) 143-149.

[53] P. Španěl, D. Smith, SIFT studies of the reactions of H_3O^+, NO^+ and O_2^+ with several ethers, International journal of mass spectrometry and ion processes, 172 (1998) 239-247.

[54] T. Wang, P. Španěl, D. Smith, Selected ion flow tube, SIFT, studies of the reactions of H_3O^+, NO^+ and O_2^+ with eleven $C_{10}H_{16}$ monoterpenes, International Journal of Mass Spectrometry, 228 (2003) 117-126.

[55] P. Španěl, D. Smith, Selected ion flow tube studies of the reactions of H_3O^+, NO^+, and O_2^+ with several amines and some other nitrogen-containing molecules, International Journal of Mass Spectrometry, 176 (1998) 203-211.

[56] T. Wang, P. Španěl, D. Smith, A selected ion flow tube, SIFT, study of the reactions of H_3O^+, NO^+ and O_2^+ ions with several N- and O-containing heterocyclic compounds in support of SIFT-MS, International Journal of Mass Spectrometry, 237 (2004) 167-174.

[57] R.S. Blake, M. Patel, P.S. Monks, A.M. Ellis, S. Inomata, H. Tanimoto, Aldehyde and ketone discrimination and quantification using two-stage proton transfer reaction mass spectrometry, International Journal of Mass Spectrometry, 278 (2008) 15-19.

[58] R.S. Blake, K.P. Wyche, A.M. Ellis, P.S. Monks, Chemical ionization reaction time-of-flight mass spectrometry: Multi-reagent analysis for determination of trace gas composition, International Journal of Mass Spectrometry, 254 (2006) 85-93.

[59] D. Smith, P. Spanel, Selected ion flow tube mass spectrometry (SIFT-MS) for on-line trace gas analysis, Mass Spectrom Rev, 24 (2005) 661-700.

[60] P. Mochalski, K. Unterkofler, P. Spanel, D. Smith, A. Amann, Product ion distributions for the reactions of NO^+ with some physiologically significant aldehydes obtained using a SRI-TOF-MS instrument, Int J Mass Spectrom, 363 (2014) 23-31.

[61] K.P. Wyche, R.S. Blake, K.A. Willis, P.S. Monks, A.M. Ellis, Differentiation of isobaric compounds using chemical ionization reaction mass spectrometry, Rapid communications in mass spectrometry : RCM, 19 (2005) 3356-3362.

[62] D. Smith, K. Sovová, P. Španěl, A selected ion flow tube study of the reactions of H_3O^+, NO^+ and O_2^+ with seven isomers of hexanol in support of SIFT-MS, International Journal of Mass Spectrometry, 319-320 (2012) 25-30.

[63] S. Inomata, H. Tanimoto, H. Yamada, Mass Spectrometric Detection of Alkanes Using NO^+ Chemical Ionization in Proton-transfer-reaction Plus Switchable Reagent Ion Mass Spectrometry, Chemistry Letters, 43 (2014) 538-540.

[64] W.B. Knighton, E.C. Fortner, S.C. Herndon, E.C. Wood, R.C. Miake-Lye, Adaptation of a proton transfer reaction mass spectrometer instrument to employ NO^+ as reagent ion for the detection of 1,3-butadiene in the ambient atmosphere, Rapid communications in mass spectrometry : RCM, 23 (2009) 3301-3308.

[65] R. Brůhová Michalčíková, P. Španěl, A selected ion flow tube study of the ion molecule association reactions of protonated (MH^+), nitrosonated (MNO^+) and

dehydroxidated $(M-OH)^+$ carboxylic acids (M) with H_2O, International Journal of Mass Spectrometry, 368 (2014) 15-22.

[66] M. Norman, A. Hansel, A. Wisthaler, O_2^+ as reagent ion in the PTR-MS instrument: Detection of gas-phase ammonia, International Journal of Mass Spectrometry, 265 (2007) 382-387.

[67] F. Grandinetti, G. Occhiucci, M.E. Crestoni, S. Fornarini, M. Speranza, Ionic Lewis superacids in the gas phase. Part 2. Reactions of gaseous CF_3^+ with oxygen bases, International journal of mass spectrometry and ion processes, 127 (1993) 123-135.

[68] M. Tsuji, M. Aizawa, Y. Nishimura, Mass-Spectrometric Study on Ion–Molecule Reactions of CF_3^+ with PhX [X= H, CH_3, and C_2H_n (n= 1, 3, 5)] at Near-Thermal Energy, Bulletin of the Chemical Society of Japan, 68 (1995) 3497-3505.

[69] C. Dehon, J. Lemaire, M. Heninger, A. Chaput, H. Mestdagh, Chemical ionization using CF_3^+: Efficient detection of small alkanes and fluorocarbons, International Journal of Mass Spectrometry, 299 (2011) 113-119.

[70] S.G. Lias, J.R. Eyler, P. Ausloos, Hydride transfer reactions involving saturated hydrocarbons and CCl_3^+, CCl_2H^+, CCl_2F^+, CF_2Cl^+, CF_2H^+, CF_3^+, NO^+, $C_2H_5^+$, sec-$C_3H_7^+$ and t-$C_4H_9^+$, International Journal of Mass Spectrometry and Ion Physics, 19 (1976) 219-239.

[71] J.R. Eyler, P. Ausloos, S.G. Lias, Novel ion-molecule reaction involving cleavage of the carbonyl bond in ketones and aldehydes, Journal of the American Chemical Society, 96 (1974) 3673-3675.

[72] J. Oomens, T.H. Morton, Fluoronium metathesis and rearrangements of fluorine-stabilized carbocations, International Journal of Mass Spectrometry, 308 (2011) 232-238.

[73] P. Ausloos, S. Lias, J.R. Eyler, Reactions of halomethyl ions with carbonyl-containing compounds, International Journal of Mass Spectrometry and Ion Physics, 18 (1975) 261-271.

Chapter Two: Experimental and Instrumentation

This chapter will deal with the experimental work in this thesis and details of the chemical ionization reaction time-of-flight-mass spectrometry (CIR-TOF-MS) which was used in this work. The parts of this instrument will be described, along with some of the fundamental aspects behind the time-of-flight mass analyser. In addition, a brief discussion on GC-MS will be given.

2.1 Chemicals and Reagents

Reagent ions were generated in the source of the CIR-TOF-MS using water at saturated vapour pressure in high purity nitrogen (BOC, 99.998 %), CF_4 (BOC special gases, 99.999 % purity) or O_2 gas (zero grade N2.6, BOC special gases).

Alkane samples, ethane, propane and n-butane were introduced into the CIR-TOF-MS as 5 ppmV mixtures in nitrogen (CP grade, BOC, Manchester). Nitrogen from the same batch (CP grade) used for the alkane samples was utilized for preparation of n-pentane and n-hexane samples in Tedlar bags, and was also used for background measurements. The concentration range of alkane gas mixtures with N_2 ranged from 0 to 5 ppmV. Samples of n-pentane and n-hexane (Sigma-Aldrich, Gillingham, Dorset, UK) were prepared in two stages using N_2 in 10 litre Tedlar bags (Thames-Restek UK, Ltd, Saunderton, Bucks., UK) to produce a range of concentrations from 0 to 50.0 ppmV; more details are given in Chapter 3.

The target VOC analytes–ethyl acetate, methyl acetate, acrylonitrile, propionitrile, acetonitrile, acetone, 2-butanone, acetaldehyde, butanedione, propanal, furan, methyl furan, pyrrole, pyridine, benzene, ethyl benzene, toluene, styrene, xylene, ethanol, octane, bromobenzene, α-pinene and pentane (Sigma-Aldrich, Gillingham, Dorset, UK)–were analysed using CF_3^+ as a novel reagent in CIR-TOF-MS and H_3O^+ for comparison. In addition, these VOCs were used to prepare standard curves. Analytes were prepared with a known concentration by two-stage dilution in 10 litre Tedlar bags; more details are given in Chapter 4.

Breath samples from smokers and non-smokers were collected in 10 litre or 3 litre Tedlar bags. The bags were prepared for use by filling with N_2 gas and keeping them in an oven at 45ºC for 15 minutes. Afterwards, the bags were flushed with N_2 gas at least three times. During the experiments, the samples in the Tedlar bags were fixed at 40ºC in an oven.

The sampling line and sample inlet were maintained at a temperature of 40ºC using heating cable and tape; more details are given in Chapter 5.

Urine samples were collected in Sterilin single use plastic bottles (Thermo Fisher Scientific, UK). During the experiment, urine samples were divided into two 8 ml portions. The first portion was poured into a Dreschel bottle that was kept in a water bath to maintain the temperature of urine sample at 40ºC. The remainder of the sample was kept refrigerated while the first portion of the sample was measured. A cylinder of 10 ppmV bromobenzene in a nitrogen calibration mix was used as the internal standard. Bromobenzene does not produce conflicting peaks in the spectra from the urine headspace samples, and it is not found to naturally exist in air. Bromobenzene was diluted further in N_2 gas to produce a final concentration of 2.5 ppmV. More details can be found in Chapter 6.

Experiments were conducted to identify VOCs in breath samples using Solid Phase Microextraction-Gas Chromatography-MS (SPME-GC-MS). This allowed one to establish the general range of VOCs in exhaled breath. Breath samples were collected in Tedlar bags. The SPME fibre type was CAR/PDMS and exposed to a breath sample for 20 minutes and after that, for protection, the fibre was retracted into the metal sheath. Finally, the fibre's contents was introduced to the GC-MS through its injection port and the extract time was 5 minutes.

2.2 Gas Chromatography-Mass Spectrometry (GC-MS)

GC-MS is one of the most important and utilized techniques for the separation quantification and analysis of VOCs [1]. The principle of GC relies on two phases, the mobile phase (carrier gas), usually helium, and a stationary phase, in which the sample is passed through very long capillary columns coated with a thin layer (1 µm) of viscous liquid on the inner wall of the column held in temperature controlled oven [2]. The sample is injected into the column and its component analytes are carried by the stream of carrier gas. The components have retention times determined by their physical properties and affinities of the stationary phase and so separate from one to another at different oven temperatures, reaching the detector at different times. See Figure 2.1.

GC has the advantages of being relatively inexpensive, reliable and relatively simple. In addition, only small volumes of the samples are required to operate (typical < 2 µl of liquid sample). It is a non-destructive analytical tool with high sensitivity and high

resolution [1, 2]. In spite of these advantages, samples with small traces of analytes may need pre-concentration to improve the detection sensitivity. One way of doing this is to use a cryogenic trap to collect the analyte. Another way to collect the component is to use adsorbent materials such as polymer (Tenax) or charcoal. Unfortunately, there is no single column that is suitable for all kinds of analytes. A non-polar column is suitable for separating hydrocarbons, while a polar column is best for oxygenated volatile organic compounds (OVOCs) such as aldehydes and ketones [2].

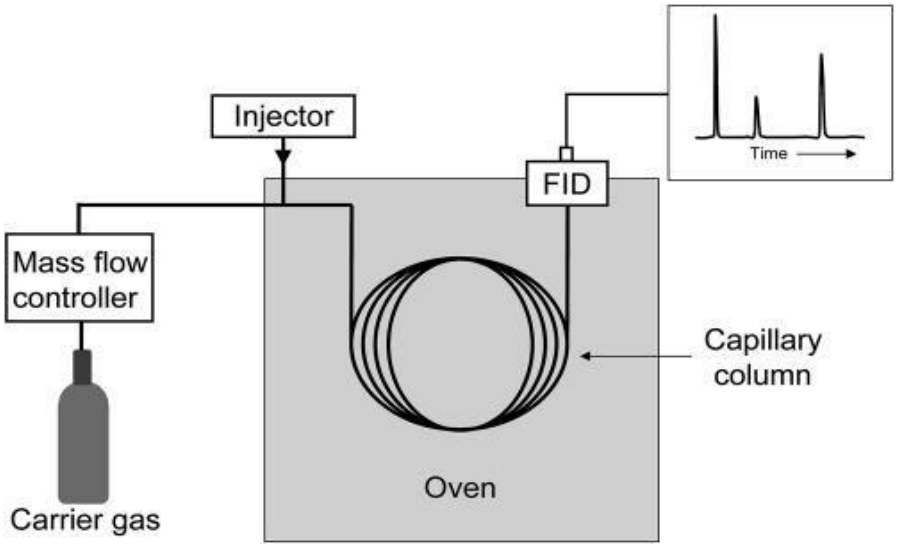

Figure 2. 1: Schematic diagram of the main components of a gas chromatogram (GC); adapted from Ellis & Mayhew [2].

2.3 Chemical Ionization Reaction Time-of-Flight-Mass Spectrometry (CIR-TOF-MS)

The focus of this work is to establish the suitability of CF_3^+/CF_2H^+ as a new reagent in CIR-TOF-MS to detect small-chain alkanes and other VOCs in breath and urine headspace for smokers and non-smokers, as compared with the more conventional precursors H_3O^+ and O_2^+ in CIR-TOF-MS.

Samples need to be ionized before being analysed by mass spectrometry. Munson and Field found that the chemical ionization (CI) technique [3], requires much lower energies compared with conventional electron ionization (EI) techniques, which results in less fragmentation of the sample molecules. Most VOCs need approximately 10 eV for ionization, the high energy of electron ionization (70 eV) leads to extensive fragmentation. While fragmentation can be used to determine structural information for analytes, identification of an analyte can become very difficult in such a complex mixture

without pre-separation [4]. CI reactions proceed with less excess energy and CI is thus often referred to as a soft ionization technique leading to little or no fragmentation [2]. CI often produces a single parent ion, simplifying the task of deconvoluting spectra as less fragmentation, and simpler analysis of real-life samples.

The CI processes depends on the chemical properties of the analyte and the chemical reagent, but generally follow four paths: proton transfer (PTR), charge transfer, hydride (H^-) transfer and adduct formation. The CI processes are shown in these examples [2, 5-8].

$$H_3O^+ + CH_3CHO \longrightarrow CH_3CHOH^+ + H_2O \quad \text{proton transfer} \quad (2.1)$$

$$NO^+ + C_6H_5OCH_3 \longrightarrow C_7H_8O^+ + NO \quad \text{charge transfer} \quad (2.2)$$

$$CF_3^+ + RH \longrightarrow CF_3H + R^+ \quad \text{hydride transfer} \quad (2.3)$$

$$NO^+ + CH_3COOH \longrightarrow NO^+\,CH_3COOH \quad \text{adduct formation} \quad (2.4)$$

Other examples have already been discussed in Chapter One.

PTR-MS, which operates through proton transfer is a form of CIR-MS using H_3O^+ as a chemical reagent. It was developed by Lindinger *et al*. in the 1990s [9]. CIR-MS instruments (which includes PTR-MS) have the following components: (1) an ion source to produce the reagent ions, (2) a drift tube where the reagent ions react with the analyte, (3) a mass analyser using either an radio frequency quadrupole (RFQ) or a time of flight device, (4) a detection system and (5) and an instrumental control system, as seen in Figure 2.2.

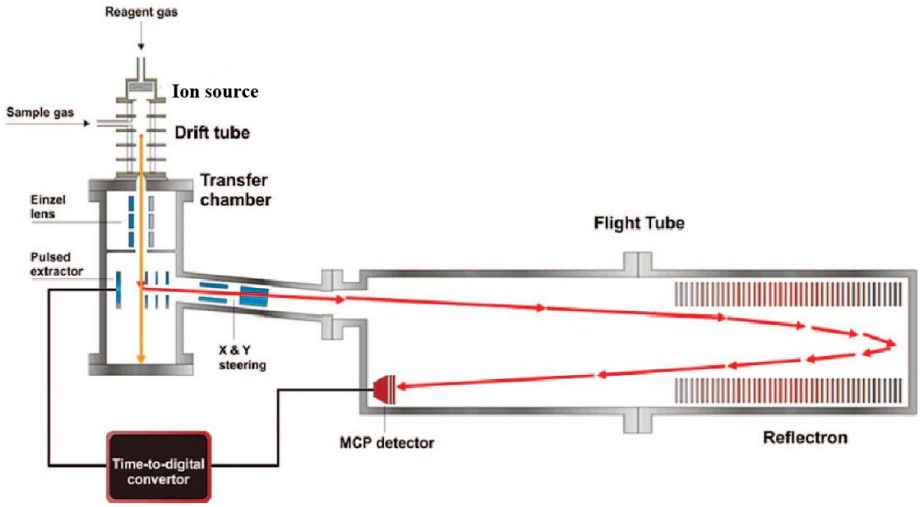

Figure 2. 2: Schematic diagram of the main components of a Time-of Flight (TOF) CIR-MS; adapted from Blake *et al* [10].

The two instruments used in this thesis were both Model 4500A instruments from Kore Technologies, Ely. Of these, the "Leicester" CIR-TOF-MS, uses a radioactive ^{241}Am ion source as the ionizing element, while the other, the "York" CIR-TOF-MS (on loan from the University of York) is equipped with a conventional hollow cathode discharge source (Figure 2.3).

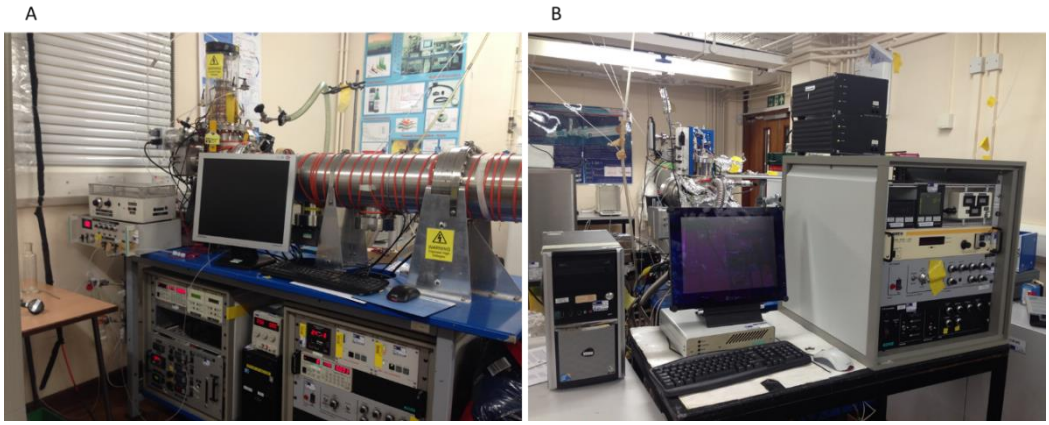

Figure 2. 3: the Leicester CIR-TOF-MS (A) and York CIR-TOF-MS (B).

2.3.1 Ion source

An electrical discharge can be generated using two planar electrodes. The electrode which has a positive potential is called the anode, whilst the other is called the cathode. Gases under normal conditions are good electrical insulators, but under the high potential deference between the two electrodes and under conditions of low gas pressure, they will become conductors and lead to a self-sustained discharge. At this stage, the voltage is known as the breakdown voltage, and this is dependent on the composition and the pressure of the gas, the voltage applied between the electrodes and the shape of the electrodes, Figure 2.4 [2, 11, 12].

The York TOF was fitted with a hollow cathode discharge (HCD) ion source. Ennis *et al*. in York were the first group to couple this to a reflectron TOF-MS [10, 13]. An HCD consists of a pair of electrodes, anode and cathode, to which an electrical potential is applied. Initially in the absence of an electrical potential difference the reagents such as H_2O and CF_4 act as insulators, but by increasing the potential difference, at one point a discharge commences in the reagent gas between the electrodes. The ion mix initially produced consists of a variety of ions and charge states. These pass through a field free source drift region where they rapidly stabilise forming H_3O^+ and CF_3^+. The reagent pressure and flow rate in HCD was 1 mbar and 5-10 sccm. Over time and continuous

operation, the performance of the HCD deteriorated and became unstable due to a build-up of contamination. Consequently, the ion source needed frequent cleaning especially when CF_3^+ was the reagent [2].

In the Leicester TOF, a radioactive ion source was driven by α-particles from a radioactive strip of ^{241}Am fixed to the inner side of a stainless-steel cylinder. The energetic (5 MeV) α-particles ionize the water vapour passing through into a variety of charged fragments which rapidly equilibrate to create H_3O^+. The advantages of this source are that there is no need for an external current driver and the ion count is more stable compared to a conventional hollow cathode source. In addition, it suffers less from contamination caused by back diffusion of the analyte gas to the ion source region owing to the high flow rate of gas (20 STP cm^3 min^{-1}) into the ion source region. The intrinsically low ion count rate is offset partially by the operating pressure of the sample (up to 13 mbar), more analyte gas can be added to the drift tube to increase ion sensitivity [2, 14-17].

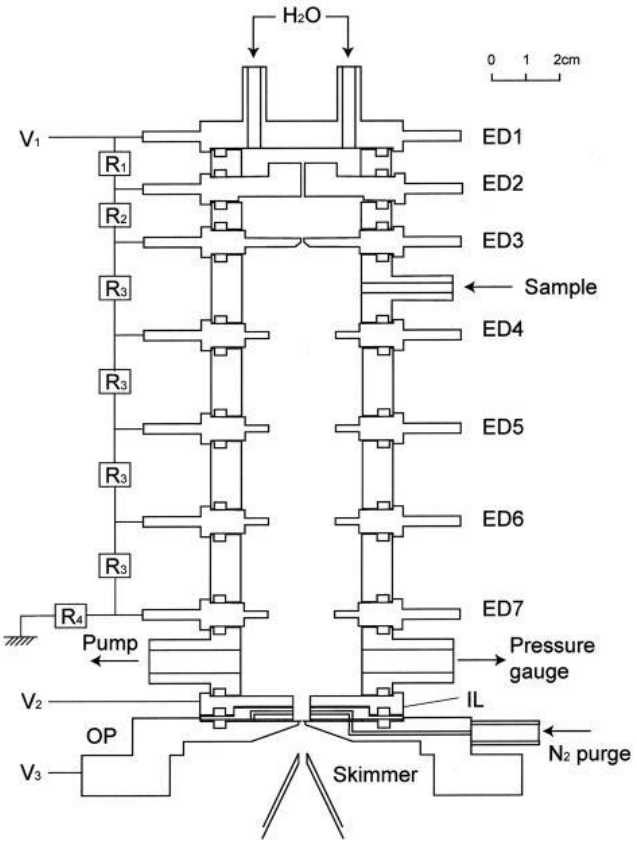

Figure 2. 4: Schematic of a discharge ion source and drift tube; adapted from Ellis *& Mayhew* [2].

In this work, the radioactive ion source of the Leicester CIR-TOF-MS was operated at 6 mbar with a water vapour flow rate of 50 sccm, while the hollow cathode discharge of the York CIR-TOF-MS was operated at 1.3 - 1.6 mbar and a CF_4 or O_2 flow rate of 5-9 sccm.

The analyte gas was supplied to the drift tubes at rates of 150 sccm and 50 sccm for the Leicester CIR-TOF-MS and York CIR-TOF-MS, respectively. The analyte molecules were chemically ionized through reactions with precursor ions produced in the ion source.

2.3.2 Drift tube

The role of the drift tube is to create a uniform electric field which directs and increases the migration velocity of the ions along the drift tube towards the entry point of the TOF-MS. As shown in Figure 2.4, the drift tube is the area between ED4 and ED7, which contains several stainless steel or brass electrodes (guard rings). The electrodes are separated by a slightly conductive insulator (Quadrant Semitron static dissipative Teflon) to maintain the applied voltage stable on each electrode while still avoiding charge build up. This special Teflon contains mica or glass which renders it slightly conductive and while it acts as a good insulator it is sufficiently conductive to dissipate the build-up of static charge, which would distort the uniform accelerating electric field in the drift tube. The analytes enter the drift tube through a sample inlet tube and mix with the now stabilised ion stream from the ion source region. There are two widely used ways to manage the flow of sample into the drift tube. The first is to use a mass flow controller which can be managed electronically. Some disadvantages of this approach are cost, and memory effects caused by some of the VOCs sticking to the inner side of the flow controller. The second method which was applied in this work, uses a critical orifice, which consists of a plate with a small hole in the centre that permits gas to enter the drift tube at a certain flow rate. It has the advantage of simplicity and reduced VOC sticking, but since the flow rate through the orifice is temperature and pressure sensitive, mass flow and rate meters are needed to maintain a stable operating environment on the upstream side. Ions are fed into the mass spectrometer through a 100-200 µm aperture at the end of the drift tube. This allows a small fraction of ions to enter the mass spectrometer while maintaining an internal operating pressure of $\leq 10^{-6}$ mbar [2].

In this work, the CIR-TOF-MS instruments were operated at a range of E/N = 50 Td - 120 Td. The E/N represent the ratio of the electric field strength to the molecular number density in the drift tube and is known as the reduced electric field, whose unit is the

Townsend (Td = 10^{-17} V cm^2) [2]. Increasing the electrical field and the collision energy or decreasing the drift tube pressure (lowering *N*) will increase the value of *E/N*.

When H_3O^+ is used as the reagent ion, H_3O^+ ions can attach to neutral water molecules in the drift tube reactor producing water cluster ions:

$$H_3O^+(H_2O)n^{-1} + H_2O + M \longrightarrow H_3O^+(H_2O)n + M \qquad (2.5)$$

Where M is a third body.

The formation of water clusters increases with high humidity in the sample as well as low values of *E/N* or both. The proton affinity of water clusters frequently differ from that of the single hydronium ion so that high concentrations of clusters can affect the observed yields from the target VOCs and complicate interpretation of mass spectra [10]. For example, acetaldehyde has a proton affinity that lies between that of the hydronium ion and its water cluster; as a result, it reacts with H_3O^+ but not with $H_3O^+(H_2O)$. Toluene has a lower proton affinity than water; as consequence, toluene will react with the cluster by ligand switching, rather than with the hydronium ion [2].

Increasing the *E/N* value in the drift tube will reduce the production of hydrated hydronium clusters. At the same time, higher *E/N* values could cause unwanted fragmentation and reduce the reaction time of the analyte in the drift tube, which in turn could affect detection sensitivity [2].

The formation of CF_3^+ and CF_2^+ from the discharge of CF_4 in the drift tube can also be influenced by the value of *E/N*. In the presence of water, CF_2H^+ is produced and the relative abundance decreases from 20% - 30% at 50 Td to 3% - 1% at 100 Td. Fortunately, unlike the case with H_2O clusters, the reaction rate of CF_2H^+ is similar to that of CF_3^+ and so does not affect the outcome. Nevertheless, every effort was made to minimise the production of CF_2H^+.

$$CF_2H^+ + RH \longrightarrow CF_2H_2 + R^+ \qquad (2.6)$$

By choosing suitable inlet sample humidity and *E/N* it was possible to increase the percentage of the main reagent CF_3^+, as compared with CF_2H^+. Where the yields were high enough it was possible to reduce the relative humidity of the sample by diluting the sample with dry N_2.

2.3.3 Mass analyser and Detection

Analyte ions in CIR-MS are created in the source by chemical ionization, and the drift tube is coupled to a TOF-MS. Square wave pulses of ions are injected into a flight tube while a TOF mass analyser measures the flight times of the ion components from the point of entry into the mass spectrometer to the detector [18]. A TOF consists of two sections. The first is a short section known as the ion accelerator and the second a longer section called the flight tube. The ion accelerator region contains two electrodes, the repeller and the extractor. The extractor electrode consists of a transmission grid which injects all the ions into the flight tube with the same energy. The ions pass the acceleration area to the flight tube [2]. The flight tube contains a series of electrodes (reflectron) working as an ion mirror which doubles the length of the flight tube and also compensates for the energy spread of ions with the same m/z so that they arrive at the same time at the detector. The ions which have higher velocities will penetrate further into the reflector array than slower moving ions with the same m/z. As a consequence, the fast ions will have a longer journey to the detector, as shown in Figure 2.5. The additional journey length of the faster ion is optimised through the choice of voltage applied to the reflectron array. This leads to the faster and slower ions of the same m/z reaching the detector at the same time. As a result, mass resolution is increased [2, 19].

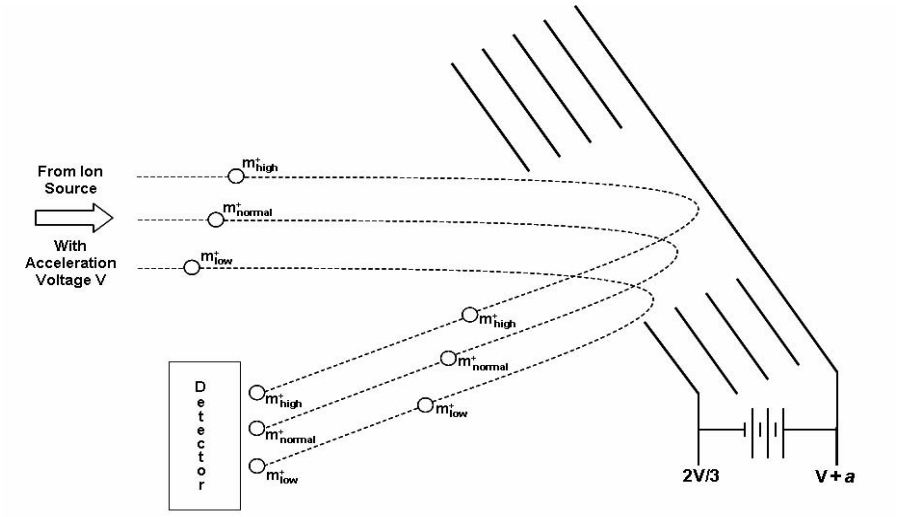

Figure 2. 5: Schematic of a Reflectron TOF-MS; adapted from Watson *et al* [19].

During the acceleration stage, all ions start off with the same kinetic energy, so that they will travel at different velocities according to their value of m/z. This results in the ions separating into groups (packets) [19].

The kinetic energy (½mv^2) of the ion is equivalent to the potential energy zeV (where m, v, z, e, q and V are ion mass, ion velocity, charge number, elementary charge, charge of ion and the potential in the acceleration area respectively).

$$E = qV = \frac{1}{2}mv^2 = \frac{1}{2}m\left(\frac{l}{t}\right)^2 \quad (2.7)$$

The time (time of flight) required for the ions to reach the detector is given by the following equation (where l is the length of flight tube):

$$t = \sqrt{\frac{l^2}{2eV}.\frac{m}{z}} \quad (2.8)$$

Thus, measuring the time-of-flight leads to the detection of m/z.

On the practical side, it is difficult to gain an accurate value for m/z by using Equation (2.8) for a number of reasons: the difference in speed between the two-stage acceleration area, the reflecting array of the reflectron and the flight tube. As a consequence, the ions will travel various distances. In addition, it is difficult to measure the starting time of the ions in order to determine their actual travel accurately. For the aforementioned reasons, a measured flight time, t, for some known ions are used to calibrate the flight times of any unknown ions [2].

TOF-MS has some advantages over quadrupole-based mass spectrometers. Firstly, it avoids the mass filter effects of quadrupoles which causes them to discriminate against heavier m/z ions and, secondly, it can achieve higher mass resolving power leading to more accurate mass measurements and better sensitivity. Otherwise, TOF-MS has some limitations such as requiring a higher vacuum compared with other MS methods, leading to a high cost and a bulky system. In addition, the need for carefully controlled temperatures to avoid the effects of the electronics and any change in the length of the flight tube [2].

After the ions are separated according to their mass, they are detected by a microchannel plate (MCP) detector. The output from the MCP is sent via a pre-amplifier to a time-to-digital converter (TDC). The TDC builds the input data as an arrival time histogram [20].

2.4 Data Collection and Normalisation

Collection of data was achieved through the GRAMS/AI software (Thermo Scientific). GRAMS/AI was used to convert the time data from the TDC into mass-to-charge ratios

(m/z). Later, the data was converted to an Excel-readable file (csv format) via in-house add-ons to the base GRAMS/AI software [20].

Generally, ion count rates are expressed as values relative to the reagent (e.g., H_3O^+, O_2^+ or CF_3^+) rather than their absolute values. This scaling (also referred to as normalizing) procedure eliminates small yield changes due to fluctuations in the reagent count rate occurring during the course of an experiment. Since historically most CIR-MS achieved absolute H_3O^+ counts near to 10^6 s^{-1}, it has become common practise to express ion yields as normalized counts per second (ncps).

In this thesis, three precursors were used in CIR-TOF-MS; H_3O^+, CF_3^+ and O_2^+. The normalisations for each reagent are shown in the following equations.

$$ncps = 10^6 \times \frac{i(MH^+)}{i(H_3O^+ + H_3O^+(H_2O))} \quad (2.9)$$

$$ncps = 10^6 \times \frac{i(MH^+)}{i(CF_3^+ + CF_2H^+)} \quad (2.10)$$

$$ncps = 10^6 \times \frac{i(MH^+)}{i(O_2^+)} \quad (2.11)$$

This means that the ion count rate for MH^+ is expressed as a signal of one million counts per second for every reagent.

2.5 Calibration

Throughout this thesis the CIR-MS instrument was calibrated using the static gas calibration method. In this method, a known quantity of a mixture of one or more VOCs in liquid phase is introduced into a Tedlar bag and diluted with an 8 litre volume of nitrogen. Although this method is relatively cheap and simple, it has some disadvantages, such as some analytes having the tendency to stick on the bag walls or undergo chemical decomposition, leading to a decrease in their apparent concentrations. Figure 2.6 and 2.7 show the calibration curves for toluene using CF_3^+ and H_3O^+ in CIR-MS.

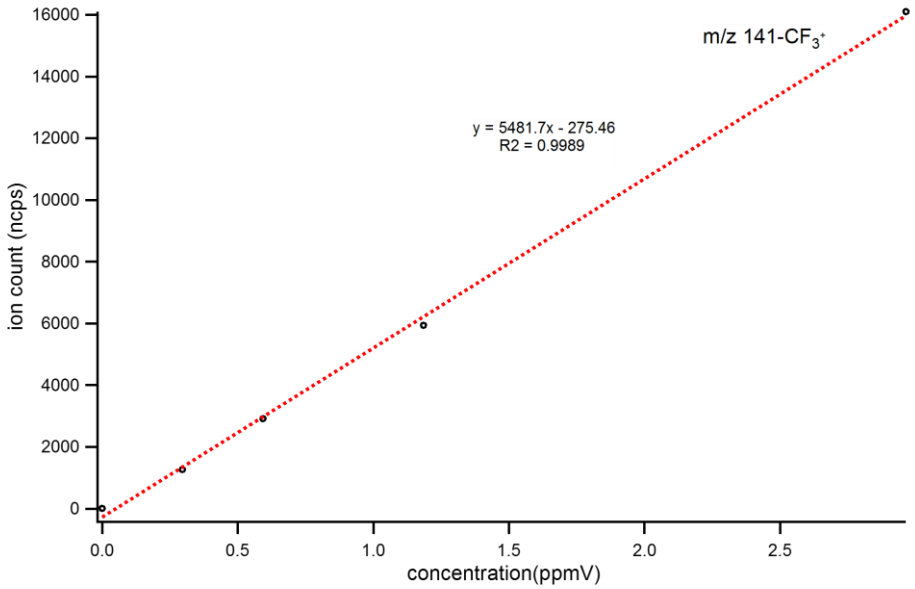

Figure 2. 6: Calibration curve for toluene using CF_3^+ as the reagent in CIR-MS.

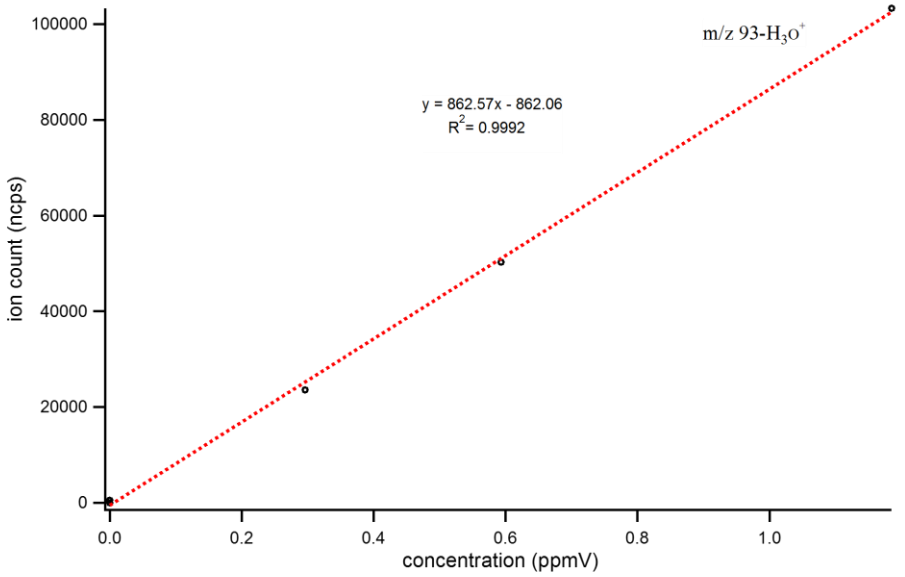

Figure 2. 7: Calibration curve for toluene using H_3O^+ as the reagent in CIR-MS.

2.6 Sensitivity

CIR-MS sensitivity can be determined by running a series of known concentrations and plotting concentration against the measured ion signal. If the relationship produced is linear the sensitivity of the instrument can be determined from the gradient of a linear fit to the data. At the same time, it is possible to estimate the value of the background signal from the intercept of the yield curve. The sensitivity (S_N) can be defined as:

$$S_N = \frac{\#}{[x]} \qquad (2.12)$$

where # is normalized ion count of the compound in ncps and [x] is the concentration in ppmV. The unit of sensitivity is thus ncps $ppmV^{-1}$

The sensitivity of the instrument can be influenced by many factors such as the humidity of the sample and *E/N*, as previously discussed. The nature of the reagent and analyte can also affect the sensitivity. As can be seen in Figures 2.6 and 2.7, the sensitivity of toluene produced by CF_3^+ as the reagent in CIR-MS is a somewhat higher (5482 ncps $ppmV^{-1}$) than the sensitivity of toluene that obtained from using H_3O^+ as the reagent in CIR-MS (863 ncps $ppmV^{-1}$).

2.7 Summary

This Chapter contains a brief discussion of GC-MS and some of the details of CIR-TOF-MS. CIR-TOF-MS is an analytical technique capable of detecting a wide range of all chemical classes at high sensitivities. The high speed of analysis by CIR-TOF-MS is advantageous as it is capable of detecting analytes and producing a mass spectrum in seconds. CIR-TOF-MS has the ability to switch between different reagents such as H_3O^+, NO^+, NH_4^+ and O_2^+. In this work we demonstrate that CIR-TOF-MS can be switched to CF_3^+ as a reagent to detect a wide range of VOCs in real samples; breath and urine headspace of smokers and non-smokers.

2.8 References

[1] H.M. McNair, E.J. Bonelli, Basic gas chromatography, in: Basic gas chromatography, Lithographed by Consolidated Printers, 1969.

[2] A.M. Ellis, C.A. Mayhew, Proton transfer reaction mass spectrometry: principles and applications, John Wiley & Sons, 2013.

[3] M.S. Munson, F.-H. Field, Chemical ionization mass spectrometry. I. General introduction, Journal of the American Chemical Society, 88 (1966) 2621-2630.

[4] E. de Hoffmann, V. Stroobant, Mass spectrometry: principles and applications, John Wiley & Sons, 2007.

[5] P. Španěl, Y. Ji, D. Smith, SIFT studies of the reactions of H_3O^+, NO^+ and O_2^+ with a series of aldehydes and ketones, International journal of mass spectrometry and ion processes, 165 (1997) 25-37.

[6] P. Španěl, D. Smith, SIFT studies of the reactions of H_3O^+, NO^+ and O_2^+ with several ethers, International journal of mass spectrometry and ion processes, 172 (1998) 239-247.

[7] S.G. Lias, J.R. Eyler, P. Ausloos, Hydride transfer reactions involving saturated hydrocarbons and CCl_3^+, CCl_2H^+, CCl_2F^+, CF_2Cl^+, CF_2H^+, CF_3^+, NO^+, $C_2H_5^+$, sec-$C_3H_7^+$ and t-$C_4H_9^+$, International Journal of Mass Spectrometry and Ion Physics, 19 (1976) 219-239.

[8] P. Ŝpaněl, D. Smith, SIFT studies of the reactions of H_3O^+, NO^+ and O_2^+ with a series of volatile carboxylic acids and esters, International journal of mass spectrometry and ion processes, 172 (1998) 137-147.

[9] W. Lindinger, A. Hansel, A. Jordan, On-line monitoring of volatile organic compounds at pptv levels by means of proton-transfer-reaction mass spectrometry (PTR-MS) medical applications, food control and environmental research, International journal of mass spectrometry and ion processes, 173 (1998) 191-241.

[10] R.S. Blake, P.S. Monks, A.M. Ellis, Proton-transfer reaction mass spectrometry, Chemical reviews, 109 (2009) 861-896.

[11] R.K. Marcus, J.A. Broekaert, Glow discharge plasmas in analytical spectroscopy, John Wiley & Sons, 2003.

[12] M.E. Pillow, A critical review of spectral and related physical properties of the hollow cathode discharge, Spectrochimica Acta Part B: Atomic Spectroscopy, 36 (1981) 821-843.

[13] C.J. Ennis, J.C. Reynolds, B.J. Keely, L.J. Carpenter, A hollow cathode proton transfer reaction time of flight mass spectrometer, International Journal of Mass Spectrometry, 247 (2005) 72-80.

[14] D. Hanson, J. Greenberg, B. Henry, E. Kosciuch, Proton transfer reaction mass spectrometry at high drift tube pressure, International Journal of Mass Spectrometry, 223 (2003) 507-518.

[15] R.S. Blake, C. Whyte, C.O. Hughes, A.M. Ellis, P.S. Monks, Demonstration of proton-transfer reaction time-of-flight mass spectrometry for real-time analysis of trace volatile organic compounds, Analytical chemistry, 76 (2004) 3841-3845.

[16] K.P. Wyche, R.S. Blake, K.A. Willis, P.S. Monks, A.M. Ellis, Differentiation of isobaric compounds using chemical ionization reaction mass spectrometry, Rapid communications in mass spectrometry : RCM, 19 (2005) 3356-3362.

[17] R.S. Blake, P.S. Monks, A.M. Ellis, Proton-transfer reaction mass spectrometry, Chemical reviews, 109 (2009) 861-896.

[18] A. Kraj, D.M. Desiderio, N.M. Nibbering, Mass spectrometry: instrumentation, interpretation, and applications, John Wiley & Sons, 2008.

[19] J.T. Watson, O.D. Sparkman, Introduction to mass spectrometry: instrumentation, applications, and strategies for data interpretation, John Wiley & Sons, 2007.

[20] R.S. Blake, Monitoring tropospheric composition using time of flight chemical ionization mass spectrometric techniques, in, University of Leicester, 2005.

Chapter Three: CF_3^+ and CF_2H^+: new reagents for n-alkane determination in chemical ionization reaction mass spectrometry

This Chapter has been published in *Analyst*, 2016, 141, 6564-6570

3.1 Introduction

Direct chemical ionization (CI) mass-spectrometry has seen widespread use in applications such as plant studies, food science, atmospheric, forensics and medical applications [1-3]. The detection of alkanes is important in many applications, such as petroleum combustion and a wide range of metabolic processes [4, 5]. In addition, alkanes have been measured in the exhaled breath of smokers [6].

C_2-C_6 alkanes are difficult or impossible to detect with conventional chemical reagents. H_3O^+ or NO^+ exhibit little or no reaction with light alkanes, while O_2^+ causes the fragmentation of short chain alkanes [1, 7]. A suitable chemical reagent is needed to react with C_2-C_6 alkanes that produces less fragmentation but has a similar sensitivity to O_2^+. The aim of this study was to demonstrate that CF_3^+ and CF_2H^+, as produced from CF_4 as a reagent in CIR-MS, meets these requirements [1]. The most prevalent mechanisms for the reactions of chemical reagents with the analytes are proton transfer, charge transfer and hydride extraction. Proton transfer reaction mass spectrometry (PTR-MS) is a particularly well-known technique for the detection of many volatile organic compounds (VOCs). PTR-MS depends on H_3O^+ as a precursor and has a proton affinity that is lower than many VOCs of interest [1, 2, 8]. The most common precursors in CIR-MS are H_3O^+ and NH_4^+, but there are other reagents that can be used to detect VOCs such as protonated acetone. For instance, Inomata *et al*. [9], applied protonated acetone as a reagent in CIR-MS to distinguish between the two isomers ethyl acetate and 1,4-dioxane [9]. Blake *et al*. [10], also used protonated acetone to differentiate between methyl vinyl ketone and methacrolein owing to the proton affinity of acetone being intermediate to these compounds [10]. H_3O^+ is unable to react with lighter *n*-alkanes (< C_6).

Charge transfer is another mechanism that occurs when the ionization potential of the analyte is lower than that of the precursor. This mechanism commonly involves NO^+ and O_2^+. Španěl and Smith have applied selected ion flow tube mass spectrometry (SIFT), to detect the reactions of H_3O^+, NO^+ and O_2^+ with various VOCs such as aromatic and aliphatic compounds [1, 7]. O_2^+ has an ionization energy (IE) of 12.07 eV, which is able to react with all *n*-alkanes with ionization energies ranging from 11.52 eV to 10.13 eV

(ethane to hexane). As the number of carbon atoms in the chain increases, the reaction becomes more exothermic. NO^+ cannot undergo charge transfer with C_2-C_4 *n*-alkanes owing to its IE being lower (9.26 eV). NO^+ can gain a degree of energy from an electrical field in a drift tube, which might then allow certain reactions with C_5 and C_6 alkanes [1].

Studies have shown that NO^+ can be applied to distinguish between isomers [11-13]. Amador- Muñoz *et al*. [14], used a switchable ionization mode ($NO^+/H_3O^+/O_2^+$) to detect a number of relatively long-chain *n*-alkanes (> C5). Arnold *et al*. [15], noticed that the threshold size of NO^+ reactions with alkanes occurred at hexane, and that these processes are mainly followed by hydride transfer . Recently, Koss *et al*. [16], conducted a survey of the results of reactions of NO^+ with a wide range of OVOCs, as measured by GC-EI-MS/GC-TOF-MS. They demonstrated that NO^+ exhibited no reaction with small-chain alkanes such as ethane, propane and *n*-butane, but they manged to estimate the sensitivity of the reaction of NO^+ with *i*-pentane using GC-EI-MS results [16]. Conversely, Wilson *et al.* [17], detected a small percentage yield of alkanes (C_3 and higher) with NO^+ and the approximate rate constants of these reactions were recorded . Apart from O_2^+, which produces more fragmentation with *n*-alkanes, no suitable reagent has been found that reacts with the lighter *n*-alkanes with little or no fragmentation [1, 18]. In order to detect lighter alkanes in oil shale, an alternative method is to use CF_3^+ as a precursor in CIR-MS rather than O_2^+. Lias *et al*. and Tsuji *et al*. used CF_4 ions (CF_3^+ and CF_2H^+) as reagents in ion-cyclotron resonance mass spectrometry (ICR-MS) to detect C_2-C_6 *n*-alkanes with lower fragmentation compared with O_2^+. The general mechanisms of these reactions is hydride extraction, [1, 19, 20].

$$CF_3^+ + RH \longrightarrow CF_3H + R^+ \qquad (3.1)$$

and

$$CF_2H^+ + RH \longrightarrow CF_2H_2 + R^+ \qquad (3.2)$$

Dehon *et al.* [21], also worked with CF_3^+ ions as reagents in fourier transform ion cyclotron resonance mass spectroscopy (FT-ICR-MS) to detect small *n*-alkanes and fluorocarbons. The authors demonstrated that the reaction of CF_3^+ and CF_2H^+ with these compounds produces less fragmentation [21]. The rate constants of some common *n*-alkanes were determined by Lias *et al.* and Dehon *et al.* and exhibited good agreement with each other [1, 19, 21]. In this Chapter, the performances of CF_3^+ and CF_2H^+ as reagents in CIR-MS are compared with O_2^+ according to percentage yield, sensitivity and

fragmentation with respect to pressure (1-10 Torr), moisture and the drift tube electric field (*E/N*).

3.2 Experimental

The type of instrument used in this work was a Kore-P-4500-a time-of-flight mass spectrometer [1, 22]. Analytes were reacted with positively charged CI reagent ions, forming charged ion products which were subsequently separated/detected by TOF-MS. The principle and operational conditions used for CIR-MS have been explained in Chapter 2 and elsewhere [11, 23, 24]. The experiments were run at *E/N* values of 50 Td and 100 Td. A typical value for *E/N* in proton transfer work is 100 Td. The value of 50 Td was chosen to minimise fragmentation at the lowest possible value of *E/N* required to operate CIR-MS.

CF_4 (BOC special gases, 99.999% purity) or O_2 (zero grade N2.6, BOC special gases) were used as reagents in the hollow cathode discharge ion source of a CIR-TOF-MS at a rate of 5-9 sccm. According to the Kyoto protocol to the United Nations Framework Convention on Climate Change, CF_4 is considered a target for reduction. As a result, care was taken to use the least amount possible. The intensity of unwanted fragments such as NO^+ and NO_2^+, which may cause spurious reactions, were kept less than 5% of the main reagent peak (CF_3^+) by adjusting the extraction voltage and discharge current as described by Knighton *et al.* [25], O_2^+ ions were created using oxygen, and the intensities of NO^+ and NO_2^+ were reduced to avoid overlap with peaks of interest arising from the analytes. Since CF_3^+ and CF_2H^+ were both present in the reactions, their combination was taken into account during normalization.

The temperature of the ion source was maintained at 70ºC to minimize the effects of ambient temperature variation. The discharge region pressure was maintained at 1.3 Torr while the sample pressure was also held at 1.3 Torr. The alkanes ethane, propane and *n*-butane were supplied as a 5 ppmV mixture in nitrogen (CP grad-BOC, Manchester). Nitrogen from the same batch that was used for the preparation of alkanes (CP grad-BOC) was provided for dilution of *n*-pentane and *n*-hexane and the measurement of the background. Concentrations ranging from 0 to 5 ppmV were prepared by mixing alkane gas with nitrogen. Stock solutions of *n*-pentane and *n*-hexane (Sigma Aldrich) were prepared by diluting 10 µl of alkane sample with nitrogen in 10 litre Tedlar bags. Samples

with concentrations range from 0 to 50.0 ppmV were prepared by dilution of the appropriate amount in 10 litre Tedlar bags.

The effect of *E/N* on CF_3^+ and CF_2H^+ production was tested using N_2 as the analyte, and the effect of humidity (0 to 90%) was measured over a range from 83 to 130 Td. In order to estimate the effect of moisture on alkane products, analyte samples were divided into streams and passed through two mass flow controllers. One stream was passed through a bubbler and then combined with a second stream. The flow rate of both streams was fixed at 500 sccm, whilst only 50 sccm was supplied to the CIR-TOF-MS while the rest was released to atmosphere. It is assumed that alkane concentrations were not affected by the humidity. The percentage of the humidity was determined via a Hygrosens Hygro-Thermometer (Hygrosens Instruments GmbH, Loffingen, Germany).

3.3 Result and discussion

Pure CF_4 ionized in an electrical discharge source gives two predominant ions, CF_3^+ and CF_2H^+, at 69 and 51 amu, respectively. CF_2H^+ was produced through the reaction of CF_2^+ with water (due to the presence of residual humidity, i.e., water). The value of *E/N* was strongly influenced by the production of CF_2H^+ so that relative abundances of CF_2H^+ ranged from 20% to 40% at 50 Td and from 3% or less at 100 Td. In proton transfer reactions, H_3O^+ and its cluster ($H_3O^+.H_2O$) possess different proton affinities, which might cause undesirable side reactions. In a similar manner, CF_3^+ and CF_2H^+ contributions can lead to undesirable side reactions. The first set of experiments were run in dry conditions (RH < 0.01%) to reduce the effects of humidity on the alkane samples.

3.3.1 Ethane

Ethane reacts with CF_3^+ as a reagent in CIR-MS to produce main fragment at m/z 29, followed by small fragment at 43 amu in both cases of *E/N*. A small peak was detected at m/z 27 which could belong to $C_2H_3^+$ at 100 Td, (see Table 3.1).

Table 3. 1*:* Results for ethane with CF_3^+ as the reagent in CIR-MS.

Name	*m/z*	fragments	% (CF_4) at 100 Td	% (CF_4) at 50 Td
Ethane C_2H_4	27	$C_2H_3^+$	3.5	
(28)	29	$C_2H_5^+$	93.3	97.9
	43		3.2	2.0

O_2^+ is considered a strong reagent in CIR-MS. The ethane results showed that the main product was at 29 amu at both *E/N* followed by a signal at 28 amu with a relative abundance that was higher at 50 Td in both products. Small fragments were observed at 26 and 27 amu at both 50 and 100 Td (see Table 3.2).

Table 3. 2: Results for ethane with O_2^+ as reagent in CIR-MS.

Name	*m/z*	fragments	% (O_2) at 100 Td	% (O_2) at 50 Td
Ethane C_2H_4	26	$C_2H_2^+$	1.3	0.4
(28)	27	$C_2H_3^+$	10.1	1.6
	28	$C_2H_4^+$	29.6	13.5
	29	$C_2H_5^+$	56.9	81.8
	43	$C_3H_7^+$	2.0	2.7

3.3.2 Propane

The main product of propane with CF_3^+ was $C_3H_7^+$ at m/z = 43 for both values of *E/N*. A small peak was detected at 29 amu at both 50 and 100 Td. Another small peak at m/z = 41 was also detected, though only at 100 Td. In general, the main peak intensity was found to be higher at 50 Td, while other fragment peaks intensities were higher at 100 Td owing to the difference in energy between 50 and 100 Td, (see Table 3.3).

Table 3. 3: Results for propane with CF_3^+ as reagent in CIR-MS.

Name	*m/z*	fragments	% (CF_4) at 100 Td	% (CF_4) at 50 Td
Propane C_3H_8	29	$C_2H_5^+$	0.8	0.6
(44)	41	$C_3H_5^+$	2.2	
	43	$C_3H_7^+$	97.0	99.4

The oxygen results showed that propane's main fragment was at m/z 43 followed by a signal at 28 amu at 50 and 100 Td. Small peaks also were detected at 26, 27, 29 and 41 amu in both cases; see Table 3.4.

Table 3. 4: Results for propane with O_2^+ as reagent in CIR-MS.

Name	*m/z*	fragments	% (O_2) at 100 Td	% (O_2) at 50 Td
Propane C_3H_8	26	$C_2H_2^+$	1.5	0.4
(44)	27	$C_2H_3^+$	2.3	0.4
	28	$C_2H_4^+$	35.8	28.1
	29	$C_2H_5^+$	10.8	3.7
	41	$C_3H_5^+$	3.8	1.4
	43	$C_3H_7^+$	45.7	62.7

3.3.3 Butane

The reaction of butane with CF_3^+ produced very similar results at both 50 and 100 Td. The predominant peak was recorded at m/z =57, which represented the most dominant

ion, followed by a small amount of molecular ion at m/z =58. The small signal at m/z = 56 could have arisen due to removal of hydrogen atoms from the molecular ion. Small fragments were also detected at m/z = 29 and 43, related to ethyl and propyl groups, respectively; see Table 3.5.

Table 3. 5: Results for butane with CF_3^+ as reagent in CIR-MS.

Name	m/z	fragments	% (CF_4) at 100 Td	% (CF_4) at 50 Td
Butane C_4H_{10} (58)	29	$C_2H_5^+$	0.7	0.8
	43	$C_3H_7^+$	0.7	0.8
	56	$C_4H_8^+$	0.2	0.2
	57	$C_4H_9^+$	95.4	95.3
	58	$C_4H_{10}^+$	3.0	2.9

Butane with O_2^+ allowed the formation of small parent and molecular ions at m/z = 57 and 58 respectively at both *E/N*. The predominant fragment was detected at 43 amu, followed by small fragments at 26, 27, 28, 29 and 41 amu in both cases. In addition, m/z = 42 was observed only at 100 Td. At *E/N* =100 Td, a greater number fragments and a reduced abundance of m/z 43 were expected due to the difference in energy between each of the values of *E/N*; see Table 3.6.

Table 3. 6: Results for butane with O_2^+ as reagent in CIR-MS.

Name	m/z	fragments	% (O_2) at 100 Td	% (O_2) at 50 Td
Butane C_4H_{10} (58)	26	$C_2H_2^+$	0.1	0.1
	27	$C_2H_3^+$	0.8	0.3
	28	$C_2H_4^+$	2.8	2.8
	29	$C_2H_5^+$	7.9	2.2
	41	$C_3H_5^+$	7.4	1.4
	42	$C_3H_6^+$	1.5	
	43	$C_3H_7^+$	74.6	70.6
	57	$C_4H_9^+$	3.9	14.6
	58	$C_4H_{10}^+$	1.1	8.1

3.3.4 Pentane

Pentane reacts with CF_3^+ to produce the dominant ion at m/z = 71, which was slightly more abundant at 50 Td, followed by a small molecular ion at m/z = 72. The fragment at 43 amu was detected for both *E/N* values, with a relatively high abundance at 100 Td. In addition, a very small signal was seen at 57 amu for an *E*/*N* of 50 Td, which may belong to $C_4H_9^+$; see Table 3.7.

Table 3. 7: Results for pentane with CF_3^+ as reagent in CIR-MS.

Name	m/z	fragments	% (CF_4) at 100 Td	% (CF_4) at 50 Td
Pentane C_5H_{12}	43	$C_3H_7^+$	24.4	5.8
(72)	57	$C_4H_9^+$		0.3
	71	$C_5H_{11}^+$	74.3	92.7
	72	$C_5H_{12}^+$	1.3	1.4

The result of pentane with oxygen showed that a small amount of parent ion at m/z = 71 formed with a slightly higher abundance at 50 Td, followed by small peak at 72 amu which was the molecular ion. Many other fragments were detected at 27, 28, 29, 41, 24, 43, 57 and 57 amu due to the cleavage at carbon bonds at C_2, C_3 and C_4. The predominant signal was at m/z = 43 at both 50 and 100 Td; see Table 3.8.

Table 3. 8: Results for pentane with O_2^+ as reagent in CIR-MS.

Name	m/z	fragments	% (O_2) at 100 Td	% (O_2) at 50 Td
Pentane C_5H_{12}	27	$C_2H_3^+$	0.5	
(72)	28			1.0
	29	$C_2H_5^+$	2.2	2.4
	41	$C_3H_5^+$	19.5	5.0
	42	$C_3H_6^+$	7.6	2.0
	43	$C_3H_7^+$	51.7	44.1
	56	$C_4H_8^+$	3.4	2.8
	57	$C_4H_9^+$	11.3	10.1
	58	$C_4H_{10}^+$	0.5	
	71	$C_5H_{11}^+$	2.9	28.4
	72	$C_5H_{12}^+$	0.5	4.2

3.3.5 Hexane

Hexane reacted with CF_3^+ to form a parent ion at m/z = 85 with relatively high intensity at 50 Td and a low intensity at 100 Td, followed by small molecular ion at 86 at 50 Td. Small fragments were recorded at 41, 43, 44, 57 and 71 amu due to the cleavage at carbon bonds at C_3 up to C_5. The predominant fragment was recorded at m/z 43; see Table 3.9.

Table 3. 9: Results for hexane with CF_3^+ as reagent in CIR-MS.

Name	m/z	fragments	% (CF_4) at 100 Td	% (CF_4) at 50 Td
Hexane C_6H_{14}	41	$C_3H_5^+$	1.8	
(86)	43	$C_3H_7^+$	47.9	18.7
	44	$C_3H_8^+$	0.9	0.6
	57	$C_4H_9^+$	6.1	4.1
	71	$C_5H_{11}^+$	0.2	0.4
	85	$C_6H_{13}^+$	43.1	73.7
	86	$C_6H_{14}^+$		2.5

Hexane with oxygen formed small amounts of parent and molecular ions at m/z = 85 and 86 respectively at both values of *E/N*. Owing to cleavage at carbon C_2 up to C_5, various

fragments were observed at 29, 41, 42, 43, 44, 56, 57, 58 and 71 amu. The highest abundance of these fragments were observed at 56 and 57 amu at 50 and 100 Td, respectively; see Table 3.10.

Table 3. 10: Results for hexane with O_2^+ as reagent in CIR-MS.

Name	m/z	fragments	% (O_2) at 100 Td	% (O_2) at 50 Td
Hexane C_6H_{14} (86)	29	$C_2H_5^+$	0.9	0.3
	41	$C_3H_5^+$	7.2	1.0
	42	$C_3H_6^+$	1.1	4.7
	43	$C_3H_7^+$	8.3	
	44	$C_3H_8^+$		27.5
	56	$C_4H_8^+$	31.0	41.0
	57	$C_4H_9^+$	46.5	1.7
	58	$C_4H_{10}^+$	1.9	2.8
	71	$C_5H_{11}^+$	2.0	15.8
	85	$C_6H_{13}^+$	1.2	5.2
	86	$C_6H_{14}^+$	0.8	0.2

The reaction of CF_4 as a reagent in CIR-MS with ethane, propane and *n*-butane exhibits very little sign of fragmentation at either 50 Td or 100 Td. The spectra of ethane, propane and *n*-butane at 100 Td clearly showed less fragmentation. Figure 3.1 shows a composite spectrum of each alkane.

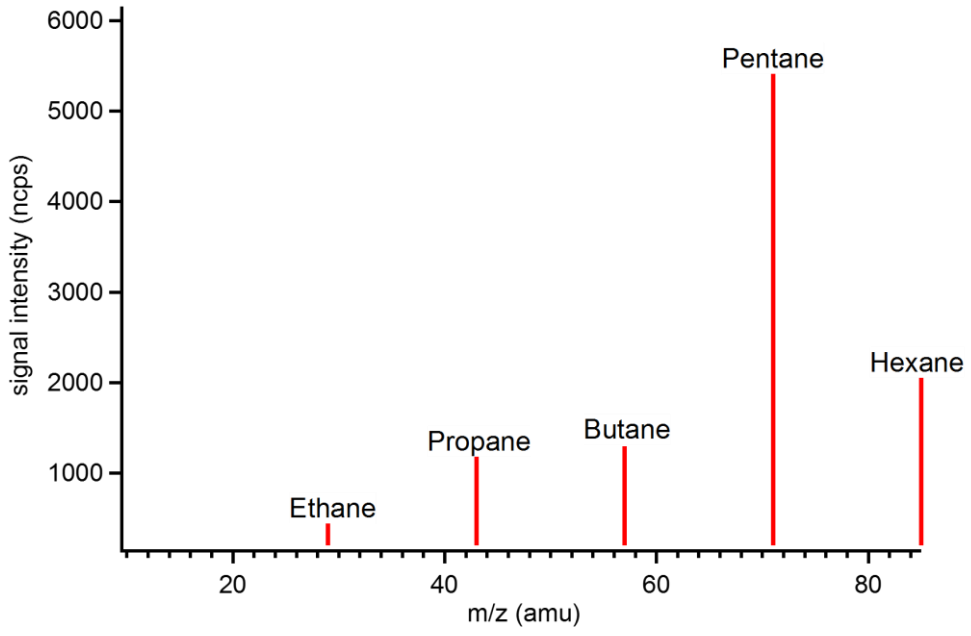

Figure 3. 1: Composite spectrum for ethane, propane, butane, pentane and hexane at *E*/*N* = 100 Td using CF_3^+ as precursor in CIR-MS [1].

Pentane and hexane experienced some fragmentation with CF_3^+, although fragmentation was minimal at 50 Td compared to 100 Td. The main products of *n*-pentane and *n*-hexane

were detected at m/z = 71 and 85, respectively, which follow a hydride extraction mechanism. The other product was detected at 43 amu ($C_3H_7^+$) which may form due to carbon-carbon bond fragmentation of the parent ions.

Pentane showed some fragmentation, in contrast to results of Dehon *et al*. [21], which exhibited complete fragmentation in pentane and weak indicators of a hydride transfer reaction in hexane.

The electron affinity (IE) of O_2^+ is 12.07 eV, and it reacts with small *n*-alkanes with the exception of methane (IE of methane is 12.61 eV). All the *n*-alkanes showed significant fragmentation with O_2^+ as a reagent in CIR-MS at 50 Td and 100 Td. The parent ions of pentane and hexane almost disappeared. CF_3^+ showed improved fragmentation patterns with the *n*-alkanes, showing almost no significant indication of any fragmentation of ethane, propane and *n*-butane. Small amounts of fragmentation with pentane and hexane were detected (Figure 3.2).

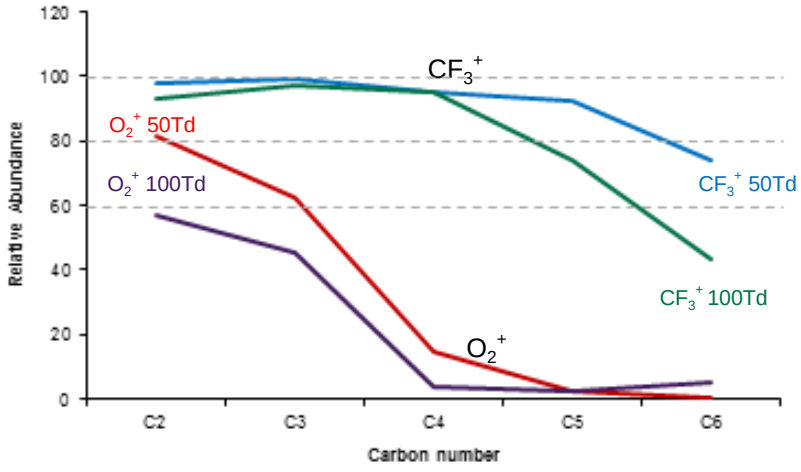

Figure 3. 2: Relative abundance of alkane molecular ions with CF_3^+ and O_2^+ at *E*/*N* = 50 and 100 Td.

3.3.6 Sensitivity

Calibration curves are important to determine the quantitative sensitivity for compound detection. Calibration curves for the alkanes were generated through their partial dilution in pure nitrogen, as shown in Figure 3.3.

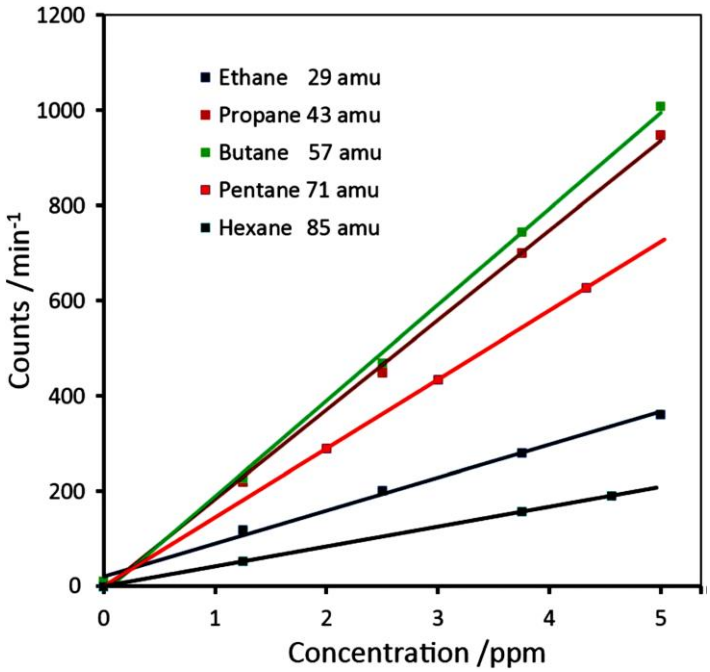

Figure 3. 3: Calibration curves for the alkanes were generated at 100 Td using CF_3^+ as reagent in CIR- MS, adapted from reference [1].

Care was taken whilst measuring the calibration of the alkanes to reduce the presence of humidity so that the effect of CF_2H^+ ions was reduced to less than 1% on the combined reactant percentage for all alkane products. The action of O_2^+ is more aggressive action than that of CF_3^+, leading to more fragmentation and producing lower signal intensities for both the parent and fragment ions.

Sensitivity can be defined as the number of product ions created in a trace gas mixing ratio of 1 ppbV and at a precursor signal of 1 million ion counts per second (ncps $ppbV^{-1}$) [1, 26]. The result of the reactions of alkanes with CF_3^+ are that slightly higher intensities were observed as compared with the results obtained using O_2^+ at 100 Td; see Table 3.11. In general, as the number of carbon atoms in the alkane increases, the overall detection sensitivities rise and more fragments are produced, particularly with O_2^+.

Table 3. 11: Detection sensitivity of the C_2- C_6 alkanes with CF_3^+ and O_2^+ at 100 Td. All sensitivities are in units of counts min^{-1} ppm^{-1}.

Target alkane	ethane[1]	propane[1]	*n*-butane[1]	*n*-pentane[1]	*n*-hexane[1]
m/z	29	43	57	71	85
Reagent					
CF_3^+	1756.5	7478.8	1864.3	282.0	34.4
O_2^+	777.8	292.5	30.8	207.1	21.2

1 = count min^{-1} ppm^{-1}

3.3.7 Limit of detection (LOD) and Signal-to-Noise (S:N)

The detection limit and signal-to-noise ratio were calculated for the alkanes (C_2-C_6) with CF_3^+ and O_2^+ as reagents in CIR-MS. It seems that the LOD for O_2^+ were higher than those for CF_3^+. A more powerful ion source and more extensive optimisation could potentially improve performance. The LOD and S:N found are shown in Tables 3.12 and 3.13.

Table 3. 12: Detection limit and signal-to-noise ratios for the alkanes with CF_3^+. The experiments were run for 10 minutes. Signal-to-noise was increased at 50 Td.

		100 Td		50 Td	
Name	Fragment	S:N	LOD (ppbV)	S:N	LOD (ppbV)
Ethane	$C_2H_5^+$	2678	6	4755	3
Propane	$C_3H_7^+$	1046	14	1277	11
n-Butane	$C_4H_9^+$	24002	1	52560	1
n-Pentane	$C_5H_{11}^+$	2253	30	2678	30
n-Hexane	$C_6H_{13}^+$	1267	17	2249	3

Table 3. 13: Detection limit and signal-to-noise ratios for the alkanes with O_2^+. The experiments were run for 10 minutes. Signal-to-noise was increased at 50 Td.

		100Td		50Td	
Name	Fragment	S:N	LOD (ppbV)	S:N	LOD (ppbV)
Ethane	$C_2H_5^+$	4475	3	8182	2
Propane	$C_3H_7^+$	4590	3	22145	1
n-Butane	$C_4H_9^+$	1172	13	18076	1
n-Pentane	$C_5H_{11}^+$	2363	6	10665	29
n-Hexane	$C_6H_{13}^+$	1942	8	5161	3

In order to assess CF_3^+ and CF_2H^+ as chemical reagents in chemical ionization mass spectrometry for use to detect VOCs in real-life samples, it is important to understand their properties and origins and other parameters that could affect their production. When working at high *E*/*N* values such as 100 Td, greater fragmentation occurs and a small amount of CF_2H^+ is produced. Operation at low *E*/*N* values such as 50 Td results in less fragmentation being observed but larger quantities of CF_2H^+ will be produced in the reagent mix and should be taken into account [1].

CF_2H^+ is thought to occur from the reaction of CF_2^+ with H_2O due to the humidity in the system by hydride transfer. Eyler *et al*. [27], noticed that small traces of the CF_2^+ ion reacted swiftly with natural species of CF_4 to produce CF_3^+ ions at a pressure of 10^{-6} Torr. So, it seems that the product, CF_2H^+, does not exist in ICR-MS within a 5 ms reaction

time [1, 27]. Ehlerding *et al*. [28], produced CF_2^+ ions in significant amounts at 0.1 Torr, whereas the CF_3^+ was produced at 1 mTorr [1, 28]. As the *E/N* is increased to 100 Td, CF_2^+ reacts with natural ions of CF_4 to produce CF_3^+, in agreement with the findings of Eyler *et al*. [1, 27].

Thermochemical calculations showed that the reaction of CF_2^+ with H_2O is only slightly exothermic (ΔH = -13.2 kJ mol^{-1}), and additional energy could be supplied by increasing the value of *E*/*N*. This may inhibit the path of CF_2H^+ production and allow CF_2^+ to react with CF_4 to form CF_3^+ (ΔH = -92.18 kJ mol^{-1}); see Table 3.14. The relative humidity in the initial set of experiments was around 0.01% to minimise interference from the H_3O^+ ion [1]. Dehon *et al*. [21], demonstrated that no reaction occurred between CF_3^+ and trace water at ambient air at pressures of 10^{-4} Torr, although a reaction between pure water vapour and CF_3^+ was observed at 10^{-4} Torr, and the slow appearance of H_3O^+ was observed while CF_3^+ ions disappeared. The existence of water may be considered to constitute the presence of an additional compound in the sample mixture which can compete with the *n*-alkanes. A significant reduction in the percentage of the alkane products and both reagents (CF_3^+ and CF_2^+) resulted from an increase in the relative humidity of the samples.

Table 3. 14: Thermochemical Calculations [1].

No	Reaction	energy
1	$CF_3^+ + H_2O \rightarrow CF_2H^+ + HOF$	ΔH = +361.7 kJ mol^{-1}
2	$CF_3^+ + H_2O \rightarrow CF_2OH^+ + HF$	ΔH = -142.8 kJ mol^{-1}
3	$CF_2^+ + H_2O \rightarrow CF_2H^+ + OH$	ΔH = -13.2 kJ mol^{-1}
4	$CF_2^{2+} + H_2O \rightarrow CF_2OH^+ + H^+$	ΔH = -1725.5 kJ mol^{-1}
5	$CF_2^+ + CF_4 \rightarrow CF_3^+ + CF^+$	ΔH = -92.185 kJ/mol^{-1}

The percentage of reactant products reduced rapidly at values of *E*/*N* < 100 Td, as seen in Figure 3.4. Figure 3.4 shows values of *E*/*N* in the region of 100 Td provided the best compromise between reactant reduction and fragmentation. The result of the n-alkanes also exhibited a decrease in yield of *n*-alkanes products, as shown in Table 3.15. It seems that moisture in the analyte affects any work at 50 Td.

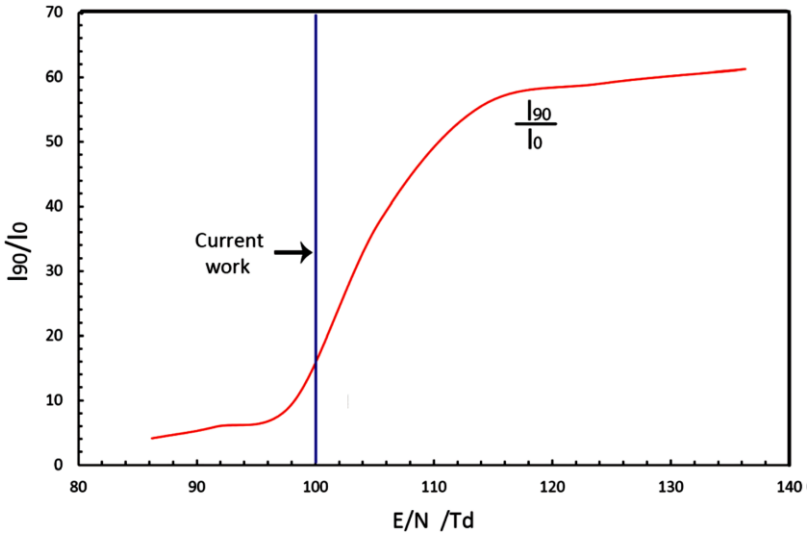

Figure 3. 4: The percentage yields of (CF_3^+ + CF_2H^+) expressed as I_{90}/I_0 for relative humidity (RH) ranging from 0% and 90% as a function of *E/N.* Adapted from ref. [1].

Table 3. 15: The main fragments of the alkane which reacted with CF_3^+ and CF_2H^+ over a range of humidities (RH) ranging from 0% to 90%. The resolution of the machine is not sufficient to distinguish between $C_2H_5^+$ and other possible fragments such as N_2H^+ or COH^+. The variation in alkane fragments was very similar.

n-Alkane	Fragment (amu)	Percentage yield			
		RH = 0%	RH = 20%	RH = 45%	RH = 90%
Ethane	29	100	-	-	40
Propane	43	100	76	57	45.4
n-Butane	57	100	82	66	44.9
n-Pentane	71	100	82	65	44.9
	43	100	78	60	41.4
n-Hexane	85	100	72	52	34.6
	57	100	77	58	44.4
	43	100	78	58	41.2

According to the calculations summarized in Table 3.14, Equation (3.3), it can be noticed that the reaction is endothermic ($\Delta H = +361.7$ kJ mol^{-1}).

$$CF_3^+ + H_2O \longrightarrow CF_2H^+ + HOF \qquad (3.3)$$

Dehon *et al.* [21], suggested that two stages occur in this reaction. The first step, a thermodynamically allowed intermediate complex, was produced; the second step, which favoured proton transfer, proceeded as shown in Equations 3.4 and 3.5 [1].

$$CF_3^+ + H_2O \longrightarrow [CF_3OH_2^+] \longrightarrow HF + CF_2OH^+ \qquad (3.4)$$

Followed by

$$CF_2OH^+ + H_2O \longrightarrow CF_2O + H_3O^+ \quad (3.5)$$

Lower values of *E/N* or higher moisture content will increase the concentration of $H_3O^{+\cdot}$ As a result, the contribution from this source must be taken into count [1].

The ethyl peak from ethane appears at 29.06 amu and, as the concentration of H_3O^+ increased, was overlapped by another peak at 29.02 amu, which obscured the $C_2H_5^+$ ethyl signal. Unfortunately, our instrument does not have sufficient resolution to distinguish the two groups. The proton affinity of H_2O (691 kJ mol^{-1}) is higher than that of N_2 (493 kJ mol^{-1}) so that the product N_2H^+, though not thermodynamically favoured, can nevertheless potentially be produced. Another possibility with the same mass is CHO^+, which has a proton affinity of 667 kJ mol^{-1}, which itself is not far from that of H_2O. There is chance that this might happen, but the associated mechanism is not clear [1].

CF_3^+ has the ability, as a reagent ion in CIR-MS, to detect the lighter *n*-alkanes. H_3O^+ and NO^+ almost do not react with lighter *n*-alkanes, but both CF_3^+ and O_2^+ do react with alkanes (C_2-C_6), and both have a similar detection sensitivity. The existence of humidity in the samples could complicate the process of analysis so, as a result, the calibration curves of known standards are needed. However, CF_3^+ leads to less fragmentation compared with O_2^+ [1].

The presence of CF_2H^+ as a reagent with CF_3^+ could complicate the results, but this particular obstacle can be overcome by the simple expedient of adjusting the value of *E/N* [1]. Earlier, using conventional reagents such as H_3O^+ and O_2^+ to detect small-chain alkanes (C_2-C_6) faces certain difficulties such as a lack of any reaction or the occurrence of extensive fragmentation; CF_3^+ appears to present new opportunities and be a worthy addition to conventional chemical ionization reagents used in CIR-MS [1].

The percentage of product in these groups increases when moving from 100 Td to 50 Td, and more precautions must be taken to avoid variations in *E*/*N* during the experiment.

3.4 Summary

Detection of lighter alkanes with conventional chemical reagent such as H_3O^+ is almost impossible owing to their basicity. It has been demonstrated that CF_3^+ and CF_2H^+ used as reagents in CIR-MS supply an effective method of detecting lighter *n*-alkanes (C_2-C_6) that would not otherwise be easily accessible. The applicability of the precursors in CIR-MS with different variables such as operating pressures of 1-10 Torr, high moisture content and electrical field in the drift tube (*E/N*) were evaluated. Chemical ionization

reagents, H_3O^+ and NO^+, react with hexane and higher, while O_2^+ will react with all analytes but result in extensive fragmentation. On the other hand, both CF_3^+ and CF_2H^+ acting together react with small-chain *n*-alkanes whilst showing almost no fragmentation. At *E/N* = 100 Td under dry conditions, the relative intensity of CF_2H^+ to CF_3^+ was less than 3%, making CF_3^+ the main precursor ion in CIR-MS. In parallel, a set of experiments using O_2^+ as the reagent were conducted, and extensive fragmentation was recorded. The sensitivity of lighter alkanes to CF_3^+ and CF_2H^+ were better compared with the O_2^+ result. Alkane mixture results showed that the reagents CF_3^+ and CF_2H^+ can be used for the detection of alkanes in real-life samples such as exhaled breath samples and urine headspace.

3.5 References

[1] R.S. Blake, S.A. Ouheda, C.J. Evans, P.S. Monks, CF_3^+ and CF_2H^+: new reagents for n-alkane determination in chemical ionisation reaction mass spectrometry, The Analyst, 141 (2016) 6564-6570.

[2] R.S. Blake, P.S. Monks, A.M. Ellis, Proton-transfer reaction mass spectrometry, Chemical reviews, 109 (2009) 861-896.

[3] D. Smith, P. Spanel, Selected ion flow tube mass spectrometry (SIFT-MS) for on-line trace gas analysis, Mass Spectrom Rev, 24 (2005) 661-700.

[4] J.J. Schauer, M.J. Kleeman, G.R. Cass, B.R. Simoneit, Measurement of emissions from air pollution sources. 5. C_1− C_{32} organic compounds from gasoline-powered motor vehicles, Environmental science & technology, 36 (2002) 1169-1180.

[5] M. Phillips, J.P. Boehmer, R.N. Cataneo, T. Cheema, H.J. Eisen, J.T. Fallon, P.E. Fisher, A. Gass, J. Greenberg, J. Kobashigawa, Heart allograft rejection: detection with breath alkanes in low levels (the HARDBALL study), The Journal of heart and lung transplantation, 23 (2004) 701-708.

[6] D.E. Euler, S.J. Dave, H. Guo, Effect of cigarette smoking on pentane excretion in alveolar breath, Clinical chemistry, 42 (1996) 303-308.

[7] P. Španěl, D. Smith, Selected ion flow tube studies of the reactions of H_3O^+, NO^+, and O_2^+ with several aromatic and aliphatic hydrocarbons, International Journal of Mass Spectrometry, 181 (1998) 1-10.

[8] A.M. Ellis, C.A. Mayhew, Proton transfer reaction mass spectrometry: principles and applications, John Wiley & Sons, 2013.

[9] S. Inomata, H. Tanimoto, Differentiation of isomeric compounds by two-stage proton transfer reaction time-of-flight mass spectrometry, Journal of the American Society for Mass Spectrometry, 19 (2008) 325-331.

[10] R.S. Blake, M. Patel, P.S. Monks, A.M. Ellis, S. Inomata, H. Tanimoto, Aldehyde and ketone discrimination and quantification using two-stage proton transfer reaction mass spectrometry, International Journal of Mass Spectrometry, 278 (2008) 15-19.

[11] K.P. Wyche, R.S. Blake, K.A. Willis, P.S. Monks, A.M. Ellis, Differentiation of isobaric compounds using chemical ionization reaction mass spectrometry, Rapid communications in mass spectrometry : RCM, 19 (2005) 3356-3362.

[12] S. Inomata, H. Tanimoto, H. Yamada, Mass Spectrometric Detection of Alkanes Using NO^+ Chemical Ionization in Proton-transfer-reaction Plus Switchable Reagent Ion Mass Spectrometry, Chemistry Letters, 43 (2014) 538-540.

[13] H. Yamada, S. Inomata, H. Tanimoto, Evaporative emissions in three-day diurnal breathing loss tests on passenger cars for the Japanese market, Atmospheric Environment, 107 (2015) 166-173.

[14] O. Amador Muñoz, P.K. Misztal, R. Weber, D.R. Worton, H. Zhang, G. Drozd, A.H. Goldstein, Sensitive detection of n-alkanes using a mixed ionization mode Proton-Transfer Reaction – Mass Spectrometer, Atmospheric Measurement Techniques Discussions, (2016) 1-21.

[15] S.T. Arnold, A. Viggiano, R.A. Morris, Rate constants and product branching fractions for the reactions of H_3O^+ and NO^+ with C_2-C_{12} alkanes, The Journal of Physical Chemistry A, 102 (1998) 8881-8887.

[16] A.R. Koss, C. Warneke, B. Yuan, M.M. Coggon, P.R. Veres, J.A. de Gouw, Evaluation of NO^+ reagent ion chemistry for on-line measurements of atmospheric volatile organic compounds, Atmospheric Measurement Techniques Discussions, (2016) 1-35.

[17] P.F. Wilson, C.G. Freeman, M.J. McEwan, Reactions of small hydrocarbons with H_3O^+, O_2^+ and NO^+ ions, International Journal of Mass Spectrometry, 229 (2003) 143-149.

[18] R. Sommariva, R.S. Blake, R.J. Cuss, R.L. Cordell, J.F. Harrington, I.R. White, P.S. Monks, Observations of the release of non-methane hydrocarbons from fractured shale, Environmental science & technology, 48 (2014) 8891-8896.

[19] S.G. Lias, J.R. Eyler, P. Ausloos, Hydride transfer reactions involving saturated hydrocarbons and CCl_3^+, CCl_2H^+, CCl_2F^+, CF_2Cl^+, CF_2H^+, CF_3^+, NO^+, $C_2H_5^+$, sec-$C_3H_7^+$ and t-$C_4H_9^+$, International Journal of Mass Spectrometry and Ion Physics, 19 (1976) 219-239.

[20] M. Tsuji, M. Aizawa, Y. Nishimura, Mass-Spectrometric Study on Ion–Molecule Reactions of CF_3^+ with PhX [X= H, CH_3, and C_2Hn (n= 1, 3, 5)] at Near-Thermal Energy, Bulletin of the Chemical Society of Japan, 68 (1995) 3497-3505.

[21] C. Dehon, J. Lemaire, M. Heninger, A. Chaput, H. Mestdagh, Chemical ionization using CF_3^+: Efficient detection of small alkanes and fluorocarbons, International Journal of Mass Spectrometry, 299 (2011) 113-119.

[22] C.J. Ennis, J.C. Reynolds, B.J. Keely, L.J. Carpenter, A hollow cathode proton transfer reaction time of flight mass spectrometer, International Journal of Mass Spectrometry, 247 (2005) 72-80.

[23] R.S. Blake, C. Whyte, C.O. Hughes, A.M. Ellis, P.S. Monks, Demonstration of proton-transfer reaction time-of-flight mass spectrometry for real-time analysis of trace volatile organic compounds, Analytical chemistry, 76 (2004) 3841-3845.

[24] R.S. Blake, K.P. Wyche, A.M. Ellis, P.S. Monks, Chemical ionization reaction time-of-flight mass spectrometry: Multi-reagent analysis for determination of trace gas composition, International Journal of Mass Spectrometry, 254 (2006) 85-93.

[25] W.B. Knighton, E.C. Fortner, S.C. Herndon, E.C. Wood, R.C. Miake-Lye, Adaptation of a proton transfer reaction mass spectrometer instrument to employ NO^+ as reagent ion for the detection of 1,3-butadiene in the ambient atmosphere, Rapid communications in mass spectrometry : RCM, 23 (2009) 3301-3308.

[26] C. Warneke, C. Van der Veen, S. Luxembourg, J. De Gouw, A. Kok, Measurements of benzene and toluene in ambient air using proton-transfer-reaction mass spectrometry: calibration, humidity dependence, and field intercomparison, International Journal of Mass Spectrometry, 207 (2001) 167-182.

[27] J.R. Eyler, P. Ausloos, S.G. Lias, Novel ion-molecule reaction involving cleavage of the carbonyl bond in ketones and aldehydes, Journal of the American Chemical Society, 96 (1974) 3673-3675.

[28] A. Ehlerding, A. Viggiano, F. Hellberg, R.D. Thomas, V. Zhaunerchyk, W.D. Geppert, H. Montaigne, M. Kaminska, F. Österdahl, M. Af Ugglas, The dissociative recombination of fluorocarbon ions III: CF_2^+ and CF_3^+ , Journal of Physics B: Atomic, Molecular and Optical Physics, 39 (2006) 805.

Chapter Four: CF_3^+ and CF_2H^+ as reagents in chemical ionization reaction mass spectrometry for the determination of VOCs

This Chapter has been published in *International Journal of Mass Spectrometry*, 2017, 421, 224-233.

4.1 Introduction

Volatile organic compounds (VOCs) possess higher vapour pressure than other organics, resulting in a large number of their molecules being in the gaseous state [1]. VOCs have two main sources: natural sources, which are often known as biogenic emissions; man-made sources, otherwise known as anthropogenic emissions [2]. It is well established that VOCs formed and emitted by the human body have a high potential for use in diagnosis in the fields of both medicine and physiology [3]. Hence, VOCs could well play an important role as non-invasive and potentially real-time methods of detecting various diseases and metabolic disorders such as early-stage cancer, asthma and the progression of therapeutic intervention [3]. A recent review reported that 1764 VOCs have been detected in human body. Among these VOCs, 874 were recorded in exhaled breath, 353 in saliva, 504 in skin emanations, 279 in urine, 130 in blood and 381 in faeces [3, 4].
Proton transfer reaction-mass spectrometry (PTR-MS) has the ability to detect various VOCs across a wide range of applications at very low concentrations and with fast response times. Blake *et al*. [5], utilized a number of different CI reagents (NO^+, NH_4^+ and O_2^+) which along with H_3O^+ in traditional PTR-MS, are grouped together as the reagent ions used in the technique chemical ionization reaction mass spectrometry (CIR-MS). CIR-MS is an online technique which allows the rapid measurement of VOCs at high time resolution [6].

In the early 1970s CF_4 was used in ion cyclotron resonance mass spectrometry (ICR-MS) as a precursor for the detection of a number of common VOCs [7-9] and more recently Dehon *et al*. [10], did similar work with some common alkanes and chloroalkanes. In Chapter 3, we showed the effectiveness of CF_3^+/ CF_2H^+ to detect small chain alkanes (C_2-C_6) [11]. In this Chapter we consider the utility of CF_3^+/CF_2H^+, as generated from CF_4^+, as reagents in CIR-TOF-MS with range of VOCs. These VOCs were chosen in accordance with the possibility of their existence in exhaled breath and human urine samples (see Chapters 5 and 6). Moreover, these compounds represent the main functional groups in organic chemistry [12] .

4.2 Experimental

The instruments used in this work were a CIR-TOF-MS (Model 4500A, Kore Technologies, Ely) which has been described in detail elsewhere (Chapter 2). All experiments were run at 100 Td or 120 Td with 60 second integration times over a mass range of 0-249 amu. One instrument used CF_4/ CF_3^+ as reagent ions whilst the second used H_2O/H_3O^+. CIR-TOF-MS instruments were supplied with CF_4 and H_2O vapour at rates of 2 and 50 ml/ min, respectively. VOC standards samples were delivered at 60 and 150 ml/ min for each of the CIR-TOF-MS instruments, respectively.

4.2.1 Stock solutions preparation

High-purity nitrogen (BOC; 99.999%) was provided for use as a dilution gas for preparation of stock of standards and for purging bags, lines and instruments. The standards (Sigma-Aldrich, Gillingham, Dorset, UK) used in this study were prepared in two stages: in the first step, 3 microlitres of the standard of interest were spiked into a Tedlar bag (Thames-Restek UK, Ltd, Saunderton, Bucks., UK) and diluted with 8 litres of N_2 to prepare a stock solution; in the second, a series of diluted standards were prepared by spiking a certain volume (concentration) of stock solution into a Tedlar bag and diluting with 8 litres N_2. A list of the VOC standards used, and their concentrations are shown in Table 4.1. The aim of producing a series of diluted standards was to create a calibration curve.

Table 4. 1: List of VOCs and their concentrations.

compound	ppmV	ppmV	compound	ppmV	ppmV
ethyl acetate	85.52	0.54	pyrrole	121.07	0.76
methyl acetate	105.68	0.66	pyridine	104.28	0.65
acrylonitrile	128.23	0.80	benzene	94.21	0.59
propionitrile	120.78	0.76	ethyl benzene	68.60	0.43
acetonitrile	160.84	1.01	toluene	79.04	0.49
acetone	114.40	0.72	styrene	73.31	0.46
2-butanone	93.77	0.57	xylene	68.13	0.43
acetaldehyde	150.27	0.94	ethanol	143.87	0.90
butanedione	96.60	0.60	octane	51.70	0.32
propanal	117.15	0.73	bromobenzene	79.98	0.50
furan	115.50	0.72	α-pinene	52.90	0.33
methyl furan	97.85	0.61	heptane	56.96	0.36
hexene	67.17	0.42	propanol	112.25	0.70
pentanone	78.90	0.49	hexanone	68.04	0.43
c. hexanone	77.75	0.49	hexanal	68.27	0.43
acrolein	125.72	0.786	DMS	113.19	0.71

4.3 Result and discussion

4.3.1 Calibration curves

Calibration curves for all VOC standards were obtained by partial dilution of stock solutions of standards with N_2. Linear responses were observed for all the VOCs analysed in this Chapter.

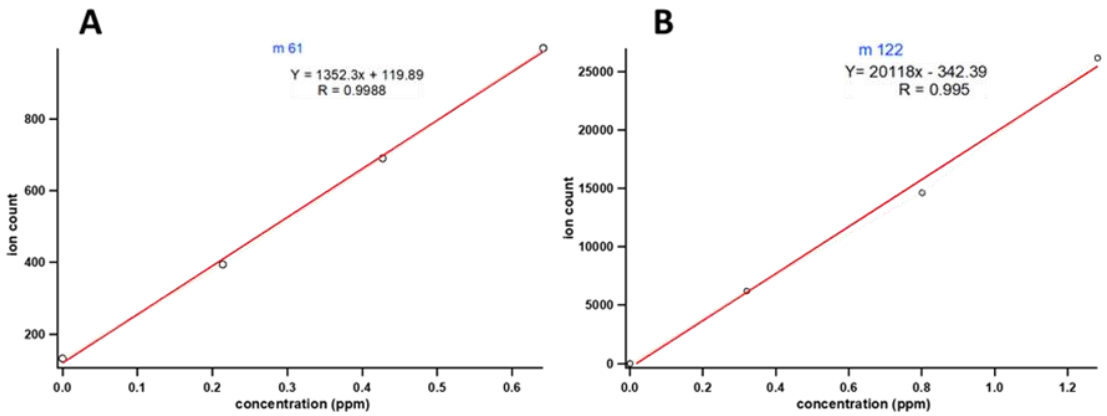

Figure 4. 1: Calibration plot from m/z 61 (carbonyl group) and m/z 122 (acrylonitrile), as produced by CF_3^+ as the reagent in CIR-MS.

4.3.2 Results and Discussion

The VOCs chosen were selected depending on the likelihood of their existence in human breath, bodily fluids and work place. Their reactions with CF_3^+ and H_3O^+ with the selected VOCs were carried out at 100 Td and 120 Td in essentially dry conditions (relative humidity < 0.01%). Under typical conditions, the main ion fragments from CF_4 in the electrical discharge source are CF_3^+ and CF_2H^+ with m/z = 69 and 51, respectively. It is believed that CF_2^+ ions have a short lifetime and may react with CF_4 to produce CF_3^+, and in some cases exist as a transitory form to produce certain other products [11, 12].

4.3.2.1 Alkanes

The results for C_2-C_6 *n*-alkanes were presented in Chapter 3 where the main mechanism was hydride transfer, as shown in Equation 4.1 [10].

$$CF_3^+ + R.H \longrightarrow R^+ + CF_4 \qquad (4.1)$$

For the longer-chain *n*-alkane, *n*-heptane and *n*-octane produce alkyl fragments as their main products. The dominant fragment ion at m/z = 57 for heptane and octane, corresponding to $C_4H_9^+$, has relative abundances of 94.7% and 50.0% respectively, followed by fragments ions for heptane and octane at m/z = 41 and 71, respectively. The results using H_3O^+ showed that no parent ion peak could be detected (see Table 4.2).

Table 4. 2: Results for alkanes with CF_3^+ and H_3O^+ as reagents in CIR-MS at *E/N* = 100 and 120 Td.

Source	Fragment	Mass	CF_3^+		H_3O^+	
			% (100 Td)	% (120 Td)	% (100Td)	% (120Td)
Heptane	$C_3H_5^+$	41	5.3	23.3	ND	ND
	$C_4H_9^+$	57	94.7	76.7		
Octane	$C_3H_5^+$	41		26.6	ND	ND
	$C_3H_6^+$	42		1.4		
	$C_3H_7^+$	43	8.2	13.6		
	$C_4H_9^+$	57	50.0	42.8		
	$C_4H_{10}^+$	58	2.0	3.2		
	$C_5H_{11}^+$	71	39.7	12.6		

Alkanes have relevance in human health, pulmonary tuberculosis has been shown to produce VOCs in human breath due to *Mycobacterium tuberculosis* infection. One of these compounds, which is considered a biomarker for pulmonary tuberculosis, is heptane [13]. Other studies have showed that *n*-heptane could be considered an exogenous contaminant [14]. Another study claimed the octane level increased in preschool children aged between 2 and 4 years during episodes of wheezing compared with other children aged 6 years with transient wheeze [15].

4.3.2.2 Alkenes

Although the main product of hexene and α-pinene with CF_3^+ as a reagent in CIR-MS is fragmentation, hexene and α-pinene also react with CF_3^+ producing a small amount of the parent ion via hydride transfer; see Tables 4.3 and 4.4.

Hexene has prominent peaks at m/z = 85, 84 and 83, which indicate parent ions of $C_6H_{13}^+$, $C_6H_{12}^+$ and $C_6H_{11}^+$, respectively, followed by fragments at m/z = 56, 43 and 41, which belong to $C_4H_8^+$, $C_4H_7^+$, and $C_4H_5^+$, respectively. The result at 120 Td showed that products arose from alkyl chain fragmentation. Similarly, the ionization of hexene with H_3O^+ produced parent ions at m/z = 85 and 86, and additionally a range of fragments. Generally, the reactions at 120 Td produced a greater amount of fragmentation compared with conditions at 100 Td. Hexene is released as a contaminant by the dialyzer materials used to treat patients with end-stage renal disease [16].

α-Pinene produces two types of peaks; principal ions at m/z = 137, 136, and 135, which belong to $C_{10}H_{17}^+$, $C_{10}H_{16}^+$ and $C_{10}H_{15}^+$, respectively, followed by fragments at m/z = 94, 93, 92, 81 and 79 which arise from $C_6H_{11}^+$, $C_7H_{10}^+$, $C_7H_9^+$, $C_6H_9^+$ and $C_6H_7^+$, respectively.

Table 4. 3: Results for hexene with CF_3^+ and H_3O^+ as reagents in CIR-MS at *E/N* = 100 and 120 Td.

Source	Fragment	Mass	CF_3^+		H_3O^+	
			% (100 Td)	% (120 Td)	% (100Td)	% (120Td)
Hexene	CH_3^+	15		8.3		
	$C_2H_3^+$	27		14.9		4.4
	$C_2H_5^+$	29		20.0		
	$C_3H_3^+$	39		6.3		2.5
	$C_3H_5^+$	41	3.7	12.7		29.1
	$C_3H_7^+$	43	33.6	14.0	26.1	43.9
	$C_4H_7^+$	55		13.6		
	$C_4H_8^+$	56	2.4			
	$C_4H_9^+$	57			5.8	12.7
	$C_5H_{11}^+$	71		7.8		
	$C_5H_{13}^+$	73	3.4			
	$C_6H_{11}^+$	83	39.0			
	$C_6H_{12}^+$	84	3.0			
	$C_6H_{13}^+$	85	4.6		63.7	7.5
	$C_6H_{14}^+$	86			4.5	
		91	10.2	2.5		

A similar result was obtained through the use of H_3O^+ with α-pinene, with a higher percentage of parent ions produced when running the experiment at 100 Td. A study conducted in coniferous forests showed that concentration of pinonaldehyde, which is produced from the oxidation of α-pinene, was highest (0.15 ppbV) in the morning, while other compounds were found to be highest around midday [17] . α-Pinene and ozone could lead to aerosol formation by photochemical oxidation during the morning in coastal regions [18]. PTR-MS measurements detected the acetone and pinonaldehyde produced by the oxidation of α-pinene in the air in the presence of NO_x [19].

Table 4. 4: Results for α-pinene with CF_3^+ and H_3O^+ as reagents in CIR-MS at *E/N* = 100 and 120 Td.

Source	Fragment	Mass	CF_3^+		H_3O^+	
			% (100 Td)	% (120 Td)	% (100Td)	% (120Td)
α-Pinene	$C_2H_3^+$	27	2.7			
	$C_3H_5^+$	41		4.1		
	$C_6H_5^+$	77		12.5		
	$C_6H_7^+$	79	3.8	3.8		
	$C_6H_9^+$	81	6.8		31.3	53.8
		82			1.8	3.6
	$C_7H_7^+$	91		17.3		
	$C_7H_8^+$	92	7.2	26.2		

continued

$C_7H_9^+$	93	40.9	28.0		
$C_7H_{10}^+$	94	3.5			
$C_6H_{11}^+$	95	2.9			
	107	7.3	4.8		
$C_{10}H_{15}^+$	135	15.6	3.3	2.7	
$C_{10}H_{16}^+$	136	4.0			
$C_{10}H_{17}^+$	137	5.7		56.5	38.8
	138			6.3	
	153			1.2	

4.3.2.3 Alcohols

In contrast to H_3O^+, which gave the protonated alcohols of ethanol, methanol and propanol with relative abundances of 78%, 99% and 88%, respectively, the alcohols do not seem to be particularly reactive with CF_3^+.

Ethanol reacts to produce alkyl fragments, which at m/z = 29 could be either $C_2H_5^+$ or HCO^+ with a relative abundance of around 50%. In addition, ethanol produces a protonated alcohol due to the competition between both precursors, CF_3^+ and H_3O^+, with a relative abundance of 25%, see Table 4.5. In a similar manner**,** propanol formed a high proportion of a fragment at m/z = 43, which could arise from $C_3H_7^+$ as a result of fragmentation of its fragile alkyl chain or from CH_3CO^+, which may result from hydride extraction, with a relative abundance of around 75%. CH_3CO^+ is the more likely of the two because the result at 120 Td showed the appearance of the $C_2H_3^+$ fragment in high abundance. Also, propanol produced a peak at m/z = 131, which may belong to $CH_3(CH_2)_2OH_2.CF_3H^+$ as a result of the combination of CF_3^+ with the alcohol. The presence of a small percentage of the protonated alcohol was also detected. Methanol seems to resist reacting with CF_3^+. Generally, the reactions at 120 Td produced a greater abundance of fragmentation compared with conditions at 100 Td; see Table 4.6.

Table 4. 5: Results for ethanol with CF_3^+ and H_3O^+ as reagents in CIR-MS at *E/N* = 100 and 120 Td.

Source	Fragment	Mass	CF_3^+		H_3O^+	
			% (100 Td)	% (120 Td)	% (100Td)	% (120Td)
Ethanol	$C_2H_3^+$	27	7.7	46.9	3.8	55.3
	$C_2H_5^+$/ HCO^+	29	55.7		15.5	
	$CH_3CH_2OH^+$	45	11.4	53.1		
	$CH_3CH_2OH_2^+$	47	25.2		77.5	44.3
	$CH_3CH_2OH_2^+$	48			3.2	

Table 4. 6: Results for methanol and propanol with CF_3^+ and H_3O^+ as reagents in CIR-MS at *E/N* = 100 and 120 Td.

Source	Fragment	Mass	CF_3^+		H_3O^+	
			% (100 Td)	% (120 Td)	% (100Td)	% (120Td)
Methanol	CH_3^+	15				1.3
	CH_3OH^+	32				1.9
	$CH_3OH_2^+$	33			98.8	95.6
	$CH_3OH_3^+$	34			1.2	1.2
Propanol	$C_2H_3^+$	27		61.6		
	$C_3H_3^+$	39		19.9		6.6
	$C_3H_5^+$	41		18.5	9.1	51.1
	$C_3H_6^+$	42				1.7
	$C_3H_7^+$/ CH_3CO^+	43	74.8		87.8	37.9
	$C_3H_8^+$	44			3.1	
	$CH_3CH_2CH_2O^+$	59	3.1			2.7
	$CH_3CH_2CFH^+$	61	4.7			
		62	3.1			
		63	2.3			
	$C_3H_7OH_2.CF_3H^+$	131	12.0			

Ethanol and methanol concentrations in endogenous breath have been found to be in the range between 0.20 to 0.70 ppbV, and 0.57 to 4.01 ppbV, respectively, in healthy individuals [20]. A higher ethanol concentration was found in the breath of patients with obesity-related liver disease and female obesity [21]. A study conducted on healthy volunteers via selected ion flow tube mass spectrometry (SIFT-MS) found that the mean concentration of ethanol was 196 ppbV, and that this level was observed to increase if food or sweet drinks had been consumed in the two hours before collecting breath samples [22]. Methanol, one of the VOCs found in human breath, is found in lower levels in patients with lung cancer compared to healthy volunteers [23]. There are two sources of nutrition for methanol; methanol as a by-product of alcoholic fermentation, and also as found in certain fruits such as apples. It has been found that apples increase the endogenous source of methanol in human breath [24]. A study revealed that the concentration of methanol and some other VOCs were increased in patients within a cancer cohort compared with healthy subjects [25]. Methanol and ethanol show significant differences in patients with cirrhosis compared to those in healthy subjects [26, 27]. A study showed that the consumption of ethanol could reduce the activity of liver alcohol dehydrogenase (ADH) [28]. A number of reports in the literature have demonstrated that 1-propanol is a VOC that could potentially act as a biomarker for lung

cancer [29]. Among 21 prespecified VOCs, the level of 2-propanol was found to be increased in patients with pulmonary arterial hypertension [30].

4.3.2.4 Ketones and aldehydes

Infrared multiple photon dissociation (IRMPD) results showed that a range of ketones exhibit a stretching action of their C=O bonds due to the CF_3^+ fragment. Similar mechanisms include an electrophilic reaction between CF_3^+ ion and the carbonyl oxygen to produce an intermediate state. This intermediate is exothermic ($\Delta H < -200$ kJ mol^{-1}) and short-lived, decaying rapidly to form a fluorine-stabilized carbocation, as per Equation 4.2 [8, 12, 31].

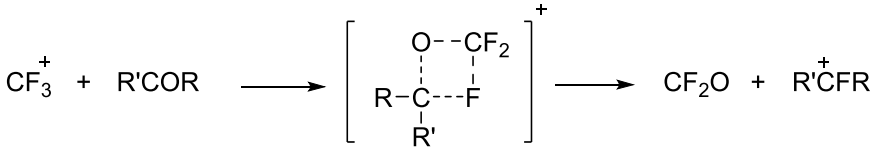

(4.2)

Displacement reactions such as one shown in Equation 4.3 have been noticed to occur where there were weak bonds in the carbonyl group [8].

$$CF_3^+ + RCOR \longrightarrow RCO^+ + R'CF_3 \quad (4.3)$$

At *E/N* = 100 Td, acetone formed the RCF_3^+ cation at m/z = 127, which may belong to $CH_3COCH_3.CF_2^+$, with a relative abundance of 64%. The peak at m/z = 61 might belong to $CH_3CFCH_3^+$, as produced by the substitution of oxygen by a fluorine atom. Another species was produced by the protonated molecule ion at m/z = 59, which arose from the competitive action between H_3O^+ with CF_3^+. Similar behaviour was observed at *E/N* = 120 Td with an extra fragment observed at m/z = 41, which may correspond to an alkyl fragment. The main product of the hydronium ion with acetone was a protonated molecule ion, as shown in Table 4.7.

Acetone represents one of the most abundant compounds in human breath, and is considered a sign of dextrose metabolism and lipolysis [32]. The concentration of acetone has been found to be higher (234 nmol/l) in patients with congestive heart failure (CHF) compared with patients without CHF (57 nmol/l) and healthy controls (47 nmol/l) [33]. Acetone concentrations were detected using GC-MS and solid-phase microextraction (SPME) with on-fibre derivatization; its concentrations were found to be 1.71 ppmV and 0.76 ppmV in diabetics' and healthy subjects' breath, respectively [34].

Table 4. 7: Results for butanone with CF_3^+ and H_3O^+ as reagents in CIR-MS at *E/N* = 100 and 120 Td.

Source	Fragment	Mass	CF_3^+		H_3O^+	
			% (100 Td)	% (120 Td)	% (100Td)	% (120Td)
Acetone	$C_3H_5^+$	41		24.2		
	$CH_3COHCH_3^+$	59	12.9	9.9	96.7	97.0
	$CH_3CHOHCH_3^+$				3.3	3.0
	$CH_3CFCH_3^+$	61	23.2	34.1		
	$CH_3COCH_3.CF_2^+$	127	63.9	31.8		

A study conducted to measure concentration of acetone in healthy volunteers for a period of six months using SIFT-MS showed the average concentration of acetone was 477 ppbV [35]. Another study showed that there was a high correlation between acetone concentration in patients with uncontrolled diabetes mellitus (0.3 ppmV to 1 ppmV) and the blood glucose concentration in the same patients [36]. It has also been demonstrated that acetone can be produced by the reaction of ozone with human skin lipids [37]. Acetone levels have been shown to be raised towards the end of perioperative periods of laparoscopic operations, which could be due to the onset of lipolysis [38]. In addition, acetone was found to be increased in cancer patients after surgery [39]. The acetone concentration in human breath increases overnight (during sleep) by a factor of up to four [40]. A study demonstrated that a positive correlation could be seen between exhaled acetone and same-day serum C-reactive protein (CRP) in pneumonia patients, with acetone concentrations and CRP levels decreasing by up to 90% from the day of admission to the day the patient was discharged [41]. Acetone is one of the VOCs which is observed to give higher concentrations in urine, ranging from 300 to 630 ppbV, with the associated variability relying on the diet of the subjects, their medical state, level of dehydration and environmental exposure [42]. Many studies have been conducted to measure VOCs in the environment and the atmosphere to find the effect and contribution of this compound on human surroundings. A study was conducted in the Mediterranean Sea using PTR-MS, which showed that burning biomass is a source of acetone, the percentage of which was 1.8% [43]. Atmospheric oxidation of terpenes seems to be a major source of acetone in the atmosphere [19]. The concentrations of acetone in the northern hemispheric boundary layer and free troposphere were 2.5 ppbV and 1.0 ppbV, respectively [44].

Butanone formed two principal product fragments, one at m/z = 75 which was produced by replacing the oxygen atom in the carbonyl group with fluorine, whilst the second at m/z = 55 which can be assigned to $C_4H_7^+$, may be the result of dehydration of the carbonyl group. More fragments were noticed when the experiment was run at *E/N* = 120 Td. H_3O^+ formed more consistent products producing protonated molecular ions at both 100 and 120 Td; see Table 4.8.

Table 4. 8: Results for butanone with CF_3^+ and H_3O^+ as reagents in CIR-MS at *E/N* = 100 and 120 Td.

Source	Fragment	Mass	CF_3^+		H_3O^+	
			% (100 Td)	% (120 Td)	% (100Td)	% (120Td)
Butanone	$C_2H_3^+$	27		19.2		
	$C_2H_5^+$	29		56.8		
	$C_3H_3^+$	39		7.4		
		47	5.5			
	$C_4H_5^+$	53		1.7		
	$C_4H_7^+$	55	41.5	14.9		
	$C_2H_5COHCH_3^+$	73	6.3		95.6	94.3
	$C_2H_5CHOHCH_3^+$	74			4.4	4.2
	$C_2H_5CFCH_3^+$	75	45.0			
	$C_2H_5COCH_3.CF_3^+$	141	1.8			

A variety of microorganisms such as *Lactococcus lactis* have been found to produce malodorous emissions from many VOCs during domestic organic waste collection using PTR-MS. Butanone is one of these compounds, which confirms a positive correlation with pure culture of *Lactococcus lactis* after two hours [45]. 2-butanone was found to be within 12 compounds made–significantly–in cirrhotic patients (CP) compared to healthy subjects [26, 46]. 2-Butanone has been reported as being a major biomarker of lung cancer [23, 29, 47, 48].

As the number of carbons increases in the ketones, cleavage to produce acetyl groups/ alky groups can occur. Pentanone formed a fragment at m/z = 43 which may correspond to either $C_3H_7^+$ or CH_3CO^+. It seems that part of the acyl group, in the presence of CF_3^+, formed $CH_3CHO.CF_3^+$ at m/z = 113 with a relative abundance of 71.4%. An increased number of fragments were noticed at 120 Td. In the accompanying PTR-MS work, H_3O^+ formed the protonated molecular ion at both 100 and 120 Td; see Table 4.9.

Urine releases a variety of VOCs which could be used to identify many diseases. A study showed that 2-pentanone may have some degree of utility in detecting lung cancer [49].

Pentanone was one of the VOCs that could distinguish cirrhotic patients (CP) from healthy controls [19, 39]. A study was conducted to detect VOCs released by rat L6 skeletal muscle cells using GC-MS. The authors found that pentanone is one of the compounds released by these cells [50].

Table 4. 9: Results for pentanone with CF_3^+ and H_3O^+ as reagents in CIR-MS at *E/N* = 100 and 120 Td.

Source	Fragment	Mass	CF_3^+		H_3O^+	
			% (100 Td)	% (120 Td)	% (100Td)	% (120Td)
Pentanone	$C_2H_3^+$	27		18.0		
	$C_2H_5^+$	29	2.7			
	$C_3H_3^+$	39		14.2		
	$C_3H_5^+$/ $CHCO^+$	41		49.0		
	$C_3H_7^+$/ CH_3CO^+	43	16.8			
	CH_3CHOH^+	45				10.0
	CH_3CFH^+	47	2.9			
	$C_4H_9^+$	57	3.3			
	$C_5H_9^+$	69				2.4
	$C_3H_7COHCH_3^+$	87			95.6	87.6
	$C_3H_7CHOHCH_3^+$	88			4.4	
	$CH_3CHO.CF_3^+$	113	71.4	18.7		
	$CH_3CHOH.CF_3^+$	114	2.9			

Hexanone formed two peaks at m/z = 83 which may correspond to $C_6H_{11}^+$ and were result of dehydration of the carbonyl group. The other peak arises at m/z = 113 which may result from a combination of the acyl group with the CF_3^+ ion. Both peaks represent a third of the product ions. In addition, there were some fragments at m/z = 43, which may belong to $C_3H_7^+$/ CH_3CO^+, and m/z = 61, which resulted from the replacement of oxygen atom in the carbonyl group with fluorine. The result at 120 Td, showed that products arose from alkyl chain fragmentation. The PTR-MS result showed that consistent products produced protonated molecular ions at both 100 and 120 Td; see Table 4.10.

Human breath and urine contain a variety of VOCs which may help to identify diseases. Hexanone was one of the compounds found exclusively in subjects who were smokers [14]. Another study showed that hexanone, one of the VOCs that may be used as a potential marker owing to its presence in human urine, can thus be verified as useful in other fields of study, such as forensics [51].

Table 4. 10: Results for hexanone with CF_3^+ and H_3O^+ as reagents in CIR-MS at *E/N* = 100 and 120 Td.

Source	Fragment	Mass	CF_3^+		H_3O^+	
			% (100Td)	% (120Td)	% (100Td)	% (120Td)
Hexanone	$C_2H_3^+$	27		10.7		
	$C_2H_5^+$	29		47.0		
	$C_3H_3^+$	39		4.8		
	$C_3H_5^+$/ $CHCO^+$	41		8.4		
	$C_3H_7^+$/ CH_3CO^+	43	11.0	10.7		
		45		4.2		
	$C_4H_7^+$	55		14.1		
	$CH_3CH_2CFH^+$	61	14.0			
	$C_6H_{11}^+$	83	32.9			
	$C_4H_9COHCH_3^+$	101	10.8		93.4	83.1
	$C_4H_9CHOHCH_3^+$	102			6.6	5.9
	$CH_3CHO.CF_3^+$	113	31.3			

Cyclohexanone formed the predominant peak at m/z = 81, which may form as a result of the dehydration of cyclohexanone. In a similar manner, the experiment conducted at 120 Td resulted in a signal at m/z = 81, but with more alkyl fragments. H_3O^+ results showed the protonated molecular ion at both 100 and 120 Td; see Table 4.11.

Human breath consists of many VOCs which are considered to have potential to characterise diseases and changes in metabolism. A study conducted on cancer patients showed cyclohexanone to be one of the VOCs which decreased during any related surgery [39].

Butanedione saw the formation of its major product at m/z = 87, which corresponds to a protonated molecular ion resulting from the competition between H_3O^+ with CF_3^+, followed by a signal at m/z = 43 which may be an acyl group fragment. The low abundance fragment at m/z = 114 may have arisen from a combination of the acyl group with CF_3^+. The low abundance peak at m/z = 135 can be assigned to $CH_3COCOCH_3.CF_2^+$. Other small unknown fragments at m/z = 117 and 127 were also detected. The mass spectrum produced at 120 Td showed that butanedione's predominant peak was at m/z = 43, which may belong to an acyl group, followed by a signal at m/z = 27 which considered to be that of $C_2H_3^+$. A small peak at m/z = 61 was recorded that belongs to a carbonyl group where the oxygen atom has been replaced by a fluorine. A protonated parent ion was detected when using H_3O^+ as the reagent in CIR-MS; see Table 4.11.

Table 4. 11: Results for cyclohexanone and butanedione with CF_3^+ and H_3O^+ as reagents in CIR-MS at *E/N* = 100 and 120 Td.

Source	Fragment	Mass	CF_3^+		H_3O^+	
			% (100Td)	% (120Td)	% (100Td)	% (120Td)
C. hexanone	$C_2H_3^+$	27		2.8		
	$C_3H_5^+$	41		9.7		
		53		3.3		
	$C_4H_7^+$	55	3.1	4.3		
	$CH_3CH_2CH_2O^+$/ CH_2CHCFH^+	59		1.8		
	$C_6H_8^+$	79		4.5		
	$C_6H_9^+$	81	81.1	67.3		5.1
	$C_6H_{10}^+$	82		4.4		
	$(CH_2)_5COH^+$	99	13.5		93.7	88.9
	$(CH_2)_5CHOH^+$	100			6.3	6.0
		125	2.2	2.0		
Butanedione	CH_3^+	15		22.1		
		41		3.2		
	CH_3CO^+	43	27.9	69.8		
		59		1.5	1.0	10.1
	$CH_3CH_2CFH^+$	61		3.4		
	$CH_3CHOCOCH_3^+$	87	44.8		99.0	82.1
	$CH_3CHOHCOCH_3^+$	88				7.8
	$CH_3CHOH.CF_3^+$	114	7.8			
		117	2.6			
		127	4.9			
		131	3.1			
	$CH_3COCOCH_3.CF_2^+$	135	8.9			

The layer of soil known as the rhizosphere is important owing to the presence of the roots of plants and is thought to supply up to 20% of photosynthetically fixed carbon. This media helps microbes to release VOCs. One of these compounds, 2,3-butanedione, has been found to be released from *Arabidopsis* roots [2, 52]. Butanedione is also released from ground roasted coffee beans after warm water (18ºC) is added [2, 53]. Animal houses emit a variety of VOCs; a study showed butanedione was one of 14 VOCs emitted from pigsties, for instance [2, 54].

Propanal shows the principle peaks in its mass spectrum at m/z = 61, 59 and 41. The peak at m/z = 61 might belong to $CH_3CFCH_3^+$, produced by the substitution of oxygen by fluorine. The signal at m/z = 59 arises from protonation of the parent ion due to competition between CF_3^+ and H_3O^+ in CIR-MS. Low abundance fragments at m/z = 62, 57 and 41were also detected. Increasing the *E/N* to 120 Td resulted in a reduced of

abundance the ion at m/z = 61 whilst an increase in the fragments were observed at m/z = 41 and 39. Proton transfer reactions with H_3O^+ produced the protonated parent ion almost exclusively at 100 Td, though with an increased number of fragments at 120 Td; see Table 4.12.

Table 4. 12: Results for propanal with CF_3^+ and H_3O^+ as reagents in CIR-MS at *E/N* = 100 and 120 Td.

Source	Fragment	Mass	CF_3^+		H_3O^+	
			% (100Td)	% (120Td)	% (100Td)	% (120Td)
Propanal	$C_3H_3^+$	39		26.1		22.6
	$C_3H_5^+$	41	12.9	43.5		7.8
	$CH_3CH_2CO^+$	57	8.1			2.4
	$CH_3CH_2CHOH^+$	59	18.4	6.5	96.7	64.9
	$CH_3(CH_2)_2OH^+$	60			3.3	2.2
	$CH_3CH_2CFH^+$	61	57.9	23.9		
	$CH_3CH_2CFH_2^+$	62	2.7			

Hexanal exhibits alkyl chain fragmentation due to its longer carbon chain. The main fragment in its mass spectrum at m/z = 83 may result from dehydration of hexanal to form hexene. The other main fragment was observed at m/z = 55 due to cleavage of the chain at C_4. Small fragments were produced at C_4 and C_6. At 120 Td, alkyl chain fragmentation arose at C_2, C_3, C_4 and C_6. The protonated molecules arising from H_3O^+ represented only around 25% of the total products, and further were only seen only at 100 Td. The final main fragment at m/z = 83 was formed by the dehydration of hexanal, and was observed at both 100 and 120 Td. Other small fragments were observed at C_4 and C_6 in both cases; see Table 4.13.

A study was conducted to measure the VOCs emitted during the exposure of human skin to UVR using PTR-MS and laser-based photoacoustic detection, the results of which showed that propanal was one of the VOCs emitted that directly reflected the damage caused by UVR [55, 56]. Human urine contains a variety of VOCs which could be used as the biomarkers for, and fingerprints of, a variety of diseases. Propanal levels have also been found to decrease significantly in healthy human urine samples stored for four days [48].

Table 4. 13: Results for hexanal with CF_3^+ and H_3O^+ as reagents in CIR-MS at *E/N* = 100 and 120 Td.

Source	Fragment	Mass	CF_3^+		H_3O^+	
			% (100Td)	% (120Td)	% (100Td)	% (120Td)
Hexanal	$C_2H_5^+$	29		44.3		
	$C_3H_3^+$	39		10.8		
	$C_3H_5^+$	41		10.8		
	$C_3H_7^+$	43		7.2		
	$C_4H_7^+$	55	45.1	19.4	2.7	33.7
	$C_4H_8^+$	56	1.9			
	$C_4H_9^+$	57	5.4			
	$C_2H_5CFH^+$	61		2.0		
	$C_6H_9^+$	81	2.5	2.3		
	$C_6H_{11}^+$	83	39.2	3.1	66.8	59.3
	$C_6H_{12}^+$	84	2.4		4.1	4.1
	$C_6H_{13}O^+$	101	3.5		24.9	
	$C_6H_{13}OH^+$	102			1.5	
	$C_6H_{12}O.H_2O^+$	117				2.0

Studies have been conducted with lung cancer patients, smokers and healthy volunteers using GC-MS, the results of which showed that hexanal was significantly higher in lung cancer patients as compared with smokers and healthy subjects [57-59]. Preliminary clinical studies have been conducted on non-small cell lung cancer (NSCLC) to investigate whether the presence of straight-chain aldehydes (C_3-C_9) such as hexanal could be used as a diagnostic tool for early lung cancer. The results showed that the levels of these aldehydes were elevated in this instance compared to healthy volunteers and volunteers who smoked [60]. Another study was conducted on a group of lung cancer patients and healthy smoker and non-smoker volunteers via the use of the SPME-GC-MS method. The statistical analysis (discriminant analysis) of the data showed that hexanal, pentanal, and nonane were only detected in cancer patients [61]. Similarly, the concentration of hexanal was found to be higher in the blood headspace of lung cancer patients as compared with healthy volunteers [62]. Hexanal urinary concentrations were found to be elevated in cancer patients (0.24-4.36 pg μL^{-1}) compared to a healthy control [63]. In addition, hexanal was found to be higher in oesophageal and gastric malignancy patients compared with a healthy control [64].

It is well known that CF_3^+ preferentially attacks the carbonyl group in aldehydes [8]. Acetaldehyde produces two main peaks at m/z = 47 and m/z = 113. The first peak is formed by the replacement of the oxygen atom in the carbonyl group with a fluorine atom to form CH_3CFH^+. The other peak at m/z = 113 emerges from the combination of

acetaldehyde ion with CF_3^+ to form $CH_3CHO.CF_3^+$. There were also some small signals at m/z = 45, 73, 75 and 110. At 120 Td, acetaldehyde produced only three peaks. Signals were seen at m/z = 113, which was similar to the 100 Td result, as was a fragment at m/z = 27 due to the higher energy used. Another peak at m/z = 45 appeared due to protonation of the parent ion, and was unusually higher in intensity than the result at 100 Td. This was confirmed by the spectra seen in PTR-MS. A low intensity was seen at m/z = 45, and was actually found to increase at 120 Td compared with the result at 100 Td (which, generally speaking, should not happen); see Table 4.14.

Table 4. 14: Results for acetaldehyde with CF_3^+ and H_3O^+ as reagents in CIR-MS at *E/N* = 100 and 120 Td.

Source	Fragment	Mass	CF_3^+		H_3O^+	
			% (100Td)	% (120Td)	% (100Td)	% (120Td)
Acetaldehyde	$C_2H_3^+$	27		45.9		
	CH_3CHOH^+	45	7.4	27.2	97.6	97.8
		46			2.4	2.2
	CH_3CFH^+	47	39.0			
		73	2.9			
		75	16.0			
		110	6.0			
	$CH_3CHO.CF_3^+$	113	28.7	26.9		

Acetaldehyde is formed mainly in the human body by enzymatic oxidation of ethanol, and which is later converted to acetic acid and water. Another ethanol-dependent source of acetaldehyde could result from bacterial fermentation in the intestines. A previous study was conducted on teetotal subjects by collecting breath samples and analysing them using GC-MS. The results of this study showed that the concentration of endogenous levels of acetaldehyde ranged from 0.7 to 11.0 ng/litre [65]. PTR-MS was used to analyse VOCs emitted by *in vitro* cultured cancerous and non-cancerous human cells. Among the VOCs detected in this study was acetaldehyde, which sees significant utilization by cancerous, but not non-cancerous, cells [66]. A study was conducted to measure the change in VOCs in metabolite emission by *Mycobacterium smegmatis* after administration of the antibiotics ciprofloxacin and gentamicin using PTR-MS; acetaldehyde was found to show a three-fold increase within four hours of administration [67]. The consumption and release of VOCs by bacteria such as *Staphylococcus aureus* and *Pseudomonas aeruginosa* could potentially represent a biomarker for ventilator-associated pneumonia. Acetaldehyde was found to be consumed by *P. aeruginosa* but

emitted by *S. aureus* [68]. A longitudinal study was conducted to measure VOCs in exhaled breath in healthy individuals using SIFT-MS, in which the concentration of acetaldehyde was found to be within the range of 0 to 104 ppbV [22]. Acetaldehyde has also been demonstrated to be present in the headspace of urine and was shown by Huang *et al*. to be one of the VOCs found to be present in relatively high amounts in patients with gastro-oesophageal cancer, as compared with healthy cohorts [25].

Acrolein (propenal) produced two mean peaks at m/z = 59 and 125, which were formed from replacement of the oxygen atom with a fluorine atom and the combination of the parent molecule with CF_3^+, respectively. It seems that changing energy, *E/N*, during an experimental run on acrolein with CF_3^+ and H_3O^+ using CIR-MS showed almost no effect on the results. A small fragment was observed at m/z = 57 which resulted from the protonated parent molecule. Hydronium reactions produced a strongly protonated molecular ion; see Table 4.15. The release of VOCs from cells such as muscle cells supplies information as to the origin of these VOCs in breath samples. Associated studies have been conducted on animal muscle cells (rat L6 skeletal muscle cells) being used as models for human skeletal muscle cells. In this study, the researchers attempted to discover the origin and metabolic fate of endogenous VOCs in breath and skin emanations. Propenal was found to be one of the aldehydes being uptaken by muscle cells [52].

Table 4. 15: Results for acrolein with CF_3^+ and H_3O^+ as reagents in CIR-MS at *E/N* = 100 and 120 Td.

Source	Fragment	Mass	CF_3^+		H_3O^+	
			% (100Td)	% (120Td)	% (100Td)	% (120Td)
Acrolein	$CH_2CHCHOH^+$	57	10	4.1	96.3	96.5
	$CH_3CH_2CHOH^+$	58			3.7	3.5
	CH_2CHCFH^+	59	40.9	53.4		
	$CH_2CHCHO.CF_3^+$	125	49.1	42.5		

4.3.2.5 Acetates

The behaviour of ethyl acetate and methyl acetate differ considerably from each other in terms of fragmentation. Ethyl acetate cleaves into CH_3CO^+, as seen at m/z = 43, and represents the most abundant ion. The other fragment was observed at m/z = 61, which represented $CH_3COOH_2^+$ or $CH_3CH_2CFH^+$, the former seeming the most likely owing to the same peak being observed with hydronium. There were also two low abundance ions

at m/z = 89, which emerged from protonation of the parent ion, and at m/z = 129, which was formed from a combination of the ethyl acetate ion with a carbonyl group (first cleavage). At 120 Td, the mass spectrum showed its main fragment to be at m/z = 43, similar to the results obtained at 100 Td, but with further fragments at m/z = 15 and 27. The results of using the hydronium ion were somewhat different from those of previous compounds, as the protonated molecule represents 61% and 4 % of the total abundance at 100 and 120 Td, respectively, while the fragment at m/z = 61 represent 35% and 82% of the total abundance at 100 and 120 Td, respectively. It seems the cleavage of ethyl acetate into the $CH_3COO^+$and CH_3CO^+ ion represents the first step in the reaction mechanism, followed by other steps such as protonation, or replacement of oxygen atom by CF^+, in the acetate group for the H_3O^+ and CF_3^+, respectively; see Table 4.16.

A study was conducted on exhaled breath samples for patients infected with *H. pylori* and healthy controls by using SPME-GC-MS, the results of which showed that ethyl acetate was one of the endogenous VOCs detected in breath samples of *H. pylori*-infected patients but not the healthy controls [69]. Many VOCs may be emitted from rhizosphere and different parts of plant such as roots which could result from biotic stresses. Some volatile organic compounds such as ethyl acetate were detected from root of Arabidopsis [2]. The atmosphere contains many anthropogenic and biogenic VOCs which may affect air quality. PTR-MS was used to detect VOCs on a rooftop in industrial and residential areas in Mexico City, where ethyl acetate was one of the thirty-eight individual ions monitored during this study [2].

Table 4. 16: Results for ethyl acetate with CF_3^+ and H_3O^+ as reagents in CIR-MS at *E/N* = 100 and 120 Td.

Source	Fragment	Mass	CF_3^+		H_3O^+	
			% (100Td)	% (120Td)	% (100Td)	% (120Td)
ethyl acetate	CH_3^+	15		22.2		
	$C_2H_3^+$	27		6.8		
	CH_3CO^+	43	67.4	65.8	1.6	12.2
	$CH_3CH_2CFH^+$/ $CH_3COOH_2^+$	61	19.8	5.2	35.0	82.1
	$CH_3CHOHOH^+$	62				1.6
	$C_2H_5OCOHCH_3^+$	89	4.3		60.9	4.1
		90			2.5	
	$C_2H_5OCOCH^+$. $COCH_3$	129	8.4			

Methyl acetate gave rise to a peak at m/z = 143 which was formed by a combination of the analyte with CF_3^+. In addition, small peaks emerged at m/z = 144 which belonged to the protonated fragment of m/z = 143. Other fragments at m/z = 75 arose from the protonated molecular ion, followed by signal at m/z = 43 that belonged to CH_3CO^+, which was formed by cleavage of the carbonyl group. A small peak that arose at m/z = 131 could have been the result of a combination of CF_3^+ with a protonated acetyl group. The results at 120 Td showed only two peaks at m/z = 143 and 43, which was similar to results found at 100 Td. H_3O^+ produced mostly the protonated parent ion at 100 Td. Ionization conducted at 120 Td also produced the protonated parent ion, with some additional fragmentation observed at m/z = 43; see Table 4.17. During exercise the dynamics of VOCs in exhaled breath can be changed. The methyl acetate concentration has been shown to change by a factor of 3-5 within 1 min during pedalling [70]. Many types of food release flavours which may be used for quality specification and control. Methyl acetate is one of the VOCs detected in exhaled breath after consuming palm oil [71].

Table 4. 17: Results for methyl acetate with CF_3^+ and H_3O^+ as reagents in CIR-MS at *E/N* = 100 and 120 Td

Source	Fragment	Mass	CF_3^+		H_3O^+	
			% (100Td)	% (120Td)	% (100Td)	% (120Td)
methyl acetate	CH_3CO^+	43	10.6	28.9		9.0
	$CH_3OCOHCH_3^+$	75	18.5		96.7	88.0
		76			3.3	2.9
	$CH_3CHOHOCF_3H^+$	131	2.6			
	$CH_3OCOCH_3.CF_3^+$	143	65.4	71.1		
	$CH_3OCOCH_3.CF_3H^+$	144	3.0			

4.3.2.6 Aromatic compounds

With aromatic compounds CF_3^+ acts as a Lewis acid (an electrophile) reacting with the nucleophilic cyclic compounds [72]. A plausible explanation for the different outcomes for the ionization of aromatic compounds with CF_3^+ may be attributed to the stability of the cations generated. O-xylene reacts with CF_3^+ in aromatic electrophilic substitution reaction, as shown in Figure 4.2 (upper part). The resulting cation has a resonance structure B (benzylic cation) which is more stable than resonance structure A. However, in the instance of styrene, electrophilic addition is the favoured mechanism because the π-electron of the vinyl group of styrene is more nucleophilic than the aromatic π-electron. The resulting cation is a stabilized benzylic cation, as shown in Figure 4.2 (lower part).

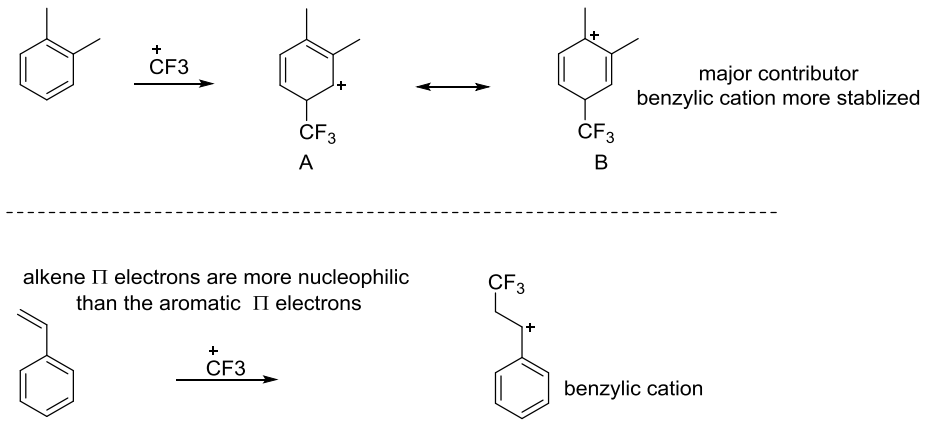

Figure 4. 2: Reaction mechanism of CF_3^+ with *o*-xylene and styrene.

The reaction of benzene and toluene with CF_3^+, however, also occurs by aromatic electrophilic substitution. Intermediate I loses HF to form benzylic cation II. The driving force for losing HF is the formation of the benzylic cation; see Figure 4.3. In the instances of xylene and styrene, the benzylic cations were generated directly from the reaction with CF_3^+ without the need for HF as a leaving group; see Figure 4.2.

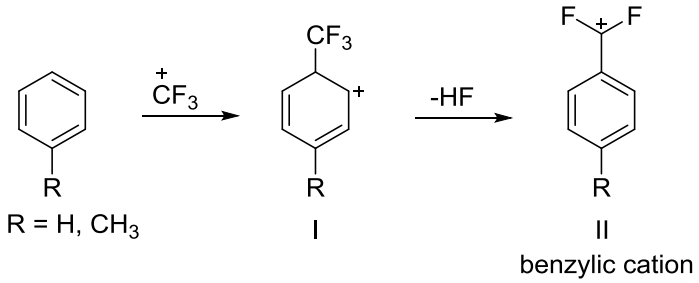

Figure 4. 3: Reaction mechanism of CF_3^+ with benzene and toluene.

Benzene's main product at m/z = 127 formed from the addition of CF_2^+ to the benzene ring. Small fragments appeared at m/z = 79 and 128, which resulted from protonation of the molecular ion, and a mass of 127, respectively. An unknown signal was detected at m/z = 109. The spectra recorded at 120 Td were similar to those recorded at 100 Td but with lower abundance of the m/z = 127 signal and additional small fragments at m/z = 43, 78, 79, 83, 109 and 128. This could have been caused by high energy of the 120 Td experiment. Hydronium reactions produced a strong protonated molecular ion signal; see Table 4.18.

Table 4. 18: Results for benzene with CF_3^+ and H_3O^+ as reagents in CIR-MS at *E/N* = 100 and 120 Td.

Source	Fragment	Mass	CF_3^+		H_3O^+	
			% (100Td)	% (120Td)	% (100Td)	% (120Td)
Benzene	$C_3H_7^+$	43		6.0		
	$C_6H_6^+$	78		4.7		
	$C_6H_7^+$	79	4.9	3.3	94.4	39.9
	$C_6H_8^+$	80			5.6	6.1
		83		2.8		
		109	2.7	4.9		
	$C_6H_5.CF_2^+$	127	87.7	73.2		
	$C_6H_5.CF_2H^+$	128	4.7	5.1		

Many VOCs emitted from the environment, exhalation and human bodily fluids have the potential to be used as markers for diseases/ disorders. A study was conducted in San Francisco (SF) and the coastal beach of California (SB) to measure benzene levels in ambient air and the exhalation of smokers and non-smokers using GC-MS. The concentration of benzene was found to be seven-fold higher in SF (2.6 ppbV) than SB (0.38 ppbV). Benzene concentrations were 3.3 ppbV and 2.5 ppbV in smokers and non-smokers, respectively. This study suggested that smoking is an additional source of benzene to outdoor VOCs [73]. A similar study was conducted on smoking and non-smoking individuals to detect VOCs in exhaled breath. Benzene and five hydrocarbons were found in higher concentrations in exhaled breath in smoking volunteers [74]. The concentration of benzene was found to decrease in smokers within an hour since they smoked their last cigarette [75]. The blood headspace of smoking and non-smoking volunteers were measured using GC-MS to detect VOCs. Among these VOCs, benzene was found to be present in significantly higher concentrations (547 ng/l) in the blood of smoking volunteers compared with non-smokers (192 ng/l) [76].

Ethylbenzene cleaves upon ionization to form an ethyl cation and methylbenzene at m/z = 27 and 91, respectively. In addition, a benzene ring could form in a transient fashion (temporarily) and combine with CF_2^+ to form the peak at m/z = 127. This product was protonated to give the small signal at m/z = 128. Small fragments were detected at m/z = 105, 106, 107, and 109, which may have resulted from the removal of hydrogen or the protonation of the parent ion. By contrast, ethylbenzene produces fewer fragments at 120 Td, where the main peak is observed at m/z = 127 followed by small signal at 128 amu. Another main peak was detected at m/z = 91 followed by small signals at m/z = 27 and

m/z = 105. The hydronium experiment showed ethylbenzene produced a protonated ion-molecule as the main product at 100 Td. In contrast, at 120 Td, the protonated species represented around half of the total products, followed by a fragment at m/z = 79; see Table 4.19.

A study was run using both lung cancer patients and healthy individuals using GC-TOF-MS and canine recognition. Ethylbenzene was one of the VOCs that had a greater concentration in exhaled breath of cancer patients than healthy controls [77]. Ethylbenzene was present in significantly lower levels in non-small cell lung cancer patients compared with chronic obstructive pulmonary disorder patients [78].

Table 4. 19: Results for ethylbenzene with CF_3^+ and H_3O^+ as reagents in CIR-MS at *E/N* = 100 and 120 Td.

Source	Fragment	Mass	CF_3^+		H_3O^+	
			% (100Td)	% (120Td)	% (100Td)	% (120Td)
Ethylbenzene	$C_2H_3^+$	27	15.1	3.4		
	$C_6H_7^+$	79			3.4	36.1
	$C_6H_8^+$	80				2.0
	$C_6H_5CH_2^+$	91	6.8	28.5		
	$C_6H_5C_2H_4^+$	105	9.0	8.7		
	$C_6H_6C_2H_4^+$	106	5.0			
	$C_6H_7C_2H_4^+$	107	14.9		89.3	56.8
	$C_6H_9C_2H_4^+$	109	10.0		7.3	5.1
	$C_6H_5.CF_2^+$	127	36.5	55.2		
	$C_6H_5.CF_2H^+$	128	2.8	4.2		

Bromobenzene sees its main fragments at m/z = 205 and 207, which resulted from cations of the two isotopes of bromine (51:49 abundance) when combined with CF_2^+. In addition, the bromine substituent was stripped off leaving the benzyl group which was seen at m/z = 77. This fragment could further react with water to form a cluster at m/z = 95. Moreover, it could react with CF_3^+ to form peaks at m/z = 145 and 146. Similar results were observed at 120 Td but with greater abundance at m/z = 77, from the formation of the benzyl ion product. H_3O^+ results showed two main products owing to the isotopes of bromine atom at m/z = 157 and 159 for both 100 Td and 120 Td; see Table 4.20.

Toluene's main signal occurred at m/z = 141 which was formed by a combination of toluene with CF_2^+, followed by small fragment at m/z = 142 resulting from protonation of the main fragment. Other fragments were seen at m/z = 91 and 93, which resulted from the loss of a hydrogen from, and protonation of, the parent molecule, respectively. Although toluene at 120 Td produced similar peaks at m/z = 91, 141 and 142, though with

slight differences in abundance, other small fragments were seen at m/z = 92 and 161, which represented the parent ion and the combination of toluene with CF_3^+, respectively. H_3O^+ produced mostly protonated molecular ions at both 100 Td and 120 Td; see Table 4.20. Environmental toluene concentrations have been found in the range of 13 to 191 mg/m^3, while the level of toluene in exhaled breath ranged from 159 to 3354 ng/L [79]. The concentration of toluene in the breath exhaled by smokers was found to be within the range from 1.29 to 8.01 µg/cig [80].

Table 4. 20: Results for bromobenzene and toluene with CF_3^+ and H_3O^+ as reagents in CIR-MS at *E/N* = 100 and 120 Td.

Source	Fragment	Mass	CF_3^+		H_3O^+	
			% (100Td)	% (120Td)	% (100Td)	% (120Td)
B. benzene		53	10.5			
	$C_6H_5^+$	77	9.9	35.3		
	$C_6H_6^+$	78		3.2		
	$C_6H_6.H_2O^+$	95	21.2	2.8		
		105	7.5			
	$C_6H_4.CF_3^+$	145	6.1	15.0		
	$C_6H_5.CF_3^+$	146	5.2	5.2		
	$C_6H_4Br^+$	156	2.6	5.1		
	$C_6H_5Br^+$	157			48.6	48.1
	$C_6H_6Br^+$	158		4.7	3.2	3.6
	$C_6H_7Br^+$	159			44.4	45.1
	$C_6H_8Br^+$	160			3.8	3.1
		205	19.8			
	$C_6H_4BrCF_2^+$	206		8.6		
	$C_6H_5Br.\ CF_2^+$	207	17.1	8.6		
Toluene	$C_7H_7^+$	91	3.2	21.7		
	$C_7H_8^+$	92		6.7		
	$C_7H_9^+$	93	15.8		92.6	92.5
	$C_7H_9^+$	94			7.4	7.5
	$C_7H_8.CF^+$	123		2.2		
	$C_7H_7.CF_2^+$	141	78.2	59.1		
	$C_7H_8.CF_2^+$	142	2.8	5.2		
	$C_7H_8.CF_3^+$	161		5.1		

Xylene saw a major fragment at 175 amu resulting from the addition of CF_3^+ to the xylene ion followed by a small fragment at m/z = 176, which formed by the protonation of the fragment at 175 amu. In addition, a relatively intense peak was observed at 155 amu that emerged from a combination of CF_2^+ with the parent molecule. Moreover, small fragments were detected at 105 and 106 amu. Similar results were observed for xylene at 120 Td, with the formation of ions at 105, 106, 155, 175 and 176 amu, though with some

differences in relative abundances. The signal at m/z = 155 has a greater abundance than at m/z = 175 compared to the results observed at 100 Td. Moreover, a relatively high peak was seen at 91 amu that resulted from the removal of a methyl group, leaving the $C_6H_4CH_3^+$ ion. Another small peak was detected at m/z = 137 which may result from a combination of the xylene ion with CF^+. On the other hand, xylene showed few signs of fragmentation in the proton transfer reactions at both 100 and 120 Td; see Table 4.21. VOCs are added to the atmosphere from a number of sources such as industrial activities and motor vehicle exhaust. Many studies have been conducted to measure VOCs in the atmosphere in urban and rural sites. PTR-MS was used to investigate various aromatic compounds such as xylenes released from traffic in Innsbruck [81].

Table 4. 21: Results for xylene with CF_3^+ and H_3O^+ as reagents in CIR-MS at *E/N* = 100 and 120 Td.

Source	Fragment	Mass	CF_3^+		H_3O^+	
			% (100Td)	% (120Td)	% (100Td)	% (120Td)
Xylene	$C_6H_4CH_3^+$	91		29.5		
	$C_8H_9^+$	105	9.6	10.9		
	$C_8H_{10}^+$	106	4.1	8.3		
	$C_8H_{11}^+$	107		3.2	92.6	91.0
	$C_8H_{12}^+$	108			7.4	9.0
	$C_8H_{10}.CF^+$	137		2.5		
	$C_8H_9.CF_2^+$	155	16.6	26.6		
	$C_8H_{10}.CF_3^+$	175	63.6	17.0		
	$C_8H_{10}.CFH_3^+$	176	6.6	2.0		

Styrene saw the formation of its main ion at m/z = 173 that resulted from a combination of the styrene ion with CF_3^+, followed by a small fragment ion at 174 amu that arose from the protonation of the fragment at m/z = 173. In addition, another combination occurred with CF_2^+ to form a fragment at m/z = 153. Moreover, a fluorine atom attached to the double bond on the ethylene group, producing a methylene leaving group and thus forming the fragment at 109 amu. The parent ion and protonated molecule were also seen at m/z = 104 and 105, respectively; see Table 4.22.

Similar results were observed at 120 Td with slight changes in abundances and additional fragments seen at m/z = 78 and 103, 110 and 154. The masses at m/z = 78 and 103 could arise from an ethylene group being stripped from styrene, leaving a benzyl ion, and the dehydrogenation of the parent molecule, respectively. An unknown fragment was also detected at 133 amu. Another fragment was seen at 154 amu which may result from

protonation of the fragment at m/z = 153. H_3O^+ produced mostly protonated molecular ions at both 100 Td and 120 Td; see Table 4.22. The VOCs in exhaled breath seems to represent a promising approach to identifying various disorders and diseases. Xylene concentrations in non-small cell lung cancer patients were lower than those in chronic obstructive pulmonary patients [58].

Table 4. 22: Results for styrene with CF_3^+ and H_3O^+ as reagents in CIR-MS at *E/N* = 100 and 120 Td.

Source	Fragment	Mass	CF_3^+		H_3O^+	
			% (100Td)	% (120Td)	% (100Td)	% (120Td)
Styrene	$C_6H_6^+$	78		4.0		
	$C_6H_9CHCH^+$	103		6.0		
	$C_6H_5CHCH_2^+$	104	4.7	16.7		
	$C_6H_5CH_2CH_2^+$	105	15.4		91.9	92.3
	$C_6H_5CH_2CH_3^+$	106			8.1	7.7
	$C_6H_5CFH^+$	109	13.2	28.9		
	$C_6H_5CFH_2^+$	110		2.2		
		133		6.5		
	$C_6H_5CHCH.CF_2^+$	153	10.5	17.1		
	$C_6H_5CHCH_2.CF_2^+$	154		1.8		
	$C_6H_5CHCH_2.CF_3^+$	173	50.9	16.7		
	$C_6H_5CHCH_2.CF_3H^+$	174	5.2			

4.3.2.7 Five- and six-membered heterocyclic compounds

Furan, pyridine and pyrrole have lone pair electrons which allows them to behave as Lewis bases, as shown in Figure 4.4.

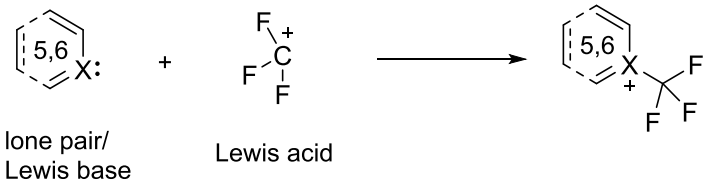

Figure 4. 4: Five and six-membered rings such as aromatic and heterocyclic compounds act as Lewis bases and react with CF_3^+ as a Lewis acid, adapted from ref [12].

Furan formed its main fragment at 137 amu, followed by fragment at m/z = 117 which arose from the combination of furan with CF_3^+ and CF_2H^+, respectively. Small fragments were seen at 68 amu which belongs to the parent ion, and unknown peaks at 89, 109 and 117 amu. Similar results were obtained at 120 Td with lower abundance of the main fragment at m/z = 137 and extra unknown fragments at 39 and 59 amu. By contrast, H_3O^+

produced mostly protonated molecular ions at 120 Td, while a lower abundance of protonated molecular ions were detected at 100 Td with some fragments at 39 and 41 amu; see Table 4.23.

Methylfuran formed its principal ions at m/z = 151, 82 and 83 and may result from the combination of the parent ion with CF_3^+, the molecular ion and its protonated ion, respectively. Other small fragments were detected at 81 amu that may have resulted from dehydrogenation of the molecular ion, whilst the peaks at m/z = 85 and 103 may have arisen from the replacement of the oxygen atom by a fluorine atoms. In addition, signals at m/z = 131 and 133 were observed that emerge from the combination of CF_2^+ with the molecular ion and its protonated ion. At 120 Td, methylfuran does not combine with CF_3^+ or CF_2^+; rather, fragments at m/z = 81, 82, 83, 85 and 103 were detected. Moreover, unknown signals were detected at 54, and 77 amu. PTR-MS produced mostly protonated molecular ions at both 100 Td and 120 Td; see Table 4.23.

Table 4. 23: Results for furan and methylfuran with CF_3^+ and H_3O^+ as reagents in CIR-MS at *E/N* = 100 and 120 Td.

Source	Fragment	Mass	CF_3^+		H_3O^+	
			% (100Td)	% (120Td)	% (100Td)	% (120Td)
Furan		39		5.1	10.4	
		41			14.0	
		59		5.4		
	$C_4H_4O^+$	68	4.2			
	$C_4H_4OH^+$	69			72.5	95.6
	$C_4H_5OH^+$	70			3.2	4.4
		89	2.5	17.1		
		109	3.6	14.5		
		117	3.8	11.9		
	$C_4H_4O.CF_2H^+$	119	11.3			
	$C_4H_4O.CF_3^+$	137	70.8	43.5		
	$C_4H_4O.CF_3H^+$	138	3.9	2.5		
Methylfuran		54		10.7		
		77		12.8		
	$C_5H_5O^+$	81	6.2	12.0		
	$C_5H_6O^+$	82	14.1	11.3		
	$C_5H_7O^+$	83	21.8	18.6	94.0	94.5
	$C_5H_8O^+$	84			5.6	5.5
	$C_5H_5FH^+$	85	4.9	12.9		
	$C_5H_5F_2^+$	103	7.3	21.6		
	$C_5H_5OCF_2^+$	131	2.9			
	$C_5H_6OCF_2H^+$	133	9.4			
	$C_5H_6OCF_3^+$	151	32.2			

Furans were found to be released in human urine samples [43]. Furan derivatives have been detected in exhaled breath using real-time high resolution tandem mass spectrometry [82].

Pyridine formed its main products at both 100 Td and 120 Td at 148 amu, which emerged from the addition of pyrrole to CF_3^+, followed by small signal at 149 amu that resulted from the protonation of this product. In addition, signals were recorded at 79, 80, 95 and 69 amu. The masses at 79 and 80 belonged to the parent ion and protonated parent ion-molecule, respectively. The mass at 95 could not be identified, but the mass at 96 amu may result from the replacement of the nitrogen atom with CF^+. On the other hand, further small, but unknown, peaks at m/z = 109, 130 and 146 were detected at 100 Td. The hydronium ion produced mostly protonated molecular ions at both 100 Td and 120 Td; see Table 4.24. Pyridine was found to be present in exhaled breath after drinking coffee [83].

Table 4. 24: Results for pyridine with CF_3^+ and H_3O^+ as reagents in CIR-MS at *E/N* = 100 and 120 Td.

Source	Fragment	Mass	CF_3^+		H_3O^+	
			% (100Td)	% (120Td)	% (100Td)	% (120Td)
Pyridine	$C_5H_5N^+$	79	3.0	16.7		
	$C_5H_5NH^+$	80	17.4	10.7	94.1	93.6
	$C_5H_5NH_2^+$	81			5.9	5.6
		95	6.5	8.8		
	$C_5H_5CF^+$	96	2.6	8.2		
		109	2.2			
		130	4.4			
		146	2.1			
	$C_5H_5N.CF_3^+$	148	53.2	50.5		
	$C_5H_5N.CF_3H^+$	149	4.3	5.0		
	$C_5H_{10}NH_2.CFH^+$	156	2.0			

Pyrrole, at both 100 Td and 120 Td, produces its main peak at m/z = 136 and 116 which emerged from the combination of the molecule with CF_3^+ and CF_2^+, respectively. Small fragments were seen at 117 and 118 amu which were related to the mass signal observed at 116. Other peaks were detected at m/z = 135 and 137 amu that may have been formed by dehydration and protonation of the mass at m/z = 136, respectively. The spectrum observed with the hydronium ion were those of protonated molecular ions for both 100 Td and 120 Td; see Table 4.25.

Dimethyl sulphide (DMS) reacts as Lewis base with CF_3^+ similar to five- and six-membered heterocyclic rings. DMS shows a preference for its parent ion to combine with CF_3^+ at m/z = 131 at both 100 Td and 120 Td. Small fragments were seen at m/z = 61, 62 and 63 which could belong to the parent ions and the protonated molecular ion, respectively. The largest abundance of protonated molecules were produced by H_3O^+ at both 100 and 120 Td; see Table 4.25. Living organisms can release VOCs, providing information on disorder or disease processes. A study showed that L6 rat skeletal muscle cell lines released DMS [49].

Table 4. 25: Results for pyrrole and DMS with CF_3^+ and H_3O^+ as reagents in CIR-MS at *E/N* = 100 and 120 Td.

Source	Fragment	Mass	CF_3^+		H_3O^+	
			% (100Td)	% (120Td)	% (100Td)	% (120Td)
Pyrrole	$C_4H_4NH_2^+$	68	8.2		95.4	95.5
		96	3.4	4.1	4.6	4.5
		98	4.3			
	$C_4H_4N.CF_2^+$	116	18.2	46.2		
	$C_4H_4NH.CF_2^+$	117		2.4		
	$C_4H_4NH.CF_2H^+$	118	8.9			
	$C_4H_4N.CF_3^+$	135	1.8	5.9		
	$C_4H_4NH.CF_3^+$	136	51.8	39.2		
	$C_4H_4NH.CF_3H^+$	137	3.7	2.3		
DMS	$CH_3SCH_2^+$	61	8.4	13.6		
	$CH_3SCH_3^+$	62	13.7	28.2		
	$CH_3SHCH_3^+$	63	8.6		93.0	92.6
	$CH_3SH_2CH_3^+$	64			2.9	3.1
	$CH_3SH_3CH_3^+$	65			4.1	4.3
	$CH_3SCH_3.CF_3^+$	131	69.4	58.2		

Acrylonitrile formed its main fragment at m/z = 122, which resulted from the addition of parent ion and CF_3^+, followed by a small peak at 123 amu. A low intensity fragment of the protonated molecule ion also was detected at 54 amu. The result at 120 Td showed that the main product also was formed at 122 amu though with a relatively lower abundance compared to the result at 100 Td. Signals were detected at 26, 27, and 29 amu which mainly arose from cyanide (CN) as a leaving group. Other peaks were detected at 31 and 70 amu, the first of which was unidentified, whilst the other may have arisen from the addition of CF^+ to the parent molecular ion. The protonated parent ion was predominant in PTR-MS results; see Table 4.26.

Cigarette smoke is a complex mixture of species that includes many VOCs in the gas phase. High exposure to these VOCs could cause increased risks to health. Acrylonitrile was one of the VOCs found in cigarette smoke [84].

Table 4. 26: Results for acrylonitrile with CF_3^+ and H_3O^+ as reagents in CIR-MS at *E/N* = 100 and 120 Td.

Source	Fragment	Mass	CF_3^+		H_3O^+	
			% (100Td)	% (120Td)	% (100Td)	% (120Td)
Acrylonitrile	$C_2H_2^+$	26		3.6		
	$C_2H_3^+$	27		4.8		
	$C_2H_5^+$	29		21.3		
		31		16.2		
	CH_2CHCNH^+	54	12.7		96.3	96.3
	$CH_2CHCHNH^+$	55			3.7	3.7
	$CH_2CHCN.CF^+$	70		11.2		
	$CH_2CHCN.CF_3^+$	122	83.4	42.8		
	$CH_2CHCN.CF_3H^+$	123	3.9			

Propionitrile produced its main fragment by complexation of its parent ion with CF_3^+, as seen at m/z = 124, followed by unidentified peak at 96 amu at both 100 and 120 Td. Moreover, the protonated adduct formation ion was detected at m/z = 125 at 100 Td. Protonated molecules were most commonly detected for both 100 and 120 Td; see Table 4.27.

Table 4. 27: Results for propionitrile with CF_3^+ and H_3O^+ as reagents in CIR-MS at *E/N* = 100 and 120 Td.

Source	Fragment	Mass	CF_3^+		H_3O^+	
			% (100Td)	% (120Td)	% (100Td)	% (120Td)
propionitrile	$CH_3CH_2CNH^+$	56	22.3		96.3	96.2
		57			3.7	3.6
		96	1.2	11.2		
	$CH_3CH_2CN.CF_3^+$	124	73.2	88.8		
	$C_2H_5CNH.CF_3H^+$	125	3.4			

Acetonitrile formed its main fragment at 110 amu followed by a small peak at 111 amu which resulted from combination of the parent ion with CF_3^+, and its protonated form, respectively, at both 100 and 120 Td. An unusual peak was detected at m/z = 42 which may belong to the protonated parent ion at 120 Td. H_3O^+ results were predominant at both 100 and 120 Td; see Table 4.28.

Table 4. 28: Results for acetonitrile with CF_3^+ and H_3O^+ as reagents in CIR-MS at *E/N* = 100 and 120 Td.

Source	Fragment	Mass	CF_3^+		H_3O^+	
			% (100Td)	% (120Td)	% (100Td)	% (120Td)
acetonitrile	CH_3CNH^+	42		18.8	97.4	97.1
	$CH_3CNH_2^+$	43			2.6	2.6
	$CH_3CNH.CF_3^+$	110	98.7	77.6		
	$CH_3CNH.CF_3H^+$	111	1.3	3.5		

Cigarette smoke contains a significant number of VOCs which may affect human health. One study showed that exhaled breath from smokers has a higher concentration of acetonitrile compared to non-smokers, and requires nearly a week to decrease to of the same level as non-smokers after stopping smoking [65], and the levels of acetonitrile in exhaled breath and the urine headspace of smokers were within the range 17-127 ppbV and 0-150 µg/L, respectively [85].

4.4 Summary

The ability of CF_3^+ to act as a chemical reagent in CIR-MS in the detection of VOCs has been tested using a number of standard VOCs. In this work, Tedlar bags were used to prepare standard solutions, and samples were, for the most part, measured using CF_3^+ as chemical reagent in CIR-TOF-MS. At the same time, samples were also measured by PTR-TOF-MS for comparative purposes. The CF_3^+ spectrum showed a number of fragments that resulted from the various reactions of CF_3^+ with the analytes. Some fragments observed arose from the protonated ion due to the reaction of certain analytes with H_3O^+. Using CF_3^+ and H_3O^+ simultaneously as reagents is considered to be a meaningful tool in the detection of VOCs via CIR-TOF-MS.

Lighter alkanes reacted with CF_3^+ via a charge transfer (hydride extraction) mechanism, whilst higher alkanes tended towards fragmentation of the C_n chain to produce alkyl fragments. Alkenes with CF_3^+ produced parent ions and other fragments. Alcohols showed little reactivity with CF_3^+, with methanol exhibiting no reaction, and other alcohols producing alkyl fragments.

CF_3^+ is a suitable reagent by which to detect various aromatic and nitrile compounds; it acts as a Lewis acid in these circumstances. Aromatic and heterocyclic compounds showed a tendency to combine with CF_3^+ / CF_2^+. Ketones and aldehydes mainly form $ROCOR.CF_3^+$, or RCO^+, or $RCO.CF_3^+$. Nitriles and DMS form RCF_3^+.

Having established that the use of CF_3^+ to detect the lighter n-alkanes with relatively little fragmentation, further work was undertaken to assess its behaviour with a wider variety of naturally occurring VOCs and in particular, with those VOCs who have been found to feature strongly in H_3O^+-based breath analysis work. Of these, those with m/z = 110, 124, 141, 143, 148, 173 and 175 are likely markers for acetonitrile, propionitrile, toluene, methyl acetate, pyridine, styrene and xylene. The results provided a small library of reference spectra, that could be used to identify several VOCs found in real-life smokers' and non-smokers' samples of exhaled breath or urine headspace.

4.5 References

[1] A. Bhatt, M.A. Parsi, T. Stevens, S. Gabbard, A. Kumaravel, S. Jang, D. Grove, R. Lopez, S. Murthy, J.J. Vargo, Volatile organic compounds in plasma for the diagnosis of esophageal adenocarcinoma: a pilot study, Gastrointestinal endoscopy, 84 (2016) 597-603.

[2] A.M. Ellis, C.A. Mayhew, Proton transfer reaction mass spectrometry: principles and applications, John Wiley & Sons, 2013.

[3] C. Kramer, P. Mochalski, K. Unterkofler, A. Agapiou, V. Ruzsanyi, K.R. Liedl, Prediction of blood:air and fat:air partition coefficients of volatile organic compounds for the interpretation of data in breath gas analysis, Journal of breath research, 10 (2016) 017103.

[4] B. de Lacy Costello, A. Amann, H. Al-Kateb, C. Flynn, W. Filipiak, T. Khalid, D. Osborne, N.M. Ratcliffe, A review of the volatiles from the healthy human body, Journal of breath research, 8 (2014) 014001.

[5] R.S. Blake, K.P. Wyche, A.M. Ellis, P.S. Monks, Chemical ionization reaction time-of-flight mass spectrometry: Multi-reagent analysis for determination of trace gas composition, International Journal of Mass Spectrometry, 254 (2006) 85-93.

[6] E. Masi, A. Romani, C. Pandolfi, D. Heimler, S. Mancuso, PTR-TOF-MS analysis of volatile compounds in olive fruits, Journal of the science of food and agriculture, 95 (2015) 1428-1434.

[7] J.R. Eyler, P. Ausloos, S.G. Lias, Novel ion-molecule reaction involving cleavage of the carbonyl bond in ketones and aldehydes, Journal of the American Chemical Society, 96 (1974) 3673-3675.

[8] P. Ausloos, S. Lias, J.R. Eyler, Reactions of halomethyl ions with carbonyl-containing compounds, International Journal of Mass Spectrometry and Ion Physics, 18 (1975) 261-271.

[9] S. Lias, P. Ausloos, Ion-molecule reactions involving halomethyl ions; heats of formation of halomethyl ions, International Journal of Mass Spectrometry and Ion Physics, 23 (1977) 273-292.

[10] C. Dehon, J. Lemaire, M. Heninger, A. Chaput, H. Mestdagh, Chemical ionization using CF_3^+: Efficient detection of small alkanes and fluorocarbons, International Journal of Mass Spectrometry, 299 (2011) 113-119.

[11] R.S. Blake, S.A. Ouheda, C.J. Evans, P.S. Monks, CF_3^+ and CF_2H^+: new reagents for n-alkane determination in chemical ionisation reaction mass spectrometry, The Analyst, 141 (2016) 6564-6570.

[12] R.S. Blake, S.A. Ouheda, E.F. Alwedi, P.S. Monks, Exploration of the utility of CF_3^+ as a reagent for chemical ionisation reaction mass spectrometry, International Journal of Mass Spectrometry, 421 (2017) 224-233.

[13] M. Phillips, R.N. Cataneo, R. Condos, G.A. Ring Erickson, J. Greenberg, V. La Bombardi, M.I. Munawar, O. Tietje, Volatile biomarkers of pulmonary tuberculosis in the breath, Tuberculosis, 87 (2007) 44-52.

[14] W. Filipiak, V. Ruzsanyi, P. Mochalski, A. Filipiak, A. Bajtarevic, C. Ager, H. Denz, W. Hilbe, H. Jamnig, M. Hackl, Dependence of exhaled breath composition on exogenous factors, smoking habits and exposure to air pollutants, Journal of breath research, 6 (2012) 036008.

[15] A. Smolinska, E.M. Klaassen, J.W. Dallinga, K.D. van de Kant, Q. Jobsis, E.J. Moonen, O.C. van Schayck, E. Dompeling, F.J. van Schooten, Profiling of volatile organic compounds in exhaled breath as a strategy to find early predictive signatures of asthma in children, PloS one, 9 (2014) e95668.

[16] P. Mochalski, J. King, M. Haas, K. Unterkofler, A. Amann, G. Mayer, Blood and breath profiles of volatile organic compounds in patients with end-stage renal disease, BMC nephrology, 15 (2014) 1.

[17] K. Müller, S. Haferkorn, W. Grabmer, A. Wisthaler, A. Hansel, J. Kreuzwieser, C. Cojocariu, H. Rennenberg, H. Herrmann, Biogenic carbonyl compounds within and above a coniferous forest in Germany, Atmospheric Environment, 40 (2006) 81-91.

[18] L. Russell, A. Mensah, E. Fischer, B. Sive, R. Varner, W. Keene, J. Stutz, A. Pszenny, Nanoparticle growth following photochemical α-and β-pinene oxidation at Appledore Island during International Consortium for Research on Transport and Transformation/Chemistry of Halogens at the Isles of Shoals 2004, Journal of Geophysical Research: Atmospheres, 112 (2007).

[19] A. Wisthaler, N. Jensen, R. Winterhalter, W. Lindinger, J. Hjorth, Measurements of acetone and other gas phase product yields from the OH-initiated oxidation of terpenes by proton-transfer-reaction mass spectrometry (PTR-MS), Atmospheric Environment, 35 (2001) 6181-6191.

[20] A. Jones, Excretion of low-molecular weight volatile substances in human breath: focus on endogenous ethanol, Journal of analytical toxicology, 9 (1985) 246-250.
[21] S. Nair, K. Cope, R.H. Terence, A.M. Diehl, Obesity and female gender increase breath ethanol concentration: potential implications for the pathogenesis of nonalcoholic steatohepatitis, The American journal of gastroenterology, 96 (2001) 1200-1204.
[22] C. Turner, P. Spanel, D. Smith, A longitudinal study of ethanol and acetaldehyde in the exhaled breath of healthy volunteers using selected-ion flow-tube mass spectrometry, Rapid communications in mass spectrometry : RCM, 20 (2006) 61-68.
[23] A. Bajtarevic, C. Ager, M. Pienz, M. Klieber, K. Schwarz, M. Ligor, T. Ligor, W. Filipiak, H. Denz, M. Fiegl, W. Hilbe, W. Weiss, P. Lukas, H. Jamnig, M. Hackl, A. Haidenberger, B. Buszewski, W. Miekisch, J. Schubert, A. Amann, Noninvasive detection of lung cancer by analysis of exhaled breath, BMC cancer, 9 (2009) 348.
[24] U. Riess, U. Tegtbur, C. Fauck, F. Fuhrmann, D. Markewitz, T. Salthammer, Experimental setup and analytical methods for the non-invasive determination of volatile organic compounds, formaldehyde and NOx in exhaled human breath, Analytica chimica acta, 669 (2010) 53-62.
[25] J. Huang, S. Kumar, N. Abbassi-Ghadi, P. Spanel, D. Smith, G.B. Hanna, Selected ion flow tube mass spectrometry analysis of volatile metabolites in urine headspace for the profiling of gastro-esophageal cancer, Analytical chemistry, 85 (2013) 3409-3416.
[26] F. Morisco, E. Aprea, V. Lembo, V. Fogliano, P. Vitaglione, G. Mazzone, L. Cappellin, F. Gasperi, S. Masone, G.D. De Palma, R. Marmo, N. Caporaso, F. Biasioli, Rapid "breath-print" of liver cirrhosis by proton transfer reaction time-of-flight mass spectrometry. A pilot study, PloS one, 8 (2013) e59658.
[27] G. Millonig, S. Praun, M. Netzer, C. Baumgartner, A. Dornauer, S. Mueller, J. Villinger, W. Vogel, Non-invasive diagnosis of liver diseases by breath analysis using an optimized ion-molecule reaction-mass spectrometry approach: a pilot study, Biomarkers : biochemical indicators of exposure, response, and susceptibility to chemicals, 15 (2010) 297-306.
[28] V. Ruzsanyi, W. Lederer, C. Seger, B. Calenic, K.R. Liedl, A. Amann, Non-(13)CO2 targeted breath tests: a feasibility study, Journal of breath research, 8 (2014) 046005.

[29] Y. Saalberg, M. Wolff, VOC breath biomarkers in lung cancer, Clinica Chimica Acta, 459 (2016) 5-9.

[30] F.S. Cikach, Jr., A.R. Tonelli, J. Barnes, K. Paschke, J. Newman, D. Grove, L. Dababneh, S. Wang, R.A. Dweik, Breath analysis in pulmonary arterial hypertension, Chest, 145 (2014) 551-558.

[31] J. Oomens, T.H. Morton, Fluoronium metathesis and rearrangements of fluorine-stabilized carbocations, International Journal of Mass Spectrometry, 308 (2011) 232-238.

[32] W. Miekisch, J.K. Schubert, G.F. Noeldge-Schomburg, Diagnostic potential of breath analysis--focus on volatile organic compounds, Clinica chimica acta; international journal of clinical chemistry, 347 (2004) 25-39.

[33] M. Kupari, J. Lommi, M. Ventilä, U. Karjalainen, Breath acetone in congestive heart failure, The American journal of cardiology, 76 (1995) 1076-1078.

[34] C. Deng, J. Zhang, X. Yu, W. Zhang, X. Zhang, Determination of acetone in human breath by gas chromatography–mass spectrometry and solid-phase microextraction with on-fiber derivatization, Journal of Chromatography B, 810 (2004) 269-275.

[35] C. Turner, P. Španěl, D. Smith, A longitudinal study of ammonia, acetone and propanol in the exhaled breath of 30 subjects using selected ion flow tube mass spectrometry, SIFT-MS, Physiological measurement, 27 (2006) 321.

[36] M.R. McCurdy, Y. Bakhirkin, G. Wysocki, R. Lewicki, F.K. Tittel, Recent advances of laser-spectroscopy-based techniques for applications in breath analysis, Journal of breath research, 1 (2007) 014001.

[37] A. Wisthaler, C.J. Weschler, Reactions of ozone with human skin lipids: sources of carbonyls, dicarbonyls, and hydroxycarbonyls in indoor air, Proceedings of the National Academy of Sciences of the United States of America, 107 (2010) 6568-6575.

[38] P.R. Boshier, J.R. Cushnir, V. Mistry, A. Knaggs, P. Spanel, D. Smith, G.B. Hanna, On-line, real time monitoring of exhaled trace gases by SIFT-MS in the perioperative setting: a feasibility study, The Analyst, 136 (2011) 3233-3237.

[39] S. Kischkel, W. Miekisch, P. Fuchs, J.K. Schubert, Breath analysis during one-lung ventilation in cancer patients, The European respiratory journal, 40 (2012) 706-713.

[40] J. King, A. Kupferthaler, B. Frauscher, H. Hackner, K. Unterkofler, G. Teschl, H. Hinterhuber, A. Amann, B. Hogl, Measurement of endogenous acetone and isoprene in exhaled breath during sleep, Physiological measurement, 33 (2012) 413-428.

[41] J. Huang, S. Kumar, A. Singanayagam, P.M. George, O.M. Kon, M. Takata, G.B. Hanna, Exhaled breath acetone for therapeutic monitoring in pneumonia using selected ion flow tube mass spectrometry (SIFT-MS), Analytical Methods, 5 (2013) 3807.

[42] P. Mochalski, A. Agapiou, M. Statheropoulos, A. Amann, Permeation profiles of potential urine-borne biomarkers of human presence over brick and concrete, The Analyst, 137 (2012) 3278-3285.

[43] R. Holzinger, J. Williams, G. Salisbury, T. Klüpfel, M.d. Reus, M. Traub, P. Crutzen, J. Lelieveld, Oxygenated compounds in aged biomass burning plumes over the Eastern Mediterranean: evidence for strong secondary production of methanol and acetone, Atmospheric Chemistry and Physics, 5 (2005) 39-46.

[44] D. Sprung, C. Jost, T. Reiner, A. Hansel, A. Wisthaler, Acetone and acetonitrile in the tropical Indian Ocean boundary layer and free troposphere: Aircraft-based intercomparison of AP-CIMS and PTR-MS measurements, Journal of Geophysical Research: Atmospheres, 106 (2001) 28511-28527.

[45] S. Mayrhofer, T. Mikoviny, S. Waldhuber, A.O. Wagner, G. Innerebner, I.H. Franke-Whittle, T.D. Mark, A. Hansel, H. Insam, Microbial community related to volatile organic compound (VOC) emission in household biowaste, Environmental microbiology, 8 (2006) 1960-1974.

[46] R. Fernandez del Rio, M.E. O'Hara, A. Holt, P. Pemberton, T. Shah, T. Whitehouse, C.A. Mayhew, Volatile Biomarkers in Breath Associated With Liver Cirrhosis - Comparisons of Pre- and Post-liver Transplant Breath Samples, EBioMedicine, 2 (2015) 1243-1250.

[47] X.A. Fu, M. Li, R.J. Knipp, M.H. Nantz, M. Bousamra, Noninvasive detection of lung cancer using exhaled breath, Cancer medicine, 3 (2014) 174-181.

[48] G. Song, T. Qin, H. Liu, G.-B. Xu, Y.-Y. Pan, F.-X. Xiong, K.-S. Gu, G.-P. Sun, Z.-D. Chen, Quantitative breath analysis of volatile organic compounds of lung cancer patients, Lung cancer, 67 (2010) 227-231.

[49] Y. Hanai, K. Shimono, K. Matsumura, A. Vachani, S. Albelda, K. Yamazaki, G.K. Beauchamp, H. Oka, Urinary volatile compounds as biomarkers for lung cancer, Bioscience, biotechnology, and biochemistry, 76 (2012) 679-684.

[50] P. Mochalski, R. Al-Zoairy, A. Niederwanger, K. Unterkofler, A. Amann, Quantitative analysis of volatile organic compounds released and consumed by rat L6 skeletal muscle cells in vitro, Journal of breath research, 8 (2014) 046003.

[51] P. Mochalski, K. Krapf, C. Ager, H. Wiesenhofer, A. Agapiou, M. Statheropoulos, D. Fuchs, E. Ellmerer, B. Buszewski, A. Amann, Temporal profiling of human urine VOCs and its potential role under the ruins of collapsed buildings, Toxicology mechanisms and methods, 22 (2012) 502-511.

[52] M. Steeghs, H.P. Bais, J. de Gouw, P. Goldan, W. Kuster, M. Northway, R. Fall, J.M. Vivanco, Proton-transfer-reaction mass spectrometry as a new tool for real time analysis of root-secreted volatile organic compounds in Arabidopsis, Plant Physiology, 135 (2004) 47-58.

[53] W. Lindinger, A. Hansel, A. Jordan, On-line monitoring of volatile organic compounds at pptv levels by means of proton-transfer-reaction mass spectrometry (PTR-MS) medical applications, food control and environmental research, International journal of mass spectrometry and ion processes, 173 (1998) 191-241.

[54] C.K. Saha, A. Feilberg, G. Zhang, A.P.S. Adamsen, Effects of airflow on odorants' emissions in a model pig house—A laboratory study using Proton-Transfer-Reaction Mass Spectrometry (PTR-MS), Science of the Total Environment, 410 (2011) 161-171.

[55] B.W. Moeskops, M.M. Steeghs, K. van Swam, S.M. Cristescu, P.T. Scheepers, F.J. Harren, Real-time trace gas sensing of ethylene, propanal and acetaldehyde from human skin in vivo, Physiological measurement, 27 (2006) 1187-1196.

[56] M.M.L. Steeghs, B.W.M. Moeskops, K. van Swam, S.M. Cristescu, P.T.J. Scheepers, F.J.M. Harren, On-line monitoring of UV-induced lipid peroxidation products from human skin in vivo using proton-transfer reaction mass spectrometry, International Journal of Mass Spectrometry, 253 (2006) 58-64.

[57] P. Fuchs, C. Loeseken, J.K. Schubert, W. Miekisch, Breath gas aldehydes as biomarkers of lung cancer, International Journal of Cancer, 126 (2010) 2663-2670.

[58] H. Handa, A. Usuba, S. Maddula, J.I. Baumbach, M. Mineshita, T. Miyazawa, Exhaled breath analysis for lung cancer detection using ion mobility spectrometry, PloS one, 9 (2014) e114555.

[59] A.G. Dent, T.G. Sutedja, P.V. Zimmerman, Exhaled breath analysis for lung cancer, Journal of thoracic disease, 5 Suppl 5 (2013) S540-550.

[60] D. Poli, M. Goldoni, M. Corradi, O. Acampa, P. Carbognani, E. Internullo, A. Casalini, A. Mutti, Determination of aldehydes in exhaled breath of patients with lung cancer by means of on-fiber-derivatisation SPME–GC/MS, Journal of Chromatography B, 878 (2010) 2643-2651.

[61] A. Ulanowska, T. Kowalkowski, E. Trawińska, B. Buszewski, The application of statistical methods using VOCs to identify patients with lung cancer, Journal of breath research, 5 (2011) 046008.

[62] C. Deng, X. Zhang, N. Li, Investigation of volatile biomarkers in lung cancer blood using solid-phase microextraction and capillary gas chromatography-mass spectrometry, Journal of chromatography. B, Analytical technologies in the biomedical and life sciences, 808 (2004) 269-277.

[63] R. Guadagni, N. Miraglia, A. Simonelli, A. Silvestre, M. Lamberti, D. Feola, A. Acampora, N. Sannolo, Solid-phase microextraction-gas chromatography-mass spectrometry method validation for the determination of endogenous substances: urinary hexanal and heptanal as lung tumor biomarkers, Analytica chimica acta, 701 (2011) 29-36.

[64] S. Kumar, J. Huang, N. Abbassi-Ghadi, H.A. Mackenzie, K.A. Veselkov, J.M. Hoare, L.B. Lovat, P. Spanel, D. Smith, G.B. Hanna, Mass Spectrometric Analysis of Exhaled Breath for the Identification of Volatile Organic Compound Biomarkers in Esophageal and Gastric Adenocarcinoma, Annals of surgery, 262 (2015) 981-990.

[65] J.R. Dannecker, E.G. Shaskan, M. Phillips, A new highly sensitive assay for breath acetaldehyde: Detection of endogenous levels in humans, Analytical biochemistry, 114 (1981) 1-7.

[66] C. Brunner, W. Szymczak, V. Hollriegl, S. Mortl, H. Oelmez, A. Bergner, R.M. Huber, C. Hoeschen, U. Oeh, Discrimination of cancerous and non-cancerous cell lines by headspace-analysis with PTR-MS, Analytical and bioanalytical chemistry, 397 (2010) 2315-2324.

[67] E. Crespo, S.M. Cristescu, H. de Ronde, S. Kuijper, A.H. Kolk, R.M. Anthony, F.J. Harren, Proton Transfer Reaction Mass Spectrometry detects rapid changes in volatile metabolite emission by Mycobacterium smegmatis after the addition of specific antimicrobial agents, J Microbiol Methods, 86 (2011) 8-15.

[68] W. Filipiak, A. Sponring, M.M. Baur, A. Filipiak, C. Ager, H. Wiesenhofer, M. Nagl, J. Troppmair, A. Amann, Molecular analysis of volatile metabolites released specifically by Staphylococcus aureus and Pseudomonas aeruginosa, BMC microbiology, 12 (2012) 113.

[69] S. Sethi, R. Nanda, T. Chakraborty, Clinical application of volatile organic compound analysis for detecting infectious diseases, Clinical microbiology reviews, 26 (2013) 462-475.

[70] J. King, P. Mochalski, A. Kupferthaler, K. Unterkofler, H. Koc, W. Filipiak, S. Teschl, H. Hinterhuber, A. Amann, Dynamic profiles of volatile organic compounds in exhaled breath as determined by a coupled PTR-MS/GC-MS study, Physiological measurement, 31 (2010) 1169-1184.

[71] O. Lasekan, S. Otto, In vivo analysis of palm wine (Elaeis guineensis) volatile organic compounds (VOCs) by proton transfer reaction-mass spectrometry, International Journal of Mass Spectrometry, 282 (2009) 45-49.

[72] G.S. Prakash, G. Rasul, A. Burrichter, K.K. Laali, G.A. Olah, Ab Initio/IGLO/GIAO-MP2 Studies of Fluorocarbocations: Experimental and Theoretical Investigation of the Cleavage Reaction of Trifluoroacetic Acid in Superacids1a, The Journal of Organic Chemistry, 61 (1996) 9253-9258.

[73] R.C. Wester, H.I. Maibach, L.D. Gruenke, J.C. Craig, Benzene levels in ambient air and breath of smokers and nonsmokers in urban and pristine environments, Journal of Toxicology and Environmental Health, Part A Current Issues, 18 (1986) 567-573.

[74] L. Wallace, E. Pellizzari, Personal air exposures and breath concentrations of benzene and other volatile hydrocarbons for smokers and nonsmokers, Toxicology letters, 35 (1987) 113-116.

[75] A. Jordan, A. Hansel, R. Holzinger, W. Lindinger, Acetonitrile and benzene in the breath of smokers and non-smokers investigated by proton transfer reaction mass spectrometry (PTR-MS), International journal of mass spectrometry and ion processes, 148 (1995) L1-L3.

[76] H. Hajimiragha, U. Ewers, A. Brockhaus, A. Boettger, Levels of benzene and other volatile aromatic compounds in the blood of non-smokers and smokers, International archives of occupational and environmental health, 61 (1989) 513-518.

[77] B. Buszewski, T. Ligor, T. Jezierski, A. Wenda-Piesik, M. Walczak, J. Rudnicka, Identification of volatile lung cancer markers by gas chromatography–mass spectrometry: comparison with discrimination by canines, Analytical and bioanalytical chemistry, 404 (2012) 141-146.

[78] D. Poli, P. Carbognani, M. Corradi, M. Goldoni, O. Acampa, B. Balbi, L. Bianchi, M. Rusca, A. Mutti, Exhaled volatile organic compounds in patients with non-small cell lung cancer: cross sectional and nested short-term follow-up study, Respiratory research, 6 (2005) 71.

[79] S. Ghittori, A. Alessio, S. Negri, L. MAESTRI, P. ZADRA, M. IMBRIANI, A field method for sampling toluene in end-exhaled air, as a biomarker of occupational exposure: correlation with other exposure indices, Industrial health, 42 (2004) 226-234.

[80] S. Moldoveanu, W. Coleman III, J. Wilkins, Determination of benzene and toluene in exhaled cigarette smoke, Beiträge zur Tabakforschung/Contributions to Tobacco Research, 23 (2008) 107-114.

[81] R. Holzinger, A. Jordan, A. Hansel, W. Lindinger, Automobile emissions of acetonitrile: Assessment of its contribution to the global source, Journal of Atmospheric Chemistry, 38 (2001) 187-193.

[82] D. García-Gómez, L. Bregy, C.s. Barrios-Collado, G. Vidal-de-Miguel, R. Zenobi, Real-time high-resolution tandem mass spectrometry identifies furan derivatives in exhaled breath, Analytical chemistry, 87 (2015) 6919-6924.

[83] L. Meier, C. Berchtold, S. Schmid, R. Zenobi, High mass resolution breath analysis using secondary electrospray ionization mass spectrometry assisted by an ion funnel, Journal of mass spectrometry : JMS, 47 (2012) 1571-1575.

[84] S. Gordon, M. Brinkman, R. Meng, G. Anderson, J. Chuang, R. Kroeger, I. Reyes, P. Clark, Effect of cigarette menthol content on mainstream smoke emissions, Chemical research in toxicology, 24 (2011) 1744-1753.

[85] S.M. Abbott, J.B. Elder, P. Španěl, D. Smith, Quantification of acetonitrile in exhaled breath and urinary headspace using selected ion flow tube mass spectrometry, International Journal of Mass Spectrometry, 228 (2003) 655-665.

Chapter Five: Application of CF_3^+/CF_2H^+ as novel reagents in chemical ionization reaction mass spectrometry for breath analysis

5.1 Introduction

Breath analysis has been known for its diagnostic potential for various diseases for a long time. Although early research in this regard was found in the writings of Hippocrates, the first attempt to quantify CO_2 in breath was undertaken by Lavoisier in 1784 [1-3]. However, it was only after the development of gas chromatography in the 1950s that the real investigation of gas molecules in breath began. Since that time, many substances have been investigated in human breath [1]. Exhaled human breath consists of 78.6% (w/v) nitrogen, 16% (w/v) oxygen, 4.5% (w/v) carbon dioxide, and 0.9% (w/v) volatile organic compounds (VOCs) and other inert gases [1]. Human breath contains more than 1000 VOCs in concentrations ranging from parts per million (ppm) to parts per trillion (ppt) [4]. These VOCs appear to originate from two sources: endogenous and exogenous. Endogenous VOCs are produced from metabolic or physiological processes and then transported to the lungs through the bloodstream to be released as exhaled gases. Among these VOCs found in human breath are hydrocarbons, alcohols, isoprene, aldehydes, nitrogen-containing compounds and sulphur-containing compounds [5]. Exogenous compounds arise from environments such as halogenated organic compounds absorbed by the human body through the process of breathing [4-7].

5.1.1 Importance of breath analysis

Breath analysis has advantages over other conventional medical tests as it is non-invasive, fast and safe. Patients usually tolerate breath analysis well and are able to provide repeat samples without any problems. In addition, breath analysis can be performed in real time and can be relatively inexpensive [8]. To date, approximately 35 compounds exhaled in breath have been considered as potential biomarkers for certain diseases and metabolic disorders [9]. Some of these VOCs will be briefly discussed.

5.1.2 Hydrocarbons

Numerous aliphatic and aromatic hydrocarbons have been detected in human exhaled breath [10, 11]. There are many sources of hydrocarbons, particularly ethane and pentane, in the human body that arise from processes such as protein metabolism, colonic bacterial metabolism, and lipid peroxidation [12]. Lipid peroxidation occurs by removal of allylic

hydrogen atoms from the lipid through attack by reactive oxygen species. Among these products are pentane and ethane, which are, respectively, produced from the peroxidation of omega-3 or omega-6 polyunsaturated fatty acids. Lipid peroxidation is considered a sign of several clinical conditions and diseases, such as inflammatory disease, cancer and atherosclerosis [13, 14]. Alkane levels in exhaled breath are age dependent; with older subjects showing higher levels of oxidative stress [15, 16]. Cigarette smoke contains a high concentration of free radicals which assist in the initiation of lipid peroxidation, leading to the production of more hydrocarbons (particularly ethane and pentane) [14].

5.1.3 Alcohols

The most abundant endogenous alcohols found in exhaled breath are ethanol and methanol. Bacteria are considered one of the major sources of small-chain alcohols. Gut bacteria produce alcohols (C_1-C_5) through anaerobic fermentation of carbohydrates [17]. Enzymes are another source of alcohol in the human body; cytochrome P450 enzymes, for instance, metabolize alkanes in the liver to produce alcohols [12, 18]. Ethanol in exhaled breath is produced in the oral cavities and is affected by sugary food consumption, however, most of the methanol in human breath is thought to be produced systemically [19-21]. The consumption of alcoholic drinks is well known to increase ethanol levels in breath. Also, the level of methanol is increased with consistent level for a long time in human breath because the presence of ethanol prevents the metabolism of methanol [22]. Relatively high concentrations of ethanol are considered a sign of non-alcoholic liver disease and obesity [23, 24]. Propanol has two sources, namely systemically and in oral cavities [19, 25]. It has been reported that elevated concentrations of propanol are found in cirrhosis patients [26], and is also considered a sign of lung cancer [27]. Propan-2-ol may arise from acetone reduction by enzymes [19, 25], and might increase in diabetics [28]. The concentration of pentanol in children's breath has been reported in low concentrations [29].

5.1.4 Ketones

Acetone is the most abundant endogenous VOC to be detected in human breath. Acetone, β-hydroxybutyric acid and acetoacetic acid are collectively referred to as ketone bodies which are generated by the degradation of lipids in the liver [30]. Decarboxylation of acetoacetic acid is the main source of acetone in human breath [31] and its level is increased during fasting and starvation [32, 33]. In addition, the level of acetone is

increased in uncontrolled diabetes due to defective insulin receptors or an insulin deficiency which inhibits glucose being absorbed from the blood; as a result, the body depends on lipids as an energy source instead [32, 34]. Moreover, high concentrations of acetone are considered a sign of congestive heart failure [35].

The other source of acetone in exhaled human breath is an enzymatic conversion of propan-2-ol [28, 31]. Ketones such as 2-butanone and 2-pentanone have also been reported in healthy people [25, 26, 36-38], though high levels of these ketones in exhaled breath have been considered a marker of liver disease [24, 26, 27].

5.1.5 Aldehydes

Many aldehydes are reported in the exhaled breath of healthy people. Aldehydes are generated during the peroxidation of lipids [5, 36, 39, 40], and the detection of the aldehydes could be a marker for various forms of cancer [27, 41-44]. Acetaldehyde has been reported as one of the most abundant aldehydes [19, 20, 36, 45, 46]. Enzymatic oxidation of ethanol is one of the pathways to acetaldehyde production [47], whilst the oral cavities represent a further source of acetaldehyde. Bacteria are responsible for generating acetaldehyde after consumption of alcohols [19, 48].

5.1.6 Other compounds

Ammonia is one of the intermediates of the nitrogen cycle which is produced from hydrolysis of urea by urease. The concentration of ammonia in exhaled human breath ranges from 0.25 to 2.9 ppmV [49, 50]. The level of ammonia has been recorded to elevate during fasting [51, 52]. Exhaled ammonia is considered to be a marker of kidney, liver function and peptic ulcer disease [49]. Another class of compound that has been detected in human breath is acetonitrile, which increases in exhaled breath collected from subjects who smoke. Therefore, acetonitrile is considered a breath marker for smokers. In addition, researchers found that acetonitrile levels are elevated in exhaled breath of smokers for up to a week after having a cigarette [52-54].

5.1.7 Breath sampling

Collection of breath samples are a critical issue and numerous articles have summarized the steps required for the collecting of breath samples [2, 55, 56]. In general, breath sampling apparatus must achieve the following elements [57, 58]: the technique must be safe and comfortable for the subjects, which means disposable mouthpieces and bacterial

filters must be provided to avoid contamination from one subject to other; the sample container must maintain the integrity of analytes and the apparatus should keep the samples at a suitable temperature during collection and measurement to avoid condensation of the samples on the walls of the tubes. Breath samples can be stored for indirect analysis or injection for online analysis. There are different ways to store the samples, such as:

- Transparent or black Tedlar bags (polytetrafluoroethylene).
- Nalophan bags (polyethylene terephthalate)
- Glass vials
- Flex foil bags (polyethylene terephthalate/nylon/aluminium foil/chlorinated polyethylene
- Thermal desorption tubes such as carbon molecular sieves
- Metal canisters – silanized or electropolished.
- Micropacked sorbent traps
- Direct injection into the analytical instrument [56].

5.2 Experimental

The instruments used in this investigation were a two CIR-TOF-MS instruments (Model 4500A, Kore Technologies, Ely) which have been described in Chapter 2. All experiments were run at 100 Td, with 60 second integration times and over a mass range of 0-249 Daltons. The CIR-TOF-MS was supplied with either CF_4 or H_2O vapour as chemical reagents at rates of 2 and 50 ml/min respectively and breath samples were delivered at 60 and 150 ml/min respectively.

High purity nitrogen (BOC: 99.999%) was used as a dilution gas for preparation of stock mixtures of standards as well as for purging the sample bags, lines and apparatus. Liquid standards based on pure samples of the VOCs (Sigma-Aldrich, Gillingham, Dorset, UK) were injected into exhaled breath samples. These were prepared by adding 3 microlitres of each standard to 8 litres of N_2 in Tedlar bags (Thames-Restek UK, Ltd, Saunderton, Bucks., UK). In order to produce a range of concentrations, 50 ml aliquots of this gaseous stock was used to spike the contents of certain bags (8 litres) producing a range of concentrations between 0.43 ppmV and 1.01 ppmV.

Two groups of volunteers were required for the breath collection: smokers and non-smokers. The samples from the non-smokers were compared with those of the smokers. The experimental procedure was explained to the volunteers before taking the test, who were then also asked to fill out consent and application forms, which included the following information:

- Date of experiment
- University ID / e-mail
- Sample code (to be filled in by the researcher)
- Age
- Sex
- Weight (kg)
- Height (cm)
- Smoker or non-smoker
- Recent food and drink consumption

Ethics approval was obtained through University of Leicester healthy volunteer ethics - ethical application reference so165-cf19a

5.2.1 Collection of exhaled breath

Smoker and non-smoker subjects from representative staff and students from University of Leicester were invited to take part in this study. The subjects were 14 smokers (9 male and 5 female) and 25 non-smokers (22 male and 3 female), ages ranged from 21 to 60 years. Breath samples of smokers were collected immediately after a cigarette.

The procedure included collecting continuous tidal exhalations over 5-minute periods. Each volunteer was asked to fill a series of Tedlar bags with exhaled breath through the mouthpiece of the sampling apparatus. Initially 10 litre Tedlar bags were used and in the latter stages 3 litre Tedlar bags were used. In order to prepare the bags for use, they were filled with N_2 gas then put in an oven at around 45ºC for 15 min and flushed with N_2 gas at least three times. During the measurement, the samples in the Tedlar bags were kept at 40ºC in an oven. The sampling line and sample inlet were maintained at a temperature of 40ºC using heating cable and tape. It was not possible to control the diet of the volunteers before collecting the breath samples, but most of the volunteers had not eaten for at least 2 hours before collection of their breath samples although they had consumed water. Two

configurations were used to collect the breath samples. Each of these is described in more detail later.

5.2.2 First design to collect breath samples

In the initial attempt two sets of seven 10 litre Tedlar bags were used to collect the exhaled breath samples. One set was used to collect samples from smokers, whilst the other was used for non-smokers. The Tedlar bags were prepared as described above and then selected VOC standards were injected into six of the bags (Table 5.1). These standards were chosen depending on the likelihood of finding them in the exhaled breath. The next step was to collect continuous tidal exhalations for a period of 5 minutes. The purpose of injecting the standards into the breath samples was to help the identification and estimation of the concentration of observed peaks in the spectra produced in the CIR-TOF-MS output.

Table 5. 1: Standards injected in Tedlar bags. The Tedlar bags used were spike with standard VOC mixtures. In view of the large choice of potential candidates, each bag received a different mix of the VOC standards.

Tedlar bags	Spiked standards
Bag1	ethyl acetate, methyl acetate, acrylonitrile, propionitrile and acetonitrile
Bag2	acetone, butanone, acetaldehyde, butanedione and propanal
Bag3	furan, methylfuran, pyrrole, pyridine, and benzene
Bag4	ethylbenzene, toluene, styrene, xylene and ethanol
Bag5	octane, pentane, α-pinene and bromobenzene
Bag6	ethane
Bag7	-

5.2.3 Second design to collect breath samples

In the second approach, the 3 litre Tedlar bags replaced the 10 litre Tedlar bags used earlier. Only one bag was spiked with bromobenzene, whilst the other bags were used only to collect breath samples. The smaller size Tedlar bags were large enough for the sample, produced less and could be cleaned more quickly (Figure 5.1). In addition, the intensity (concentration) of bromobenzene observed was used to estimate the concentration of the analytes of interest.

Figure 5. 1: Assembly of seven 3 litre Tedlar bags used to collect breath samples.

Breath samples contain high relatively humidity, the percentage of which varies from subject to subject. CF_3^+ reacts with moisture so that its availability as a reagent is very sensitive to humidity and the value of *E/N*; for more details see Chapters 3 and 4. Mainly water reacts with CF_3^+ to produce CF_2H^+ but other secondary reactions also occur leading to a significant reduction in the intensity of CF_3^+ as the main reagent. For these reasons, online and offline sampling has been developed using the same design to allow for comparison of results from each method depending on the change in ion count associated with the humidity in breath samples; for more details, see Blake *et al.* [59]. The analytes of interest mainly react with CF_3^+ and CF_2H^+. Breath samples were also measured using PTR-TOF-MS to use as a guide for interpretation of breath data. We will focus on the products which result from reaction of analytes with CF_3^+ and CF_2H^+ as precursors and will further compare with PTR-MS results. Data for CF_3^+ and H_3O^+ were normalized by summation of 69 + 51 amu and 19 amu, respectively. The data obtained from online sampling could not be included as it was not possible to obtain data of satisfactory quality in the time available.

5.2.4 Standards preparation

Initially, 3 microlitres from each standard were injected into Tedlar bags according to their groups (Table 5.1) and diluted to a final volume of 8 litres using nitrogen, in order to prepare a stock solution. 50 ml of each stock solution (gas-phase) were injected into Tedlar bags containing 8 litres of nitrogen to obtain a second dilution. The concentrations of the diluted standards produced in this step are shown in Table 5.2.

Table 5. 2: Concentration of standards in second dilution.

Compound	ppmV	compound	ppmV
ethyl acetate	0.54	pyrrole	0.76
methyl acetate	0.66	pyridine	0.65
acrylonitrile	0.80	benzene	0.59
propionitrile	0.76	ethyl benzene	0.43
acetonitrile	1.01	toluene	0.49
acetone	0.72	styrene	0.46
2-butanone	0.59	o-xylene	0.43
acetaldehyde	0.94	ethanol	0.90
butanedione	0.60	octane	0.32
propanal	0.73	pentane	0.45
furan	0.72	α-pinene	0.33
methyl furan	0.61	bromobenzene	0.50

5.3 Result and discussion

5.3.1 Analysis of chemical standards

The main fragmentation characteristics of the standards were measured with the CIR-TOF-MS using CF_3^+ and H_3O^+ as reagents. These results were used to interpret the breath samples. The results of first group of standards produced by the precursors CF_3^+ and H_3O^+ are shown in Figure 5.2. The signals at m/z = 43 and 61 (using CF_3^+) were characteristic of ethyl acetate, whilst peaks m/z =122, 124 and 143 were are believed to originate from acrylonitrile, propionitrile and methyl acetate respectively. In addition, the presence of substantial H_3O^+ contributed to protonated ions such as m/z = 54, 56 and 75 from acrylonitrile, propionitrile and methyl acetate respectively. These are shown in the upper part of Figure 5.2. The results for PTR-MS showed prominent peaks at m/z = 54, 56, and 75, which were ascribed to acrylonitrile, propionitrile and methyl acetate, respectively, while m/z = 61 and m/z = 89 were produced from ethyl acetate. These are shown the lower part of Figure 5.2.

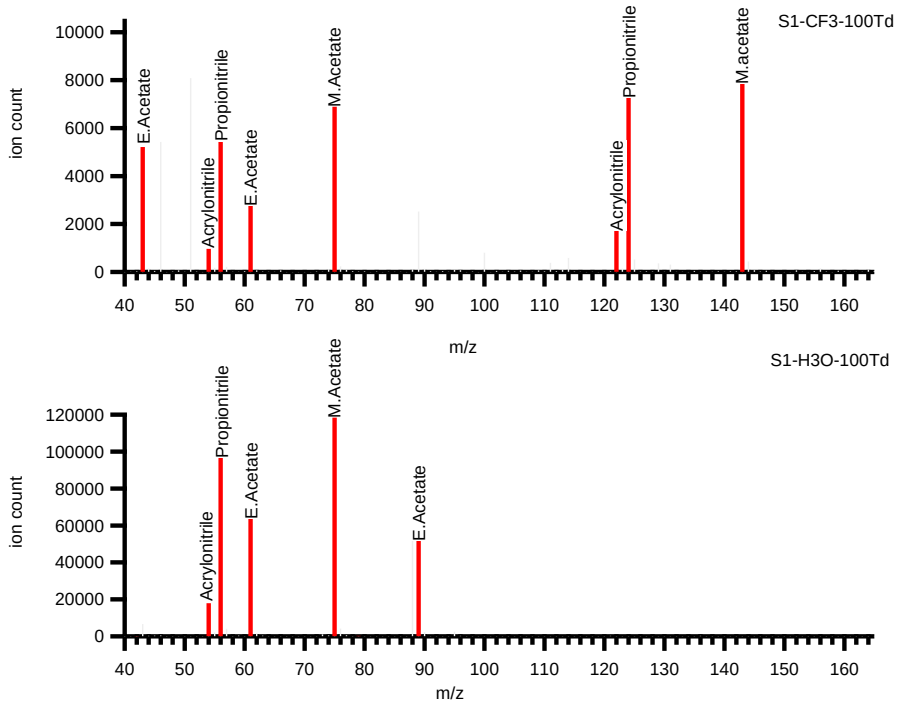

Figure 5. 2: First group of standards (S1).

The results for the second group of standards are shown in Figure 5.3. Peaks at m/z = 43 and m/z = 75 belong to butanedione and 2-butanone, respectively. The signal m/z = 61 arose from acetone or propanal, whilst the signal at m/z = 127 arose from acetone or benzene. Acetaldehyde and acetone produced protonated molecular ion at m/z = 47 and 59 respectively. As a consequence, CF_3^+ as reagent in CIR-TOF-MS was able to differentiate between the members isobaric twins (acetone and propanal). The lower part of Figure 5.3 shows PTR-TOF- MS spectra obtained from these standards. Peaks at m/z = 43, 59, 73, and 87 correspond to acetaldehyde, acetone (or a fragment of propanal), butanone and butanedione, respectively.

The spectra showed peaks at m/z = 80, 136 and 148 derived from pyridine, followed by fragments due to methyl furan at m/z = 82, 83, and 151. Other peaks at m/z = 127 and 147 belong to benzene (or acetone) and furan, respectively. The results obtained here are confirmed by the PTR-TO-MS spectra. These compounds belong to the third group of standards (Figure 5.4).

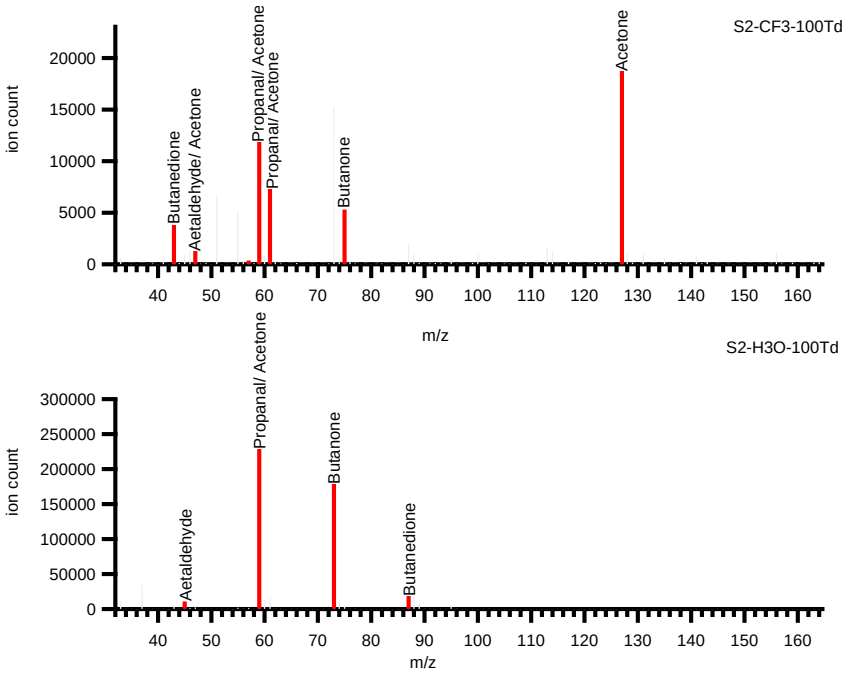

Figure 5. 3: Second group of standards (S2).

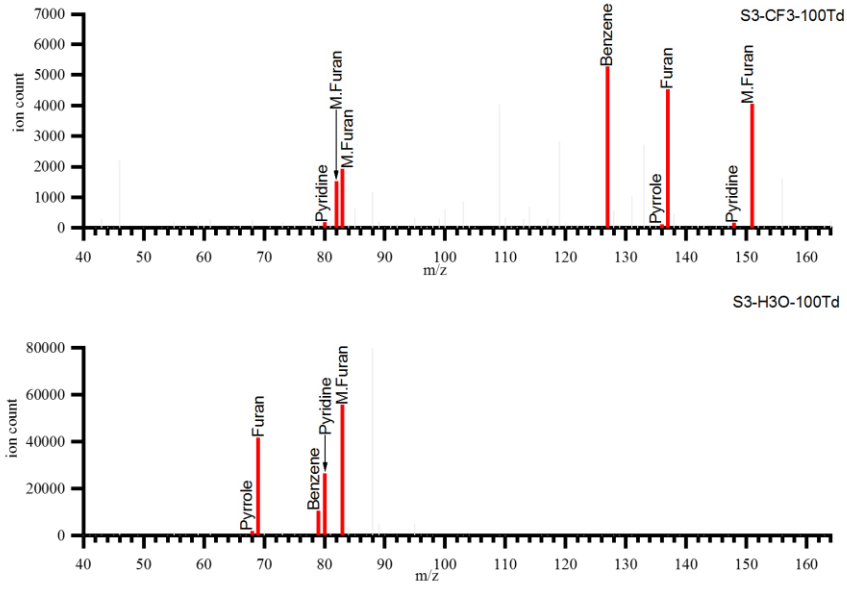

Figure 5. 4: Third group of standards (S3).

The mass spectra presented in Figure 5.5 were produced from the reaction of CF_3^+ and H_3O^+ as reagents in CIR-MS with the fourth group of standards. The signal at m/z = 127 was thought to correspond to benzene, ethyl benzene and acetone. Fragments at m/z = 141 and 173 belong to toluene and styrene by addition of CF_2, respectively. Meanwhile, both signals at m/z = 155 and 175 were assigned to xylene. The protonated molecular ion

at m/z = 47 corresponds to ethanol. The results obtained from PTR-TOF-MS support these findings.

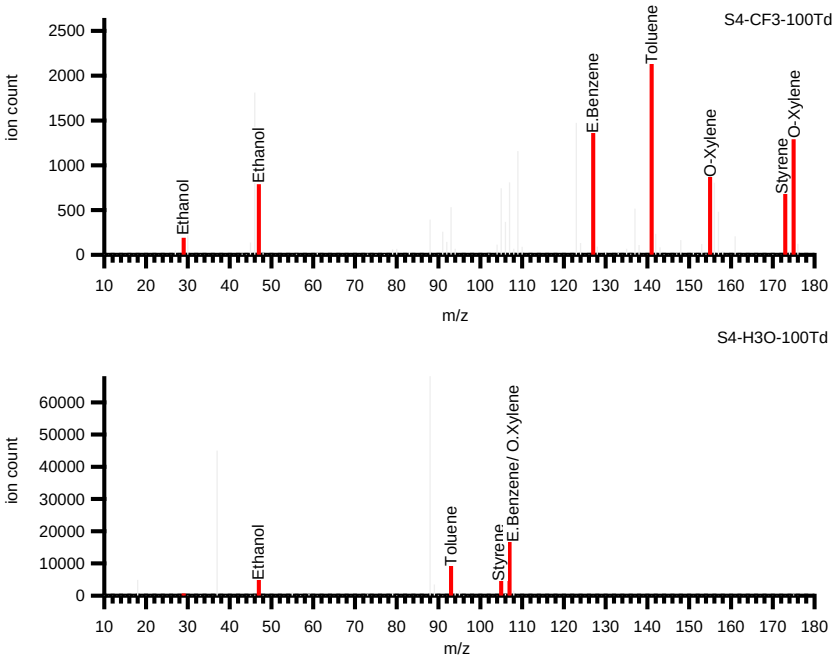

Figure 5. 5: Fourth group of standards (S4).

In the fifth group of standards, pentane was detected at m/z = 71 using CF_3^+ as a reagent in CIR-MS, though it was not detected using PTR-TOF-MS. Other peaks at m/z = 93 and 135 are believed to belong to α-pinene Figure 5.6.

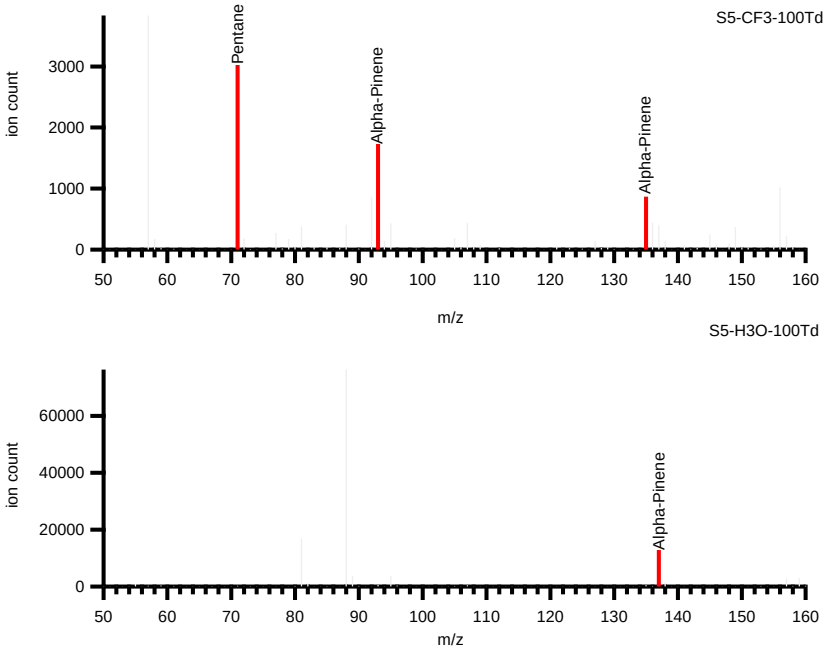

Figure 5. 6: Fifth group of standards (S5).

5.3.2 Estimating relative concentrations of particular VOCs in exhaled breath using injected standards

In order to quantify (in terms of the difference in amount between smokers and non-smokers) the VOCs in breath samples of human subjects, the ion signals for breath samples with and without standards were acquired. These values were used in Equation 5.1 to estimate the relative concentration of the compounds of interest in subjects who were smokers and non-smokers. The results for CF_3^+ are shown in Table 5.3 and Figure 5.7, whilst the results for H_3O^+ are shown in Table 5.4.

$$the\ range\ of\ estimated\ relative\ concentration = \frac{ion\ count\ of\ breath\ sample * concentration\ of\ injected\ standard}{the\ ion\ count\ of\ breath\ with\ standard} \quad (5.1)$$

Table 5. 3: Estimated relative concentrations in breath sample, as detected by CF_3^+ as a reagent in CIR-MS.

Compound	mass	relative con. Range, smoker	relative con. range, non-smoker
octane	57	0.06-0.12 ppmV	0.05-0.11 ppmV
butanone	75	0.13-0.37 ppmV	0.05-0.06 ppmV
acrylonitrile	122	0.44-0.68 ppmV	0.24-0.24 ppmV
benzene	127	0.28-0.42 ppmV	0.10-0.16 ppmV
toluene	141	0.10-0.13 ppmV	0.07-0.12 ppmV
methyl acetate	143	0.10-0.14 ppmV	0.04-0.12 ppmV

Table 5. 4: Estimated relative concentration in breath sample detected by H_3O^+ as reagent in CIR-MS.

compound	mass	relative con. Range, smoker	relative con. range, n-smoker
acetonitrile	42	1.17-1.60 ppmV	0.19-0.62 ppmV
ethanol	47	0.16-0.48 ppmV	0.04-0.06 ppmV
acrylonitrile	54	0.14-0.27 ppmV	0.13-0.21 ppmV
acetone	59	0.07-0.15 ppmV	0.06-0.07 ppmV
ethyl acetate,	61	0.02-0.05 ppmV	≤0.01 ppmV
butanone	73	0.20-0.36 ppmV	≤0.01 ppmV
methyl acetate	75	0.01-0.11 ppmV	≤0.01 ppmV
benzene	79	0.28-0.86 ppmV	0.34-0.48 ppmV

Variations in estimating the total volume of the Tedlar bags employed for the injected standard method introduced an additional uncertainty into the error estimation for the breath sample of approximately 10%.

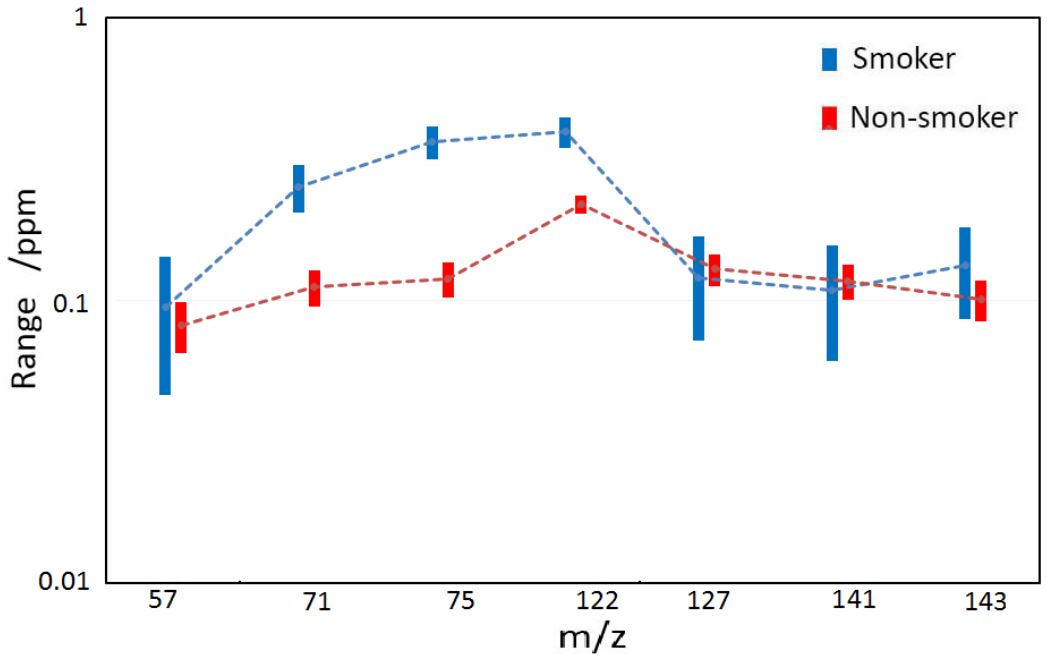

Figure 5. 7: Concentration range of detected compounds for smokers and non-smokers, as detected by CF_3^+ as a reagent in CIR-MS, is shown in ppmV. Error bars represent the minimum and maximum concentrations per m/z value. Internal standard method.

5.3.3 Bromobenzene as a single standard

In the previous section, two sets of data were produced. One set was produced from the breath samples only and compared to another set with standards added. However, the two samples could differ in humidity and volume, thereby introducing additional uncertainty in the estimation of the concentration of the compounds of interest. In an attempt to reduce the sources of error, the design of the experimental procedure was amended. Tedlar bags with a capacity of 3 litres were used to collect breath samples. These required less to fill and would be easier to clean. In this series of experiments bromobenzene (50 ml of 1.33 ppmV) was injected only into one bag to estimate the relative concentration of compounds of interest in breath samples. Later volunteers were asked to fill these bags with their exhaled breath.

5.3.3.1 Estimate of the relative concentration of VOCs of interest using bromobenzene as an internal standard

Breath samples with and without bromobenzene were measured via CIR-TOF-MS using both reagents. The ion count for breath samples with and without bromobenzene were

acquired and used for estimation of the relative concentrations of various VOCs. Equation 5.2 shows how to calculate the relative concentration of an analyte in breath samples. The result obtained with CF_3^+ is shown in Table 5.5 and Figure 5.8, and the results for H_3O^+ are shown in Table 5.6.

$$concentration = \frac{signal\ of\ analyte * concentration\ of\ bromobenzene}{signal\ of\ bromobenzene} \quad (5.2)$$

Table 5. 5: Estimated relative concentrations in breath sample detected by CF_3^+ as reagent in CIR-MS.

compound	mass	relative con. range, smoker	relative con. range, n-smoker
octane	57	0.37-0.43 ppmV	0.25-0.5 ppmV
pentane	71	0.29-0.32 ppmV	0.21-0.27 ppmV
butanone	75	0.17-0.24 ppmV	0.09-0.15 ppmV
acrylonitrile	122	0.08-0.11 ppmV	0.03-0.13 ppmV
acrolein	125	0.15-0.17 ppmV	0.08-0.13 ppmV
ben/carbonyl	127	1.94-2.15 ppmV	1.26-2.78 ppmV
toluene	141	0.13-0.19 ppmV	0.06-0.19 ppmV
methyl acetate	143	0.51-0.52 ppmV	0.45-0.79 ppmV

Table 5. 6: Estimated relative concentrations in breath samples detected by H_3O^+ as reagent in CIR-MS.

compound	mass	relative con. range, smoker	relative con. range, n-smoker
ethanol	47	0.29-1.52 ppmV	1.09-2.61 ppmV
acrylonitrile	54	0.26-1.67 ppmV	0.33-0.64 ppmV
ethyl acetate,	61	0.20-0.56 ppmV	0.56-0.78 ppmV
butanone	73	0.52-1.59 ppmV	0.46-0.79 ppmV

In the initial set of measurements, samples were taken from two bags: one containing the sample alone, with the other containing the sample injected with a standard of known strength. However, owing to the variable humidity in breath samples which caused instability in the equipment, it was not easy to achieve reproducible results.

In the second attempt (Equation 5.2), only one bag was injected with the bromobenzene standard. The remaining bags contained no additives but all were assumed to have the same composition. It was hoped that this would eliminate errors arising from comparing separate runs. Moreover, the amended design allows the measurement of more than one bag for same sample. Instabilities in the operation of the CIR-TOF-MS made it impossible to obtain satisfactory results from two separate breath samples. This method has the same

limitations as previous one viz: the test volume uncertainty (± 10%) and sensitivity of bromobenzene which could change during the experiment.

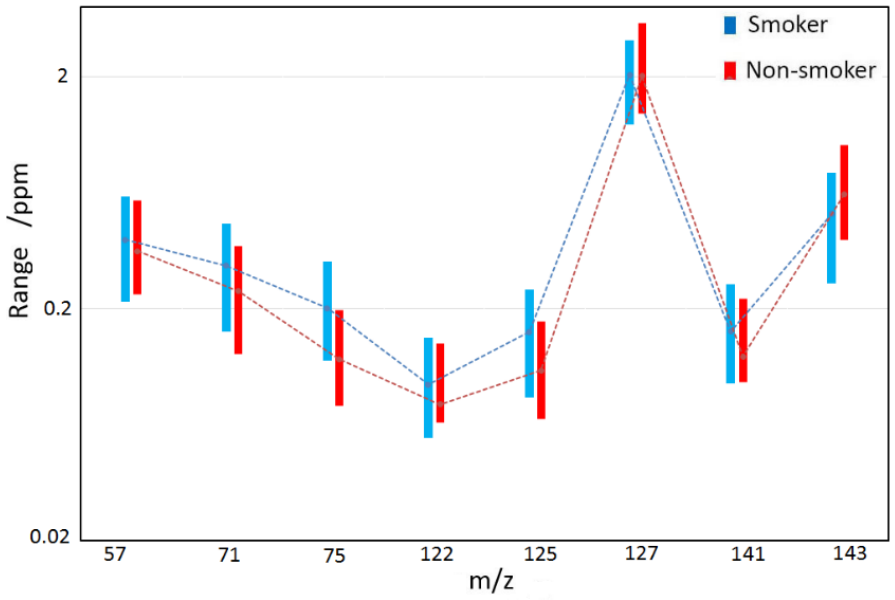

Figure 5. 8: The bromobenzene method results. The concentration of the range of detected compounds for smokers and non-smokers, using CF_3^+ as the reagent in CIR-TOF-MS and using bromobenzene in ppmV (Table 5.5). The error bars represent the minimum and maximum concentration per m/z value. The y-axis is formatted in a log scale to accommodate the large range of yields observed.

5.3.4 Estimated concentration of VOCs in breath using calibration curves

In design two, the estimation of the concentration of a number of the detectable masses in exhaled breath samples was found to introduce unacceptable levels of uncertainty. Errors could arise from the imprecise estimates of the volume of the breath sample in each bag and the sensitivity of bromobenzene. As a result, a series of standard solutions were prepared and measured to calculate the sensitivity of the VOCs of interest that could be used to estimate the concentration of compounds detected in exhaled breath.

5.3.4.1 Calibration curves

Related stock solutions and a series of diluted standards were prepared as discussed in Chapter 4 and reported in Table 5.1. The sensitivities of these compounds were estimated from the gradient of their calibration curves. Figure 5.9 shows a standard curve for mass 122 as detected by CF_3^+ as reagent in CIR-TOF-MS.

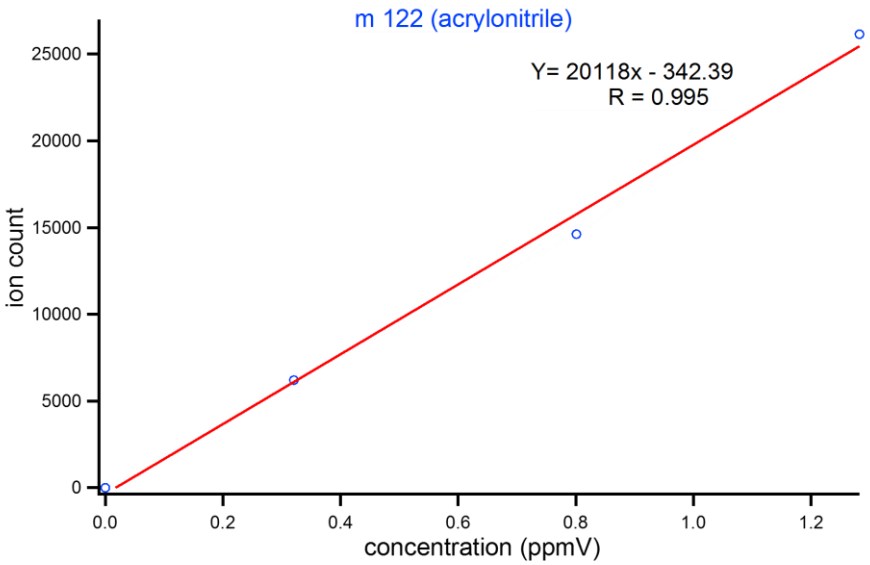

Figure 5. 9: Calibration curves for m/z = 122, the major fragment of acrylonitrile.

5.3.4.2 Calculation of VOCs concentrations using calibration method

The sensitivity of compounds detected in breath samples were estimated from the gradients of standards of these compounds. Equation 5.3 show how sensitivity can be used to calculate the concentration of compounds detected in breath samples.

$$S_N = \frac{\#}{[x]} \qquad (5.3)$$

S_N = sensitivity of the compound, [x] = concentration (ppmV) and # = normalized ion count of the compound (ncps). The sensitivity is therefore in units of ncps $ppmV^{-1}$. The results for the concentrations of detected compounds are shown in Tables 5.7 and 5.8, and illustrated in Figure 5.10.

Table 5. 7: Estimated concentration in breath samples detected by CF_3^+ as reagent in CIR-MS.

compound	mass	relative con. range, smoker	relative con. range, n-smoker
octane/butane	57	1.31-1.4 ppmV	0.67-1.20 ppmV
butanone	75	0.09-0.14 ppmV	0.05-0.06 ppmV
acetonitrile	110	0.13-0.21 ppmV	0.01-0.02 ppmV
acrylonitrile	122	0.12-0.16 ppmV	0.03-0.06 ppmV
acrolein	125	0.04-0.05 ppmV	0.03-0.04 ppmV
acetone/benzene	127	0.49-0.74 ppmV	0.11-0.34 ppmV
toluene	141	0.12-0.24 ppmV	0.08-0.16 ppmV
methyl acetate	143	0.31-0.39 ppmV	0.27-0.32 ppmV

Table 5. 8: Estimated concentration in breath samples detected by H_3O^+ as reagent in CIR-MS.

compound	mass	relative con. range, smoker	relative con. range, n-smoker
ethanol	47	0.12-0.23 ppmV	0.08-0.09 ppmV
acrylonitrile	54	<0.01 ppm V	<0.01 ppmV
acrolein	57	0.05-0.05 ppmV	0.04-0.05 ppmV
acetone	59	0.15-0.20 ppmV	0.03-0.060 ppmV
ethyl acetate	61	0.02-0.03 ppmV	0.01-0.02 ppmV
butanone	73	0.02-0.03 ppmV	<0.01 ppmV
acetonitrile	42	0.11-0.24 ppmV	0.01-0.02 ppmV

The calibration curve method also has a number of limitations. For example, fragments from several compounds having the same value of m/z. Benzene and acetone appear at m/z = 127 with different abundances. As a consequence, the concentration of benzene, as estimated using m/z = 127, could not only contain benzene but could also be due to the presence of a CF_3 adduct of acetone.

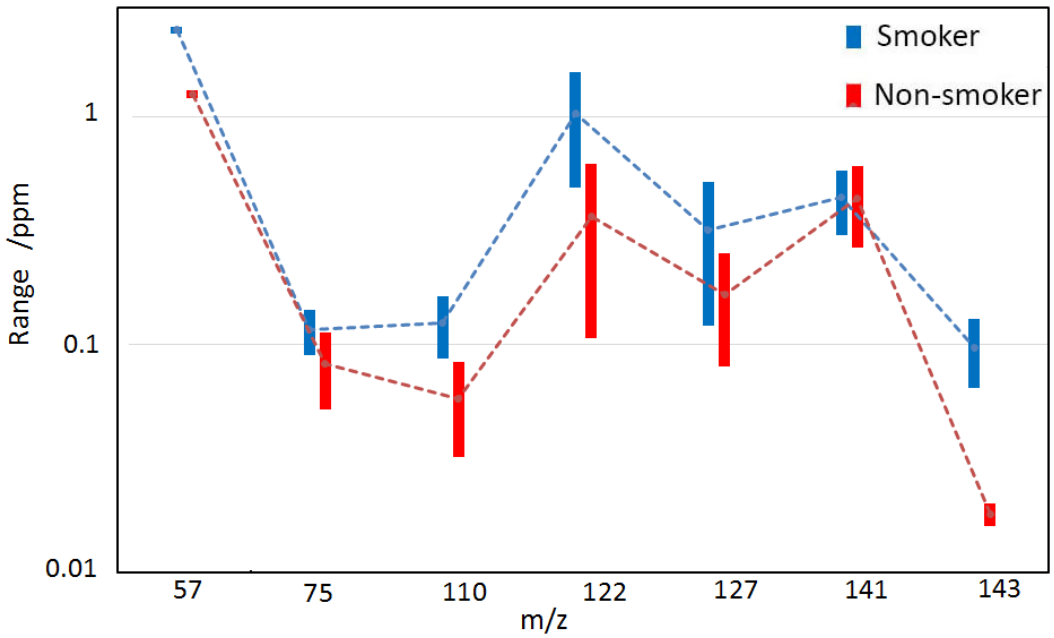

Figure 5. 10: Concentration range of detected compounds for smokers and non-smokers, as detected by CF_3^+ as reagent in CIR-MS and using a calibration curve; concentrations are shown in ppmV. Error bars represent the minimum and maximum concentration for each m/z value.

5.3.5 Evaluation of the three concentration methods

The first method to estimate the concentration range of compounds detected for smoking and non-smoking subjects used internal standards of the expected compounds, injected

into the breath samples. This method relied on a comparison of the intensity of the compound of interest in breath with and without standards. The sensitivity of this method is satisfactory but suffers from limitations such as uncertainty of the sample volume. Other sources of error could arise from dependence of the CF_3^+ ion count from one sample to another on ambient humidity.

In the second method, bromobenzene was used as an internal standard to estimate concentrations in breath samples from smoker and non-smoker volunteers. This method depends on injection of a known concentration of bromobenzene into one of the Tedlar bags holding the breath samples. Here again, the uncertainty from estimating the sample volume was reduced when using 3 litre Tedlar bags. In addition, the sample-to-sample variation in humidity was avoided since the composition of the participating bags derived from a single breath collection. In spite of this, this method still suffers from a variation of intensity (sensitivity) of bromobenzene during the associated measurements (between samples).

In the third method, calibration curves were generated using standards of compounds expected in breath samples. The sensitivity extracted from the gradient of the calibration curves was used to estimate the concentration of the species detected. In this method, the error from the uncertainty in sample volume was eliminated.

Of the three alternatives, the calibration curve method offered the best approach.

Some considerable variation in the concentrations were noticed between the result of CF_3^+ and H_3O^+ for some compounds, such as butanone and acrylonitrile. This could be expected as different chemical mechanisms were involved when CF_3^+ and H_3O^+ are the reagents. As noted in Chapter 3, some compounds such as the lighter n-alkanes are detected by CF_3^+, but not by H_3O^+, and alcohols while insensitive to reacting with CF_3^+, react strongly with H_3O^+. The main aim of this Chapter was to identify the VOCs detected in breath samples using a novel reagent in CIR-TOF-MS rather than estimation the concentrations of the samples. In spite of the uncertainty in the methods of estimating the concentration of VOCs in exhaled breath such as errors in the volume and humidity of breath samples, the results showed the intensity of some of VOCs in exhaled breath were consistently higher in smokers' breath compared with non-smokers, as shown in Figures 5.8, 5.9 and 5.11.

5.3.6 Alkanes (C_2-C_6) in breath

Proton transfer reactions do not occur with the lighter n-alkanes ($\leq C_6$), whereas the remaining VOCs provided an interesting comparison from when using H_3O^+ as well as CF_3^+ [59]. The alkane data showed that the average of the yields for smokers is greater than those of non-smokers, as seen in Figure 5.11.

In the present investigation, a minor fragment of ethane, $C_2H_3^+$ (m/z=27) was selected as the indicator for the presence of ethane. This fragment is too small to be useful if *E/N* = 100 Td but at 120 Td fragmentation of ethane is apparent. The molecular ion group for propane at m/z = 43 is believed to contain fragment contributions from other VOCs, including butane and pentane so that it cannot be considered a marker for propane ($C_3H_7^+$). Butane, pentane and hexane whose molecular ion fragments at m/z = 57, 71 and 85 all were able to differentiate unambiguously between smokers and non-smokers. Alcohol reactions with CF_3^+ are very weak and the yields obtained are negligible whereas in PTR reactions alcohols could be detected without difficulty.

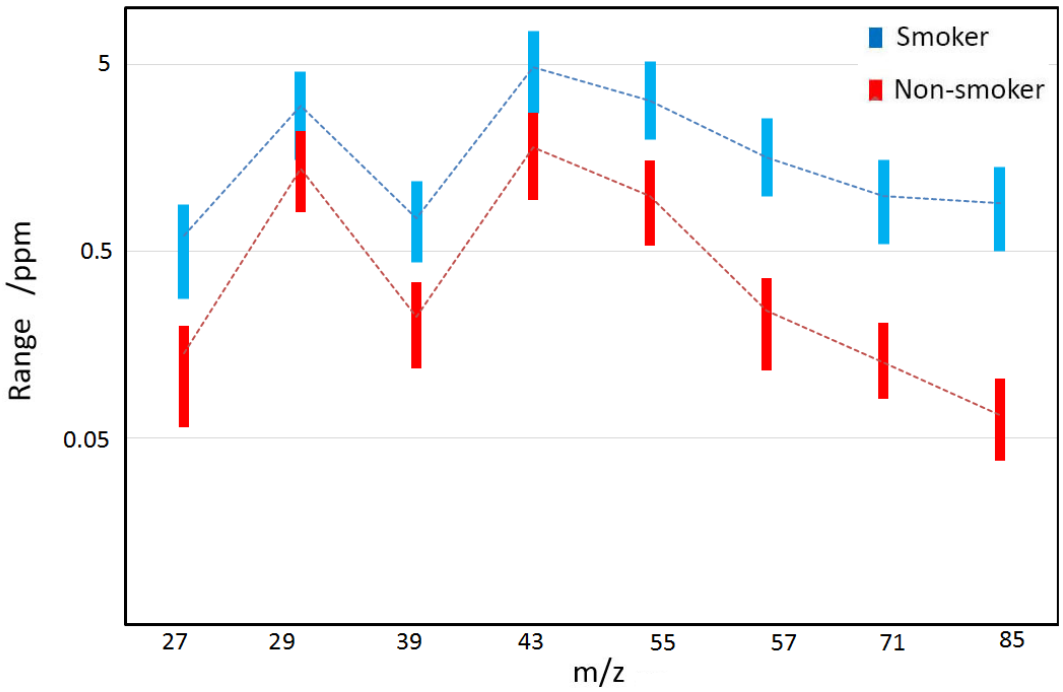

Figure 5. 11: Comparison of the yields of C_2-C_6 alkane molecular ions and fragments.

5.3.7 Interpretation of breath spectra

PTR-TOF-MS measurements cannot distinguish structural isomers or nominally isobaric species [60]. As result, it is not always possible to identify specific peaks in the mass

spectrum and impossible when two or more VOCs or fragments have the same mass. Moreover, fragmentation and clustering of products make this process even more complicated. Using CF_3^+ as a precursor, however, it is possible to identify small-chain alkanes which do not react with H_3O^+ [59]. In addition, CF_3^+ offers a variety of reaction routes so is able to react preferentially with certain target VOCs and differentiate VOCs. The end products of the two reagents rarely have the same m/z. For example, certain compounds, such as the nitriles, or functional groups, such as the carbonyl group readily form CF_3-adducts or normal protonated ions, depending on the reagent type [61].

Figures 5.12 and 5.13 show the results of smoking and non-smoking volunteers, respectively, where the upper charts represent the results of breath samples measured by CIR-TOF-MS using CF_3^+ as the precursor, and the lower charts the results obtained with the CIR-TOF-MS using H_3O^+ as the precursor.

Predominant and expected known peaks in the exhaled breath of smoking and non-smoking volunteers will be discussed in more detail.

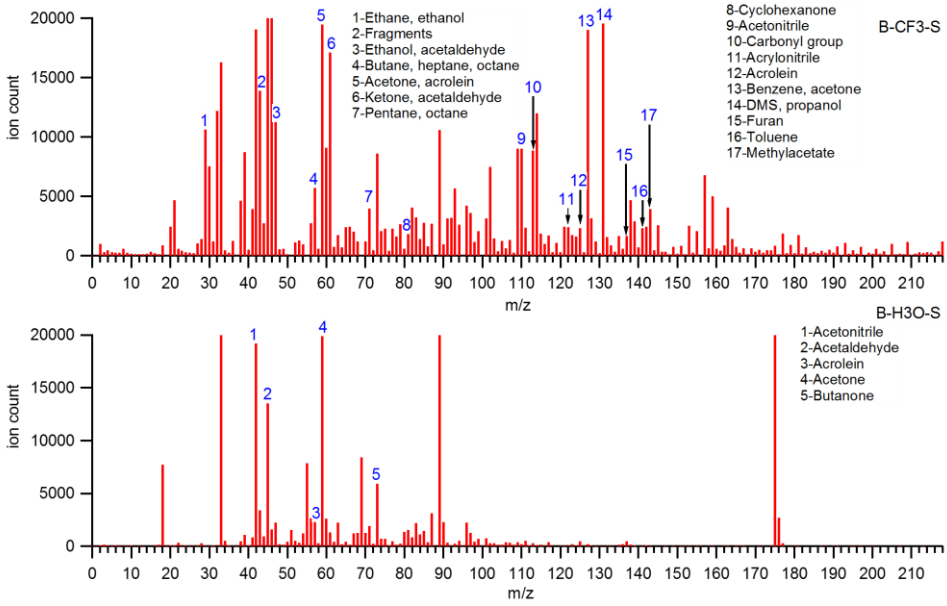

Figure 5. 12: Expected compounds in breath smoker, resulting from the use of CF_3^+ (upper chart) and H_3O^+ (lower chart) as precursors. Background spectra due to lab air was subtracted.

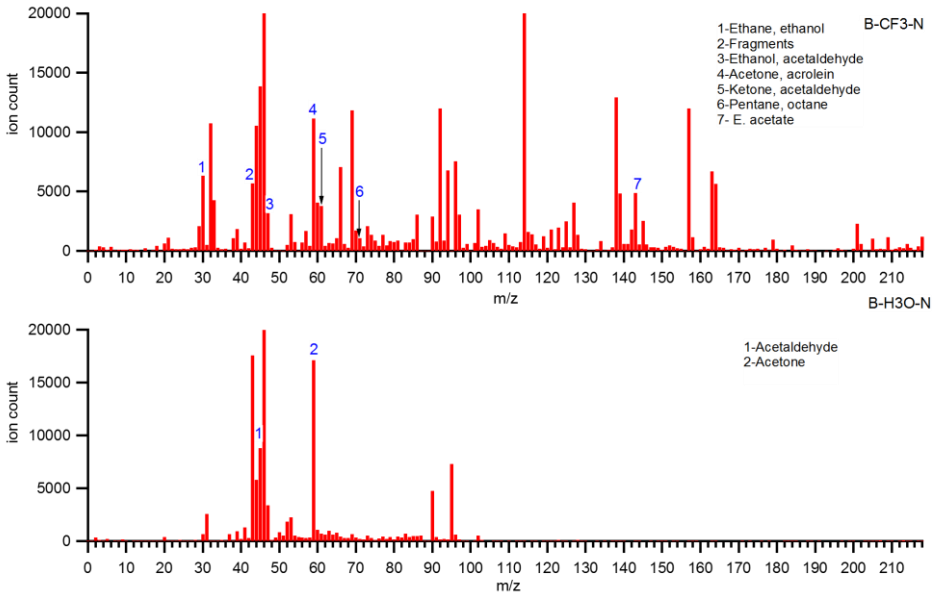

Figure 5. 13: Expected compounds in the breath non-smokers, where CF_3^+ (upper chart) and H_3O^+ (lower chart) are used as precursors. Background spectra due to lab air was subtracted.

5.3.7.1 m/z = 29

A peak at m/z = 29 is produced by reaction of a breath sample using CF_3^+ as the reagent. Blake *et al.* [61], found that pentanone and ethanol give fragments of $C_2H_5^+$ with relative abundances of 3% and 56%, respectively. In another study, Blake *et al.* [59], reported that the parent ion of ethane, $C_2H_5^+$, has a 94% relative abundance. It seems that m/z = 29 contains contributions from ethane as well as ethanol. Further investigation in the mass spectral region of m/z = 29 shows evidence of two overlapping groups: firstly, from the source reaction of CF_3^+ with an alkane (most likely ethane) to form $C_2H_5^+$ at m/z = 29.0611, as shown in equation 5.4.

$$CF_3^+ + C_2H_6 \longrightarrow C_2H_5^+ + CF_3H \qquad (5.4)$$

Another peak with the same mass (m/z = 29.0176) is CHO^+ but it is not obvious by what mechanism it would be created [61].

The CIR-TOF-MS instruments used in this work do not have sufficient resolution (m/Δm ~1000) to separate these peaks, so software was used to resolve the data into its two constituents to estimate the contribution of $C_2H_5^+$. In conditions of high humidity, the interfering group was dominant and the percentage of hydrocarbons contributed only 5% of the total of m/z = 29 yield in the exhaled breath samples. Figure 5.14 illustrates a

situation in which the contribution of the $C_2H_5^+$ is dominant, a situation not encountered in conditions of high humidity.

VOCs have the potential to be used as biomarkers for many disorder in the human body. The concentration of ethane has been detected previously by GC-MS and been found to be raised in human breath immediately after smoking, returning to baseline within three hours [62]. In addition, Handelman *et al*. and Stevenson *et al*. [63, 64], found that ethane in breath increased significantly in 52% of haemodialysis patients when compared to a control group. The authors suggested that long-term metabolic processes were responsible for this elevation of ethane. The concentration of ethane in breath has also been found to be increased in inflammatory disease, and with patients with asthma, and is produced by lipid peroxidation [5]. On the other hand, another study claims that ethane and pentane are in fact not biomarkers of airway inflammation or oxidative stress [65]. Finally, ethane is one of the species that is considered to be a biomarker of oxidative stress and schizophrenia [49, 66-68].

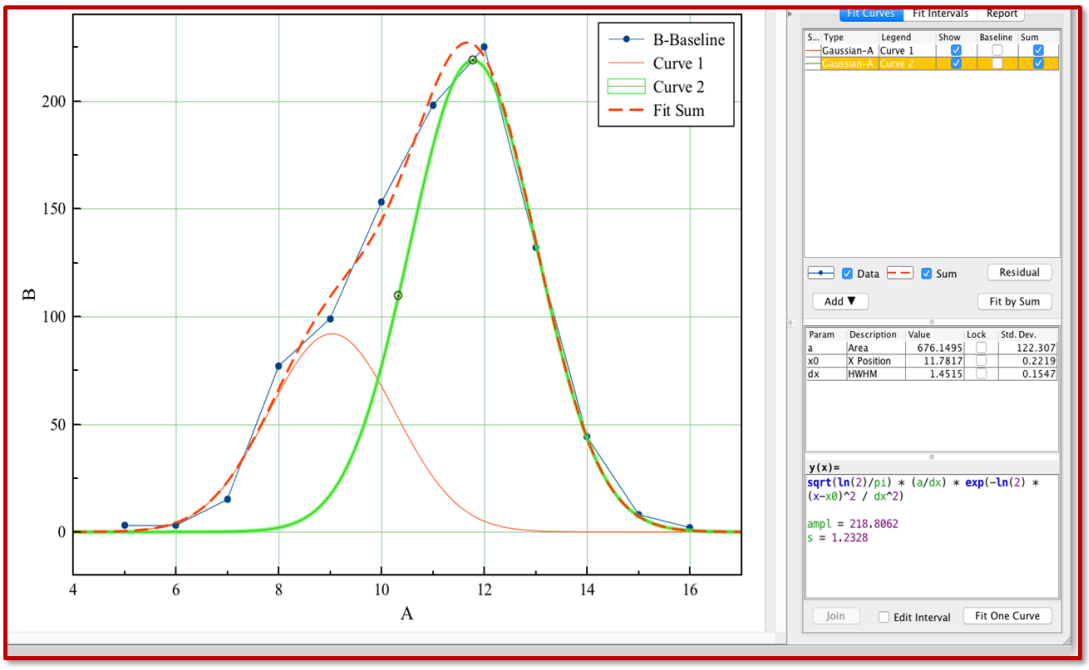

Figure 5. 14: Estimated hydrocarbon percentage from the total intensity at m/z = 29. The software used was MagicPlot Student (St. Petersburg).

From the library (Chapter 4) it appears that m/z =29 more likely is composed of a mixture of the fragments $C_2H_5^+$ and CHO^+. As a result there are problems using m/z = 29 as marker but it is a useful predictor for ethane and ethanol when humidity is low, in the case of high humidity, the CHO^+ fragment can dominate.

5.3.7.2 m/z = 57

In the alkane work, the peak at m/z = 57 may be attributed to butane or fragments from heptane or octane. Blake *et al.* [59, 61], found that butane produces a parent ion at m/z = 57 with a relative abundance of 96%, while heptane and octane produce main fragments at m/z = 57 with relative abundances of 95% and 50%, respectively [59, 61]. Blood-borne butane may originate from protein oxidation and/ or bacteria activity in the colon. The concentration of butane in human breath has been shown to be in the range from 0.6 to 6.5 ppb [69]. Butane was found to be one of five VOCs which were significantly different between subjects with healthy and diseased lungs [70]. In addition, butane was found to decrease after surgery on diseased lungs, suggesting that butane is linked to tumour growth [70]. Our results show that m/z = 57, which may belong to butane, is higher in smokers than non-smokers. This could support the apparent relationship between smoking and diseased lungs. It seems that owing to the observed overlap of m/z = 57, it cannot be used as biomarker for a specific compound but it does give indication to the existence of the hydrocarbons i.e. butane, octane or heptane.

5.3.7.3 m/z = 61

A significant peak was observed at m/z = 61, which was thought mainly to belong to aldehydes and ketones. Blake *et al*. [61], (Ch. 4 results), demonstrated that propanal, acetone, ethyl acetate, hexanone, DMS and propanol react with CF_3^+ as reagent and gave fragments at m/z = 61 with relative abundances of 58, 23, 20, 14, 8 and 4%, respectively. It is likely that the m/z = 61 is useful as a marker of some compounds possessing a carbonyl group, mainly acetone and propanal where fluorine replaces oxygen in $–COH^+$ to form $-CFH^+$.

5.3.7.4 m/z = 71

The ion with m/z = 71 is likely associated with pentane or octane. Blake *et al.* (results of Ch. 4) found that pentane and octane produced fragments at m/z = 71 with relative abundances of 74.3 and 39.7 %, respectively, in the CIR-TOF-MS work using CF_3^+ as the reagent [59, 61]. Pentane and octane produced no meaningful PTR-TOF-MS results. A study was conducted on preschool children (2-4 years) with preclinical asthma using GC-TOF-MS; octane was one of the VOCs which increased during episodes of wheezing compared with children with transient wheezing at 6 years of age [71]. Elevated levels of pentane in breath can be correlated with the progression of sickness in inflammatory

bowel disease patients [72]. Our findings exhibit the signal at m/z = 71, which could belong to pentane, was higher in smokers compared to non-smokers. This could provide some evidence that smoking may play a part in the occurrence of the disease mentioned above. While m/z =71 cannot be attributed to a definite compound, it could be used as sigh of existing pentane and/or octane.

5.3.7.5 m/z = 75

The small signal observed at m/z = 75 might be produced by 2-butanone. Blake *et al.* [61], found that 2-butanone gave predominant peaks at m/z = 75 and 55, with relative abundances of 45 and 41%, respectively, with CF_3^+ as a precursor. Figures 5.12 and 5.13 (lower part - H_3O^+ results) show a peak at m/z = 73 which could belong to 2-butanone. In addition, our GC-MS measurements showed that 2-butanone was one of the compounds present in breath samples (Table 5.9). Amal al *et al.* [73], conducted a study on breath samples of patients with gastric cancer using GC-MS and cross-reactive nanoarrays combined with pattern recognition. The results of this study showed that eight VOCs, one of them 2-butanone, were significantly different across the cases considered in this study [73]. 2-butanone is one of the ketones whose concentration varies significantly in cirrhotic patients compared to healthy volunteers in a study conducted using PTR-TOF-MS [74]. A study was conducted to quantify carbonyl volatile organic compounds in lung cancer patients, the authors of which used silicon microreactor technology to capture carbonyl VOCs which were then measured by FT-ICR-MS. The results of this study showed that one of these compounds, 2-butanone, has a higher concentration in the exhaled breath of lung cancer patients compared with healthy controls [75, 76]. Another study showed that 2-butanone, 2-pentanone, methanol, limonene, and carbon disulphide are markers for early-stage liver disease [77]. Our data showed that the concentration of butanone in smokers is twice as high as that in non-smokers. Meanwhile m/z = 75 appears to be a useful biomarker of 2-butanone (smokers) particularly when compared with PTR-MS result.

5.3.7.6 m/z = 110

Another significant peak at m/z = 110 resulted from the addition of CF_3^+ to the molecular ion and can be assigned to acetonitrile. From Figure 5.12 (lower part), the peak at m/z = 42 arises from the reaction of H_3O^+ and acetonitrile. As consequence, both CF_3^+ and H_3O^+ can be used to confirm the presence of acetonitrile in smoker samples. A study was

conducted to detect acetonitrile in smokers and non-smokers using SIFT-MS. The concentration range of acetonitrile was found to be 17-124 ppb [78]. Our own concentrations were higher in smokers than non-smokers. Research indicates the effects of different sampling techniques such as mixed expiratory, alveolar, and time-controlled samples on the results of breath analysis. The author found the concentration of endogenous VOCs is higher in alveolar samples, and the ratios C_{alv}/C_{mixed} for acetonitrile were within the range 1-1.5 [79]. The concentration of acetonitrile in the breath of smokers was found to increase while using thermal desorption tubes (TD) during measurement with PTR-MS [80]. Breath samples (smokers, passive smokers, and non-smokers) were measured using extractive electrospray ionization mass spectrometry. The results showed that the concentration of acetonitrile reaches a maximum (around 30 ng/L) within 1-4 hours after smoking, returning to background levels within seven days [81].

Our library (Blake *et al*. [61], and Chapter 4), indicate that m/z = 110 could be used as biomarker to identify acetonitrile.

5.3.7.7 m/z = 122

A small peak at m/z = 122 resulted from the reaction of CF_3^+, and is thought to belong to acrylonitrile. Our findings in Chapter 4 demonstrated that acrylonitrile produces a fragment at m/z = 122 with a relative abundance of 83.4 %. As seen in the lower part of Figure 5.12, PTR-MS measurements produced a peak at 54 amu which may belong to the protonated parent of acrylonitrile. Acrylonitrile concentrations have been found to be elevated in individuals exposed to tobacco smoke [82]. A study conducted to detect VOCs in the plasma of oesophageal adenocarcinoma (EAC) and gastroesophageal reflux-diseased patients showed that acrylonitrile was one of nine VOCs that decreased significantly in the plasma headspace of EAC patients compared to those without EAC [83]. Acrylonitrile is considered one of the component of vapour phase of mainstream cigarette smoke [84]. Our data showed that acrylonitrile level is higher in smokers compared with non-smokers. m/z = 122 is a good biomarker for smokers.

5.3.7.8 m/z = 125

The small signal at m/z = 125 has been assigned to acrolein. Blake *et al*. [61], found that acrolein with CF_3^+ produced a product of mass 125 ($CH_2CHCHO.CF_3^+$) with a relative abundance of around 50%. Another peak with m/z = 59 has a relative abundance of 41% [1]. Figure 5.12, (lower) shows a corresponding signal at m/z = 57, which would be

expected from the reaction with H_3O^+. As a consequence, both precursors produce a positive result. A study conducted on normal tobacco and E-cigarette smoke found the amount of acrolein released from cigarettes ranged from 0.17 to 8.27 μg (cig. eq.) [85]. Another study detected acrolein in human breast cancer cells [86].

5.3.7.9 m/z = 127

A significant peak at m/z = 127 was observed from the reaction of CF_3^+ with the sample. Blake *et al.* [61], found the m/z = 127 groups could result from reactions with acetone, benzene and bromobenzene with relative abundances of 63.9, 87.7, and 36.5%, respectively. As seen in Figures 5.12 and 5.13, of the peak at m/z = 59 (reaction with H_3O^+) was prominent using both CF_3^+ and H_3O^+, where it is suggested that m/z = 127 is more likely to stem from the CF_3-adduct with acetone. The average concentration of acetone in normal healthy breath is lower than 0.83 ppmV, while the average concentration of acetone in diabetic breath is found to be above 1.11 ppmV [87]. One study showed that acetone concentrations ranged widely from 100 ppb to 1000 ppb [88], whilst another study found the range to be 148-2744 ppb [50]. The concentration of acetone was found to be lower (458.7 ppb) in lung cancer patients than in healthy controls (627.5 ppb) [89]. Schwarz *et al.* [90], investigated variations of acetone concentrations in breath with changes in body-mass index (BMI), age and gender. The study found no significant differences between acetone concentrations in breath and these factors. Acetone is one of the compounds which has been observed to increase in the breath of anaesthetized patients during laparoscopic surgery; this could be due to the onset of lipolysis [91]. The concentration of acetone in breath increases overnight during sleep (575-1460 ppb) compared to the daytime (234-580 ppb) [92]. There is a positive correlation between the concentration of acetone and serum C-reactive protein (CRP). The levels of these compounds were found to be in lower on the day of discharge compared with the day of admission in community-acquired pneumonia patients [93]. Endogenous acetone concentrations have been found to be significantly raised in cancer patients during lung surgery as a result of long periods of fasting and lipid hydrolysis [71]. Natural intra-individual biological and diet may result in variations of the concentration of acetone in breath. As a result, it is not easy to use acetone in breath to monitor blood glucose [94]. Benzene is one of the hydrocarbons which has a higher concentration in smokers' breath. Studies showed the concentration of benzene was significantly higher in smokers and passive smokers than with non-smokers [53, 95].

Unfortunately, m/z =127 cannot be used as marker for a single compound but could be used as indication of the presence of acetone/ or benzene/or ethylbenzene or a mixture of any of these.

5.3.7.10 m/z = 141

A small peak at m/z = 141 could be assigned to toluene. Blake *et al.*[61], found that toluene gave a predominant peak at m/z = 141 with a relative abundance of 78.2% with CF_3^+ as the precursor [61]. Our GC-MS measurements showed that toluene was one of the compounds present in breath samples (Table 5.9). A literature search for a list of 98 hazardous smoke compounds found toluene as one such compound [82]. A study in alveolar and blood of hospital staff showed toluene concentrations of 1-22 ng/l, which were higher in smoking than non-smoking volunteers [96]. In addition, our results indicated that level of toluene in smokers is higher approximately twice as high than found for non-smokers. Hence m/z = 141 qualifies as a useful marker for toluene.

5.3.7.11 m/z = 143

An ion observed at m/z = 143 was thought to be methyl acetate. The results in Chapter 4 found that the reaction of CF_3^+ with methyl acetate produced its principal fragment at m/z = 143 with a relative abundance of 65.4%. The PTR-MS results showed a small signal at m/z = 75 which could belong to methyl acetate (Figure 5.12 and 5.13) [61]. Several studies were conducted to measure the change in VOCs as a result of physical exercise. King *et al.* [69], showed that methyl acetate showed a drastic increase in concentration by a factor of 3-5 shortly after starting exercise Our results show that methyl acetate in smokers is slightly higher compared with non-smokers, so that m/z = 143 is useful as a potential marker for methyl acetate.

5.3.7.12 other peaks

The peak at m/z = 43 arises from propane ($C_3H_7^+$), but also from the fragmentation of various compounds with longer alkyl chains. In addition, some peaks, such as m/z = 59 and 47, arose from competitive H_3O^+ secondary reactions which become significant as the humidity increased in the sample. These belonged to acetone and ethanol/acetaldehyde, respectively.

It is clear that CF_3^+ acts as an excellent reagent in CIR-MS in terms of the detection of the numerous different VOCs in the exhaled breath of smokers and non-smokers. As seen

in CF_3^+ and H_3O^+ spectra, it seems that CF_3^+ has the greater ability to detect VOCs and small-chain alkanes compared with H_3O^+ in CIR-MS. As a result, CF_3^+ is complementary to H_3O^+ in CIR-MS to identify VOCs in exhaled breath with greater specificity and accuracy.

5.4 Statistical investigation

Multivariate analysis is an important tool for the examination of all variables in complex datasets to extract the underlying patterns from this data [97, 98]. Analysis of breath via CIR-TOF-MS using CF_3^+ as a reagent provided an extensive dataset by which to identify the many VOCs in human breath. In total, 39 samples (14 smokers and 25 non-smokers) and 39 variables (m/z values) were analysed statistically and subjected to principal component analysis (PCA), agglomerative hierarchical clustering analysis (AHC), and partial least squares - discriminant analysis (PLS-DA) using XL STAT [99]. Masses of reagents (CF_3^+, H_3O^+), clusters and undetectable masses were manually excluded from the mass range before running statistical analyses to avoid complications in output data. Figure 5.15 shows the differentiation of smoker and non-smoker data by PCA in two dimensions. Observation of the resultant graph shows that if data are represented on only one axis, the variability may still be high (56.81%) and the two axes represent 71.74% of the initial variability of the data.

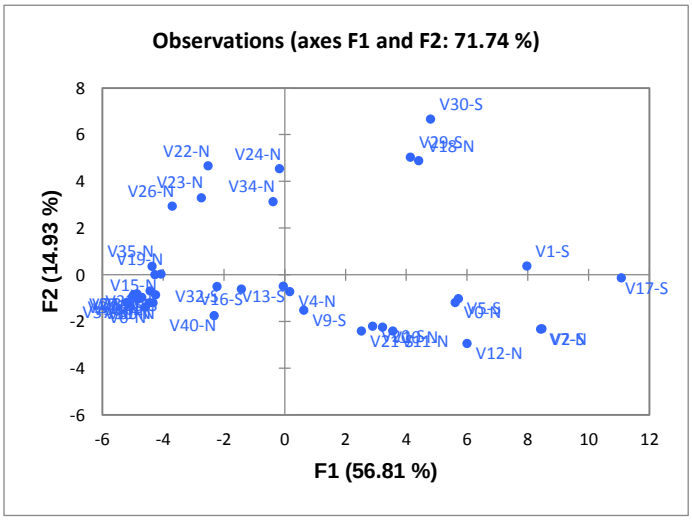

Figure 5. 15: Principal Component Analysis of smoking and non-smoking volunteers (samples ending with S and N represent smokers and non-smokers, respectively).

A cluster analysis was performed in order to find the similarities and dissimilarities between the VOCs in smoker and non-smoker samples. The dendrogram (Figure 5.16)

shows that the results were grouped into two main groupings depending on the state of volunteer smokers or non-smokers, and indeed other conditions such as the humidity of the sample. The first group on the right side of Figure 5.16 has two main subgroups, the first with the red colour being more likely to represent non-smoker samples. The second subgroup includes the subgroups in green and light purple which represent the mix between smoking and non-smoking samples. This area is believed to represent the overlap between these two groups of individuals. The main group on the left-hand side of the dendrogram represents the smokers within the samples. The difference between the two main areas in the dendrogram are related to the difference/ concentration of VOCs in breath samples between smokers and non-smokers.

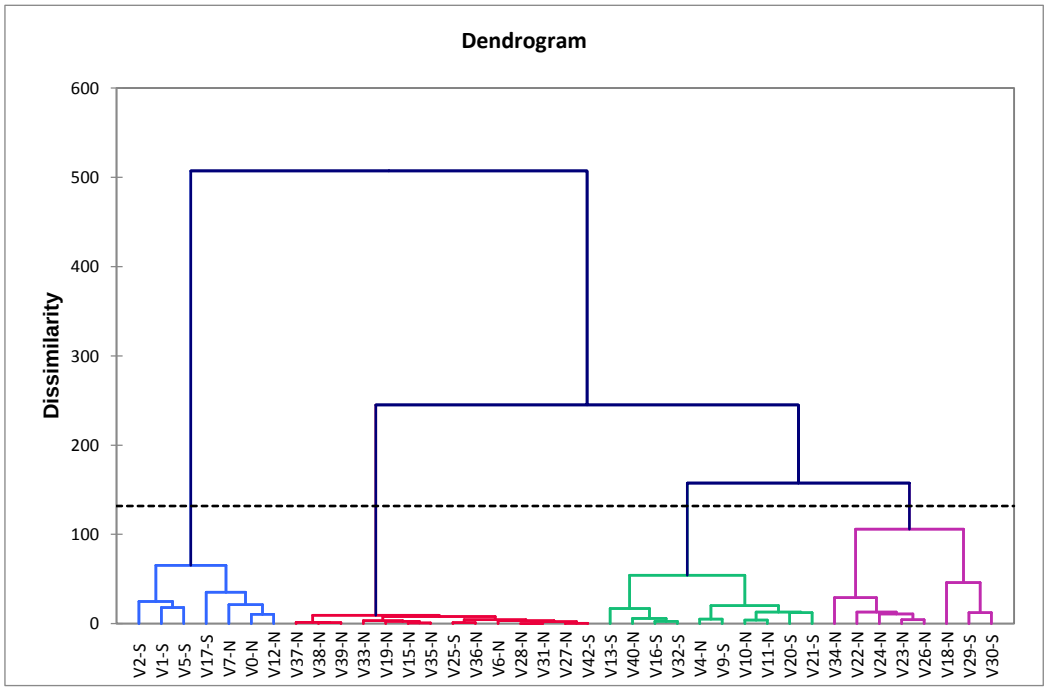

Figure 5. 16: shows the dendrogram. The bottom (x-axis) nodes represent the individual subjects (smokers and non-smokers), which are distributed along the x-axis according to their Euclidean distances, so that similar subjects are plotted close to one another. The other nodes belong to the clusters to which subjects belong, spaced along y-axis depend on the level of dissimilarity.

PLS-DA was conducted in order to discriminate between the breath of smoker and non-smoker samples. The receiver operating characteristic curve (ROC) is a function of the specificity and the sensitivity of every value in the model. ROC is a measure of true positive vs false positive. A plot of sensitivity against the reciprocal of specificity produces the ROC (Figure 5.17). The area under this curve also called the c-statistic, and

has range from 0.5 (minimum or no discrimination) to 1 (maximum discrimination) [100]. As can be seen from inspection of Figure 5.17, PLS-DA has the ability to distinguish between the smoking and non-smoking groups, where the value of the ROC is 0.994.

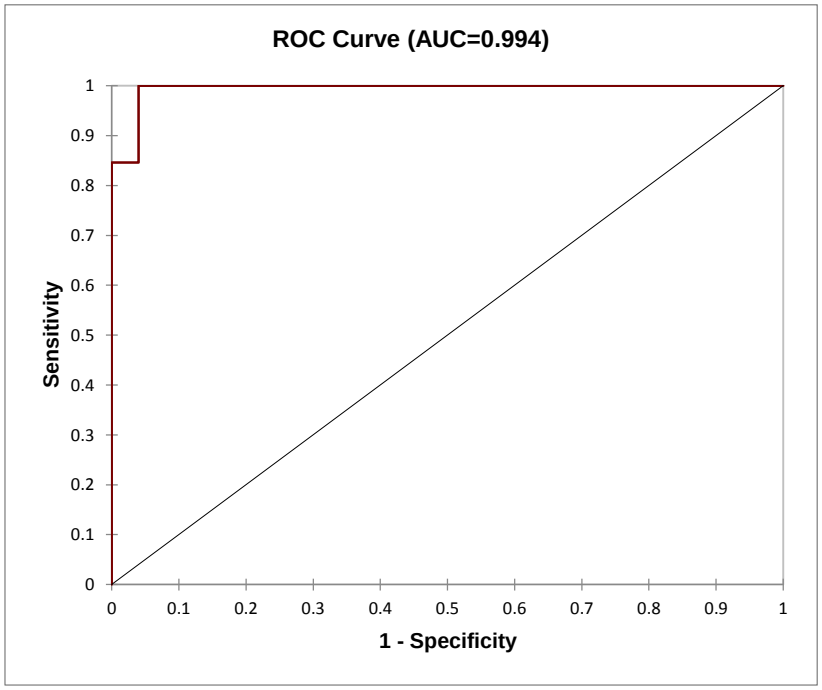

Figure 5. 17: Receiver operating characteristics curve (ROC) has a high outcome value of 0.994 meaning the PLS-DA model's performance is high, which shows that PLS-DA makes a clear distinction between the two groups (smokers and non-smokers).

Inspection of the observation on the two axes (Figure 5.18), shows a meaningful separation between the smokers (green colour) and non-smokers (blue colour). Partial overlap between the two groups indicate some smoker subjects have VOC profiles similar to non-smokers, and vice versa. Furthermore, the overlap could be related to the habits of certain smokers. In addition, the number of samples might not be enough to allow for good separation in the model.

Figure 5.19 shows the variables important to enable good discrimination between the two groups (smokers and non-smokers) in PLS-DA. Masses such as 29, 33, 59, 61, 110, 127, 131, and 141 have a higher influence on allowing for the separation of the smoker group from the non-smoker group. These masses, such as that at 110, could belong to acetonitrile, which are more likely to be a marker of a smoker subject.

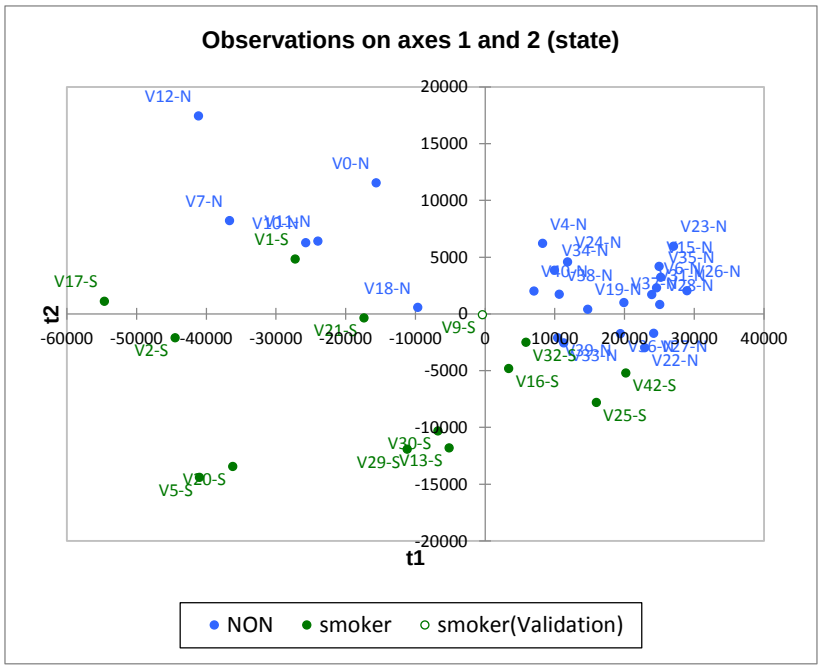

Figure 5. 18: PLS-DA shows the separation that exists between the two groups (smokers and non-smokers). The green and blue entries represent the smoker area and non-smoker area respectively in the model.

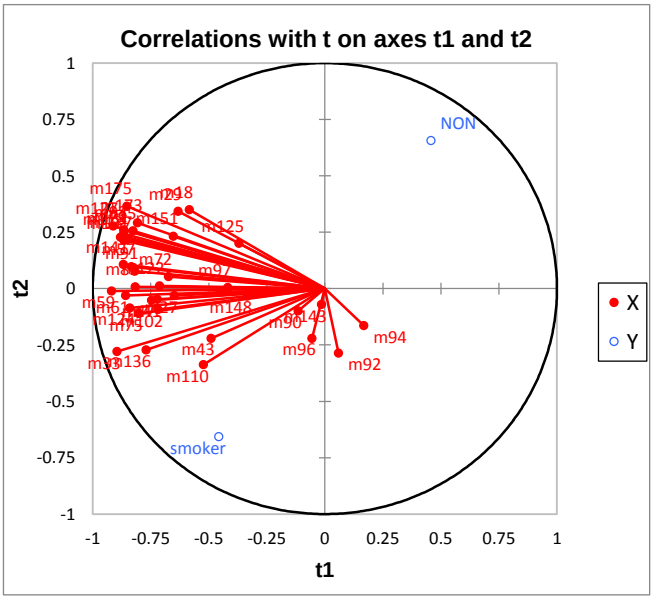

Figure 5. 19: PLS-DA shows the important variables (masses) that allow for discrimination between two sets of data (smokers and non-smokers).

The negative area in Figure 5.19 shows masses that to separate between smokers and non-smokers demonstrated more clearly in Figure 5.20. From Figure 5.20 it can be seen that masses 110 amu and 61 amu, which may belong to acetonitrile and carbonyl group, have

the strong effect on the separation of smokers and non-smokers. Masses which have more possibility to arise from one compound are shown in Table 5.9.

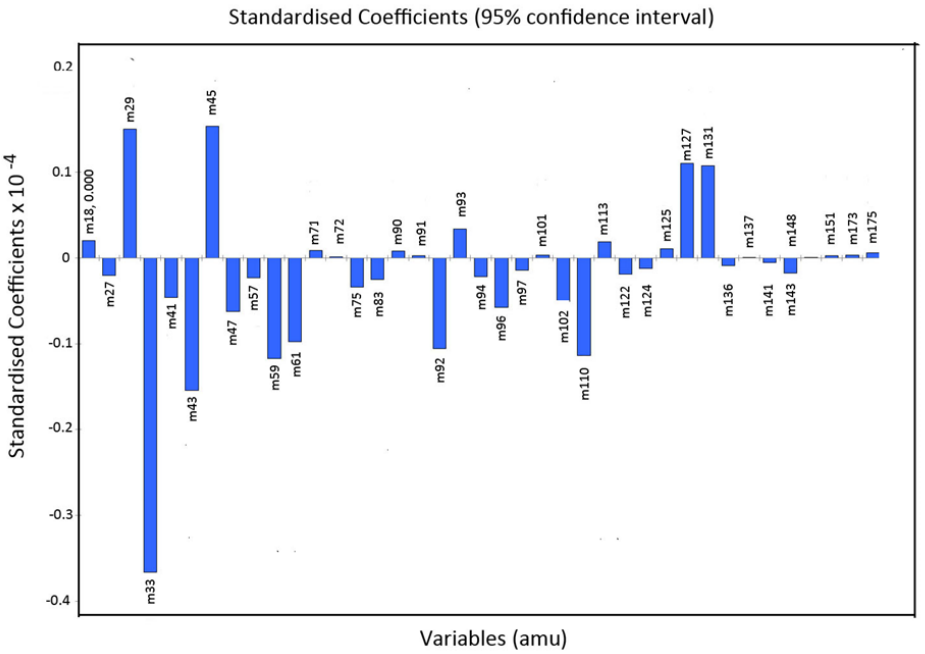

Figure 5. 20: PLS-DA coefficients for discrimination between smokers and non-smokers.

Table 5. 9: Masses and compounds that distinguish between smokers and non-smokers.

tentative assignment	mass	Structure (CF_3^+)	CF_3^+	H_3O^+	GC-MS[1]
methanol	32	CH_3OH^+	-	m33	
C_4, C_8, C_9	57	$C_4H_9^+$	-	m57	✓
acetone	58	$CH_3COHCH_3^+$	-	m59	✓
butanone	72	$CH_3CH_2CFCH_3^+$	m75		✓
acetonitrile	41	$CH_3CNH.CF_3^+$	m110		✓
acrylonitrile	53	$CH_2CHCN.CF_3^+$	m122		✓
propionitrile	55	$CH_3CH_2CNH.CF_3^+$	m124		
pyrrole	67	$C_4H_4NH.CF_3^+$	m136		
toluene	92	$C_7H_7.CF_2^+$	m141		✓
methylacetate	74	$CH_3OCOCH_3.CF_3^+$	m143		

[1]Data obtained by measuring breath samples with GC-MS

5.5 Summary

The utility of CF_3^+ as chemical precursor in chemical ionization time-of-flight mass spectrometry (CIR-TOF-MS) to identify volatile organic compounds (VOCs) has been tested in breath samples from smokers and non-smokers. CF_3^+ reacts with a wide range of VOCs in exhaled breath samples. In this work, Tedlar bags were used to collect exhaled breath samples. Samples were measured using CF_3^+ as a chemical reagent in CIR-TOF-

MS and by PTR-TOF-MS for comparative purposes. The CF_3^+ spectra showed various fragments belonging to compounds resulting from the reaction of CF_3^+ with the analytes. In the same spectra, the protonated parent ion could be seen for certain compounds, by products from the reaction of H_3O^+ (generated from the high humidity samples and in competition with CF_3^+). Using more than one precursor is helpful in the detection of VOCs in real-time and from the same sample, which could react with one or both chemical reagents, CF_3^+ and H_3O^+.

Certain fragments are more likely to belong to, or be produced, from one analyte such as at m/z = 122, 137, 141 and 143 which can be assigned to acrylonitrile, furan, toluene and methyl acetate, respectively. Some fragments could result from more than one analyte, such as m/z = 29, which may arise due to either ethane, ethanol or CHO^+. The signal at m/z = 43 ($C_3H_7^+$) is a common fragment for many compounds as well as the molecular ion of propane. The fragment at m/z = 57 could be assigned to molecular ion of butane as well as fragments from heptane or octane. The peak at m/z = 61 represents ketone and aldehyde groups, while m/z = 71 belongs to pentane (molecular ion) or a fragment from octane.

Some analytes favour the production of a protonated ion from proton transfer such as ethanol/acetaldehyde and acetone at m/z = 47 and 59, respectively. Other analytes such as the n-alkanes can react with CF_3^+ but not H_3O^+.

Multivariate analysis is an excellent tool with which to test all the variables in complex datasets to extract the underlying patterns from the associated data. PCA, AHC and PLS-DA were used to discriminate between exhaled breath samples of smokers and non-smokers. The results showed that PLS-DA has the ability to distinguish between samples obtained from smoker and non-smoker subjects, where the value of the ROC is 0.994.

5.6 References

[1] T. Hibbard, A.J. Killard, Breath Ammonia Analysis: Clinical Application and Measurement, Critical Reviews in Analytical Chemistry, 41 (2011) 21-35.

[2] T.H. Risby, S.F. Solga, Current status of clinical breath analysis, Applied Physics B, 85 (2006) 421-426.

[3] S. Tan, M. Hu, Antoine-Laurent Lavoisier (1743-1794): founder of modern chemistry, in, 2004.

[4] W. Cao, Y. Duan, Breath analysis: potential for clinical diagnosis and exposure assessment, Clinical chemistry, 52 (2006) 800-811.

[5] W. Miekisch, J.K. Schubert, G.F. Noeldge-Schomburg, Diagnostic potential of breath analysis--focus on volatile organic compounds, Clinica chimica acta; international journal of clinical chemistry, 347 (2004) 25-39.

[6] M. Phillips, J. Herrera, S. Krishnan, M. Zain, J. Greenberg, R.N. Cataneo, Variation in volatile organic compounds in the breath of normal humans, Journal of Chromatography B: Biomedical Sciences and Applications, 729 (1999) 75-88.

[7] R. Mukhopadhyay, Don't waste your breath, in, ACS Publications, 2004.

[8] K.H. Kim, S.A. Jahan, E. Kabir, A review of breath analysis for diagnosis of human health, TrAC Trends in Analytical Chemistry, 33 (2012) 1-8.

[9] C. Wang, P. Sahay, Breath analysis using laser spectroscopic techniques: breath biomarkers, spectral fingerprints, and detection limits, Sensors, 9 (2009) 8230-8262.

[10] K. Skeldon, L. McMillan, C. Wyse, S. Monk, G. Gibson, C. Patterson, T. France, C. Longbottom, M. Padgett, Application of laser spectroscopy for measurement of exhaled ethane in patients with lung cancer, Respiratory medicine, 100 (2006) 300-306.

[11] E. Zarling, M. Clapper, Technique for gas-chromatographic measurement of volatile alkanes from single-breath samples, Clinical chemistry, 33 (1987) 140-141.

[12] C.F. Kneepkens, G. Lepage, C.C. Roy, The potential of the hydrocarbon breath test as a measure of lipid peroxidation, Free Radical Biology and Medicine, 17 (1994) 127-160.

[13] J. Pereira, P. Porto-Figueira, C. Cavaco, K. Taunk, S. Rapole, R. Dhakne, H. Nagarajaram, J.S. Câmara, Breath analysis as a potential and non-invasive frontier in disease diagnosis: an overview, Metabolites, 5 (2015) 3-55.

[14] E. Aghdassi, J.P. Allard, Breath alkanes as a marker of oxidative stress in different clinical conditions, Free Radical Biology and Medicine, 28 (2000) 880-886.

[15] S. Mendis, P.A. Sobotka, D.E. Euler, Pentane and isoprene in expired air from humans: gas-chromatographic analysis of single breath, Clinical chemistry, 40 (1994) 1485-1488.

[16] M. Phillips, J. Greenberg, R.N. Cataneo, Effect of age on the profile of alkanes in normal human breath, Free radical research, 33 (2000) 57-63.

[17] A. Amann, D. Smith, Breath Analysis for Clinical Diagnosis and Therapeutic Monitoring:(With CD-ROM), World Scientific, 2005.

[18] M. Phillips, R.N. Cataneo, A.R.C. Cummin, A.J. Gagliardi, K. Gleeson, J. Greenberg, R.A. Maxfield, W.N. Rom, Detection of Lung Cancer With Volatile Markers in the Breatha, Chest, 123 (2003) 2115-2123.

[19] T. Wang, A. Pysanenko, K. Dryahina, P. Španěl, D. Smith, Analysis of breath, exhaled via the mouth and nose, and the air in the oral cavity, Journal of breath research, 2 (2008) 037013.

[20] C. Turner, P. Spanel, D. Smith, A longitudinal study of ethanol and acetaldehyde in the exhaled breath of healthy volunteers using selected-ion flow-tube mass spectrometry, Rapid communications in mass spectrometry : RCM, 20 (2006) 61-68.

[21] P. Španěl, C. Turner, T. Wang, R. Bloor, D. Smith, Generation of volatile compounds on mouth exposure to urea and sucrose: implications for exhaled breath analysis, Physiological measurement, 27 (2005) N7.

[22] A. Jones, Elimination Half-life of Methanol During Hangover, Basic & Clinical Pharmacology & Toxicology, 60 (1987) 217-220.

[23] S. Nair, K. Cope, R.H. Terence, A.M. Diehl, Obesity and female gender increase breath ethanol concentration: potential implications for the pathogenesis of nonalcoholic steatohepatitis, The American journal of gastroenterology, 96 (2001) 1200-1204.

[24] S. Solga, A. Alkhuraishe, K. Cope, A. Tabesh, J. Clark, M. Torbenson, P. Schwartz, T. Magnuson, A. Diehl, T. Risby, Breath biomarkers and non-alcoholic fatty liver disease: preliminary observations, Biomarkers : biochemical indicators of exposure, response, and susceptibility to chemicals, 11 (2006) 174-183.

[25] S. Van den Velde, M. Quirynen, D. van Steenberghe, Halitosis associated volatiles in breath of healthy subjects, Journal of Chromatography B, 853 (2007) 54-61.
[26] A. Hansel, A. Jordan, R. Holzinger, P. Prazeller, W. Vogel, W. Lindinger, Proton transfer reaction mass spectrometry: on-line trace gas analysis at the ppb level, International journal of mass spectrometry and ion processes, 149 (1995) 609-619.
[27] A. Wehinger, A. Schmid, S. Mechtcheriakov, M. Ledochowski, C. Grabmer, G.A. Gastl, A. Amann, Lung cancer detection by proton transfer reaction mass-spectrometric analysis of human breath gas, International Journal of Mass Spectrometry, 265 (2007) 49-59.
[28] A.E. Jones, R.L. Summers, Detection of isopropyl alcohol in a patient with diabetic ketoacidosis, The Journal of emergency medicine, 19 (2000) 165-168.
[29] B. Enderby, W. Lenney, M. Brady, C. Emmett, P. Španěl, D. Smith, Concentrations of some metabolites in the breath of healthy children aged 7–18 years measured using selected ion flow tube mass spectrometry (SIFT-MS), Journal of breath research, 3 (2009) 036001.
[30] L. Laffel, Ketone bodies: a review of physiology, pathophysiology and application of monitoring to diabetes, Diabetes/metabolism research and reviews, 15 (1999) 412-426.
[31] M.P. Kalapos, On the mammalian acetone metabolism: from chemistry to clinical implications, Biochimica et Biophysica Acta (BBA)-General Subjects, 1621 (2003) 122-139.
[32] B. Novak, D. Blake, S. Meinardi, F. Rowland, A. Pontello, D. Cooper, P. Galassetti, Exhaled methyl nitrate as a noninvasive marker of hyperglycemia in type 1 diabetes, Proceedings of the National Academy of Sciences, 104 (2007) 15613-15618.
[33] M. Statheropoulos, A. Agapiou, A. Georgiadou, Analysis of expired air of fasting male monks at Mount Athos, Journal of Chromatography B, 832 (2006) 274-279.
[34] C. Deng, J. Zhang, X. Yu, W. Zhang, X. Zhang, Determination of acetone in human breath by gas chromatography–mass spectrometry and solid-phase microextraction with on-fiber derivatization, Journal of Chromatography B, 810 (2004) 269-275.
[35] M. Kupari, J. Lommi, M. Ventilä, U. Karjalainen, Breath acetone in congestive heart failure, The American journal of cardiology, 76 (1995) 1076-1078.

[36] Y. Lin, S.R. Dueker, A.D. Jones, S.E. Ebeler, A.J. Clifford, Protocol for collection and HPLC analysis of volatile carbonyl compounds in breath, Clinical chemistry, 41 (1995) 1028-1032.

[37] S. Van den Velde, M. Quirynen, P. van Hee, D. van Steenberghe, Differences between alveolar air and mouth air, Analytical chemistry, 79 (2007) 3425-3429.

[38] S. Van den Velde, F. Nevens, D. van Steenberghe, M. Quirynen, GC–MS analysis of breath odor compounds in liver patients, Journal of Chromatography B, 875 (2008) 344-348.

[39] M.M.L. Steeghs, B.W.M. Moeskops, K. van Swam, S.M. Cristescu, P.T.J. Scheepers, F.J.M. Harren, On-line monitoring of UV-induced lipid peroxidation products from human skin in vivo using proton-transfer reaction mass spectrometry, International Journal of Mass Spectrometry, 253 (2006) 58-64.

[40] M. Corradi, I. Rubinstein, R. Andreoli, P. Manini, A. Caglieri, D. Poli, R. Alinovi, A. Mutti, Aldehydes in exhaled breath condensate of patients with chronic obstructive pulmonary disease, American Journal of Respiratory and Critical Care Medicine, 167 (2003) 1380-1386.

[41] P. Španěl, D. Smith, T.A. Holland, W.A. Singary, J.B. Elder, Analysis of formaldehyde in the headspace of urine from bladder and prostate cancer patients using selected ion flow tube mass spectrometry, Rapid communications in mass spectrometry, 13 (1999) 1354-1359.

[42] C. Deng, X. Zhang, N. Li, Investigation of volatile biomarkers in lung cancer blood using solid-phase microextraction and capillary gas chromatography-mass spectrometry, Journal of chromatography. B, Analytical technologies in the biomedical and life sciences, 808 (2004) 269-277.

[43] S.E. Ebeler, A.J. Clifford, T. Shibamoto, Quantitative analysis by gas chromatography of volatile carbonyl compounds in expired air from mice and human, Journal of Chromatography B: Biomedical Sciences and Applications, 702 (1997) 211-215.

[44] D. Smith, T. Wang, J. Sule-Suso, P. Spanel, A. El Haj, Quantification of acetaldehyde released by lung cancer cells in vitro using selected ion flow tube mass spectrometry, Rapid communications in mass spectrometry : RCM, 17 (2003) 845-850.

[45] J.R. Dannecker, E.G. Shaskan, M. Phillips, A new highly sensitive assay for breath acetaldehyde: Detection of endogenous levels in humans, Analytical biochemistry, 114 (1981) 1-7.

[46] S. Svensson, M. Lärstad, K. Broo, A.-C. Olin, Determination of aldehydes in human breath by on-fibre derivatization, solid-phase microextraction and GC–MS, Journal of Chromatography B, 860 (2007) 86-91.

[47] R. Swift, Direct measurement of alcohol and its metabolites, Addiction, 98 (2003) 73-80.

[48] D. Smith, T. Wang, P. Spanel, On-line, simultaneous quantification of ethanol, some metabolites and water vapour in breath following the ingestion of alcohol, Physiological measurement, 23 (2002) 477.

[49] M.R. McCurdy, Y. Bakhirkin, G. Wysocki, R. Lewicki, F.K. Tittel, Recent advances of laser-spectroscopy-based techniques for applications in breath analysis, Journal of breath research, 1 (2007) 014001.

[50] C. Turner, P. Španěl, D. Smith, A longitudinal study of ammonia, acetone and propanol in the exhaled breath of 30 subjects using selected ion flow tube mass spectrometry, SIFT-MS, Physiological measurement, 27 (2006) 321.

[51] D. Smith, P. Spanel, S. Davies, Trace gases in breath of healthy volunteers when fasting and after a protein-calorie meal: a preliminary study, Journal of applied physiology, 87 (1999) 1584-1588.

[52] P. Prazeller, T. Karl, A. Jordan, R. Holzinger, A. Hansel, W. Lindinger, Quantification of passive smoking using proton-transfer-reaction mass spectrometry, International Journal of Mass Spectrometry, 178 (1998) L1-L4.

[53] A. Jordan, A. Hansel, R. Holzinger, W. Lindinger, Acetonitrile and benzene in the breath of smokers and non-smokers investigated by proton transfer reaction mass spectrometry (PTR-MS), International journal of mass spectrometry and ion processes, 148 (1995) L1-L3.

[54] A.M. Ellis, C.A. Mayhew, Proton transfer reaction mass spectrometry: principles and applications, John Wiley & Sons, 2013.

[55] A. Manolis, The diagnostic potential of breath analysis, Clinical chemistry, 29 (1983) 5-15.

[56] H.K. Wilson, Breath analysis: physiological basis and sampling techniques, Scandinavian Journal of Work, Environment & Health, (1986) 174-192.
[57] M. Phillips, Method for the collection and assay of volatile organic compounds in breath, Analytical biochemistry, 247 (1997) 272-278.
[58] H. Wilson, A. Monster, New technologies in the use of exhaled breath analysis for biological monitoring, Occupational and environmental medicine, 56 (1999) 753-757.
[59] R.S. Blake, S.A. Ouheda, C.J. Evans, P.S. Monks, CF_3^+ and CF_2H^+: new reagents for n-alkane determination in chemical ionization reaction mass spectrometry, The Analyst, 141 (2016) 6564-6570.
[60] K.P. Wyche, R.S. Blake, K.A. Willis, P.S. Monks, A.M. Ellis, Differentiation of isobaric compounds using chemical ionization reaction mass spectrometry, Rapid communications in mass spectrometry : RCM, 19 (2005) 3356-3362.
[61] R.S. Blake, S.A. Ouheda, E.F. Alwedi, P.S. Monks, Exploration of the utility of CF_3^+ as a reagent for chemical ionization reaction mass spectrometry, International Journal of Mass Spectrometry, 421 (2017) 224-233.
[62] M.P. Habib, N.C. Clements, H.S. Garewal, Cigarette smoking and ethane exhalation in humans, American Journal of Respiratory and Critical Care Medicine, 151 (1995) 1368-1372.
[63] G. Handelman, Breath ethane in dialysis patients and control subjects, Free Radical Biology and Medicine, 35 (2003) 17-23.
[64] K.S. Stevenson, K. Radhakrishnan, C.S. Patterson, L.C. McMillan, K.D. Skeldon, L. Buist, M.J. Padgett, P.G. Shiels, Breath ethane peaks during a single haemodialysis session and is associated with time on dialysis, Journal of breath research, 2 (2008) 026004.
[65] K.A. Gorham, M.P. Sulbaek Andersen, S. Meinardi, R.J. Delfino, N. Staimer, T. Tjoa, F.S. Rowland, D.R. Blake, Ethane and n-pentane in exhaled breath are biomarkers of exposure not effect, Biomarkers : biochemical indicators of exposure, response, and susceptibility to chemicals, 14 (2009) 17-25.
[66] M.A. Larstad, K. Toren, B. Bake, A.C. Olin, Determination of ethane, pentane and isoprene in exhaled air--effects of breath-holding, flow rate and purified air, Acta physiologica, 189 (2007) 87-98.

[67] B.M. Ross, I. Glen, Breath ethane concentrations in healthy volunteers correlate with a systemic marker of lipid peroxidation but not with omega-3 Fatty Acid availability, Metabolites, 4 (2014) 572-579.
[68] B.M. Ross, S. Shah, M. Peet, Increased breath ethane and pentane concentrations in currently unmedicated patients with schizophrenia, Open Journal of Psychiatry, 01 (2011) 1-7.
[69] J. King, P. Mochalski, A. Kupferthaler, K. Unterkofler, H. Koc, W. Filipiak, S. Teschl, H. Hinterhuber, A. Amann, Dynamic profiles of volatile organic compounds in exhaled breath as determined by a coupled PTR-MS/GC-MS study, Physiological measurement, 31 (2010) 1169-1184.
[70] S. Kischkel, W. Miekisch, P. Fuchs, J.K. Schubert, Breath analysis during one-lung ventilation in cancer patients, The European respiratory journal, 40 (2012) 706-713.
[71] A. Smolinska, E.M. Klaassen, J.W. Dallinga, K.D. van de Kant, Q. Jobsis, E.J. Moonen, O.C. van Schayck, E. Dompeling, F.J. van Schooten, Profiling of volatile organic compounds in exhaled breath as a strategy to find early predictive signatures of asthma in children, PloS one, 9 (2014) e95668.
[72] S. Kurada, N. Alkhouri, C. Fiocchi, R. Dweik, F. Rieder, Review article: breath analysis in inflammatory bowel diseases, Alimentary pharmacology & therapeutics, 41 (2015) 329-341.
[73] H. Amal, M. Leja, K. Funka, R. Skapars, A. Sivins, G. Ancans, I. Liepniece-Karele, I. Kikuste, I. Lasina, H. Haick, Detection of precancerous gastric lesions and gastric cancer through exhaled breath, Gut, 65 (2016) 400-407.
[74] F. Morisco, E. Aprea, V. Lembo, V. Fogliano, P. Vitaglione, G. Mazzone, L. Cappellin, F. Gasperi, S. Masone, G.D. De Palma, R. Marmo, N. Caporaso, F. Biasioli, Rapid "breath-print" of liver cirrhosis by proton transfer reaction time-of-flight mass spectrometry. A pilot study, PloS one, 8 (2013) e59658.
[75] X.A. Fu, M. Li, R.J. Knipp, M.H. Nantz, M. Bousamra, Noninvasive detection of lung cancer using exhaled breath, Cancer medicine, 3 (2014) 174-181.
[76] Y. Saalberg, M. Wolff, VOC breath biomarkers in lung cancer, Clinica Chimica Acta, 459 (2016) 5-9.
[77] R. Fernandez Del Rio, M.E. O'Hara, A. Holt, P. Pemberton, T. Shah, T. Whitehouse, C.A. Mayhew, Volatile Biomarkers in Breath Associated With Liver Cirrhosis -

Comparisons of Pre- and Post-liver Transplant Breath Samples, EBioMedicine, 2 (2015) 1243-1250.

[78] S.M. Abbott, J.B. Elder, P. Španěl, D. Smith, Quantification of acetonitrile in exhaled breath and urinary headspace using selected ion flow tube mass spectrometry, International Journal of Mass Spectrometry, 228 (2003) 655-665.

[79] W. Miekisch, S. Kischkel, A. Sawacki, T. Liebau, M. Mieth, J.K. Schubert, Impact of sampling procedures on the results of breath analysis, Journal of breath research, 2 (2008) 026007.

[80] E. Crespo, S. Devasena, C. Sikkens, R. Centeno, S.M. Cristescu, F.J. Harren, Proton-transfer reaction mass spectrometry (PTRMS) in combination with thermal desorption (TD) for sensitive off-line analysis of volatiles, Rapid communications in mass spectrometry : RCM, 26 (2012) 990-996.

[81] M. Li, J. Ding, H. Gu, Y. Zhang, S. Pan, N. Xu, H. Chen, H. Li, Facilitated diffusion of acetonitrile revealed by quantitative breath analysis using extractive electrospray ionization mass spectrometry, Scientific reports, 3 (2013) 1205.

[82] R. Talhout, T. Schulz, E. Florek, J. Van Benthem, P. Wester, A. Opperhuizen, Hazardous compounds in tobacco smoke, International journal of environmental research and public health, 8 (2011) 613-628.

[83] A. Bhatt, M.A. Parsi, T. Stevens, S. Gabbard, A. Kumaravel, S. Jang, D. Grove, R. Lopez, S. Murthy, J.J. Vargo, Volatile organic compounds in plasma for the diagnosis of esophageal adenocarcinoma: a pilot study, Gastrointestinal endoscopy, 84 (2016) 597-603.

[84] S.C. Moldoveanu, Analysis of Acrylonitrile and alpha-Methacrylonitrile in Vapor Phase of Mainstream Cigarette Smoke Using a Charcoal Trap for Collection, Beiträge zur Tabakforschung/Contributions to Tobacco Research, 24 (2010) 145-156.

[85] R. Papoušek, Z. Pataj, P. Nováková, K. Lemr, P. Barták, Determination of acrylamide and acrolein in smoke from tobacco and e-cigarettes, Chromatographia, 77 (2014) 1145-1151.

[86] S. Kato, G.C. Post, V.M. Bierbaum, T.H. Koch, Chemical ionization mass spectrometric determination of acrolein in human breast cancer cells, Analytical biochemistry, 305 (2002) 251-259.

[87] A. Rydosz, Micropreconcentrator in LTCC Technology with Mass Spectrometry for the Detection of Acetone in Healthy and Type-1 Diabetes Mellitus Patient Breath, Metabolites, 4 (2014) 921-931.

[88] U. Riess, U. Tegtbur, C. Fauck, F. Fuhrmann, D. Markewitz, T. Salthammer, Experimental setup and analytical methods for the non-invasive determination of volatile organic compounds, formaldehyde and NOx in exhaled human breath, Analytica chimica acta, 669 (2010) 53-62.

[89] A. Bajtarevic, C. Ager, M. Pienz, M. Klieber, K. Schwarz, M. Ligor, T. Ligor, W. Filipiak, H. Denz, M. Fiegl, W. Hilbe, W. Weiss, P. Lukas, H. Jamnig, M. Hackl, A. Haidenberger, B. Buszewski, W. Miekisch, J. Schubert, A. Amann, Noninvasive detection of lung cancer by analysis of exhaled breath, BMC cancer, 9 (2009) 348.

[90] K. Schwarz, A. Pizzini, B. Arendacka, K. Zerlauth, W. Filipiak, A. Schmid, A. Dzien, S. Neuner, M. Lechleitner, S. Scholl-Burgi, W. Miekisch, J. Schubert, K. Unterkofler, V. Witkovsky, G. Gastl, A. Amann, Breath acetone-aspects of normal physiology related to age and gender as determined in a PTR-MS study, Journal of breath research, 3 (2009) 027003.

[91] P.R. Boshier, J.R. Cushnir, V. Mistry, A. Knaggs, P. Spanel, D. Smith, G.B. Hanna, On-line, real time monitoring of exhaled trace gases by SIFT-MS in the perioperative setting: a feasibility study, The Analyst, 136 (2011) 3233-3237.

[92] J. King, A. Kupferthaler, B. Frauscher, H. Hackner, K. Unterkofler, G. Teschl, H. Hinterhuber, A. Amann, B. Hogl, Measurement of endogenous acetone and isoprene in exhaled breath during sleep, Physiological measurement, 33 (2012) 413-428.

[93] J. Huang, S. Kumar, A. Singanayagam, P.M. George, O.M. Kon, M. Takata, G.B. Hanna, Exhaled breath acetone for therapeutic monitoring in pneumonia using selected ion flow tube mass spectrometry (SIFT-MS), Analytical Methods, 5 (2013) 3807.

[94] P. Spanel, K. Dryahina, A. Rejskova, T.W. Chippendale, D. Smith, Breath acetone concentration; biological variability and the influence of diet, Physiological measurement, 32 (2011) N23-31.

[95] L. Wallace, E. Pellizzari, Personal air exposures and breath concentrations of benzene and other volatile hydrocarbons for smokers and nonsmokers, Toxicology letters, 35 (1987) 113-116.

[96] F. Brugnone, L. Perbellini, G. Faccini, F. Pasini, G. Maranelli, L. Romeo, M. Gobbi, A. Zedde, Breath and blood levels of benzene, toluene, cumene and styrene in non-occupational exposure, International archives of occupational and environmental health, 61 (1989) 303-311.

[97] B.S. Everitt, G. Dunn, Applied multivariate data analysis, Wiley Online Library, 2001.

[98] S. Kuppusami, M. Clokie, T. Panayi, A. Ellis, P. Monks, Metabolite profiling of Clostridium difficile ribotypes using small molecular weight volatile organic compounds, Metabolomics, 11 (2015) 251-260.

[99] XLSTAT 2017: Data Analysis and Statistical Solution for Microsoft Excel. , in, Addnsoft, France, 2017.

[100] N.R. Cook, Use and misuse of the receiver operating characteristic curve in risk prediction, Circulation, 115 (2007) 928-935.

Chapter 6: Determination of VOCs in urine headspace by CF_3^+/CF_2H^+ chemical ionization reaction mass spectrometry

6.1 Introduction

To avoid the problems of analyte extraction from complex liquid sample matrices headspace analysis can be carried out to determine volatile organic compounds (VOCs) content using direct-mass spectrometry, such as chemical ionization mass spectrometry (CIR-MS) [1]. Analytes detected in the headspace VOC profile have potential to be used as markers of disorder or disease [2, 3].

Urine can be used to supply information on the physiological state of an individual. Analysis of urine is fast, relatively low cost, and routinely employed for diagnostic testing for diabetes mellitus, pregnancy and infection assessment [4]. Linus Pauling (1971) was the first to detect over 280 VOCs in urine vapour using gas chromatography. More recently, researchers have identified VOCs related to specific disorders and disease states such as a diagnostic test for gastro-oesophageal cancer [4]. Urine is considered a useful biofluid for medical analysis because it is non-invasive, easily accessible and available in relatively large volumes [4, 5].

Urine has been used as a biomarker of many disorders and diseases since 4000 BC. Hippocrates and Galen believed that urine was a filtrate from humours and blood, and begun using urine as biomarker to diagnose disease [6]. More recently, urine analysis has been established as a tool to diagnosis many disorders and diseases. It is a classical method used in clinical practice to analyse urine samples as it can be applied to near-patient testing or laboratory testing. Near-patient testing employs a reagent strip or a dipstick sample collection and is applied prior to comprehensive, more complex and expensive laboratory techniques. Dipstick testing is widely applied owing to its simplicity and ability for near-patient testing [7-12]. Some applications of dipstick tests are the measurement of urinary pH, diabetes insipidus and haematuria. Laboratory testing includes routine, or indeed less routine, measurement of metabolites to acquire quantitative data. These data are used for diagnostic purposes such as determining metabolite concentration, metabolic pathways and drug interactions [13-16].

Gas chromatography is widely used to detect VOCs in urinary metabolites. Pasikanti *et al*. [17], have utilized GC-quadrupole MS to undertake global profiling of human urine samples owing to the sensitivity, peak resolution and reproducibility of GC-MS. The

results of this study identified the presence of 150 endogenous compounds. These were classified as 29% organic acids, 23% sugars, 10% amino acids, 3% aromatic, 2% fatty acids, 1% glycerols, 29 other chemical classes as well as 3% unknown compounds.

6.2 Urine sampling and storage accessible

As previously stated, urine is considered an accessible analytical tool owing to a number of clear advantages over other body fluids. It can be collected in sufficient quantities in a manner that is non-invasive. An analytical advantage is that urine needs far less complex sample pre-treatment as it contains fewer proteins and is stable from a thermodynamical perspective. Urine samples can be collected as random samples, timed samples or 24-h samples. The timing of urine collection has advantages and disadvantages. Random samples can be collected at any time, but ignore diurnal variation of exertion and do not give a direct measurement of the volume of urine excreted. Timed samples require greater subject compliance and 24 hour samples supply a more complete picture of excretion, although this method is cumbersome [18, 19].

Integrity and stability of urine samples during storage has been shown to be important. Samples of urine must be stable to supply valid data. In a study by Ryan. *et al*.[19], urine samples were either immediately frozen at -80 ºC or kept at 4 ºC for 24 h before being frozen [19]. Later, before measuring, urine samples were thawed and then examined by gas chromatography time-of-flight mass spectrometry (GC-TOF-MS) which found that the samples contained a total of more than 700 metabolite peaks. In any one sample over 200 peaks were recorded. Statistical methods such as principal component analysis (PCA) were applied to the samples, stored in the two different ways to find any significant differences. In general, neither method of storage showed any statistically significant difference in the metabolic profile. In addition, analytical variance from repeat analysis of the same sample was found to be the same as the variance between samples that were stored in the two ways [19].

In this Chapter, chemical ionization time-of-flight mass spectrometry (CIR-TOF-MS) with a novel reagent (CF_3^+) was used to determine its suitability for detecting the VOCs particular to the urine headspace from smoking and non-smoking subjects. As we have seen in Chapters 3 and 4, CF_3^+ reacts with small chain hydrocarbons (C_2-C_6) and a wide range of VOCs. H_3O^+ as reagent in CIR-TOF-MS was also used to detect VOCs in urine headspace as a comparative method. Using more than one precursor can be helpful to

complement the gaps in the real-time detection of VOCs from the same sample, providing VOCs react with both reagent ions, CF_3^+ and H_3O^+.

6.3 Experimental

6.3.1 Instruments

Two CIR-TOF-MS (Model 4500A, Kore Technologies, Ely) were used in this study, as described in detail in Chapter 2. All experiments were run at 100 Td using 60 second integration times covering a mass range of 0 - 249 amu. The pair of CIR-TOF-MS were supplied with CF_4 or H_2O vapour as chemical reagents at a rate of 2 and 50 ml/min, respectively. The urine headspace was sampled at a flow rate of 60 and 150 ml/min respectively to achieve a value of 100 Td in both systems.

6.3.2 Chemicals

The standards (Sigma-Aldrich, Gillingham, Dorset, UK) described in Chapter 4 were used to prepare calibration mixtures. A stock solution of these standards was prepared by adding 3 microlitres of each to 8 litres of N_2 in Tedlar bags (Thames-Restek UK, Ltd, Saunderton, Bucks., UK). Subsequently, a series of standards were prepared by secondary dilution using in a Tedlar bag and diluting the selected sample with 8 litres of nitrogen (see Chapters 4 and 5). High purity nitrogen (BOC; 99.999%) was used as a carrier gas for the urine headspace for the CIR-TOF-MS systems. An internal standard of 10 ppm bromobenzene in nitrogen (BOC) was used for estimating VOC concentrations.

6.3.3 Sample collection and storage

Smoker and non-smoker subjects from University of Leicester staff and students were invited to take part in this study. The subjects were 11 smokers (10 male and 1 female) and 20 non-smokers (17 male and 3 female), ages ranged from 24 to 50 years.
As before, smoking and non-smoking volunteers were required for urine collection. The method of urine collection was explained to the volunteers, who were asked to fill out consent and application forms which included the following information:

- Date of experiment
- University ID/ e-mail
- Sample code (to be completed by the researcher)
- Age
- Sex

- Weight (kg)
- Height (cm)
- Smoking state
- Recent food and drink consumption.

Ethics approval was through the University of Leicester- ethical application reference so165-cf19a.

Urine samples were collected into 20 ml sterile plastic containers (Thermo Scientific). Urine samples of smokers were collected immediately after a cigarette. Urine samples were measured fresh where possible, but otherwise were kept in refrigerator and analysed within 1 hour of collection.

6.3.4 Design of experiment

Urine samples were divided into two 8 ml portions. The first 8 ml of urine sample was injected into a Dreschel bottle kept in a water bath to maintain the sample temperature at 40 ºC. The second part of the sample was refrigerated while the first part of the sample was being processed. Figure 6.1 shows the apparatus used for urine headspace analysis.

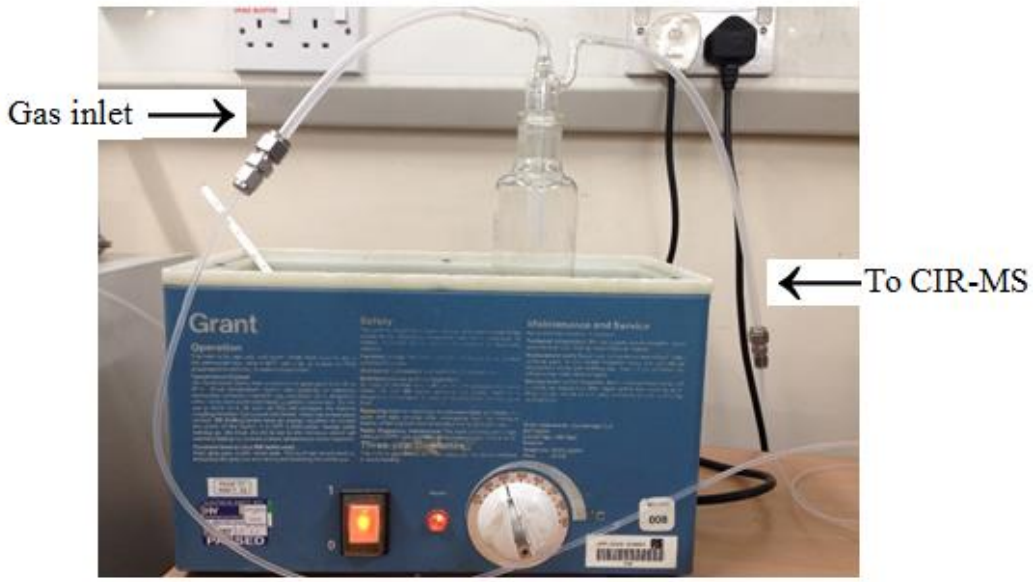

Figure 6. 1: Urine headspace and water bath.

6.3.5 Sample measurements

Headspace from the urine samples were measured by both CIR-TOF-MS using CF_3^+ and H_3O^+ as reagents to detect the various VOCs in smoking and non-smoking samples. In the first part of the experiment and prior to the addition of the urine sample, pure N_2 gas was passed through the empty Dreschel bottle to measure the background using CF_3^+ and H_3O^+ as precursors. Next, 8 ml of urine sample was introduced into the Dreschel bottle in the water bath and allowed to equilibrate for around 5 minutes before taking any measurements. Pure N_2 gas fed the headspace gases (VOCs) as carrier gas for the two CIR-TOF-MS. In the second part of the experiment, a mixture of bromobenzene/nitrogen (2.0 ppm) was supplied to an empty Dreschel bottle and used to obtain background measurements. Then, 8 ml of a new portion of urine sample was added to the Dreschel bottle in the water bath and allowed to stand for 5 minutes to reach 40 ºC after which time measurements were taken. Finally, a mixture of bromobenzene/nitrogen was delivered to the urine sample in the bottle and the measurements repeated. Both reagents were used in CIR-TOF-MS to detect VOCs in the urine samples. The purpose of adding the mixture of bromobenzene/nitrogen in second part of the experiment was so that it could be used subsequently as an internal standard to estimate the concentrations of the VOCs detected. A diagram of the urine headspace experiment is shown in Figure 6.2.

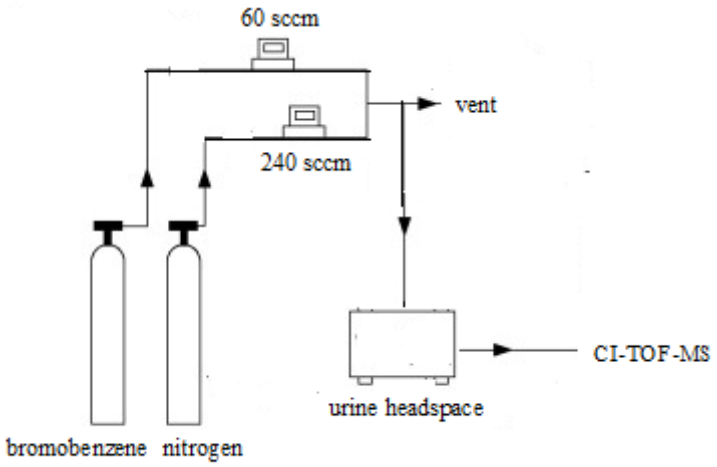

Figure 6. 2: Diagram shows injected bromobenzene in urine headspace; adapted from reference [20].

6.3.6 Estimation of the concentration of VOCs in urine headspace using bromobenzene as an external standard

Every sample of urine was divided into two portions. One portion of the urine headspace sample was carried in pure nitrogen to the CIR-TOF-MS whilst the other was carried in a mixture of bromobenzene/nitrogen (10 ppm). The mixture of bromobenzene/ nitrogen was prepared by mixing 60 ml/min of 10 ppm bromobenzene stock mixture with 240 ml/min of pure nitrogen and delivering this mix to the urine headspace using flow controllers, as shown in Figure 6.2. The final concentration of the diluted mixture of bromobenzene in the urine headspace was 2.0 ppm. The ion count due to the urine headspace sample with and without bromobenzene were acquired and used to estimate the relative concentration of the VOCs present. The relative concentration of the analyte in the urine headspace samples is shown in Equation 6.1. Tables 6.1 and Figure 6.3 show the relative concentrations of candidate compounds or fragments from the urine headspace samples. The PTR-TOF-MS results exhibited a few compounds such as ammonia and acetone. In the PTR-MS experiment the high concentration of ammonia and its large proton affinity (853.6 kJ mol^{-1}) present in the samples prevented protonation of many of the expected compounds.

$$concentration = \frac{signal\ of\ analyte * concentration\ of\ bromobenzene}{signal\ of\ bromobenzene} \qquad (6.1)$$

Table 6. 1: Concentrations of VOCs detected in urine headspace using CF_3^+ as the reagent and bromobenzene as the external standard.

compound	mass	relative con. range, smoker	relative con. range, n-smoker
octane	57	1.45-1.85 ppmV	0.71-0.84 ppmV
butanone	75	0.18-0.48 ppmV	0.20-0.38 ppmV
acetonitrile	110	0.65-1.10 ppmV	0.14-0.50 ppmV
acrylonitrile	122	0.37-0.59 ppmV	0.12-0.17 ppmV
toluene	141	0.54-0.72 ppmV	0.18-0.39 ppmV
methyl acetate	143	0.50-0.92 ppmV	0.29-0.59 ppmV
pentane	71	0.24-0.45 ppmV	0.15-0.34 ppmV

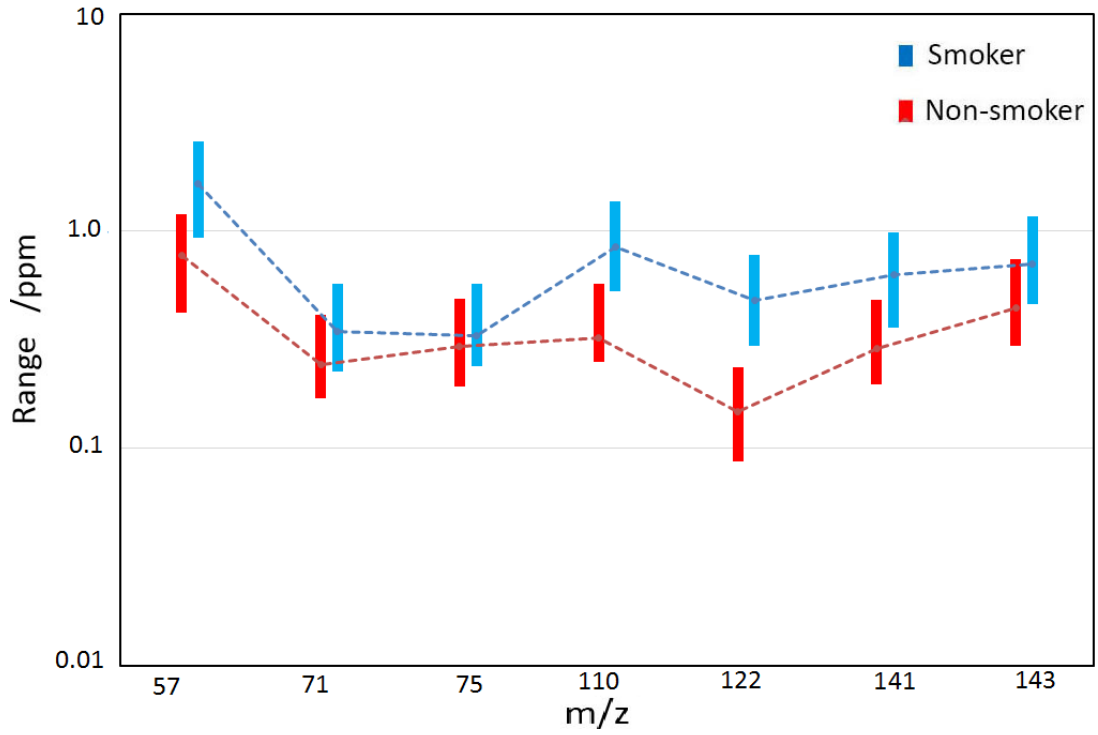

Figure 6. 3: Estimated concentrations of detected masses for smokers and non-smokers, as detected by CF_3^+ as a reagent in CIR-TOF-MS, is shown in ppmV. Error bars represent the minimum and maximum concentrations per m/z value. Bromobenzene calibration method.

6.3.7 Estimated concentration of VOCs in urine headspace using calibration curve

The estimated concentrations of VOCs in the urine headspace calculated using bromobenzene as external standard may have some associated uncertainties. Errors could arise from a change of sensitivity of bromobenzene from one experiment to another. As a consequence, standard curves were constructed to estimate the concentration of detectable VOCs in the urine headspace samples for smoking and non-smoking subjects.

A series of standard solutions for VOCs were prepared and measured. Calibration curves were extrapolated to calculate the sensitivity of these standards. The sensitivity of the VOCs of interest were used to estimate the concentration of VOCs in the urine headspace. Figure 6.4 shows example of these curves, as detected by CF_3^+ as the reagent in CIR-TOF-MS.

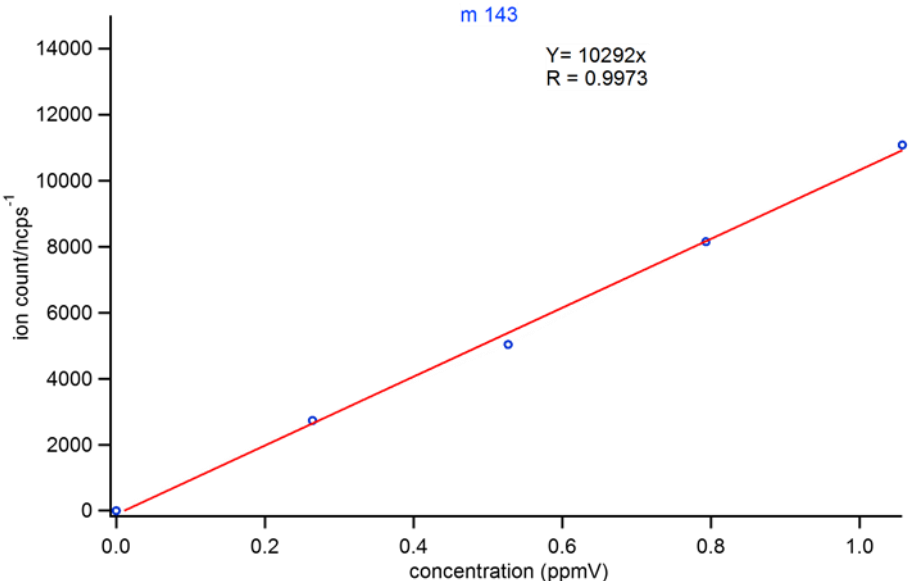

Figure 6. 4: Calibration curve for methyl acetate (m143).

The sensitivity of compounds of interest in the urine headspace samples (S_N) were estimated from the gradients of the calibration curves performed for the standards of these compounds. (Equation 6.2).

$$S_N = \frac{\#}{[x]} \qquad (6.2)$$

S_N = sensitivity of the compound, [x] = concentration (ppmV) and # = normalized ion count of the compound (ncps). The sensitivity is therefore in units of ncps $ppmV^{-1}$.

The concentrations of compounds of interest detected by CF_3^+ as the reagent are shown in Table 6.2. Only ammonia and acetone are clearly detected by H_3O^+ as the reagent in this case. The remainder were either not protonated at all or affected by the low H_3O^+ count rate resulting in small yields.

Table 6. 2: Concentrations of samples in urine headspace detected using CF_3^+ as the reagent (calibration curve method).

compound	mass	relative con. range, smoker	relative con. range, n-smoker
octane	57	0.68-1.21 ppmV	0.34-0.83 ppmV
butanone	75	0.32-0.85 ppmV	0.18-0.36 ppmV
acetonitrile	110	0.01-0.02 ppmV	$\leq$ 0.01 ppmV
acrylonitrile	122	0.09-0.15 ppmV	0.01-0.12 ppmV
benzene	127	0.25-0.57 ppmV	0.16-0.43 ppmV
toluene	141	0.09-0.15 ppmV	0.04-0.10 ppmV
methyl acetate	143	0.02-0.08 ppmV	0.02-0.06 ppmV

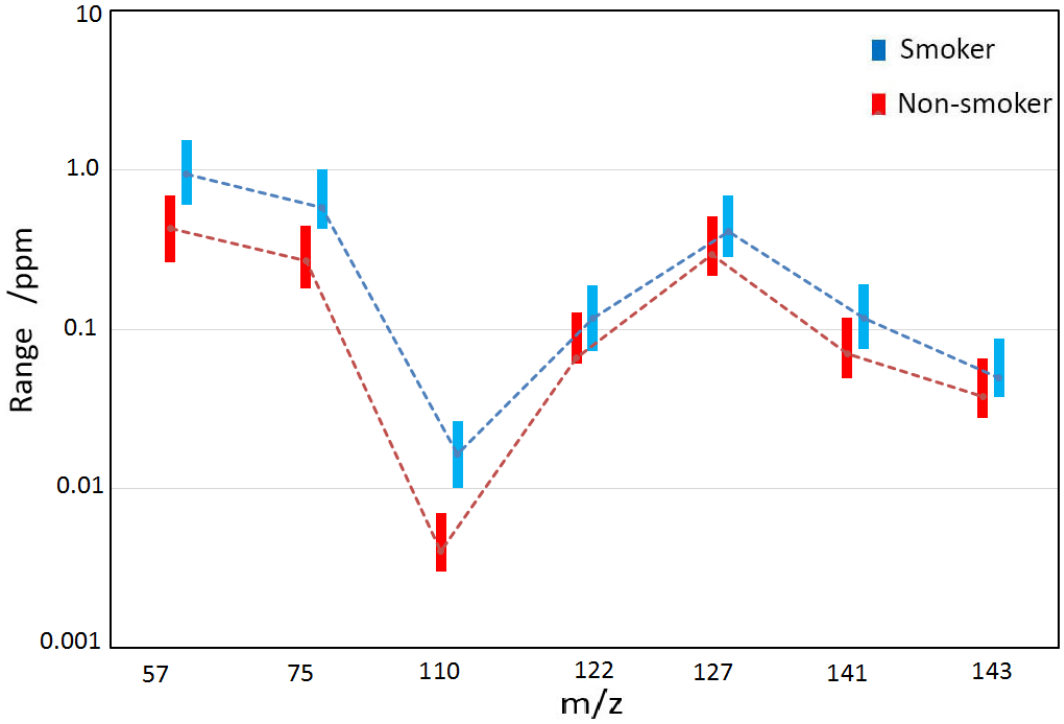

Figure 6. 5: Estimated concentrations of detected masses for smokers and non-smokers, as detected by CF_3^+ as a reagent in CIR-MS, is shown in ppmV. Error bars represent the minimum and maximum concentrations per m/z value. The conversion details were obtained from calibration curves.

6.3.8 Evaluation of concentration methods

Bromobenzene was used as an internal standard to determine concentrations of VOCs in the urine headspace of samples from smokers and non-smokers. Two flow controllers were used to mix known volumes of nitrogen and bromobenzene to produce adjustable concentrations for passing through the urine headspace. It was inevitable that there would be some errors in estimating the contentions of the analytes due to the variation of intensity (sensitivity) of bromobenzene during these measurements and allowance had to be made for them.

Calibration curves were created using standards of analytes expected to exist in urine headspace samples. The concentration was calculated using the gradient of the calibration curves. In this method, the error from the uncertainty could have resulted from the difference in humidity between the standards used to generate the calibration curves and the urine headspace samples themselves.

The aim of this Chapter is to identify VOCs in the urine headspace of smokers and non-smokers using a novel reagent in CIR-TOF-MS rather than estimation the concentrations of the samples. However, even with the possible sources of errors, the differences in concentrations of related compounds in the urine headspaces of smokers and non-smokers can still be seen, as discussed in the following section.

6.4 Results and Discussion

The urine sample headspace has a relatively high humidity. The humidity will affect the percentage of CF_3^+/CF_2H^+ [21]. As the humidity increases, the CF_3^+ ion count decreases and CF_2H^+ ion count will increase. As a consequence, it was ensured that the CF_3^+ ion count did not fall below 10% of the value in dry conditions for all experiments. In this Chapter, we will focus on the products resulting from the reaction of the analytes with CF_3^+ and CF_2H^+ as reagents and compared with those from the parallel PTR-TOF-MS results. Data for the urine headspace measured by CF_3^+ and H_3O^+ as reagents were normalized by summation of 69 + 51 amu and 19 + 37 amu, respectively.

6.4.1 Concentration ranges in smoker and non-smoker urine headspace samples

An important cause of variation in the results is the profile and recent history of the volunteers. In spite of the uncertainty in the methods of estimating the concentrations of VOCs in urine headspace, owing to such issues as the humidity of the urine headspace samples and sensitivity of bromobenzene, the results still showed the positive differentiation of some of the VOCs in urine headspace. Prominent among these is butanone, which proved to be higher in smokers' samples that those from non-smokers, as shown in Figures 6.3 and 6.5.

PTR-MS is used widely to identify volatile organic molecules in the gas phase. The use of H_3O^+ as reagent in CIR-TOF-MS has some limitations such as distinguishing between compounds of the same m/z (isobaric molecules), like aldehydes and ketones [22]. In addition, PTR-MS cannot detect small chain alkenes (C_2-C_6) owing to the proton affinity of these compounds being lower than the proton affinity of water. CF_3^+, which does not react via protonation, has the potential to be an alternative precursor in CIR-TOF-MS. CF_3^+ can be used detects the presence of small alkanes (C_2-C_6) and various VOCs in the exhaled breath of smoker and non-smoker subjects, (Chapters 3, 4, and 5) [21, 23].

As a consequence, CF_3^+ with H_3O^+ together as dual precursors have the potential to give a clearer picture of the participating VOCs. Figures 6.6 and 6.7 show results obtained for VOCs in the urine headspace of smoker and non-smoker subjects, respectively. The upper charts represent the results of urine headspaces measured using CF_3^+ as the reagent in CIR-TOF-MS. The lower charts show the results from urine headspace samples as measured by PTR-TOF-MS.

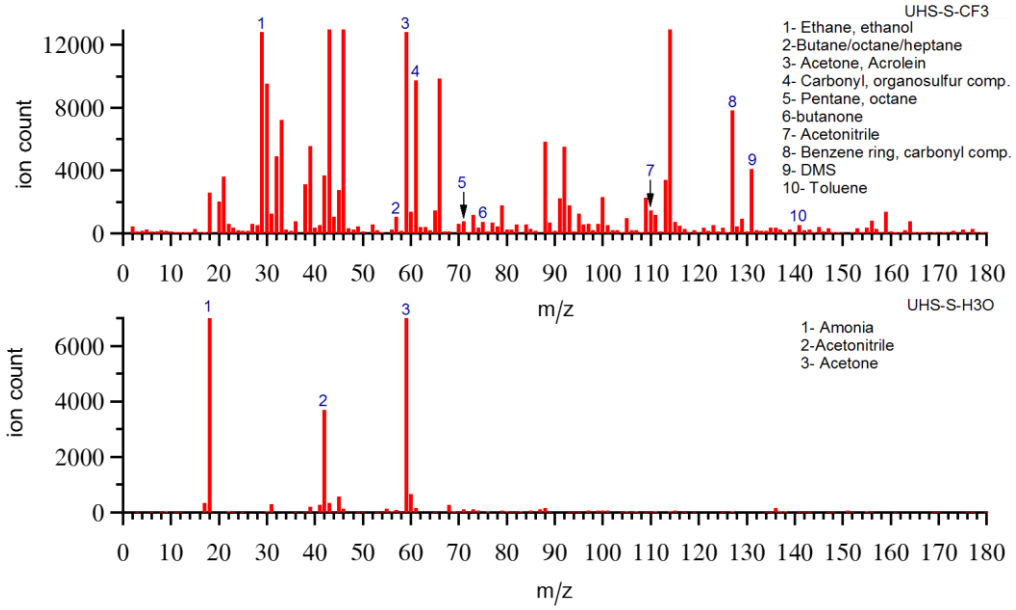

Figure 6. 6: Compounds in smoker urine headspace as a result of the use of CF_3^+ (above chart) and H_3O^+ (lower chart) as reagents in CIR-MS. The H_3O^+ spectra are relatively sparse due to the high proton affinity of large amounts of ammonia in the sample which suppress the protonation of many of the other VOCs in the sample. Background spectrum has been subtracted.

As seen in Figures 6.6 and 6.7, the PTR-TOF-MS results show fewer peaks except certain VOCs such as tentative ammonia, acetonitrile and acetone. As a consequence, we will focus only on the results of examining urine headspaces with CF_3^+ as the reagent in CIR-MS.

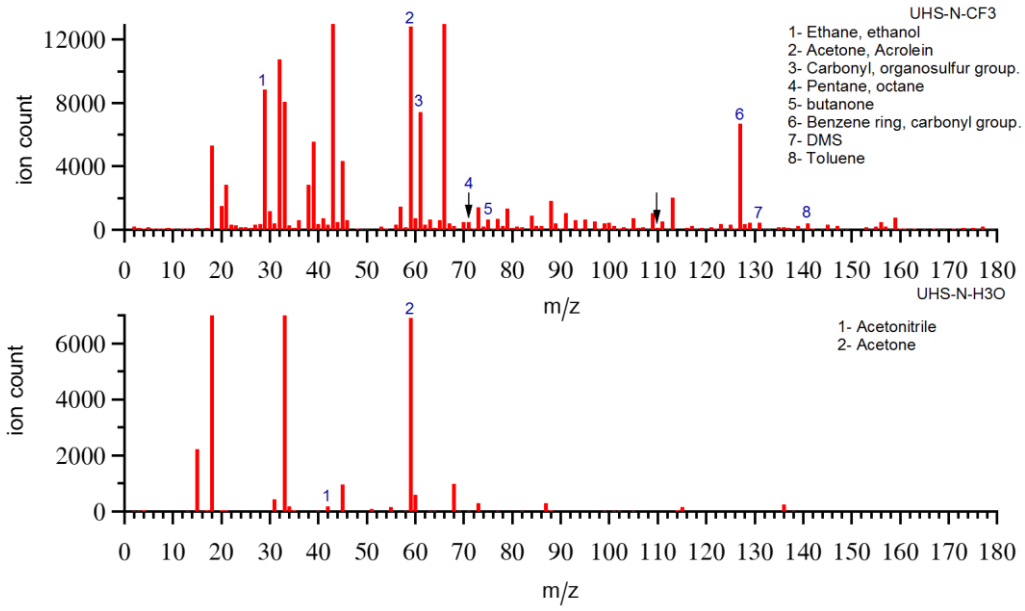

Figure 6. 7: VOCs observed in non-smoker urine headspace using CF_3^+ (upper) and H_3O^+ (lower) as reagents. Background spectrum has been subtracted.

6.4.2 m/z = 29

The reaction of the CF_3^+ with the urine headspace produced a predominant signal at m/z 29. Pentanone and ethanol produce fragments of $C_2H_5^+$ with relative abundances of 3 and 56 %, respectively [23]. Blake *et al*. [21], demonstrated that ethane produces the $C_2H_5^+$ fragment with a relative abundance of 94%. It seems that 29 amu stems partially from ethane along with a contribution of COH^+ as noted in Chapter 5. The contribution of dehydrated ethanol (m/z 29) was weak as yield at m/z = 47 of which it is a minor fragment did not itself contribute.

6.4.3 m/z = 57

The small peak detected at m/z 57 in the urine headspace samples could belong to hydrocarbons such as butane, or fragments of octane and heptane. CF_3^+ reacts with these three species to produce its most significant signal at m/z = 57. The relative abundance of this fragment in butane and heptane is above 95%, while 57 amu represents 50% octane [21, 23]. VOCs are well established as biomarkers for many disorders in the human body. Perbellini *et al*.[24], identified *n*-heptane metabolites in the urine of rats using GC-MS. The author found that heptane converts to alcohols and ketones [24, 25].

6.4.4 m/z = 61

A significant signal intensity was observed at m/z 61 which could belong to aldehydes and ketones. CF_3^+ as the reagent in CIR-MS reacts with propanal, acetone, ethyl acetate, hexanone, DMS and propanol to produce peaks at 61 amu with relative abundances of 58, 23, 20, 14, 8 and 4%, respectively [23]. Juzheng *et al*. [4], found that there was a significant difference in concentration of some VOCs such as acetone in urine headspace samples in cancer groups compared with healthy groups of individuals. Other compounds such as propanol exhibited no significant differences between the two groups. Another study showed that acetone concentrations in urine headspaces were found to be increased by up to 12-fold during the time of ovulation compared with healthy female subjects [26]. m/z = 61 cannot be used as marker of a specific compound, but can be used as sign for carbonyl group from compounds such as propanal and acetone.

6.4.5 m/z = 71

The small peak at m/z 71 was noticed in the mass spectra of urine headspaces, which may belong to pentane or octane. Pentane and octane react with CF_3^+ as a precursor in CIR-MS to produce their main fragment at 71 amu with relative abundances of 74.3 and 39.7 %, respectively [21, 23].

6.4.6 m/z = 75

The peak at m/z 75 is likely to belong to 2-butanone. CF_3^+ as a reagent in CIR-TOF-MS reacts with 2-butanone to produce its predominant signal at 75 amu with a relative abundance of 45%. 2-butanone is one of the compounds found in urine headspace in relatively high abundance, usually more than 10 ppbV [27]. Anton *et al*. [2], used a headspace sampler, a programmed temperature vaporizer in a solvent-vent injection mode, and a mass spectrometer (HS-PTV-MS) to detect VOCs in the urine headspace of lung cancer patients. The authors found that 2-butanone and 2-ethyl-1-hexanol provided good discrimination between individuals suffering from lung cancer and healthy control samples. Smith *et al*. [28], conducted a study on urine headspace using GC-MS to find the effect of pH change on VOCs. They concluded that 2-butanone was one of five compounds that was ubiquitous, irrespective of pH [28, 29]. Mochalski *et al*. [25], conducted a study to find potential biomarkers in human urine that could be utilized as chemical markers in some events such as human presence in collapsed buildings during natural and man-made disasters. The authors found the emission of 2-butanone to be

increased four-fold. In the present work the yield of this biomarker was the second lowest of those considered but is included because of its importance. The yields do not show much difference in the range of yields of the smokers or non-smokers.

6.4.7 m/z = 110

The significant peak at m/z 110 resulted from the reaction of CF_3^+ with the sample and most likely arises from acetonitrile. CF_3^+ reacts with acetonitrile to produce its principal fragment at 110 amu with a relative abundance 98.7% [23]. Emission of VOCs from urine headspace samples are not constant and have concentration profiles that vary with time. Acetonitrile is a VOC that has a long wash-out time [27]. Abbott *et al*.[30], conducted an experiment to detect and quantify acetonitrile in urinary headspace and exhaled breath, the results of which showed that the concentration of acetonitrile in urine headspace was in the range of 0-150 µg/L [30]. Other studies have showed that the mean concentration of acetonitrile in urine headspace of non-smokers was 3.74 ppbV. This concentration was found to increase with the number of cigarettes smoked daily, with the highest mean concentration reaching up to 28.04 ppbV [31].

6.4.8 m/z = 127

A significant signal at 127 amu produced from the reaction of CF_3^+ with the sample may have been related to acetone or benzene, or other benzene derivatives. Blake *et al.* [23], found m/z 127 could result from the reaction with acetone and benzene with relative abundances of 63.9 and 87.7%, respectively. Ghittori *et al*. [32], conducted an experiment to measure the concentration of benzene in urine headspace in smokers, non-smokers and workers (smoker and non-smoker) exposed to benzene in chemical plants. The results showed that the mean concentrations were 790 and 131 ng/L for smokers and non-smokers who are not exposed to benzene respectively. The mean concentrations for a smoker and non-smoker exposed to benzene were 2576 and 1259 ng/L respectively. In both cases (exposed and non-exposed), smokers still have higher concentration of benzene. Another study showed that the concentrations of benzene in the urine headspace of non-smokers, light smokers and heavy smokers were 123, 347 and 441 ng/L, respectively [33].

6.4.9 m/z = 131

The small signal detected at 131 amu be attributed to dimethyl sulphide (DMS). CF_3^+ reacts with DMS to form the main reaction fragment at 131 amu with a relative abundance

69.4% [23]. Urine headspace contains many VOCs. The most represented classes of compound within such are ketones, aldehydes and sulphur-containing compounds such as dimethyl sulphide (DMS) [25].

6.4.10 m/z = 141

The small peak recorded at 141 amu may belong to toluene. CF_3^+ reacts with toluene in CIR-MS and produces its main fragment at m/z 141 with a relative abundance of 78.2% [23]. VOCs may be used as biomarkers for many diseases and disorders. Research has shown that toluene remains stable and does not fulfil this assumed criterion [25, 34, 35]. Fustinoni *et al*. [33], showed that the concentrations of toluene in the urine headspace of non-smokers, light smokers and heavy smokers were 215, 265 and 336 ng/L, respectively.

6.5 Statistical investigation

The analysis of urine headspace via CIR-TOF-MS using a CF_3^+ reagent provided an extensive dataset of the many VOCs present in the urine headspace. Multivariate analysis is a useful technique to examine the role of variables in complex datasets [36]. In total, 31 urine headspace samples (11 smokers and 20 non-smokers) and 42 variables (m/z values) were analysed and used as input for principal component analysis (PCA), agglomerative hierarchical clustering analysis (AHC), and partial least squares discriminant analysis (PLS-DA) using XL STAT [37]. The masses of precursors (CF_3^+, H_3O^+), clusters and unidentified masses were manually removed beforehand. Ideally two-dimensional PCA would be sufficient to differentiate between smokers and non-smokers. As can be seen in Figure 6.8, if data are represented on only one axis, the variability may still be significant (46.68%), whilst two axes represents 59.06% of the initial variability of the data.

Cluster analysis was used to extract the similarities and dissimilarities between the VOCs in the urine headspaces (Figure 6.9). In the dendrogram which resulted, two main groupings resulted identified as coming from smokers or non-smokers. Extraneous factors such as the food or drink consumed before taking a urine sample, could also affect the results. Generally, most samples from smokers were grouped on the left. The second group (on the right) mainly included samples from non-smokers. Each group contains two subgroups which in turn had further sub-groupings. The distinction between these groups could not be clearly determined probably due to the small number of samples available (see Figure 6.9).

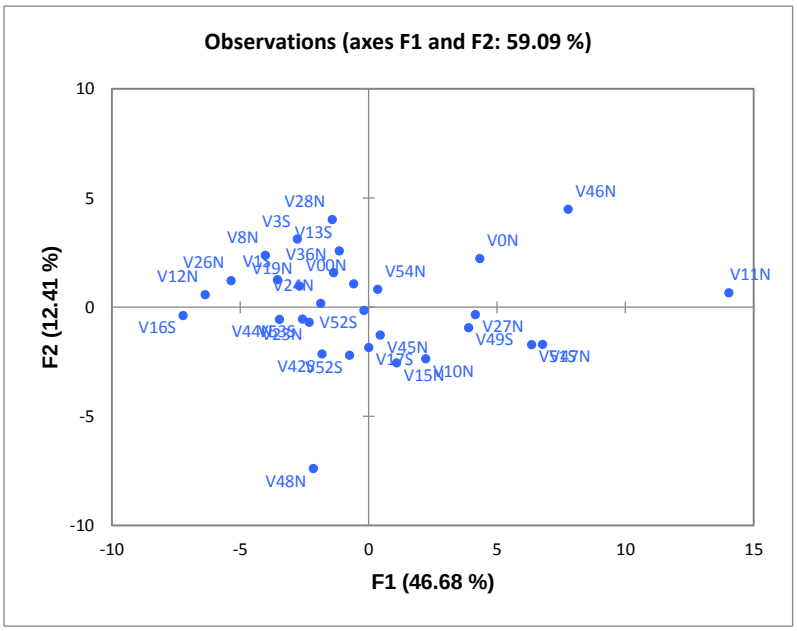

Figure 6. 8: Principal component analysis of the urine headspace of smoking and non-smoking volunteers (samples ending with S and N represent smokers and non-smokers, respectively).

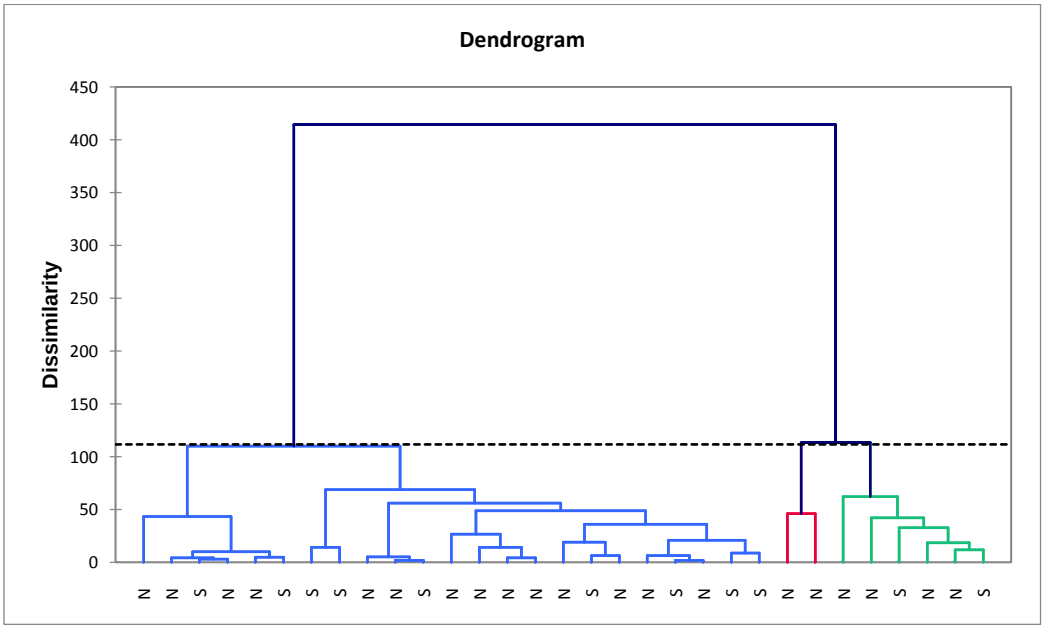

Figure 6. 9: Agglomerative hierarchical clustering (AHC). Clusters form using each observation, starting with small, similar groups leading ultimately to larger groups. In this method, it is possible to identify similar groups from a larger collection of groups.

Better discrimination between the urine headspace samples of smokers and non-smokers was observed using PLS-DA. The specificity and the sensitivity of the values in the model are demonstrated by the receiver operating characteristic curve (ROC). The probability of a negative result is represented by the specificity, while that of a positive value can be represented by the sensitivity. A plot of sensitivity against the reciprocal of specificity creates the ROC curve (Figure 6.10). The area under this curve also called the c statistic which ranges from 0.5 (minimum meaning no discrimination detected) to 1 (maximum discrimination observed) [38].

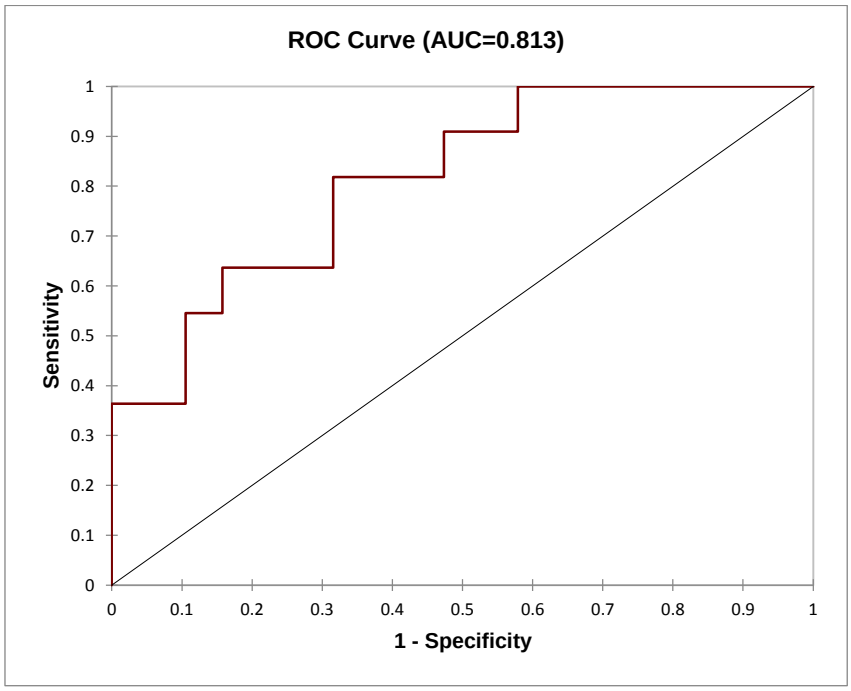

Figure 6. 10: Receiver operating characteristics curve (ROC) has a significant outcome value of 0.813, meaning the PLS-DA model's performance is good. This shows that PLS-DA is capable of distinguishing between the two groups of urine headspace samples.

PLS-DA (Figure 6.11) shows how it is possible to distinguish between the urine headspace samples of smokers and non-smokers when the value of the ROC is 0.813. Further examination of Figure 6.10, shows some separation between the urine headspaces of smokers and non-smokers. The smokers' area is located in the middle and the bottom of the left side of the graph, while the non-smoking subjects are located in middle, upper left side and lower right side of the graph. The non-smokers' area is wider than that of the smokers. There is also a degree of overlap between the two groups, which is located

around the middle of the left side, which means that some VOC profiles are common to the two groups. The separation between the two groups is not as distinct in the urine headspace data as it is in the breath data (Chapter 5). There are several reasons why this should be so. Firstly, not all the expected VOCs produced from smoking could be transfer from the lungs to the urine. Secondly the overlap could be due to the variety of food or drink consumed by certain subjects prior to testing. Thirdly, the number of samples might not be sufficient to allow for good separation in the model, and finally, it was difficult to find a sufficient number of volunteers to collect more samples.

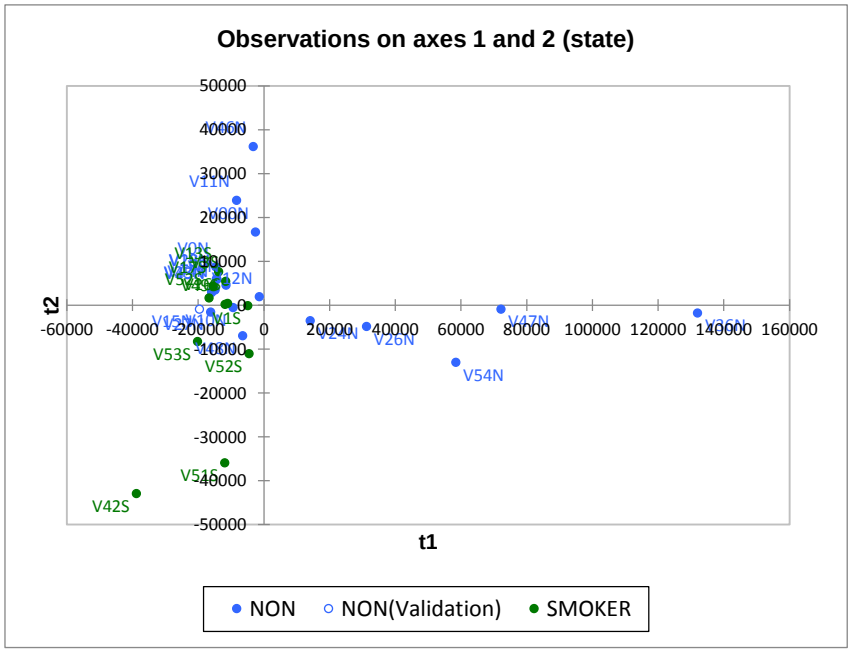

Figure 6. 11: PLS-DA shows that some separation that exists between the two groups of urine headspace samples (smokers and non-smokers). The coloured symbols on the plot are the areas that the model believes belong to each group. The green and blue symbols represent the smoker and non-smoker areas, respectively, in the model.

Figure 6.12 shows the prominent variables (masses) located in the bottom of the left side (negative area) could influence the distinction between the two groups of urine headspace data in PLS-DA. It seems that masses such as 59, 110, 127, 57, 56, 75, 136 and 141 amu are prominent candidate VOCs able to influence the separation between the two groups. The VOC at m/z = 110, is formed from acetonitrile, a well-known marker for smokers. The interesting thing is that mass 59, which may belong to protonated acetone and is thus a byproduct of a reaction with a hydronium contamination. It has a strong affect on the model in terms of distinguishing between the two groups.

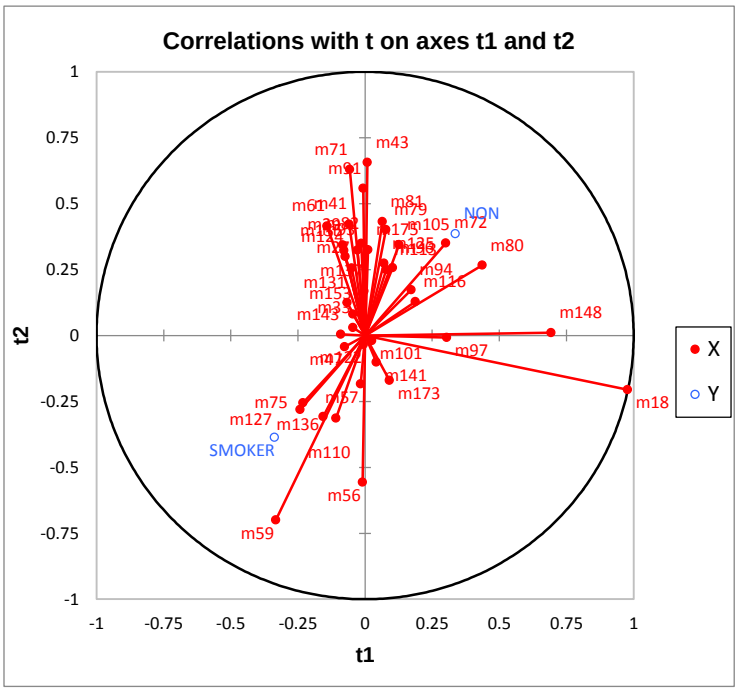

Figure 6. 12: PLS-DA shows the important variables (masses) that allow for the distinction to be made between the two groups of urine headspace data (smokers and non-smokers).

The negative area in Figure 6.12 shows masses that separate between smokers and non-smokers, which is demonstrated more clearly in Figure 6.13. From this Figure can be seen that masses 59 amu and 110 amu, which may belong to acetone and acetonitrile, have the strongest effect on the separation of smokers and non-smokers. m/z 56, m/z 57 (alkane C_4, C_8, and C_9 fragments), m/z 75 (butanone tentative assignment) and m/z 127 (benzene tentative assignment) have a more moderate effect on the separation between two groups. While m/z 136 (pyrrole tentative assignment), m/z 141 (toluene tentative assignment) and m/z 173 (styrene tentative assignment) have the lowest effect on the separation between the groups; results are shown in Table 6.3.

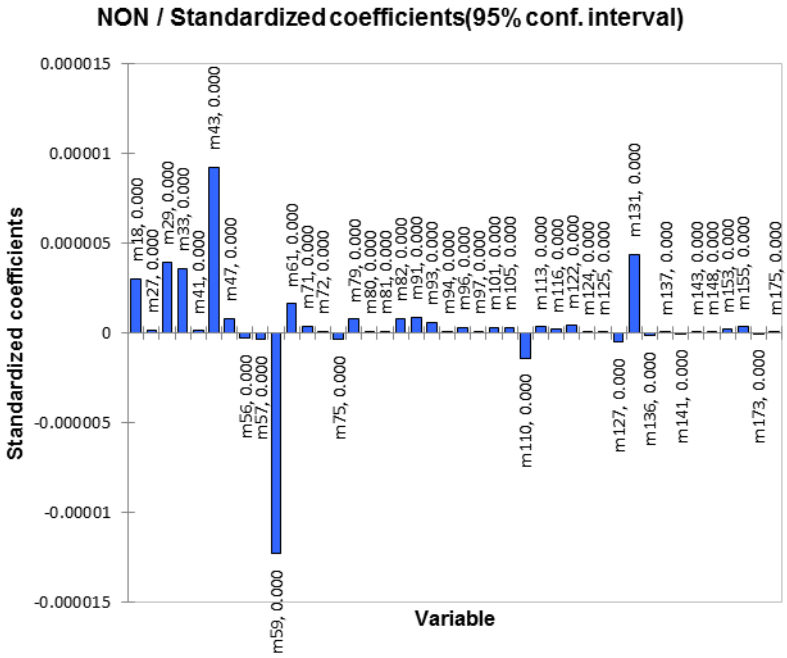

Figure 6. 13: PLS-DA coefficients for discrimination between smokers and non-smokers

Table 6. 3: Masses and compounds that distinguish between smokers and non-smokers.

tentative assignment	mass	structure	tentative assignment	mass	structure
acetone	59	$CH_3COHCH_3^+$	butanone	75	$CH_3CH_2CFCH_3^+$
acetonitrile	110	$CH_3CNH.CF_3^+$	pyrrole	136	$C_4H_4NH.CF_3^+$
benzene	127	$C_6H_5.CF_2^+$	toluene	141	$C_7H_7.CF_2^+$
	56	$C_4H_8^+$	styrene	173	$C_6H_5CHCH_2.CF_3^+$
	57	$C_4H_9^+$	-	-	-

6.6 Summary

The ability of CF_3^+ to act as a reagent in chemical ionization time-of-flight mass spectrometry (CIR-TOF-MS) has been tested to detect VOCs in the urine headspace of smokers and non-smokers. CF_3^+ reacts with several VOCs in urine headspace samples but the differentiation of the yields between smokers and non-smokers are not as apparent as in the tests on the breath emissions.

The CF_3^+ data showed several fragments that belong to compounds produced by the reaction of CF_3^+ with the analytes. Some protonated parent ions were also detected in the same spectra such as m/z 59, tentatively assigned to acetone. These peaks were produced by the reaction of H_3O^+ (as humidity and in competition with CF_3^+ in CI-TOF-MS) with the analytes.

Some signals are more likely related to, or be detected from, one analyte (compound) such as at m/z = 75, 110, 131 and 141, which may belong to butanone, acetonitrile, dimethyl sulphide and toluene, respectively. Some peaks could arise due to contributions from more than one analyte (compound), such as m/z 29 which may be assigned to either ethane, ethanol or CHO^+. The signal at m/z 43 may belong to $C_3H_7^+$ and is considered a common fragment for many compounds. The signal at 57 amu could represent butane, heptane or octane, while the fragment at 61 amu could belong to ketone or aldehyde groups. The fragment at 71 amu may arise from pentane or octane.

Some analytes prefer to react with H_3O^+, which is in competition with CF_3^+, to produce a protonated parent ion such as acetone at 59 amu.

PTR-TOF-MS data showed only a few signals such as 18, 42 and 59 amu which may belong to ammonia, acetonitrile and acetone, respectively. It seems that the reason for detecting only a few signals when using H_3O^+ as a reagent in CIR-MS is that the concentration of ammonia is relatively high in urine samples. The ammonia competes with the analytes to react with H_3O^+, and as a result the ion count of this reagent will be significantly reduced.

Generally, using more than one precursor is helpful in the detection of VOCs in real time and from the same sample, which could react with one or both chemical reagents, CF_3^+ and H_3O^+.

6.7 References

[1] Y. He, A. Vargas, Y.-J. Kang, Headspace liquid-phase microextraction of methamphetamine and amphetamine in urine by an aqueous drop, Analytica chimica acta, 589 (2007) 225-230.

[2] A.P. Antón, Á.G. Ramos, M. del Nogal Sánchez, J.L.P. Pavón, B.M. Cordero, Á.P.C. Pozas, Headspace-programmed temperature vaporization-mass spectrometry for the rapid determination of possible volatile biomarkers of lung cancer in urine, Analytical and bioanalytical chemistry, 408 (2016) 5239-5246.

[3] M. Mamas, W.B. Dunn, L. Neyses, R. Goodacre, The role of metabolites and metabolomics in clinically applicable biomarkers of disease, Archives of toxicology, 85 (2011) 5-17.

[4] J. Huang, S. Kumar, N. Abbassi-Ghadi, P. Spanel, D. Smith, G.B. Hanna, Selected ion flow tube mass spectrometry analysis of volatile metabolites in urine headspace for the profiling of gastro-esophageal cancer, Analytical chemistry, 85 (2013) 3409-3416.

[5] L. Pauling, A.B. Robinson, R. Teranishi, P. Cary, Quantitative analysis of urine vapor and breath by gas-liquid partition chromatography, Proceedings of the National Academy of Sciences, 68 (1971) 2374-2376.

[6] J.A. Armstrong, Urinalysis in Western culture: A brief history, Kidney International, 71 (2007) 384-387.

[7] J. Eigbefoh, P. Isabu, E. Okpere, J. Abebe, The diagnostic accuracy of the rapid dipstick test to predict asymptomatic urinary tract infection of pregnancy, Journal of Obstetrics and Gynaecology, 28 (2008) 490-495.

[8] D. Firestone, A. Wos, J.P. Killeen, T.C. Chan, K. Guluma, D.P. Davis, G.M. Vilke, Can Urine Dipstick be Used as a Surrogate for Serum Creatinine in Emergency Department Patients Who Undergo Contrast Studies?, The Journal of emergency medicine, 33 (2007) 119-122.

[9] D.N. Firestone, R.A. Band, J.E. Hollander, E. Castillo, G.M. Vilke, Use of a urine dipstick and brief clinical questionnaire to predict an abnormal serum creatinine in the emergency department, Academic Emergency Medicine, 16 (2009) 699-703.

[10] M.S. Graziani, G. Gambaro, L. Mantovani, A. Sorio, T. Yabarek, C. Abaterusso, A. Lupo, P. Rizzotti, Diagnostic accuracy of a reagent strip for assessing urinary albumin

excretion in the general population, Nephrology Dialysis Transplantation, 24 (2008) 1490-1494.

[11] P. Little, S. Turner, K. Rumsby, G. Warner, M. Moore, J.A. Lowes, H. Smith, C. Hawke, M. Mullee, Developing clinical rules to predict urinary tract infection in primary care settings: sensitivity and specificity of near patient tests (dipsticks) and clinical scores, Br J Gen Pract, 56 (2006) 606-612.

[12] S. Mayo, D. Acevedo, C. Quiñones-Torrelo, I. Canós, M. Sancho, Clinical laboratory automated urinalysis: comparison among automated microscopy, flow cytometry, two test strips analyzers, and manual microscopic examination of the urine sediments, Journal of clinical laboratory analysis, 22 (2008) 262-270.

[13] Z. Xu, J. Okada, A.R. Timerbaev, T. Hirokawa, Sensitive profiling of biogenic amines in urine using CE with transient isotachophoretic preconcentration, Journal of separation science, 32 (2009) 4143-4147.

[14] R. Krüger, K. Bruns, S. Grünhage, H. Rossmann, J. Reinke, M. Beck, K.J. Lackner, Determination of globotriaosylceramide in plasma and urine by mass spectrometry, Clinical chemistry and laboratory medicine, 48 (2010) 189-198.

[15] C.-W. Hu, M.-R. Chao, C.-H. Sie, Urinary analysis of 8-oxo-7,8-dihydroguanine and 8-oxo-7,8-dihydro-2'-deoxyguanosine by isotope-dilution LC-MS/MS with automated solid-phase extraction: Study of 8-oxo-7,8-dihydroguanine stability, Free Radical Biology and Medicine, 48 (2010) 89-97.

[16] N.L. Korpi-Steiner, B.C. Netzel, J.C. Seegmiller, J.B. Hagan, R.J. Singh, Liquid chromatography–tandem mass spectrometry analysis of urinary fluticasone propionate-17beta-carboxylic acid for monitoring compliance with inhaled-fluticasone propionate therapy, Steroids, 75 (2010) 77-82.

[17] K.K. Pasikanti, P.C. Ho, E.C. Chan, Development and validation of a gas chromatography/mass spectrometry metabonomic platform for the global profiling of urinary metabolites, Rapid communications in mass spectrometry, 22 (2008) 2984-2992.

[18] A. Zhang, H. Sun, P. Wang, Y. Han, X. Wang, Recent and potential developments of biofluid analyses in metabolomics, Journal of Proteomics, 75 (2012) 1079-1088.

[19] D. Ryan, K. Robards, P.D. Prenzler, M. Kendall, Recent and potential developments in the analysis of urine: A review, Analytica chimica acta, 684 (2011) 17-29.

[20] L. Jin, Y. Li, L. Lin, L. Zou, H. Hu, Drying characteristic and kinetics of Huolinhe lignite in nitrogen and methane atmospheres, Fuel, 152 (2015) 80-87.

[21] R.S. Blake, S.A. Ouheda, C.J. Evans, P.S. Monks, CF_3^+ and CF_2H^+: new reagents for n-alkane determination in chemical ionization reaction mass spectrometry, The Analyst, 141 (2016) 6564-6570.

[22] K.P. Wyche, R.S. Blake, K.A. Willis, P.S. Monks, A.M. Ellis, Differentiation of isobaric compounds using chemical ionization reaction mass spectrometry, Rapid communications in mass spectrometry : RCM, 19 (2005) 3356-3362.

[23] R.S. Blake, S.A. Ouheda, E.F. Alwedi, P.S. Monks, Exploration of the utility of CF_3^+ as a reagent for chemical ionization reaction mass spectrometry, International Journal of Mass Spectrometry, 421 (2017) 224-233.

[24] L. Perbellini, F. Brugnone, V. Cocheo, E. De Rosa, G.B. Bartolucci, Identification of the n-heptane metabolites in rat and human urine, Archives of toxicology, 58 (1986) 229-234.

[25] P. Mochalski, K. Krapf, C. Ager, H. Wiesenhofer, A. Agapiou, M. Statheropoulos, D. Fuchs, E. Ellmerer, B. Buszewski, A. Amann, Temporal profiling of human urine VOCs and its potential role under the ruins of collapsed buildings, Toxicology mechanisms and methods, 22 (2012) 502-511.

[26] A.M. Diskin, P. Spanel, D. Smith, Increase of acetone and ammonia in urine headspace and breath during ovulation quantified using selected ion flow tube mass spectrometry, Physiological measurement, 24 (2003) 191.

[27] P. Mochalski, A. Agapiou, M. Statheropoulos, A. Amann, Permeation profiles of potential urine-borne biomarkers of human presence over brick and concrete, The Analyst, 137 (2012) 3278-3285.

[28] S. Smith, H. Burden, R. Persad, K. Whittington, B. de Lacy Costello, N.M. Ratcliffe, C. Probert, A comparative study of the analysis of human urine headspace using gas chromatography–mass spectrometry, Journal of breath research, 2 (2008) 037022.

[29] B. de Lacy Costello, A. Amann, H. Al-Kateb, C. Flynn, W. Filipiak, T. Khalid, D. Osborne, N.M. Ratcliffe, A review of the volatiles from the healthy human body, Journal of breath research, 8 (2014) 014001.

[30] S.M. Abbott, J.B. Elder, P. Španěl, D. Smith, Quantification of acetonitrile in exhaled breath and urinary headspace using selected ion flow tube mass spectrometry, International Journal of Mass Spectrometry, 228 (2003) 655-665.

[31] G.M. Pinggera, P. Lirk, F. Bodogri, R. Herwig, G. Steckel-Berger, G. Bartsch, J. Rieder, Urinary acetonitrile concentrations correlate with recent smoking behaviour, BJU international, 95 (2005) 306-309.

[32] S. Ghittori, M. Fiorentino, L. Maestri, G. Cordioli, M. Imbriani, Urinary excretion of unmetabolized benzene as an indicator of benzene exposure, Journal of Toxicology and Environmental Health, Part A Current Issues, 38 (1993) 233-243.

[33] S. Fustinoni, R. Giampiccolo, S. Pulvirenti, M. Buratti, A. Colombi, Headspace solid-phase microextraction for the determination of benzene, toluene, ethylbenzene and xylenes in urine, Journal of Chromatography B: Biomedical Sciences and Applications, 723 (1999) 105-115.

[34] A. Zlatkis, W. Bertsch, H. Lichtenstein, A. Tishbee, F. Shunbo, H. Liebich, A. Coscia, N. Fleischer, Profile of volatile metabolites in urine by gas chromatography-mass spectrometry, Analytical chemistry, 45 (1973) 763-767.

[35] M. Statheropoulos, E. Sianos, A. Agapiou, A. Georgiadou, A. Pappa, N. Tzamtzis, H. Giotaki, C. Papageorgiou, D. Kolostoumbis, Preliminary investigation of using volatile organic compounds from human expired air, blood and urine for locating entrapped people in earthquakes, Journal of Chromatography B, 822 (2005) 112-117.

[36] C. Guallar-Hoyas, Prospecting for markers of disease in respiratory diseases, in, PhD Thesis, Loughborough University, 2013.

[37] XLSTAT 2017: Data Analysis and Statistical Solution for Microsoft Excel. , in, Addnsoft, France, 2017.

[38] N.R. Cook, Use and misuse of the receiver operating characteristic curve in risk prediction, Circulation, 115 (2007) 928-935.

Chapter Seven: Summary and Conclusion

7.1 Introduction

The ability to measure volatile organic compounds (VOCs) is useful in many areas of study, including atmospheric chemistry, food science, homeland security and medical diagnosis [1]. Several techniques can be used to detect a number of VOCs, including gas chromatography-mass spectrometry (GC-MS), selected ion flow tube mass spectrometry (SIFT-MS) and chemical ionization reaction mass spectrometry (CIR-MS). CIR-MS is a soft ionization technique which offers good sensitivity and can be low cost, compact and have excellent mass resolution. H_3O^+ as a reagent in CIR-MS is widely used in a range of applications, but other precursors, such as O_2^+ and NH_4^+, have also been used successfully [2]. In this thesis, CF_3^+ was demonstrated to be a novel reagent in CIR-MS when applied to the quantification of several VOC classes which are difficult to detect using conventional reagents.

Chapter One detailed some of the common reagent ions used in chemical ionization mass spectrometry techniques; namely H_3O^+, O_2^+, NO^+, NH_4^+ and CF_3^+. The reaction of H_3O^+ with different organic compounds with various functional groups (including aldehydes, ketones, alcohols, carboxylic acids, and N- and O-containing heterocyclic compounds) in mass spectrometric techniques such as SIFT-MS and CIR-MS was explored in some detail. Proton transfer reaction mass spectrometry (PTR-MS) applications in environmental measurements and medical science were explored with examples. In a similar manner, the reactions of O_2^+, NO^+ and NH_4^+ with different VOCs were explained, and the fragmentation pattern produced with these precursors demonstrated.

Historically, the first exploration of the reactions of CF_3^+ with different compounds were performed on a compact Fourier transform-ion cyclotron resonance (FT-ICR) spectrometer. The action of this reagent in FT-ICR was explored and the mechanism and the fragmentation pattern of a number of VOCs showed that CF_3^+ reacts with alkanes C_2-C_2 via hydride transfer. In addition, CF_3^+ reacts as an electrophilic reagent with variety of VOCs such as carbonyl compounds causing cleavage of their C-O bond owing to migration of the fluorine atom.

Chapter Two put the fundamentals of GC-MS and CIR-MS into context, explaining why these techniques are useful tools for establishing the qualitative and quantitative composition of gaseous mixtures. The main components of CIR-MS, namely the ion

source, drift tube, mass spectrometry and ion detectors, were described. Aspects of CIR-MS such as calibration techniques, effect of humidity, accuracy, precision and detection limits were also briefly discussed.

7.2 CF_3^+ as a new reagent in CIR-MS for the detection of small chain alkanes

In Chapter Three, it was demonstrated that CF_3^+ was a novel reagent in CIR-MS useful for the detection of lighter *n*-alkanes (C_2-C_6), which are impossible to detect using the most widely used chemical reagent, H_3O^+ owing to their low proton affinities. Another chemical ionization reagent examined was O_2^+ which produced extensive fragmentation with n-alkanes. CF_3^+ on the other hand was found to react with these alkanes with almost no fragmentation. The results also showed that the sensitivity to small chain *n*-alkanes with CF_3^+ was better than that of O_2^+. The alkane results showed that CF_3^+ could be used for measurements of alkanes in real-life samples such as exhaled breath and polluted air.

7.3 CF_3^+ as a reagent in CIR-MS for the detection of a wide range of VOCs

In Chapter Four, the ability of CF_3^+ to react with a wide range of VOC functionality in CIR-MS was examined. The VOCs in this instance were represented by organic groups such as alcohols, ketones, aldehydes, aromatics and *n*-heterocyclic compounds. These VOCs were selected based on the suspected likelihood of their occurrence in exhaled human breath, urine headspace and the environment. The results showed that CF_3^+ is good reagent to detect several aromatic and nitrile compounds, particularly those that are electron-rich and act as Lewis acids. The reaction of CF_3^+ with ketones and aldehydes mainly produced ROCOR.CF_3^+, ROC.CF_3^+ or RCO^+ although those with longer alkyl chains preferred to shed fragments of the chain in preference. Nitriles and DMS preferred to produce RCF_3^+. Generally, alcohols exhibited little reactivity with CF_3^+: no reaction with methanol was observed, though other alcohols, where they showed signs of reacting, resulted in alkyl fragments being produced. Alkenes produced molecular ions with some fragmentation.

7.4 CF_3^+ as a reagent in CIR-MS for detection of VOCs in exhaled breath

In Chapter Five, the ability of CF_3^+ to act as a chemical reagent in CIR-MS to detect VOCs in the exhaled breath of smoking and non-smoking volunteers was examined. In this work, different designs were used to collect breath samples in Tedlar bags. For comparison, PTR-TOF-MS was also used to measure the VOCs in breath samples, so that the contributions of interference by PTR products in the CF_3^+ reactions could be estimated.

The CF_3^+ spectra showed fragments originating from one parent analyte (compound) such *m/z* = 110 (acetonitrile), while other fragments such as that at *m/z* = 29 could contain contributions from several sources (ethane, ethanol and CHO^+). Some fragments produced a protonated parent ion such as *m/z* 59 (acetone) and m/z 61 from CF_3^+ where an oxygen atom is replaced by a fluorine atom. Using both reagents, CF_3^+ and H_3O^+, in CIR-MS is useful for the measurement of VOCs in real-life samples.

Multivariate analysis such as principal component analysis (PCA), agglomerative hierarchical clustering analysis (AHC) and partial least-squares discriminant analysis (PLS-DA) of the results were carried out and found to represent excellent tools for distinguishing between the breath data obtained from smokers and non-smokers.

7.5 CF_3^+ as a reagent in CIR-MS for detection of VOCs in urine headspace

In Chapter 6, several VOCs in the urine headspace of smokers and non-smokers were detected using CF_3^+ as a reagent in CIR-MS. Samples were collected in sterile plastic containers, which were then transferred to a head-spacing vessel. N_2 gas was used as carrier gas and measured with CIR-MS using CF_3^+ as the reagent. For comparative purposes, samples were also examined using H_3O^+ as a precursor in CIR-MS.

Generally, CF_3^+ spectra showed three types of signals: the first type represents the signals which are most likely related formed from one analyte for example *m/z* 110, for acetonitrile. In the second type, the signal could be produced as a fragment from more than one analyte, such as *m/z* 57 which could represent butane, heptane or octane fragments. In the third type, some analytes preferred to react with the H_3O^+, producing a protonated parent ion such as at *m/z* 59 which could belong to acetone.

Unfortunately, only a few signals were detected using PTR-MS such as m/z 18, 42 and 59 tentatively assigned to ammonia, acetonitrile and acetone, respectively. One reason behind the low detection could be the high concentration of ammonia, which would compete with other analytes and significantly reduce the fragment ion counts. This could lead to low sensitivity of most analytes.

CF_3^+ and H_3O^+ as reagents in CIR-MS could produce a clear picture when detecting VOCs in real-life samples although the distinction between smokers and non-smokers was not as marked as was found in the breath analysis experiments.

Multivariate analyses such as PCA, AHC and PLS-DA were applied to find the variations, if present, between smokers and non-smokers. Only some distinctions between smokers and non-smokers could be determined. It could be that some of VOCs related to cigarette smoke were not present at detectable levels. Another reason could be that the amount of data collected were not sufficient to allow for reasonable discrimination between smokers and non-smokers.

7.6 Further work

CF_3^+ as a reagent in CIR-MS is an excellent tool for the detection of VOCs in fields such as exhaled breath and urine headspace analysis. CF_3^+ and H_3O^+ as reagents in CIR-MS seem to be complementary to each other in the identification of several VOCs.

Further work will be needed to test the ability of CF_3^+ as a reagent in CIR-MS to identify methane, other alkanes, and other organic species such as aldehydes, ketones, carboxylic acids and heterocyclic compounds. As a result, a relatively large library of spectra could be created to help in the interpretation of data obtained from real-life samples.

Owing to the success of this research in the application of CF_3^+ in CIR-MS to identify several VOCs present in the exhaled breath and urine headspace of smokers and non-smokers, it might be useful to conduct further work using CF_3^+ as precursor in CIR-MS to determine the VOCs in patients caused by diseases such as asthma and/or cancer.

Many organisms such as *Clostridium difficile* bacteria release many VOCs such as dimethyl sulfide and N-containing compounds. This type of bacteria is responsible for around 500,000 infections caused every year and the treatment and management of *C. difficile* infection is considered to be a major economic issue. In the UK, For example, treatment of a single *Clostridium difficile* infection case costs approximately £7,000[3].

CF_3^+ as reagent in CIR-MS could be a good method to investigate the behaviour of VOCs release from bacterial metabolism and the effect of treatment with different phages on the bacteria.

CF_3^+ as precursor in CIR-MS allows numerous VOCs from natural and man-made sources to be identified and quantified at high resolution and sensitivity.

7.7 References

[1] R.S. Blake, S.A. Ouheda, C.J. Evans, P.S. Monks, CF_3^+ and CF_2H^+: new reagents for n-alkane determination in chemical ionization reaction mass spectrometry, The Analyst, 141 (2016) 6564-6570.

[2] R.S. Blake, S.A. Ouheda, E.F. Alwedi, P.S. Monks, Exploration of the utility of CF_3^+ as a reagent for chemical ionization reaction mass spectrometry, International Journal of Mass Spectrometry, 421 (2017) 224-233.

[3] A.M. Thanki, Development of a phage-based diagnostic test for the identification of Clostridium difficile, in, PhD Thesis, Loughborough Uinversity, 2016.